



HAL
open science

Design of poly(3-hydroxybutyrate-co-3-hydroxyvalerate) based films for flexible food packaging in contact with fatty food and under frozen conditions

Benjamin Le Delliou

► To cite this version:

Benjamin Le Delliou. Design of poly(3-hydroxybutyrate-co-3-hydroxyvalerate) based films for flexible food packaging in contact with fatty food and under frozen conditions. Chemical and Process Engineering. Université Paris-Saclay, 2021. English. NNT : 2021UPASB033 . tel-04815501

HAL Id: tel-04815501

<https://pastel.hal.science/tel-04815501v1>

Submitted on 3 Dec 2024

HAL is a multi-disciplinary open access archive for the deposit and dissemination of scientific research documents, whether they are published or not. The documents may come from teaching and research institutions in France or abroad, or from public or private research centers.

L'archive ouverte pluridisciplinaire **HAL**, est destinée au dépôt et à la diffusion de documents scientifiques de niveau recherche, publiés ou non, émanant des établissements d'enseignement et de recherche français ou étrangers, des laboratoires publics ou privés.

Design of poly(3-hydroxybutyrate-co-3-hydroxyvalerate) based films for flexible food packaging in contact with fatty food and under frozen conditions

Conception de films de poly(3-hydroxybutyrate-co-3-hydroxyvalerate) pour l'emballage alimentaire flexible en contact avec des aliments gras et dans des conditions de surgélation

Thèse de doctorat de l'université Paris-Saclay

École doctorale n° 581 Agriculture, alimentation, biologie, environnement et santé (ABIES)

Spécialité de doctorat : Génie des procédés

Unité de recherche : Université Paris-Saclay, INRAE, AgroParisTech, UMR SayFood, 91300, Massy, France..

Référent : AgroParisTech

**Thèse présentée et soutenue à Paris-Saclay,
le 12/07/2021, par**

Benjamin LE DELLIU

Composition du Jury

Gilles TRYSTRAM

Professeur, AgroParisTech

Président

Loïc HILLIOU

Senior Researcher, Université de Minho (Portugal)

Rapporteur & Examineur

Véronique BOUNOR-LEGARE

Directrice de Recherche, CNRS (Université Lyon 1)

Rapporteur & Examinatrice

Cyrille SOLLOGOUB

Professeur, CNAM

Examineur

Jean-Charles BENEZET

Professeur, Mines d'Alès

Examineur

Paola FABBRI

Associate Professor, Université de Bologne (Italie)

Examinatrice

Direction de la thèse

Sandra DOMENEK

Maître de conférences (HDR), AgroParisTech

Directrice de thèse

Olivier VITRAC

Chargé de recherche (HDR), INRAE-Centre IdF-Jouy-en-Josas-Antony

Co-Directeur & Examineur

Frédéric MERLE

Euramaterials

Invité

Pierre GONDÉ

Docteur, McCain Alimentaire S.A.S

Invité

Acknowledgment

Ces travaux de thèse ont été réalisés dans le cadre d'un projet CIFRE avec l'entreprise McCain Alimentaire S.A.S et je souhaite remercier toutes les personnes que j'ai eu l'occasion de croiser et avec qui j'ai pu discuter au cours de ces trois ans. Je tiens également à remercier l'ANRT pour son support financier (CIFRE agreement n°2017/1574). Je souhaite remercier l'UMR SayFood n°0782 AgroParisTech, INRAE et l'ensemble de ses collaborateurs de m'avoir hébergé au cours de ces trois ans.

Toute ma gratitude est adressée à mes directeurs de thèse, Oliver Vitrac et Sandra Domenek. Vous m'avez donné l'opportunité d'évoluer à vos côtés, de faire murir ma réflexion scientifique, de m'avoir encadré avec bienveillance et de m'avoir transmis vos très nombreuses connaissances scientifiques. Vous m'avez poussé au-delà de ma zone de confort tout en m'accompagnant. Merci à vous deux.

I am very grateful to Loic Hilliou, Senior researcher at University of Minho (Portugal), and Véronique Bounor-Legaret, Director of Research at CNRS, who accepted to take time to review this manuscript and be part of the jury. I am also grateful to Cyrille Sollogoub, Professor at CNAM, Gilles Trystram, Professor at AgroParisTech, Jean Charles Benezet, Professor at Mines d'Alès, and Paola Fabbri, Associate Professor at University of Bologna (Italy), to be part of the jury.

Je souhaite exprimer mes plus sincères remerciements à Pierre Gondé. Au-delà d'avoir été mon encadrant de thèse côté industriel, tu as été pour moi un réel moteur de motivation en me prodiguant tes conseils, tes connaissances et surtout en m'encourageant tout au long de ces trois ans. Tu m'as donné ta confiance en me permettant d'aller au-delà de ma zone de confort, d'avoir promu mes travaux de thèse et d'acquérir une expérience professionnelle inestimable. J'espère pouvoir faire une aussi belle carrière que la tienne. Je retiendrai que je dois rester moi-même car le fruit de notre travail sera toujours récompensé. Je te souhaite la plus belle des retraites qui soit, que tu puisses t'épanouir dans le sud entouré de tes oliviers. Je souhaite également adresser mes sincères remerciements à Frédéric Merle. Merci d'avoir accepté de suivre mon travail et d'avoir su poser les bonnes questions. Vous formez un beau duo et j'ai eu un immense plaisir à travailler avec vous. Merci encore.

La réalisation de ces travaux de thèse n'aurait pas été rendu possible sans les collaborations avec les partenaires suivants : **The following partnerships are acknowledged :**

- Lab-scale extrusion took place at the CTCPA, Bourg-en-Bresse (France) in cooperation with Patrice Dole.
- Melt rheology measurements were performed at the IRDL in cooperation with Michael Castro and Stéphane Bruzard.
- Process scale up to pilot scale film blowing extrusion was carried out at the PIMM in cooperation with Alain Guinault.
- Tensile test under freezer conditions, impact test and melt flow index were performed at the LNE in cooperation with Jean Mario Julien and Phuong Mai Nguyen

Je souhaite par ailleurs remercier Nathalie Ruscassier (Centrale Supélec), Mathilde Charters (Centrale Supélec), Anne Grandmontagne (PIMM), Florian Catinot (CTCPA) et Antoine Kervoelen (IRDL) pour m'avoir aidé dans la réalisation de mes travaux. Je remercie également mes deux stagiaires Sami et Valentin ainsi que l'ensemble des étudiants AgroParisTech qui ont travaillé sur ma thématique et que j'ai eu plaisir à encadrer.

Je souhaite remercier les personnes que j'ai côtoyé le plus au cours de ces trois dernières années : Robert, Richard, Michelle, Zinith, Toinou, Didier, Marie, Claire, Wafa, Celine, Marie-Laure, Anir (qui a fait un travail considérable), Flavien, Manon LG., Manon G., Cédric, Magali, Julien, Yan et en espérant n'avoir oublié personne.

Je souhaite remercier mes plus proches collègues et amis : Hajar, Maxime, et Mai.

Je tiens également à remercier l'ensemble de mes amis et de ma famille pour votre soutien et plus particulièrement : Axelle, Hugo, Fanny, Manuel, Violette, Vincent, mon Loulou, mes beaux-parents.

Je tiens à exprimer ma plus grande gratitude à mes parents et à ma sœur. Merci pour votre soutien et votre amour indéfectible qui font de moi ce que je suis aujourd'hui.

Ces derniers mots seront pour toi, Johanna, toi la femme que j'aime, ton amour et ton soutien auront été infailible. La naissance de notre merveilleux fils est la résultante de notre amour.

A mon fils Owen

Table of content

| | |
|---|-----------|
| ACKNOWLEDGMENT | 1 |
| TABLE OF CONTENT | 2 |
| SCIENTIFIC CONTRIBUTIONS | 5 |
| LIST OF FIGURES | 6 |
| LIST OF TABLES | 13 |
| GENERAL INTRODUCTION | 1 |
| I.1. SOCIETAL AND INDUSTRIAL CONTEXT..... | 1 |
| I.2. ROLES OF FOOD PACKAGING | 1 |
| I.3. CURRENT END-OF-LIFE TREATMENT OF LDPE IN FRANCE | 3 |
| I.4. THESIS CONTEXT | 5 |
| I.5. STRATEGY DEVELOPED TO DELIVER AN ALTERNATIVE TO POLYETHYLENE PACKAGING | 6 |
| CHAPTER I | 9 |
| I.1. PART I : BACKGROUND STUDY | 10 |
| I.2. PART II : LITERATURE REVIEW | 19 |
| I.3. OBJECTIVES AND APPROACH | 53 |
| CHAPTER II MATERIALS, METHODS AND IMPLEMENTATION PROCESSES | 56 |
| II.1. MATERIALS | 57 |
| II.2. EXPERIMENTAL METHODS..... | 58 |
| II.3. CHARACTERIZATION METHODS | 77 |
| CHAPTER III CHARACTERIZATION OF NEW BIO-BASED AND BIODEGRADABLE POLYMER BLEND: APPLICATION TO POLY(3-HYDROXYBUTYRATE-CO-3-HYDROXYVALERATE) / POLY(BUTYLENE-CO-SUCCINATE-CO-ADIPATE) BLENDS | 83 |
| III.1. ABSTRACT | 84 |
| III.2. INTRODUCTION | 85 |
| III.3. EXPERIMENTAL SECTION | 87 |
| III.4. RESULTS AND DISCUSSION..... | 90 |
| III.5. CONCLUSION | 104 |
| SUPPORTING INFORMATION | 106 |
| S.1. INTERNAL MIXING OF PHBV/PBSA BLENDS | 106 |

| | | |
|------|---|-----|
| S.2. | THERMO-GRAVIMETRIC ANALYSIS OF PHBV/PBSA BLENDS | 107 |
| S.3. | THERMAL STABILITY OF PHBV | 108 |
| S.4. | DETERMINATION OF THE EQUILIBRIUM MELTING TEMPERATURE T_m^0 | 108 |
| S.5. | AVRAMI-JEZIorny ANALYSIS OF NON-ISOTHERMAL CRYSTALLIZATION KINETICS | 109 |
| S.6. | DYNAMIC MECHANICAL ANALYSIS | 116 |
| S.7. | EQUIVALENT BOX MODEL..... | 116 |

CHAPTER IV IN-SITU COMPATIBILIZATION OF BINARY POLY(3-HYDROXYBUTYRATE-CO-3-HYDROXYVALERATE) / POLY(BUTYLENE-CO-SUCCINATE-CO-ADIPATE) BLENDS USING FREE RADICAL INITIATOR: BATCH-MIXER TO FILM BLOWING OF PHBV-BASED FOR FOOD PACKAGING 121

| | | |
|-------|--|-----|
| IV.1. | ABSTRACT | 122 |
| IV.2. | MATERIALS AND METHODS | 125 |
| IV.3. | RESULTS AND DISCUSSION..... | 130 |
| IV.4. | FILM-BLOWING OF <i>IN-SITU</i> COMPATIBILIZED PHBV/PBSA BLENDS | 140 |
| IV.5. | CONCLUSION | 145 |

CHAPTER V PART I: IMPROVEMENT OF THE THERMO-MECHANICAL PROPERTIES OF PHBV-BASED BLEND THROUGH PLASTICIZATION USING ACETYL TRIBUTYL CITRATE147

| | | |
|------|------------------------------|-----|
| V.1. | INTRODUCTION | 148 |
| V.2. | MATERIALS AND METHODS | 149 |
| V.3. | RESULTS AND DISCUSSION | 152 |
| V.4. | CONCLUSION | 158 |

CHAPTER V: PART II: DESIGN OF POLY(3-HYDROXYBUTYRATE-CO-3-HYDROXYVALERATE)-BASED FLEXIBLE PACKAGING FOR FROZEN FOOD: FROM BATCH-MIXER TO FILM BLOWING161

| | | |
|------|-----------------------------|-----|
| V.5. | INTRODUCTION | 162 |
| V.6. | MATERIALS AND METHODS | 163 |
| V.7. | RESULTS AND DISCUSSION..... | 167 |
| V.8. | CONCLUSION | 177 |

CHAPTER VI VALORIZATION OF POTATO PEELS AND THEIR CONSTITUENTS179

| | | |
|-------|---|-----|
| VI.1. | INTRODUCTION | 180 |
| VI.2. | LITERATURE REVIEW ON THE VALORIZATION OF POTATO PEELS AND THEIR CONSTITUENTS..... | 183 |
| VI.3. | MATERIALS AND METHODS..... | 196 |
| VI.4. | RESULTS AND DISCUSSION | 201 |

| | |
|---|------------|
| VI.5. CONCLUSION | 209 |
| CONCLUSION AND PERSPECTIVES..... | 211 |
| CHAPTER VII RESUME DU TRAVAIL DE THESE EN FRANÇAIS | 215 |
| VII.1. INTRODUCTION GENERALE..... | 216 |
| VII.2. POSITIONNEMENT DE LA THESE | 217 |
| VII.3. OBJECTIFS ET APPROCHE | 218 |
| VII.4. PRINCIPAUX RESULTATS | 219 |
| VII.5. PRINCIPALES CONCLUSIONS | 228 |
| REFERENCES | 230 |

Scientific contributions

Book Chapter Le Delliou B, Vitrac O, Domenek S (2020) Bringing New Function to Packaging Materials by Agricultural By-Products. In: Chong PA, Newman DJ, Steinmacher DA (eds) *Agricultural, Forestry and Bioindustry Biotechnology and Biodiscovery*. Springer International Publishing, Cham, pp 227-257. doi:10.1007/978-3-030-51358-0_13

Publication Le Delliou B., Vitrac O., Castro M., Bruzard S. Domenek S, «Characterization of new bio-based and biodegradable polymer blend: Application to poly(3-hydroxybutyrate-co-3-hydroxyvalerate) / poly(butylene-co-succinate-co-adipate) blends», Submitted to *Journal of Applied Polymer Science*; 2021

Oral presentation Le Delliou B., Vitrac O., Domenek S. , «Development of biodegradable poly(hydroxybutyrate-co-hydroxyvalerate) and poly(butylene succinate-co-adipate) blends: toughening effect », - *BIOPOL*, June 17-19, 2019, Stockholm, Sweden

Poster presentation Le Delliou B, Vitrac O, Domenek S., « Your packaging from your local farms to your fridge », -*MATBIM*, May 8-10, 2019, Milan, Italy

Poster presentation Le Delliou B., Vitrac O., Domenek S., « Development of biodegradable poly(hydroxybutyrate-co-hydroxyvalerate) and poly(butylene succinate-co-adipate) blends: toughening effect» - *JCAT*, June 3-5, 2019, St Valéry en Caux, France

Poster presentation Le Delliou B., Vitrac O., Domenek S., « Development of biodegradable poly(hydroxybutyrate-co-hydroxyvalerate) and poly(butylene succinate-co-adipate) blends: toughening effect » - *EPF*, June 9-14, 2019, Hersonissos, Greece

List of Figures

| | |
|---|----|
| Figure 0.1: Principles of co-production of food and its packaging components | 6 |
| Figure I.1: Classification of biodegradable polymers (reproduced from (Averous & Boquillon, 2004)) | 10 |
| Figure I.2: Classification of thermoplastic polymers based on the origin of their monomers and their bioedgradable character..... | 11 |
| Figure I.3: Global production capacities of bioplastics from 2018 to 2024 | 12 |
| Figure I.4: Global production capacities of bioplastics in 2019 (by market segment)..... | 12 |
| Figure I.5: Global production capacities of bioplastics in 2019 (by material type) | 12 |
| Figure I.6: Biodegradable plastic 2019 vs. 2024..... | 12 |
| Figure I.7: Consummation habits with focus on frozen food..... | 14 |
| Figure I.8: Selection criteria between brands on the frozen potato products(215 answers) | 15 |
| Figure I.9: Importance of packaging features (214 answers) | 15 |
| Figure I.10: Awareness of consumers on the meaning of logos for sorting packaging..... | 16 |
| Figure I.11: Replacing conventional packaging with recycled or bio-based and biodegradable packaging . | 17 |
| Figure I.12: Selection of a packaging based on the material, touch and visual appearance for a recycled or a bio-based and biodegradable packaging..... | 17 |
| Figure I.13: Presence of a home compost for vegetable waste sorting | 18 |
| Figure I.14: Chemical structure of PHBV | 19 |
| Figure I.15: General mechanism of thermal degradation of PHBV, from (Q.-S. Liu, Zhu, Wu, & Qin, 2009) | 22 |
| Figure I.16: .Schematic representation of a blown film molding extruder. Picture adapted from (Eric, 2010) | 24 |
| Figure I.17: Chemical structure of PBSA..... | 26 |
| Figure I.18: Evolution of blend morphology between two immiscible polymers depending on blend ratio, figured modified from (Landreau, 2008)..... | 28 |
| Figure I.19: Breakup mechanisms (i) into two droplets and (ii) strip of droplets) from Rayleigh instabilities | 29 |
| Figure I.20: Critical capillary number as a function of viscosity ratio (Grace† 1982)..... | 29 |
| Figure I.21: Coalescence mechanism (Delamare & Vergnes, 1996) | 30 |
| Figure I.22: Evolution of $\tan \delta$ vs Temperature for various types of polymer blends, figure reproduced from (Robeson, 2007) | 31 |
| Figure I.23: Schematic representation of an equivalent box model (EBM) for a binary blend..... | 32 |

| | |
|--|----|
| Figure I.24: Schematic of morphology development during melt blending. As pellets or powder of the minor phase soften, layers peel off. These stretch out into sheets which break up into fibers and then droplets from (Macosko et al., 1996)..... | 35 |
| Figure I.25: Schematic illustrations of in situ reactive blending of PBS-PLLA, PLLA, PBS in the melt in the presence of (PLLA-b-PGMA) ₃ : (A) represents PBS-g-(PLLA-b-PGMA) ₃ -g-PLLA copolymer; (B) represents (PBS-PLLA)-g-(PLLA-b-PGMA) ₃ -g-PLLA copolymer; (C) represents (PBS-PLLA)-g-(PLLA-b-PGMA) ₃ -g-PBS copolymer; (D) represents PBS-g-(PLLA-b-PGMA) ₃ -g-(PBS-PLLA)-g-(PLLA-b-PGMA) ₃ -g-PLLA copolymer. PLLA-b-PBS-b-PLLA represents PBS-PLLA, g represents graft from (B. Zhang et al., 2017)..... | 36 |
| Figure I.26: TEM images of the PHBV/PBS (80/20) blends with DCP content of (a)0, (b) 0.2, (c) 0.5, (d) 1.0wt% from(Ma, Hristova-Bogaerds et al. 2012)..... | 39 |
| Figure I.27: Impact performance of the ternary blends where P: PLA/S: PBS/T: PBAT and I _x : peroxide content, figure modified from (Wu et al., 2019)..... | 40 |
| Figure I.28: Possible reaction mechanisms for co-polymer formation in the presence of peroxide and TAIC, figure from(Zytner et al., 2020)..... | 41 |
| Figure I.29: Principles of safety assessment applied in EU (a) for the authorization of new substances, (b) for the verification of specific migration limits, (c-d) principles in multimaterials (here a laminate intended to be in contact with food). DFR = Simulant D..... | 51 |
| Figure I.30: Example of the different environments that the packaging will be subjected over the whole manufacturing process in the case of frozen food..... | 53 |
| Figure II.1: Residual Humidity of PHBV and PBSA as a function of drying time..... | 58 |
| Figure II.2: Picture of a SCAMEX batch mixer..... | 59 |
| Figure II.3: Schematic representation of thermo-compression molding machine..... | 64 |
| Figure II.4: Experimental protocol for compression molding..... | 64 |
| Figure II.5: (a) Twin-screw extruder scamex Rheoscam ... D, (b) twin-screw profile, (c) schematic representation of the twin-screw profile..... | 65 |
| Figure II.6: Single screw extrudeur SCAMEX Rheoscam 20mm 11D..... | 67 |
| Figure II.7: Assembly of the single-screw machine with film blowing module..... | 67 |
| Figure II.8: Screw profile for production of PHBV/PBSA masterbatch..... | 68 |
| Figure II.9: Schematic representation of the twin-screw extrusion line 16D. L/D=32:1..... | 68 |
| Figure II.10: Film blowing machine MAPRE/COLLIN..... | 70 |
| Figure II.11: (a) Overview of the film blowing extrusion module and (b) view of the filter holder and 450µm filters..... | 71 |
| Figure II.12: Images of the die head and the spiral mandrel with the magnification of the spiral showing one inlet and one outlet, images kindly provided by Alain Guinault Ph.D. Thesis with modifications..... | 72 |

| | |
|---|-----|
| Figure II.13: Die outlet and blowing ring configuration (extracted from (Laffargue, 2003)) | 73 |
| Figure II.14: Example of bubble shape depending on (a) low cooling rate and (b) high cooling rate, images extracted from (Laffargue, 2003) | 73 |
| Figure II.15: Schematic representation of the different DSC protocols | 78 |
| Figure II.16: Schematic representation of hot sealed bags filled with frozen French fries | 81 |
| Figure III.1 : Schematic representation of the different DSC protocols..... | 89 |
| Figure III.2 : Mechanical spectrum of (a) storage modulus and (b) complex viscosity for neat PHBV, PBSA (inset in (a)), and PHBV/PBSA blends at 185°C after batch mixing. Data were recorded starting with high frequencies. | 91 |
| Figure III.3 : Complex viscosity as a function of PBSA content. The solid line represents the values calculated from the mixing rule | 92 |
| Figure III.4 : SEM images of cryo-fractured neat PHBV, PBSA and PHBV/PBSA blends: (a) neat PHBV,(b) neat PBSA ,(c) 70/30, (d) 50/50, (e) 30/70..... | 93 |
| Figure III.5 : DSC curves of neat PHBV, neat PBSA and PHBV/PBSA blends recorded in the second heating scan following the protocol I..... | 94 |
| Figure III.6 : DSC curves of neat PHBV, neat PBSA and PHBV/PBSA blends aged at (a) -10°C and (b) -40°C | 95 |
| Figure III.7: Non-isothermal crystallization of neat PHBV, neat PBSA, and PHBV/PBSA blends recorded during cooling at -10 °C/min (protocol II) | 96 |
| Figure III.8 : Evolution of (a) the elastic modulus and (b) $\tan\delta$ as function of Temperature for neat PHBV, neat PBSA and PHBV/PBSA blends | 100 |
| Figure III.9 : (a) Typical stress-strain curves of tensile test of PHBV/PBSA blends except neat PBSA and (b) Evolution of the elastic modulus of PHBV/PBSA blends depending on PBSA content (Tensile test measurements)..... | 101 |
| Figure III.10 : (a) Stress-oscillation of PBSA samples during tensile testing and (b) Evolution of the tensile stress of PHBV/PBSA blends with representation of EBM model at different level of interfacial adhesion (A) | 104 |
| Figure IV.1 : Differential scanning calorimetry measurement protocol..... | 127 |
| Figure IV.2: Measurement of torque over time during melt mixing of compatibilized PHBV/PBSA blends at constant weight ratio 70/30 with different content of dicumyl peroxide..... | 130 |
| Figure IV.3: FTIR spectra of a) neat PHBV and neat PBSA in the region 4000-650 cm^{-1} and PHBV/PBSA/DCP blends in the region b) 1800-1600 cm^{-1} and c) 1500-700 cm^{-1} | 132 |
| Figure IV.4: Evolution of the complex viscosity as a function of frequencies resulting from (a) batch mixing and (b) selected formulation from twin-screw extrusion of PHBV/PBSA with varying content of DCP at 185°C | 134 |

| | |
|--|-----|
| Figure IV.5: Cole-Cole plots of PHBV/PBSA 70/30 and the compatibilized PHBV/PBSA blends with dicumyl peroxyde from 0.02 to 1phr (batch mixer) | 135 |
| Figure IV.6: SEM images of cryo-fractured surfaces of compatibilized PHBV/PBSA blends(batch mixer) with different DCP content, (a) 0 phr, (b)0.02 phr, (c) 0.1 phr and (d)0.2 phr..... | 136 |
| Figure IV.7 : Schematic illustration of the location of the observations on the SEM samples after failure of the tensile test..... | 139 |
| Figure IV.8: SEM images of the cross-section after tensile test of compatibilized PHBV/PBSA blends with different DCP content, (a) 0 phr, (b)0.02 phr, (c) 0.1 phr, (d)0.2 phr and f) 1 phr at different localization within sample marked as A and B..... | 140 |
| Figure IV.9: Film blowing of PHBV/PBSA with addition of dicumyl peroxyde (DCP) resulting from in-situ reactive extrusion | 141 |
| Figure IV.10: Evolution of (a) the elastic modulus and (b) elongation at break and (c) stress at break of the different PHBV/PBSA blends in the presence of dicumyl peroxyde with varying experimental temperatures (Tensile test measurements), ⁽¹⁾ Elastic Modulus and stress at break values for neat PHBV and neat PBSA were directly from pellets..... | 143 |
| Figure IV.11: Hot sealed film of PHBV/PBSA + 0.1phr DCP filled with frozen French fries..... | 143 |
| Figure IV.12: Evolution of (a) the elastic modulus and (b) the elongation at break of PHBV/PBSA 70/3+ 0.1 phr DCP in contact with frozen French fries after being stored at -20°C over various period of time (Tensile test measurements) | 144 |
| Figure V.1 : Differential scanning calorimetry measurement protocol..... | 150 |
| Figure V.2: Measurement of torque over time during melt mixing of plasticized and unplasticized PHBV/PBSA/ATBC+ DCP with different ATBC content | 152 |
| Figure V.3: Different scanning calorimetry curves of (a) cooling curves and (b) melting behavior resulting from 2nd heating scan of the plasticized PHBV/PBSA blends with varying ATBC content of 0, 5, 10, 15 and 20 wt % | 154 |
| Figure V.4:Glass transition temperature of the two distinct PHBV and PBSA phases as a function of ATBC with (a) PBSA/ATBC and (b) PHBV/ATBC (DSC measurements). Experimental results (empty symbols) and Fox equation (dashed line) | 155 |
| Figure V.5: Experimental mechanical properties of of the plasticized PHBV/PBSA blends with evolution of (a) elastic modulus and (b) elongation at break with varying ATBC content of 0, 5, 10, 15 wt %..... | 156 |
| Figure V.6: SEM images of the cross-section after tensile test of unplasticized and plasticized PHBV/PBSA/ATBC+DCP with ATBC content of a) 0 wt %, b) 5 wt %, c) 10 wt %, d) 15 wt %, e) 20 wt % | 158 |
| Figure V. 1 : Differential scanning calorimetry measurement protocol..... | 165 |

| | |
|--|-----|
| Figure V.2: Torque evolution with time during melt mixing of PHBV/PBSA blend with or without the addition of ATBC and as a function of Luperox® content, i.e. 0.1 and 0.2 phr | 167 |
| Figure V.3: Different scanning calorimetry curves of a) cooling curves and b) melting behavior resulting from 2nd heating scan of the plasticized and unplasticized PHBV/PBSA blends with varying content of Luperox® | 169 |
| Figure V.4: Evolution of the complex viscosity as function of frequencies of plasticized and unplasticized PHBV/PBSA 70/30+ 0.2 phr Luperox at 185°C, ⁽¹⁾ values taken from previous work (Chapter IV) | 172 |
| Figure V.5: Film blowing of a) unplasticized PHBV/PBSA 70/30+ 0.2 phr Luperox® with BUR of about 2.4 and b) plasticized PHBV/PBSA/ATBC 63/27/10+ 0.2 phr Luperox® with BUR of about 3.8, height of the blow film process is about 180 cm | 173 |
| Figure V.6: Typical stress/strain curves of PHBV-based blends with addition of ATBC at 23 et -20 °C with inset of SEM images of the cross-section after tensile test (23 °C) of (a) unplasticized and (b) plasticized PHBV/PBSA/Luperox | 176 |
| Figure V.7: Hot sealed film of PHBV/PBSA/ATBC 63/27/10 + 0.2 phr luperox filled with 625 g of frozen French fries..... | 177 |
| Figure VI.1: Principles of new ways of valorization of agri-food industries by-products in added value products | 182 |
| Figure VI.2: Chemical structure of amylose and amylopectin figure reproduced from (Niranjana Prabhu & Prashantha, 2018)..... | 184 |
| Figure VI.3: Schematic representation of starch granule ultrastructure, figure modified from (Buléon et al., 1998) | 184 |
| Figure VI.4: Evolution of the elongation and yield at break of potato starch films as function of glycerol content, figure reproduced from (Lourdin et al., 1997)..... | 185 |
| Figure VI.5: Schematic representation of starch process: from native to plasticized starch, figure reproduced from (Avérous, 2004)..... | 186 |
| Figure VI.6: Cellulose repeating unit, figure adapted from (Nechyporchuk et al. 2016)..... | 186 |
| Figure VI.7: Experimental procedure of MCF films using a semiautomatic sheet former, figure reproduced from (Sehaqui et al., 2010)..... | 187 |
| Figure VI.8: Schematic representation of lignin molecules (R. Sun, Lawther, & Banks, 1997)..... | 189 |
| Figure VI.9: The three building blocks of lignin (Chakar & Ragauskas, 2004)..... | 189 |
| Figure VI.10: Chemical structure of hydroxycinnamic acids of A) chlorogenic acid, B) caffeic acid, C) p-coumaric acid, D) ferulic acid, figure modified from (Schieber & Saldaña, 2009) | 190 |
| Figure VI.11: (a) Different edible plant wastes in diverse forms and (b) typical stress-strain curves for pure cellulose (MCC), spinach, parsley, cocoa and rice , images reproduced from (Bayer et al., 2014)..... | 192 |

| | |
|---|-----|
| Figure VI.12: Images of bioplastic films of A) Carrot , B) Parsley, C Radicchio and, D) Cauliflower, image reproduced from (Giovanni Perotto et al., 2018) | 193 |
| Figure VI.13 :Evolution the mechanical properties of carrot-based films as a function of relative humidity, figure reproduced and modified from (G. Perotto et al., 2020)..... | 194 |
| Figure VI.14: Schematic representation of BIOTREM technology, image reproduced from (BIOTREM., 2016) | 195 |
| Figure VI.15: Biochemical analysis work flow..... | 197 |
| Figure VI.16: General diagram of the determination of cellulose/hemicelluloses content with successive hydrolysis using TFA and H ₂ SO ₄ followed by HPLC analysis..... | 199 |
| Figure VI.17: Chromatogram of the molecules determined by HPLC on extractible residue obtained ultrasound assisted extraction..... | 203 |
| Figure VI.18: Schematic representation of a potential extraction and purification process of high value-added molecules implemented a biorefinery type approach..... | 204 |
| Figure VI.19: Appearance of starch: potato peels blend films with addition of glycerol with varying weight ratio a)100:0, b) 80:20, c) 50:50, d) 20:80, e) 0:100, f) 20:80 made from larger scale | 206 |
| Figure VI.20: Experimental results after thermocompression molding for varying weight ratio of starch: potato peels..... | 207 |
| Figure VI.21: Successive steps for fabrication of starch: potato peels items from thermo-compression molding | 208 |
| Figure VI.22: Visual aspects of thermo-compressed items of starch: potato peels upon varying weight ratio with a) 29:71 w/w %, b) 44:54 w/w %, c) 50:50 w/w % and d) 66:33 w/w % | 208 |
| Figure VII.1: Principe de co-production de l'aliment et des composants de l'emballage | 217 |
| Figure VII.2: illustration des différentes températures auxquelles sera soumis l'emballage de sa mise en œuvre par extrusion soufflage de gaine à son application finale pour l'emballage des aliments surgelés.. | 218 |
| Figure VII.3: Evolution de la viscosité complexe du PHBV, PBSA et des mélanges PHBV/PBSA à 185 °C après mélangeur interne. Les données ont été enregistrée en débutant des hautes fréquences. | 220 |
| Figure VII.4: Images MEB des échantillons cryo-fracturés de PHBV, PBSA et mélanges PHBV/PBSA avec: (a) PHBV, (b) PBSA, (c) 70/30, (d) 50/50 et (e) 30/70..... | 221 |
| Figure VII.5: Évolution de la contrainte de traction des mélanges PHBV/PBSA avec représentation du modèle EBM avec différents niveaux d'adhésion interfaciale (A) entre le PHBV et le PBSA | 222 |
| Figure VII.6: Evolution de la viscosité complexe en fonction de la fréquence des mélanges PHBV/PBSA avec différentes teneurs en peroxyde de dicumyle à 185 °C et (b) teneur en gel en fonction de la teneur en peroxyde de dicumyle | 223 |

| | |
|--|-----|
| Figure VII.7: (a) Extrusion soufflage de gain du PHBV/PBSA avec addition de peroxyde de dicumyle après extrusion réactive, évolution de (a) la contrainte maximale et (b) de l'élongation à la rupture des mélanges de PHBV/PBSA en fonction de la teneur en DCP | 224 |
| Figure VII.8: Température de transition vitreuse des phases de (a) PHBV et (b) PBSA en fonction de la teneur en ATBC. Les résultats expérimentaux sont représentés sous forme de symbole tandis que l'équation de Fox est représenté en pointillée | 226 |
| Figure VII.9: Extrusion-soufflage de gaine de la formulation plastifiée PHBV/PBSA/ATBC 63/27/10+ 0.2 phr Luperox® avec un Blow Up Ratio de 3.8, la taille de la bulle est d'environ 180 cm..... | 227 |

List of Tables

| | |
|---|-----|
| Table I.1: Thermo-mechanical properties of different PHBV copolymers: | 22 |
| Table I.2: Thermal-mechanical properties of PBS and its copolymers PBSA (from (Xu & Guo, 2010)) ... | 27 |
| Table I.3: Thermo-mechanical properties of PHBV or PBSA based blend with biodegradable polyester in presence or an organic peroxide | 37 |
| Table I.4: Thermo-mechanical properties of PHBV plasticized with polymeric external plasticizers..... | 45 |
| Table I.5: Test conditions for evaluating overall migration limits | 52 |
| Table II.1: : Thermo-mechanical properties collected from Data Sheet | 57 |
| Table II.2: Chemical formula and molar mass of used additives within the present study | 57 |
| Table II.3: Preliminary experimental procedures of mixing for PHBV/PBSA blends using a batch mixer . | 59 |
| Table II.4: Experimental protocol for physical blends of PHBV/PBSA prepared with batch mixer | 61 |
| Table II.5: Experimental protocol for compatibilized PHBV/PBSA with dicumyl peroxide prepared with batch mixer:..... | 62 |
| Table II.6: Experimental protocol for compatibilized PHBV/PBSA with dicumyl peroxide and ATBC prepared with batch mixer:..... | 62 |
| Table II.7: Compounding experimental design of compatibilized PHBV/PBSA blends with dicumyl peroxide | 65 |
| Table II.8:Blown-film experimental design of compatibilized PHBV/PBSA blends with dicumyl peroxide | 66 |
| Table II.9: : Compounding experimental design of compatibilized PHBV/PBSA blends at semi- pilot scale | 69 |
| Table III.1 : Thermal properties of PHBV/PBSA blends evaluated by DSC from the second heating and cooling scans | 94 |
| Table III.2 : Avrami–Jeziorny parameters during nonisothermal crystallization of neat PHV, neat PBSA, and PHBV/PBSA blends..... | 97 |
| Table III.3 : Liu parameters during nonisothermal crystallization of neat PHBV, neat PBSA and PHBV/PBSA blends..... | 99 |
| Table III.4 : Determination of Storage Modulus E' and Mechanical properties of PHBV/PBSA blends obtained from DMA and tensile test measurements. respectively | 101 |
| Table IV.1: Film blowing parameters | 126 |
| Table IV.2: Melt Flow Index and Gel content of PHBV/PBSA with varying content of DCP as function of implementation process | 133 |

| | |
|--|-----|
| Table IV.3: Thermal properties of neat PHBV, PHBV/PBSA 70/30 and compatibilized PHBV/PBSA blends with different content of dicumyl peroxide evaluated by DSC from the second heating scan and ageing method..... | 137 |
| Table IV.4: Mechanical properties of PHBV/PBSA blends with varying content of DCP obtained from tensile test measurements | 138 |
| Table V.1: Formulations and nomenclature | 149 |
| Table V.2: Gel content of plasticized and unplasticized PHBV-based blends with varying ATBC content | 153 |
| Table V.3: Thermal properties of plasticized PHBV/PBSA blends evaluated by DSC from the second heating and cooling scans | 155 |
| Table V.4: Mechanical properties of plasticized PHBV/PBSA blends obtained from tensile test measurements | 157 |
| Table V.1: Film blowing parameters..... | 164 |
| Table V.2: Gel content of plasticized and unplasticized PHBV/PBSA blends with varying content of Luperox® and compared with plasticized and unplasticized PHBV/PBSA/ATBC+ DCP..... | 168 |
| Table V.3: Thermal properties of plasticized PHBV/PBSA/Luperox blends evaluated by DSC from the second heating and cooling scans..... | 170 |
| Table V.4: Mechanical properties of plasticized and unplasticized PHBV/PBSA blends with addition of either DCP or Luperox obtained from batch mixer, results are obtained from tensile test measurements..... | 171 |
| Table V.5: Mechanical properties of plasticized and unplasticized PHBV/PBSA/Luperox blends obtained from tensile test measurements under both ambient and freezer conditions | 174 |
| Table VI.1: Chemical composition of potato peels | 189 |
| Table VI.2: Mechanical properties for potato peel-based films with addition of external plasticizer..... | 195 |
| Table VI.3: Experimental design for preparation of potato peels:starch blends with glycerol | 201 |
| Table VI.4: Chemical composition of potato peel mass with different extraction methods | 202 |
| Table VI.5: Extraction quantities of phenolic compounds after sonication extraction | 203 |
| Table VII.1: Détermination des propriétés mécaniques des mélanges PHBV/PBSA par tests de traction . | 221 |
| Table VII.2: Tableau synoptique des propriétés de la formulation PHBV/PBSA/ATBC 63/27/10+ 0.2 phr Luperox® obtenu par extrusion gonflage..... | 228 |

General introduction

I.1.Societal and industrial context

Most of the existing and future packaging materials, including bio-based and biodegradable ones, share a common drawback: they are sourced, processed, and used at very different places and rely on globalized supply chains. Each packaged food travels on average three thousand kilometers before reaching our plate, and including transport due to recycling increases the total distance. Energy is required for transportation, purification/cleaning, stabilization (for biodegradable components), and processing. Short supply chains of food have been created in response to a growing demand for the valorization of local resources and the development of local businesses. The central idea is to shorten all supply chains, including the food and the packaging chain of values. When the model is stretched to include food and packaging, it can be translated into transforming the food industry's by-products into material compounds on the same site as the food production lines. The advantages could be multiple for food plants: producing bio-based blends by recycling the energy dissipated by the food operation units (e.g., superheated steam, hot air), valorizing local biomass, reducing waste and effluent treatments, etc. New operation units devoted to material production (blending, processing, fermentation) and compatible with food production standards should be devised in this new framework. The goal of the thesis is to explore materials including by-products from the frying industry and capable of replacing polyethylene for the packaging and distribution of parfried frozen products, such as French fries.

I.2.Roles of food packaging

Food packaging is essential to food production, distribution, retailing, and consumption, as it is designed and used today. It is a necessary waste, but it becomes a useless waste as soon as it loses its original function. Due to environmental concerns and the globalization of food trade, a balance needs to be met between food preservation, convenience, and environmental impacts (Marsh & Bugusu, 2007). Only food safety cannot be compromised and must remain unchanged.

General Introduction

Food packaging plays several roles, listed hereafter.

- **Food transformation.** Vacuum cooking, asepsia (hot or aseptic filling, pasteurization, sterilization), modified atmosphere require sealed and individual packaging to operate. By enabling the standardization and industrialization of food transformation, food packaging reduced costs and fought hunger.
- **Food distribution and retailing.** Primary packaging contains preweighted and identified food, which facilitates its transportation, distribution, and retailing at frozen, chilled, or room temperature. Cooked products such as ready-to-eat meals can also be sold at hot temperatures.
- **Protection and preservation.** Food packaging preserves safety, nutritional and organoleptic quality during storage by preventing external contamination, whatever its origin (biological, microbiological, chemical, physical).
- **Minimizing food waste.** Packaging contributes to extending the shelf-life of the food product and, therefore, reduces food wastes.
- **Consumer information and traceability.** Information supporting traceability, authenticity, nutritional values, and storage conditions are supported by the packaging system and its components (labels, intelligent systems).
- **Convenience.** Facilitating handling, food preparation, and disposal is also an essential role.

Depending on the application and technical specifications (temperature tolerances, processability, printability, food contact type), the selection of materials is critical in food packaging design. Polyolefins, including polyethylene (PE) and isotactic polypropylene (PP), are the most widely used group of thermoplastic materials in food packaging. These commodity polymers combine excellent thermo-mechanical properties, processability, and low price. Their superiority for frozen products can be summarized as follows for low-density polyethylene (LDPE).

- The low glass transition temperature (typically -100°C) grants good ductility at -20°C ;
- Good mechanical properties over an extensive temperature range with high elongation at break, good tear strength, and dart drop over $5\text{ g}/\mu\text{m}$.
- Its highly branched structure creates an extensional viscosity compatible film blowing extrusion.

General Introduction

- It is a low-cost polymer obtained by gaseous polymerization.
- It can be polymerized from bio-based monomers.
- Several grades (i.e., formulation, catalysts, processing aids) have been validated for food contact applications.

PE is, however, highly persistent in the environment and not recycled for food contact. It contributes significantly to marine litter, where it represents the floating fraction. Flexible packaging is essentially single-use. Two strategies can contribute to reducing its impacts on the environment:

- Recycling for the same application or a less technical applications;
- Change to new materials with a lower footprint, such as biodegradable and bio-based polymers

I.3.Current end-of-life treatment of LDPE in France

Low-density polyethylene (LDPE) is the most used thermoplastic polymer regardless of the considered application. Its waste represents an significant input for the recycling industries. However, only industrial PEs are recycled today because they can be collected in relatively pure fractions and are not printed. Recycling post-consumer PE is far more difficult because of sorting issues and the low competitiveness of recycled resins compared to virgin ones. In 2017, only 10 % of PE film put on the French market, *i.e.*, 12,000 tons, were recycled. More post-consumer LDPE will have to be sorted with the new recycling directives coming into force in 2022 (CITEO, 2019). This should increase the amount of post-consumer LDPE recycled. Today in France, only two companies in France are specialized in LDPE recycling. The company *Barbier* recycles high-density polyethylene (HDPE) from industrial sources. *Machaon* is specialized in the recycling of post-consumer LDPE, with a current production capacity of 30,000 tons of recycled LDPE (rLDPE) per year ("Machaon : l'usine de recyclage de demain,").

I.3.1.Technical barriers to post-consumer LDPE recycling

The recycling process of LDPE involves several treatment stages. LDPE materials are sorted and shredded into smaller pieces before being washed and, finally, being regenerated into plastic granules by extrusion. Plastic processors then typically use a mixture of these recycled and virgin granules in varying proportions for their new applications to meet the specifications. However, recycling LDPE is not easy because it needs a thorough cleaning and the difficulty

General Introduction

to separate LDPE from other floating materials ("Machaon : l'usine de recyclage de demain,"). Recycling LDPE for food contact may pose a severe threat to consumers' health, and no viable process has been validated by the European Food Safety Authority. The legal basis for authorizing plastics for food contact is directly by the European Commission, whereas the European parliament manages the legal basis for the Environment.

I.3.2.Legal barriers

Recycled food contact materials as all materials in contact must comply with the European framework regulation (EC) 1935/2004 and offer the same safety as virgin ones. Plastic materials must obey to purity criteria, and only monomers and additives positively listed in the relation (EC) 10/2011 can be used for food contact. The overall migration must be lower than 10 mg/dm² of packaging; additional restrictions (~600) known as specific migration limits and must be verified. The use of non-evaluated substances is accepted if they are not carcinogenic, present behind a functional barrier, and migrate into the food below the standard detection limit of 10 µg/kg of food. The framework regulation (EC) 2023/2006 encourages the industry to set their own good manufacturing practices and paved the way for authorizing recycled plastics. The regulation (EC) 282/2008 confirmed this possibility and imposed any industrial recycling process, mechanical or chemical, to be approved by the European Food Safety Authority (EFSA). EFSA, such as the US FDA, maintains a list of approved processes and the conditions of using recycled materials for food contact (e.g., wet/dry, oily, low or high temperature). The control of the sourcing and quality management procedures are essential to get approval. Post-consumer recycled PE rarely fulfills this condition. Today PE can not be recycled back to food contact materials, except when placed behind a functional layer.

I.3.3.Chemical recycling: existing facilities and perspectives.

Chemical recycling of polyolefins (Rahimi & Garcia, 2017) appears to be the best option for obtaining food-grade recycled LDPE (rLDPE). Chemical recycling of polyethylene generally involves different methods to depolymerize the macromolecular chain to oligomers or its constitutive monomer, ethylene. Thermal cracking leads to the random breakdown of the polymer chain, which results in an oil composed of multiple molecules, which can be refined using existing oil refining techniques. The result is the synthesis of fuels made of alkanes,

General Introduction

alkenes, carbonyl group, aldehyde, and ketones (Serrano, Aguado, & Escola, 2012). It is also possible to reach a high conversion yield up to 80% by thermal cracking with a catalyst (Shah, Jan, Mabood, & Jabeen, 2010). Cracking requires high energy with temperatures ranging between 400°C-900°C. Produced fuels can be used to synthesize several plastics like PE. From a regulatory perspective, recycled monomers are equivalent to virgin ones if they meet purity standards. The expectations are huge, but both the profitability and volumes are not met yet. To our best of knowledge, only one French company, namely LEYGATECH, has received its certification for chemical recycling of polyethylene with food contact approval.

Traceability, risk assessment, and the lack of sellers of rLDPE limit its application for food contact. Theoretically, a lower grade of rLDPE could be tolerated behind a functional barrier. These possibilities are studied jointly by the UMR 0782 SayFood and LNE via their joint technological unit SafeMat (UMT ACTIA 17.09), but for more barrier polymers, such as recycled polyethylene terephthalate, recycled isotactic polypropylene, and recycled high-density polyethylene. Using a functional barrier with fat products even at freezing temperature looks premature and risky for long shelf-life products.

I.4. Thesis context

The PhD thesis takes place in an industrial context that aims to design a bio-based and biodegradable material for flexible food packaging produced with a short supply chain. Frozen products are conditioned in PE bags and are stored under frozen conditions.

Among the candidates, poly(3-hydroxybutyrate-*co*-3-hydroxyvalerate) (PHBV) is one of the most promising by meeting the requirements by being bio-based and biodegradable and with the possibility to be produced from vegetable's by-products. The overall concept of the thesis is summarized in Figure 0.1. It conjugates the design of bio-based and compostable home packaging with the valorization of food industry by-products enrolled in a circular economy.

General Introduction

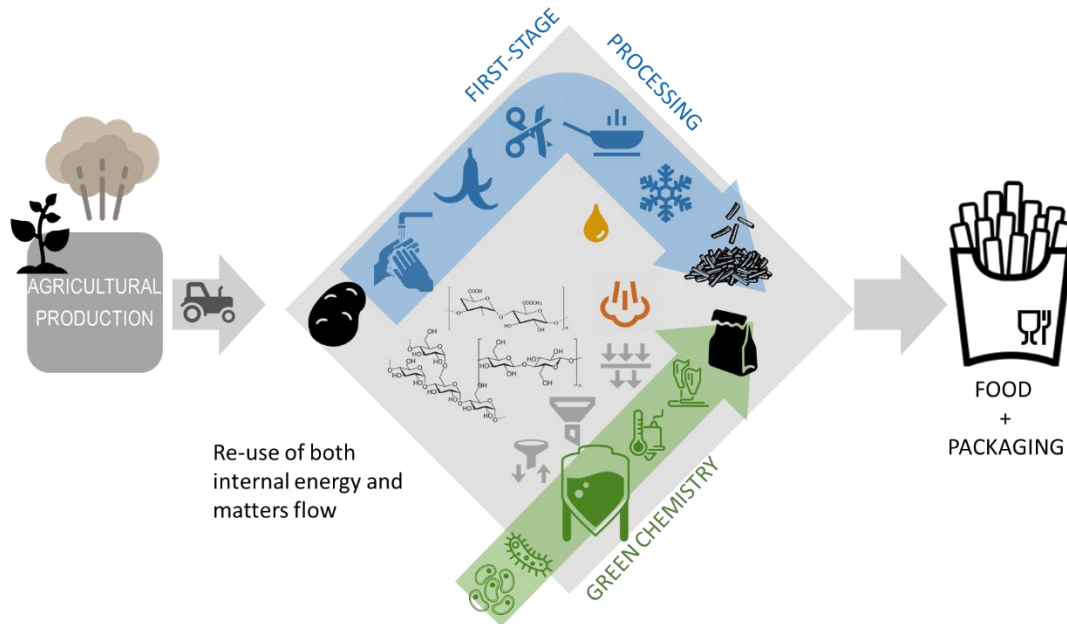


Figure 0.1: Principles of co-production of food and its packaging components

Involved in a circular economy, the ability to synthesize short-chain length polyhydroxyalkanoates (*scl*-PHAs), using by-products of agri-food industries as fermentation substrate, appears as a viable solution. Nowadays, only one type of PHA is largely available, which complies with food contact regulation available on the market, PHBV-3HV. PHBV-3HV meets the two essential requirements by being bio-based and biodegradable, but they miss sufficient mechanical performances to be incorporated in films or laminates. PHBV polymers exhibit, indeed, relatively high stiffness and brittleness. Moreover, PHBV also have a low shear viscosity and melt elastic strength, which impacts their processability negatively in blow extrusion (Anjum et al., 2016; Cunha, Fernandes, Covas, Vicente, & Hilliou, 2016). The modification of their thermo-mechanical properties is enabled by the modulation of their HV content. However, despite the ability to modulate the HV content in PHBV, its thermo-mechanical properties will not fit the severe technical specification required for frozen food packaging application.

I.5. Strategy developed to deliver an alternative to polyethylene packaging

The lack of ductility of PHBV hinders its use as an alternative to polyethylene for flexible packaging. To overcome this drawback, melt blending with the biodegradable aliphatic

General Introduction

polyester, PBSA, was drawn as the main strategy of the present thesis (Chapter III). In this way, internal mixer was used to prepare blends of PHBV and PBSA followed by the evaluation of their properties. This study, was followed by the evaluation of the impact of reactive extrusion through *in-situ* compatibilization. This study was conducted from internal mixer up to the lab-scale validation of the processability by film blowing technology (Chapter IV). Selected formulation was further modified with introduction of a plasticizer (Chapter V, Part I). Finally, scale-up of extrusion film blowing process of the most promising formulations was done followed by analysis of food/packaging interactions: performance and aging under freezer conditions.

Beyond the replacement of polyethylene, development of new materials based on vegetable by-products was investigated (Chapter VI).

Chapter I

Chapter I

I.1. Part I : Background study

I.1.1. Current situation of bio-based and biodegradable polymers

The global annual production capacity of polymers is now 360 Million tons and is almost exclusively based on petrochemical resources. Around 40 % of the annual production is used in short-lived applications, mainly packaging. The combination of mass production of processed food and the short shelf-life of food leads to the environmental impact of single-use plastics used in food packaging applications. The depletion of fossil resources and the generation of persistent pollution due to insufficient collection, reuse, recycling are aggravating factors. Biopolymers have been developed as one of the answers to those issues.

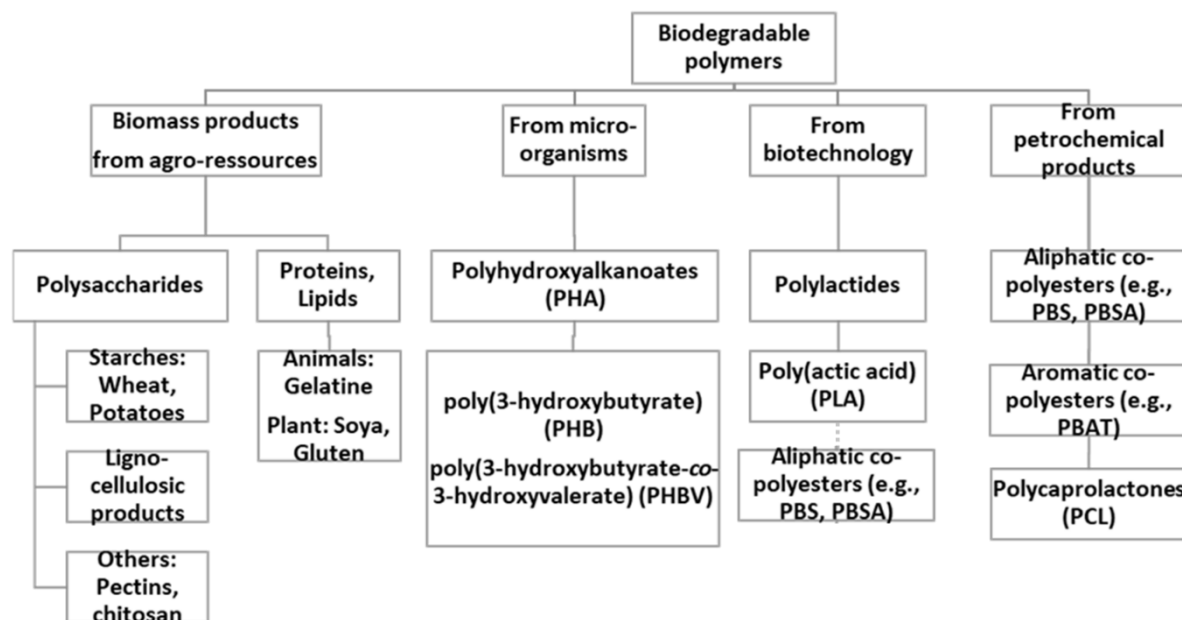


Figure I.1: Classification of biodegradable polymers (reproduced from (Averous & Boquillon, 2004))

Biopolymer is an umbrella term that encloses many polymers that differ depending on their origin and end-of-life behavior (Figure I.1). Most of the developments sought thermoplastic behaviors and commodity products such as food containers. Thermoplastic polymers are broadly used in many areas, from automotive, aeronautic, and building to food containers, due to their good mechanical and barrier properties, processing ease, and low price. The European Bioplastics Association classifies them as biobased (using EN 16760) or biodegradable (EN 13432) or both (Figure I.2). Nowadays, most conventional plastics, e.g. Polyethylene, can be synthesized from renewable resources, making the final product partially or fully bio-based.

Chapter I

Their non-biodegradable character remains, however, unchanged. As a result, increasing their market share will not resolve the pollution of the environment by plastics. Hence, there is a need to replace non-biodegradable plastics with partially or fully bio-based and biodegradable ones. (Averous & Boquillon, 2004) classified biodegradable polymers into four groups:

- agropolymers (e.g., polysaccharides) derived from agro-resources
- polyesters obtained from bacterial fermentation of by-products or sugars (e.g., polyhydroxyalkanoates)
- polyesters obtained by polymerizing monomers derived from biomass (e.g., polylactic acid)
- polyesters synthesized (partly or fully) from fossil fuel resources (e.g., aliphatic or aromatic polyesters)

Alternative thermoplastic materials for food packaging applications are fossil-based or partially bio-based polyesters, which are biodegradable. Without being exhaustive, they include: poly(butylene succinate) (PBS), poly(butylene succinate-co-adipate) (PBSA), and poly(butylene adipate-co-a terephthalate) (PBAT). The best candidates are both bio-based and biodegradable. Starch, Poly(lactic acid) (PLA), or poly(hydroxyalkanoates) (PHA) offer the best perspectives to tackle the environmental challenge (Laycock, Halley, Pratt, Werker, & Lant, 2014).

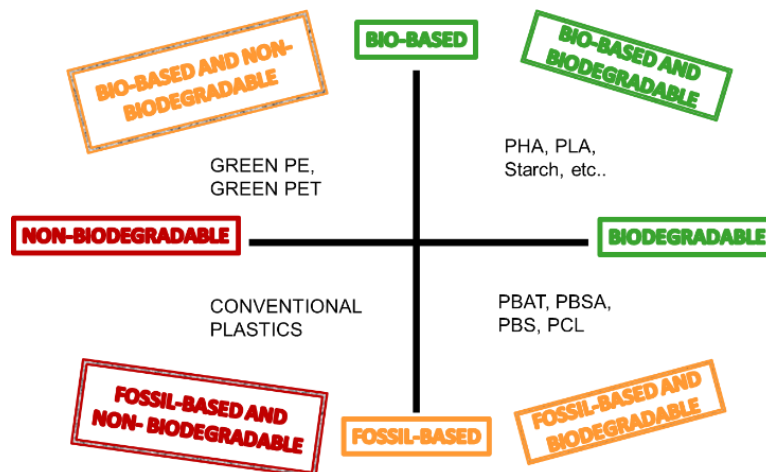


Figure I.2: Classification of thermoplastic polymers based on the origin of their monomers and their biodegradable character

The annual bioplastic production is approximately one percent of the total plastic production, 360 million tonnes/year. The production of bioplastics will grow in the coming years (Figure I.3). Flexible and rigid packaging represent up to 53 % of the global production of bioplastics

Chapter I

(Figure I.4). Flexible packaging has been preferred initially for solid and frozen food products, but its use expands to liquid contents.

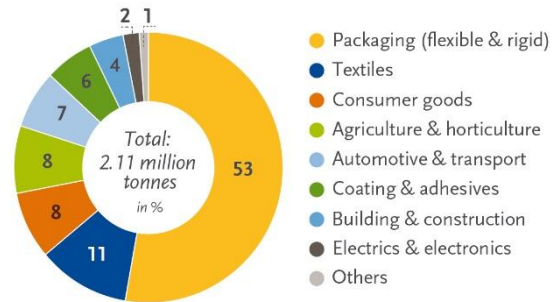
Global production capacities of bioplastics



Source: European Bioplastics, nova-Institute (2019)
More information: www.european-bioplastics.org/market and www.bio-based.eu/markets

Figure I.3: Global production capacities of bioplastics from 2018 to 2024

Global production capacities of bioplastics in 2019 (by market segment)

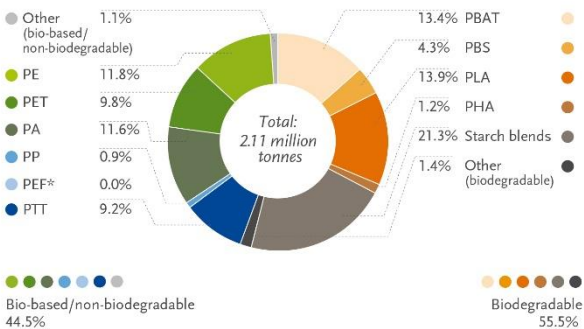


Source: European Bioplastics, nova-Institute (2019). More information: www.european-bioplastics.org/market and www.bio-based.eu/markets

Figure I.4: Global production capacities of bioplastics in 2019 (by market segment)

Fifty percent of the global production capacities of bioplastics are devoted to bio-based and biodegradable plastics. Figure I.5 shows that polyesters dominate with PBAT, PBS, PLA, and PHA. In 2019, polyhydroxyalkanoates represented only 1.2% of bioplastics, but their increasing production is anticipated in the next five years, as shown in Figure I.6.

Global production capacities of bioplastics 2019 (by material type)

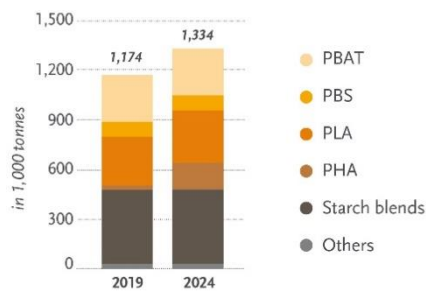


*PEF is currently in development and predicted to be available in commercial scale in 2023.

Source: European Bioplastics, nova-Institute (2019)
More information: www.european-bioplastics.org/market and www.bio-based.eu/markets

Figure I.5: Global production capacities of bioplastics in 2019 (by material type)

Biodegradable bioplastics 2019 vs. 2024



Source: European Bioplastics, nova-Institute (2019)
More information: www.european-bioplastics.org/market and www.bio-based.eu/markets

Figure I.6: Biodegradable plastic 2019 vs. 2024

Chapter I

Key points

Because most polymers' durability extends well beyond food shelf-life and their service time, their wastes cause significant environmental pollution when their collection and end-of-life are not managed adequately (Verghese, Lewis, Lockrey, & Williams, 2015). Alternative biobased and biodegradable materials offer credible food packaging alternatives, especially when combined with short and optimized food supply chains (Peelman et al., 2013). Flexible packaging for frozen, fresh, and chilled foods are dominated today by polyolefins, making them an excellent target for substitution by biobased and biodegradable polymers. Agri-food industries will be prone to replace petroleum-based plastics with bio-based and/or biodegradable ones. The transition will be rapid if the alternative materials have the same food contact suitability and similar processability during calendaring, printing, package filling, sealing, etc. Changing the format, packaging system and adapting the conditions will require more profound changes in the food industry.

I.1.2. Alternative packaging: customer poll

Replacing polyethylene layers in laminates with bio-based and biodegradable materials would reduce the environmental impact of flexible packaging. The new packaging system needs to be compatible with its process and storage conditions (e.g., oily contact and freezing temperature for parfried frozen products) and accepted by consumers. New regulations in Europe call for the phasing out of single-use plastics and, as a result, the acceleration of the adoption of environmentally friendly plastic materials. The anti-waste law AGECE 2020 (LOI n° 2020-105 du 10 février 2020 relative à la lutte contre le gaspillage et à l'économie circulaire) and Directive SUP (Directive (EU) 2019/904) set minimum amounts of recycled materials. The more general mention of compostable has replaced the biodegradable ones, but by emphasizing that all packaging materials, including biodegradable ones, should also be recyclable. Agro-food industries shifted their R&D programs to find alternatives to their conventional packaging. In order to understand what consumers are expecting from food industries and support the initiative of replacing polyethylene in frozen food products, a consumer poll was realized during this thesis.

I.1.2.1. Methodology

The poll was drafted and validated within a preliminary study before being deployed. It aims at determining whether consumers are ready to accept alternative packaging, either recyclable or bio-based and biodegradable.

Chapter I

I.1.2.1.1. Preliminary study

The preliminary study involved 20 people with various socio-demographic profiles. They were interviewed for 15 to 45 minutes. The proportions of gender, age, type, and location of their housing, diplomas, and professional activities were balanced. The answers were used to optimize the final survey, prepared as “Google forms.”

I.1.2.1.2. Consumer poll

The questionnaire contained 41 questions and was organized as funnel questions starting from consumption habits and focusing on frozen food products to specific packaging questions. It was divided into five parts: consumption habits, responsible consumption and Corporate Social Responsibility, sorting of household waste and packaging recycling, alternative solutions, and information about the respondent. The poll was sent on social media. It targeted frozen food consumers and received 401 answers. Respondents were mainly between the ages of 18 and 50, lived in families, and had college degrees. It showed a slight deviation compared to INSEE information (INSEE, 14/01/2020).

Motivation of purchase

More than 70 % of respondents bought frozen products at least once a month, and 55.4 % of them bought potato products (Figure I.7). Consumers well perceived frozen foods. For people buying frozen potato products, quality and pleasure were the most prominent criteria for choosing between two products. Asked about packaging, 44 % of respondents declared that it was not important for their purchase behavior (Figure I.8).

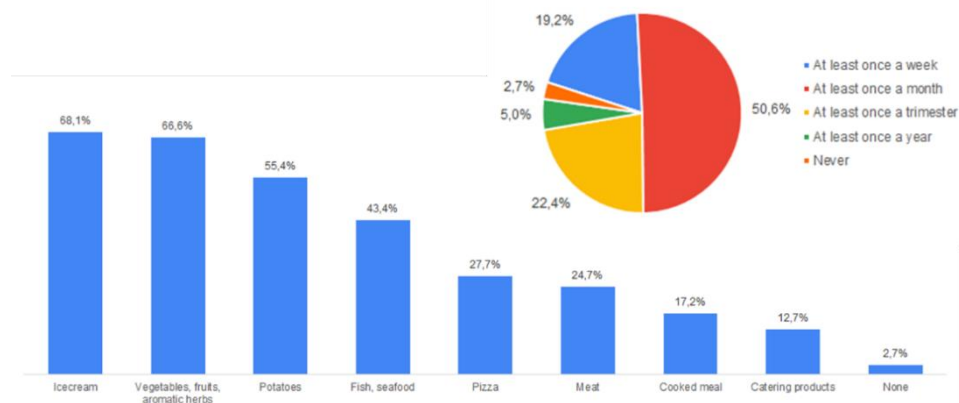


Figure I.7: Consumption habits with focus on frozen food

Chapter I

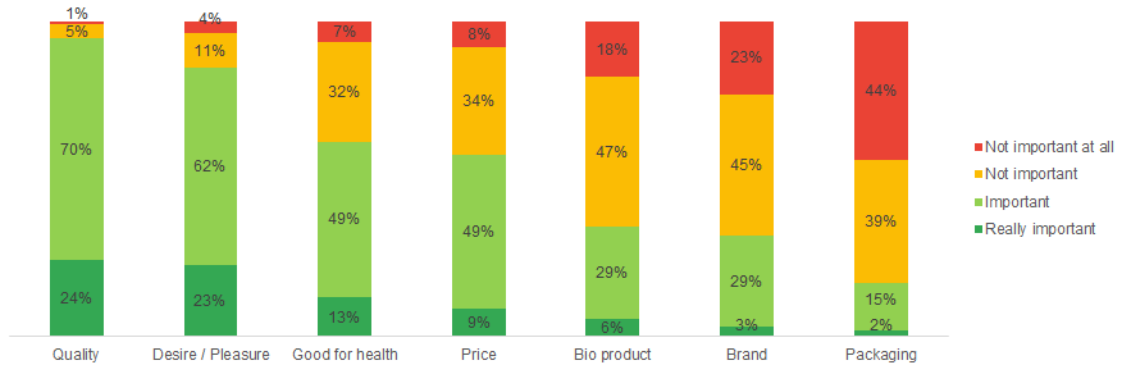


Figure I.8: Selection criteria between brands on the frozen potato products (215 answers)

Place of the packaging in the purchase intention

Specifically, Figure I.9 shows that the absence of overwrapping was important for more than 70 % of respondents. Overwrapping was often perceived not to bring added value to the customer experience. In contrast, the importance given to the proper material of the packaging, the touch, and the visual appearance were declared not to be decisive criteria for product selection.

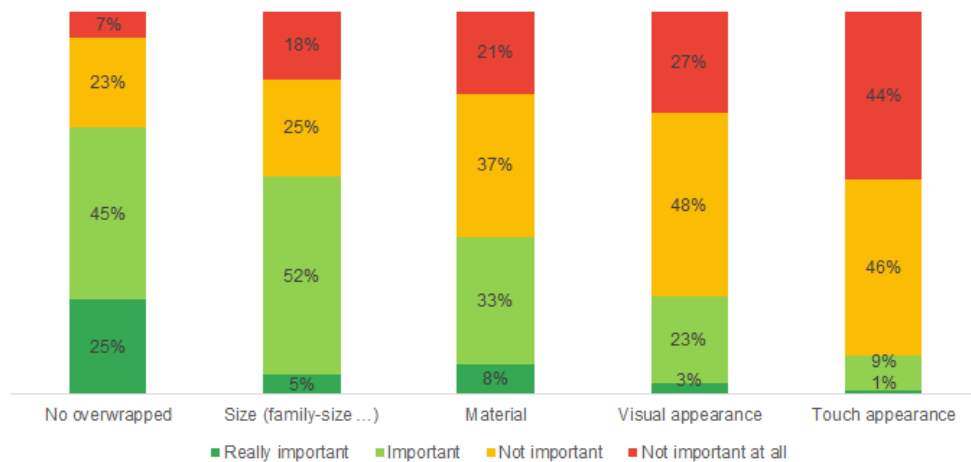


Figure I.9: Importance of packaging features (214 answers)

Awareness on bio-based and biodegradable packaging

The information printed on bio-based and biodegradable packaging may significantly influence consumer awareness of the environment. The lack of standards and the multiplicity of logos and labels may, however, blur the message. The understanding of different logos was tested by asking the responder to choose the proper definition from a list of different formulations. Figure I.10 shows that only one logo was correctly understood: the Tidy man. For all the others, less

Chapter I

than half of consumers chose the proper definition. The Triman, the green dot, and the biodegradable logo were the most frequently misinterpreted logos. The compostable logo was partly understood, but “biodegradable” and “compostable” were confused. However, in the 81,3% of incomplete answers, “compostable” was rightly identified from its logo. Authorities have already recognized this problem, and the French anti-waste law will ban the mention of “biodegradable” by 2022 and will replace by the “compostable” one.

Poorly identified logos may generate sorting errors. Educating consumers and good practices of logo use are of great importance for efficient waste collection and to prevent packaging materials from being wrongly released in nature because they are thought biodegradable when they are only compostable.

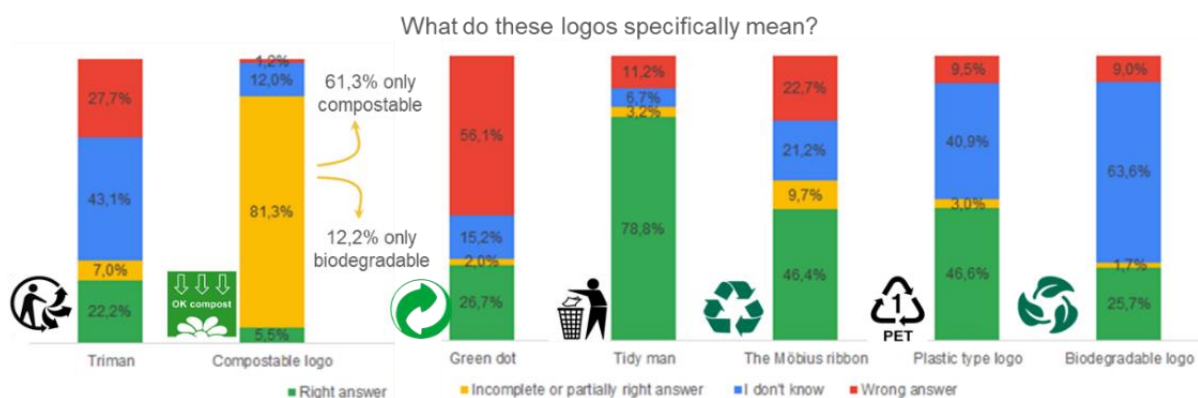


Figure I.10: Awareness of consumers on the meaning of logos for sorting packaging

Packaging placement for frozen products was tested by proposing a list of multiple choices: replacing a fossile packaging with a bio-sourced one, a non-recyclable with a recyclable one, non-recyclable by a compostable, and finally a recyclable by a compostable. Figure I.10 highlight that two preferences emerged from the proposed alternatives. Replacing non-recyclable materials with either recyclable or compostable packaging systems retained most of the approbation of consumers. Preferences for eco-friendly packaging was in line with the new SUP directive. Interestingly, the use of recyclable or compostable materials seemed to have almost equal acceptance. Changing a packaging from a recyclable to a biodegradable one obtained only 52 % of approbation (Figure I.11).

Chapter I

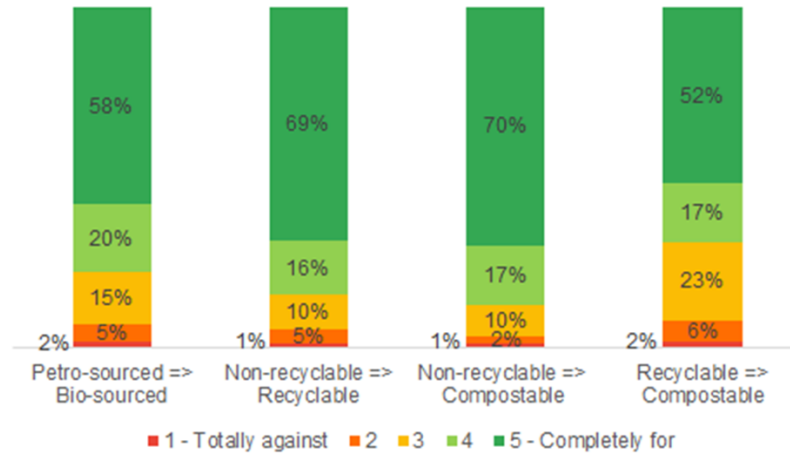


Figure I.11: Replacing conventional packaging with recycled or bio-based and biodegradable packaging

Figure I.8 and Figure I.9 show that the packaging alone is not enough to decide which product will be preferably bought. For comparable products proposed in different packagings, the visual appearance and the touch are decisive (Figure I.12). These perceptions outweigh environmental considerations. The mate and brown packaging depicted in Figure I.12 (number 1) is preferred whatever if the packaging is recycled or biodegradable. The choice may be unconscious, and 20% of respondents did not have any preference.



Figure I.12: Selection of a packaging based on the material, touch and visual appearance for a recycled or a bio-based and biodegradable packaging

The lack of composters by households may explain the equal appreciation packaging for compostable and recyclable packaging (Figure I.13). In addition, there is no specific system or procedure for sorting compostable packaging from non-compostable ones. The French anti-

Chapter I

waste law enforces compostable systems to be also recyclable to encourage closed loops and avoid energy and material wastes

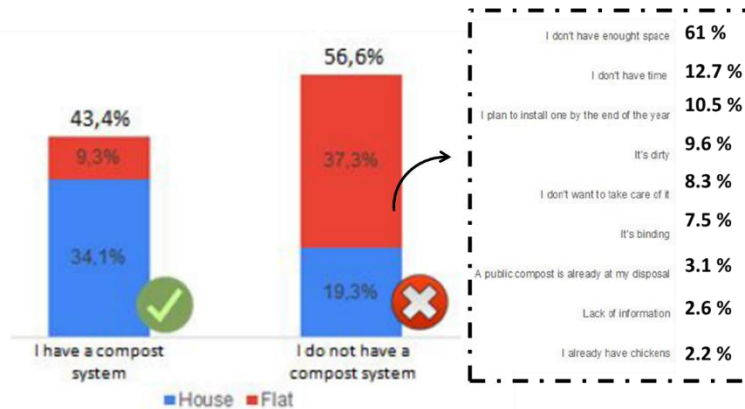


Figure I.13: Presence of a home compost for vegetable waste sorting

Key points

By addressing the replacement of flexible packaging by more sustainable alternatives, this work contributes to the European Green Deal ((Comission, 2021)) goals: “boost the efficient use of resources by moving to a clean, circular economy; restore biodiversity and cut pollution.” Since up to 80% of products’ environmental impacts are determined at the design phase the thesis explores the possibilities offered by current biodegradable polymers and investigates their ability to use for mass production and distribution of parfried frozen products. Freezing and oily contact conditions are rarely reported in the literature but are essential to envisage the substitution of polyethylene. The following section reviews the main properties of biodegradable polymers

I.2. Part II : Literature review

Adapted from (Le Delliou, Vitrac, & Domenek, 2020)

I.2.1. Polyhydroxyalkanoates

I.2.1.1. Introduction on PHAs

Polyhydroxyalkanoates (PHAs), discovered in the 1920s by Maurice Lemoigne, are fully biodegradable thermoplastic polyesters produced by microorganisms as carbon and energy storage compounds in the presence of excess carbon and limited macronutrients, such as oxygen, nitrogen, or phosphorus. Depending on the number of carbons of the monomer unit, they can be classified into short-chain or medium-chain length PHAs. The most prominent group is short-chain-length PHAs, mainly represented poly(3-hydroxybutyrate) P(3HB) and the copolymer P(3HB-co-3HV) (Figure I.14) (Laycock et al., 2014; Pakalapati, Chang, Show, Arumugasamy, & Lan, 2018).

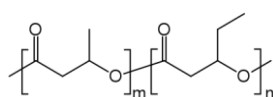


Figure I.14: Chemical structure of PHBV

The general fabrication process consists of a two-step fermentation, where the first step consists in the microbial growth until obtaining high cell densities and the second step in macronutrient limitation to trigger PHA production and intracellular accumulation. The downstream processing consists of breaking down the microbial cells to liberate the PHA granules and their purification by solvent or surfactant-based extraction techniques. This process is relatively cost-intensive as compared to standard polymer synthesis. Apart from the costs linked to downstream and purification, degrees of freedom for cost reduction are the type of fermentation, pure or mixed cultures, and the choice of fermentation substrates (pure sugars, byproducts, wastes) (Laycock et al., 2014; Pakalapati et al., 2018).

The pure culture process in sterile conditions of P(3HB) was first patented in 1959 by W.R. Grace and Company (Baptist, 1965). This process is still in use, and the few commercially available PHAs grade are synthesized *via* pure culture fermentation using, in most cases *Cupriavidus necator*. PHA production based on mixed cultures offers a viable solution with decreased processing costs because microbial consortia are stable without aseptic conditions

Chapter I

(Laycock et al., 2014). Synthesis of PHAs in mixed cultures was first observed in 1974 in wastewater treatment plants designed for biological phosphorus removal (Wallen & Rohwedder, 1974). An additional advantage is that mixed cultures can adapt to various complex feedstocks, opening the door for cost reductions using agricultural by-products.

I.2.1.2. Use of agricultural byproducts for PHA production

Production of PHA requires the use of a carbon source as fermentation substrate. However, the cost of the carbon source dramatically contributes to the overall cost of PHA production and can be as high as 40 % of the total operating cost (Leong et al., 2017; Posada, Naranjo, Lopez, Higuera, & Cardona, 2011). Using carbon sources from waste or by-products of agriculture and the food industry is an appealing solution for cost reduction. Furthermore, revalorization of wastes is a possibility to step towards a more circular economy. The change of the carbon source can have a significant impact on the productivity of the microbial culture. A trade-off needs to be reached between the cost of fermentation substrates and PHA productivity. This topic has consequently received considerable industrial and academic interest. For example, (Kumar, Ray, & Kalia, 2016) used four types of food industry wastes, including hydrolysates of pea-shell, apple pomace, potato peels, and onion peels. They were tested for PHA production individually or mixed with different pea-shell ratios. The authors found that all hydrolysates were suitable for the growth and PHA production by *B. cereus* EGU43 and *B. thuringiensis* EGU45. Biowaste combinations allowed to achieve high PHA yield. The combination of potato peels and pea-shell achieved the highest PHB yield but depended on the PS:PP ratio where pea-shell: potato peels 1:2 and 2:1 produced 20 and 405 mg/L of PHB, respectively. The addition of glucose effectively enhanced PHB yield but varied upon pea-shell: potato peels ratio from 485 to 335 mg/L at 1:2+1% glucose supplementation and 2:1+1%G, respectively. In another example, wastewater from different fruits and vegetables processing plants was used as carbon sources for PHBV with very high HV content (up to 35 mol%) (Elain et al., 2016) (Lemechko, Le Fellic, & Bruzard, 2019).

Vegetable oils represent another inexpensive carbon source to produce PHAs at a lower cost than a carbon source of high purity. Their interest as feedstock is linked to their chemical composition, including esters of glycerin and high concentration of monocarboxylic acids. Olive oil, corn oil, and palm oil are reported to produce the homo-poly(3-hydroxybutyrate) using *Cupriavidus necator* H16 (Fukui & Doi, 1998). Virgin and waste sesame oil could be successfully used as a carbon source for PHBV production by *C. necator* H16 (Taniguchi,

Chapter I

Kagotani, & Kimura, 2003). Similarly, waste frying oil could be used to synthesize PHB with homopolymer concentration similar to PHBV from glucose (Verlinden et al., 2011).

Another promising way to obtain PHAs at a lower cost comes from microalgae. Microalgae are part of a heterogeneous group of microorganisms, photosynthetic, eukaryotic or prokaryotic, and gram-negative (Olaizola, 2003). Their photosynthetic behavior offers the ability to use light as source of energy and inorganic nutrients for growth and to synthesize valuable compounds. Species, culture conditions, and extraction methods still need to be defined to take full advantage of microalgae as a viable source to produce PHAs (Costa, Miranda, De Moraes, Costa, & Druzian, 2019).

I.2.1.3. Physical-chemical properties of PHAs

PHAs are rubbery materials at room temperature (glass transition temperature, T_g , of PHB is typically 5 °C), wherefore they are in literature often compared to polyolefins. Even if the tensile strength of PHBV is comparable to the yield stress to polypropylene (PP), ca. 25 MPa, or polyethylene (PE) at ca. 35 MPa and 25 MPa, respectively (Lopez-Manchado, Valentini, Biagiotti, & Kenny, 2005; Vaccaro, DiBenedetto, & Huang, 1997). However, the elongation at break is largely inferior (elongation of break typically 400 % for PP and 600-700 % for LDPE), (Table I.1). Typically, PHBVs attain less than 5 % of maximum elongation, which makes them extremely brittle materials. Also, their impact strength is low, fracture propagating readily through the material. The reason is most likely the occurrence of very large spherulites with poor coupling between crystalline and amorphous phases. The use of nucleating agents for decreasing spherulite sizes was shown to be a successful means for slightly increasing mechanical properties (Laycock et al., 2014). Moreover, physical aging kinetics is fast, bringing about rapid embrittlement of the polymers. The embrittlement is favored by cold crystallization of PHA, because their cold crystallization temperature is near room temperature (Gérard, 2013). The most commonly used PHBV, contains 3 mol% HV and shows a Young Modulus of about 2.9 GPa, a tensile strength of 38 MPa and very poor elongation at break of about 3 %. The thermo-mechanical properties of PHBV can be tuned by increasing the percentage of HV in PHBV copolymer (Anjum et al., 2016), but even at high 3HV ratios, the polymer remains relatively brittle (Table I.1). Several authors have already discussed that the brittle behavior of PHBV can be caused by i) the cold crystallization of the amorphous phase at ambient temperature, ii) glass transition temperature close to room temperature, and iii) radial or circumferential cracks potentially contained in spherulites of PHBV with low content of 3HV

Chapter I

(Barham & Keller, 1986; El-Hadi, Schnabel, Straube, Müller, & Henning, 2002). The existence of these cracks is supposed to be caused by the difference in the thermal expansion coefficients of the material along the radius and the circumference of crystallites, which generates drastic internal stresses. (Laycock et al., 2014)

PHBV has a narrow processing window furthermore and degrades rapidly upon melting. Earlier works (Grassie, Murray, & Holmes, 1984a, 1984b, 1984c) show that thermal degradation of PHBV results from chain scission, which occurs from the six-membered ring ester decomposition process as represented in Figure I.15. The authors have shown that the main by-products resulting from thermal degradation are crotonic acid and its oligomers. PHBV also has a low shear viscosity and melt elastic strength, impacting their processability negatively in blow extrusion (Anjum et al., 2016; Cunha et al., 2016). This is strongly limiting the industrial application because most flexible packaging and thin films are obtained by blow extrusion.

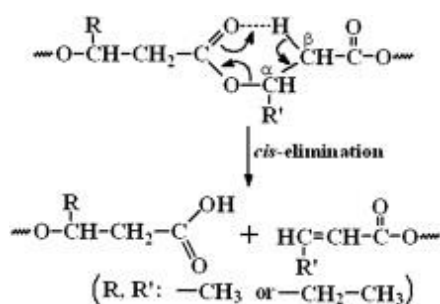


Figure I.15: General mechanism of thermal degradation of PHBV, from (Q.-S. Liu, Zhu, Wu, & Qin, 2009)

Table I.1: Thermo-mechanical properties of different PHBV copolymers:

| Polymer | 3HV content (mol%) | Young Modulus (GPa) | Tensile strength (MPa) | Elongation at break % | T _m (°C) | T _g (°C) | Reference |
|---------------|--------------------|---------------------|------------------------|-----------------------|---------------------|---------------------|--|
| P(3HB) | 0 | 3.5-4 | 40 | 3-8 | 173-180 | 5-8 | (Anjum et al., 2016) |
| P3(HB-co-3HV) | 3 | 2.6 | 32 | 3.5 | 167 | N/A | (Corre, Bruzaud, Audic, & Grohens, 2012) |
| | 9 | 1.9 | 37 | N/A | 162 | N/A | (Anjum et al., 2016) |
| | 15 | 0.5 | 11 | 9 | 142 | -5 | (Lemechko et al., 2019) |
| | 35 | 0.04 | 1.2 | 13 | 150 | -12 | |

I.2.1.4. Blown Film Extrusion

Thermoplastic polymers can be processed via different modalities, including thermoforming, cast extrusion, injection molding, or film blowing extrusion. For flexible packaging, blowing extrusion process is preferred due to its ease of implementation. However, several specifications need to be fulfilled, including melt strength, linear and extensional viscosity and crystallization kinetic.

Blown film extrusion is one of the most-used processes to produce flexible polymer films at an industrial scale. In the film extrusion process, an extruder melts and conveys the polymer to a ring die. In the present case, a ring die is used. The tube formed at the end of the die is stretched using pinch rolls, as shown in Figure I.16. The pinch roll speed allows controlling the longitudinal stretching of the film.

While the film is stretched, inflating air is injected via a hole located in the middle of the die. It leads to the formation of a bubble. When the wanted dimension of the bubble is reached, the air supply is closed. A constant volume of air is trapped.

Thanks to the film blowing extrusion process, bi-axial stretching is induced in the film. Hence, a longitudinal contribution is introduced by the pinch rolls and a transverse one by inflating. The bubble is cooled by a cooling ring which conveys cooled air on the outer side of the film. Hence, crystallization temperature is reached, and the polymer self-solidifies. The position where it happens is designated as the Frost line Height. Above it, the diameter and the thickness of the film are constant (Eric, 2010).

Two parameters allow to characterize the bi-axial stretching undergone by the film:

- The Take-Up Ratio (TUR) defines the longitudinal stretching of the film induced by the pinch rolls:

$$\text{Take - Up Ratio (TUR)} = (\text{Die gap}/\text{Film thickness})/BUR, \quad \text{Eq. I.1}$$

where R and R_0 are the duct and punch radius, respectively. Eq. I.1 defines the longitudinal stretching of the film induced by the pinch rolls:

- The Blow Up Ration (BUR) represents the transverse stretching induced by the inflated bubble: which characterizes the ratio between the radius at the freeze line and the initial ratio with:

$$BUR = \frac{R_f}{R_0} \quad \text{Eq. I.2}$$

Where R_f and R_0 represent the ratio between the radius at the freeze line and the initial ratio, respectively.

Chapter I

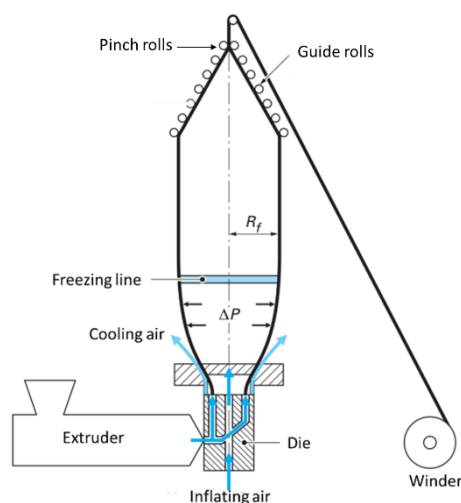


Figure I.16: .Schematic representation of a blown film molding extruder. Picture adapted from (Eric, 2010)

I.2.1.4.1. Film blowing of PHBV

The film blowing technique requires high melt strength and extensional viscosity, while PHBV exhibits both low shear viscosity and elastic melt strength (Cunha et al., 2016). Very few studies reported successful film blowing of PHBV blends (Cunha et al., 2016; Jandas, Mohanty, & Nayak, 2013; S. Sun, Liu, Ji, Hou, & Dong, 2017; Teixeira, Covas, Suarez, Angulo, & Hilliou, 2020). For neat PHBV, film blowing was found unfeasible due to the lack of melt strength (Cunha, Fernandes, Covas, Vicente, & Hilliou, 2015; Teixeira et al., 2020). (Teixeira et al., 2020). In another attempt, extrusion-blowing was achieved using PHB modified with the addition of an organic peroxide. The film exhibited improved melt strength as evidenced by its ability to be blown, but the bubble showed a lack of stability.

The ability to conduct film blowing experiments was driven by two strategies. The first strategy relies on melt blending with another polymer. Film blowing of PLA/PHB with the addition of maleic anhydride as a reactive compatibilizer was successfully achieved (Jandas et al., 2013). The best results were obtained for PLA/PHB/MA 70/30/7 resulting from maleic anhydride acting as bridging unit among PLA and PHB macromolecules through dipole-dipole or intermolecular hydrogen bonding. Blends of hydroxypropyl di-starch phosphate (HPDSP) and poly(3-hydroxybutyrate-co-4-hydroxybutyrate) (P3H4HB) were analyzed by (S. Sun et al., 2017). Although successful film blowing, elongation at break of the film was found impacted when PHA was added at ca. 36 % because of lack of compatibility. (Cunha et al., 2016) produced PHBV/PBAT films by film blowing using either a blend structure or a co-extruded

Chapter I

multilayer structure. The second strategy relies on the addition of a sacrificial layer in a bi-layer coextrusion process. In this way, (Teixeira et al., 2020) successfully produced co-extruded PHBV/PBAT films using either DCP or a multifunctional epoxide styrene-acrylic oligomeric chain extender (CE) with PBAT as an external layer.

Key points

- PHBV need to be blended with another material and is not the major polymer in the extruded film
- Above 50 wt % PHBV, the inclusion of a sacrificial layer is necessary

I.2.1.5. Conclusion

The promise to diminish the environmental footprint of packaging imparts new bio-based and biodegradable thermoplastic material. Among them, PHBV, which is commercially available, complies with the promise of being bio-based and biodegradable. With the potential to produce PHBV from food by-products or vegetable waste. Agri-food industries could position themselves strongly on this new polymer by being at the same time user but also the producer of these emerging home compostable polymers. Moreover, this approach fits perfectly with the French anti-waste law. However, from a material point of view, tremendous challenges need to be overcome to reach large-scale production towards flexible packaging. PHBV polymers exhibit, indeed, relatively high stiffness and brittleness while their lack of melt strength and premature degradation imparts their processability. In this way, three strategies have emerged to improve material properties. The first strategy relies on melt blending with another polyester without sacrificing its bio-based and biodegradable character. While being processed from the film blowing process for large-scale production, the developed material must comply with packaging application for fresh, chilled, and frozen food. Therefore, the selected polymer should be highly ductile to counterbalance the mechanical properties of PHBV but also have a low T_g with the expectation to broaden PHBV's glass transition temperature towards lower temperatures. PBSA shows high ductility, low T_g , and excellent rheological properties and has already been shown that the addition of PBSA within PLA can exhibit strain hardening behavior, making it more suitable for film blowing (Eslami & Kamal, 2013b).

I.2.2. Polybutylene succinate-co-adipate

The blending strategy requires a second, ductile polymer. Among the biodegradable plastics suitable for replacing conventional thermoplastic polymer, poly(butylene succinate) (PBS) and its copolymers are great candidates by being partially or fully bio-based and biodegradable. They show excellent biodegradability, thermoplastic properties, and mechanical properties. One of the most promising copolymer is poly(butylene succinate-co-adipate) (PBSA), with the general formula shown in Figure I.17. This is argued from its ability to be fully bio-based, home compostable, highly ductile over a large temperature thanks to its low T_g and its lower degree of crystallinity (Xu & Guo, 2010).

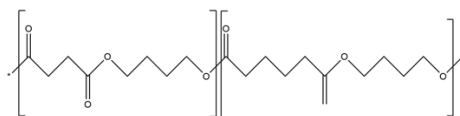


Figure I.17: Chemical structure of PBSA

Poly(butylene succinate-co-adipate) is synthesized from 1,4-butanediol, succinic acid, and adipic acid monomers through successive steps of esterification and polycondensation (Xu & Guo, 2010). Moreover, PBSA can be fully bio-based since its monomers can be obtained from renewable resources, i.e., succinic acid from bacteria fermentation (Song & Lee, 2006), adipic acid derived from lignin (Vardon et al., 2015), or 1,4-Butanediol from a strain of *Escherichia coli* (Yim et al., 2011).

I.2.2.1. Physical-chemical properties of PBSA

What makes PBSA interesting compared to PBS is that the butylene adipate unit (BA), which can self-crystallized, remains in the amorphous state when integrated with low proportion in copolymer PBSA. Consequently, the addition of butylene adipate units results in the depression of the overall degree of crystallinity (Ren et al., 2005). Table I.2 summarizes the thermomechanical of PBS and its copolymers PBSA. For BA content between 5 and 15 mol%, crystallinity degree is higher than that of PBS. However, at 20 mol% tensile strength, T_m and crystallinity degree are decreased, and elongation at break is increased compared to PBS. For food packaging films, the higher elongation at break of PBSA and its lower T_g (-45°C) makes PBSA superior to PBS. In addition, the lower crystallinity of PBSA compared to PBS accelerates its biodegradation (Tserki, Matzinos, Pavlidou, Vachliotis, & Panayiotou, 2006).

Chapter I

Table I.2: Thermal-mechanical properties of PBS and its copolymers PBSA (from (Xu & Guo, 2010))

| | Tensile strength (MPa) | Elongation at break (%) | T _m (°C) | T _g (°C) | Crystallinity degree χ (%) |
|---------|------------------------|-------------------------|---------------------|---------------------|---------------------------------|
| PBS | 35 | 85 | 112 | -18 | 61.1 |
| PBSA-5 | 46 | 155 | 108 | -21 | 87 |
| PBSA-10 | 32 | 145 | 103 | -23 | 65.7 |
| PBSA-15 | 25 | 320 | 99 | -27 | 72.3 |
| PBSA-20 | 21 | 185 | 92 | -34 | 53.9 |

I.2.3.Polymer blends

I.2.3.1.Morphology of polymer blends

Polymer blends appear as an efficient strategy to develop new and tailor-made materials by a combination of their properties in a synergetic way. The most important feature of binary (or more) blends is the organization of immiscible phases. Polymer blends can exhibit miscibility, complete phase separation, or various level of mixing (Robeson, 2007).

I.2.3.1.1.Miscibility

Miscibility returns to a thermodynamic notion and is expressed as the free energy of mixing, which reads:

$$\Delta G_m = \Delta H_m - T\Delta S_m \quad \text{Eq. I.3}$$

Where: ΔG_m is the free energy of mixing, ΔH_m the enthalpy of mixing, ΔS_m the entropy of mixing and T the temperature

For miscible polymer blends, the free energy of mixing must verify $\Delta G_m < 0$. For high molecular weight polymers, the entropy of mixing ΔS_m is small and can be neglected so that ΔG_m is dominated by ΔH_m . In general, ΔH_m is positive (endothermic), but in the presence of two interacting polymers (e.g., involving multiple hydrogen bonds), the mixture can be exothermic. Exothermic mixing has been reported for several miscible polymer blends such as poly(ethylene oxide) (PEO)/ poly(methyl methacrylate) (PMMA) (Colby, 1989) or polyisoprene (PI)/poly(vinylethylene) (PVE) (Roland & Ngai, 1991). Further evidence of miscibility in polymer blends comes from a single composition-dependent glass transition temperature (Lu & Weiss, 1992).

I.2.3.1.2. Partially miscible or immiscible polymer blends

Most of the polymers are non-miscible, and this will lead to phase separation resulting in different blend morphology depending on blend composition (Figure I.18). In general, a droplet-in-matrix morphology is depicted when either polymer A or polymer B are in majority. Droplets of the less concentrated polymer are dispersed in the matrix of the major constituent. Except when polymer ratios are getting closer, a threshold will be reached, leading to a co-continuous phase morphology until phase inversion.

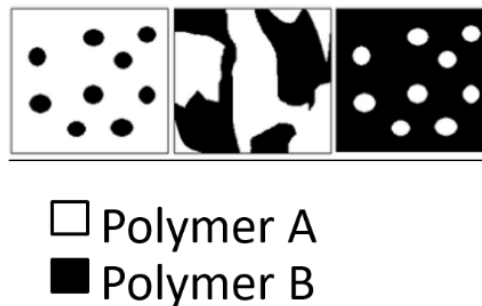


Figure I.18: Evolution of blend morphology between two immiscible polymers depending on blend ratio, figured modified from (Landreau, 2008)

The developed nodule size in a droplet-in-matrix morphology is dependent on viscosity, interfacial properties, blend ratio, and processing conditions (Koning, Van Duin, Pagnouille, & Jerome, 1998). The final morphology of the dispersed phase results from an equilibrium between two mechanisms comprising droplet break-up, which causes droplet size reduction and coalescence which causes an increase in droplet size.

Droplet break up

First studies on droplet break-up were conducted by Taylor (Taylor, 1932, 1934), who studied the deformation and rupture of Newtonian drops dispersed in a Newtonian fluid. Droplet deformation results from an equilibrium between interfacial tension forces, which tend to maintain the spherical shape of the droplet, and shear forces which tend to elongate the droplets, respectively. As a result, the ratio between both forces is defined by the Capillary number:

$$Ca = \frac{\eta_m \dot{\gamma} R}{\sigma_{AB}}, \quad \text{Eq. I.4}$$

where η_m is the matrix viscosity, R droplet radius and σ_{AB} the interfacial tension.

Chapter I

Introducing a critical value of Capillary number, Ca^* different cases can be established: i) considering $Ca < Ca^*$, then the initial spherical shape of the droplet will deform towards the flow direction but will not break, ii) for $Ca > Ca^*$, droplets can break following two modes as shown in Figure I.19:

- If $Ca > Ca^*$, simple break-up occurs and an extended drop is split into two droplets
- If $Ca \gg Ca^*$, Rayleigh break-up occurs, and highly extended fiber breaks into a much larger number of droplets.

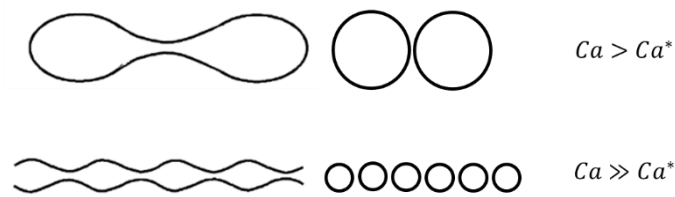


Figure I.19: Breakup mechanisms (i) into two droplets and (ii) strip of droplets) from Rayleigh instabilities

The theory by Taylor (Taylor, 1932, 1934) enables to estimate the smallest possible diameter D , when $Ca = Ca^*$. However, this theory is only valid for viscosity ratios lower than 2.5. (Grace†, 1982) showed that for the break-up of Newtonian droplets in stationary flow, Ca^* depends only on the type of flow, either simple shear or extensional flow, and the viscosity ratio $\lambda = \frac{\eta_d}{\eta_m}$ (where η_d is the viscosity of the dispersed phase). In simple shear flow, droplet break-up becomes impossible as soon as $\lambda > 4$. While for extensional flow, breakage remains possible over the entire range of the viscosity ratio.

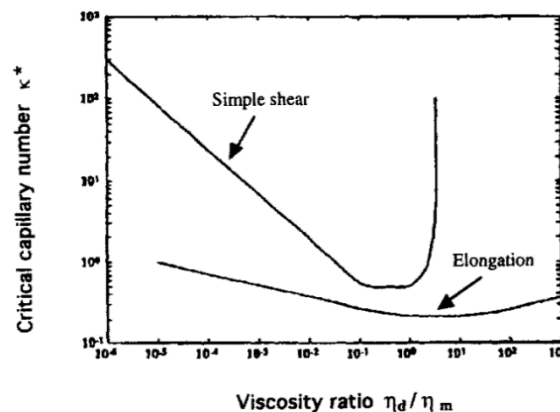


Figure I.20: Critical capillary number as a function of viscosity ratio (Grace† 1982)

Chapter I

Droplet coalescence

The second mechanism that influences the developed morphology and which acts as the opposite of breakup is coalescence. The equilibrium between breakage and coalescence phenomena determines the morphology of immiscible polymer blends. Coalescence is the fusion of two distinct droplets by rupture of the interfacial film between them, as shown in Figure I.21. It has to be considered that contact time between both drops should be sufficient to allow flow-out of the interfacial matrix film situated in-between.

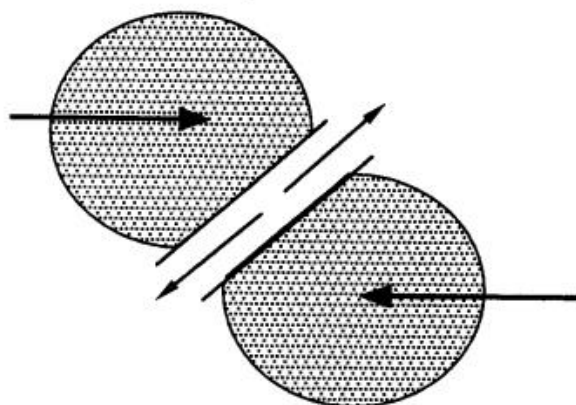


Figure I.21: Coalescence mechanism (Delamare & Vergnes, 1996)

I.2.3.2. Evaluation of affinity in binary polymer blends

The structure and related properties in polymer blends can be scrutinized with a broad spectrum of techniques.

I.2.3.2.1. Evaluation of thermal properties

The thermal properties can be influenced by the affinity between both polymers. The glass transition temperature, T_g , which is characteristic of the amorphous phase of polymers, depends on the miscibility level between polymers. Its value can be assessed from various methods, including differential scanning calorimetry (DSC), dynamic mechanical analysis (DMA), or dielectric analysis. Figure I.22 illustrates the different configurations that may happen from blending and characterized from evolution $\tan \delta$ as a function of temperature. For a single phase blend, only one T_g will be observed (Lu & Weiss, 1992).

On the contrary, an immiscible blend displays two distinct T_g with values of neat constituents. Finally, a median behavior can be observed in partially miscible blends exists. T_g shifts or broadens inwards or towards one component.

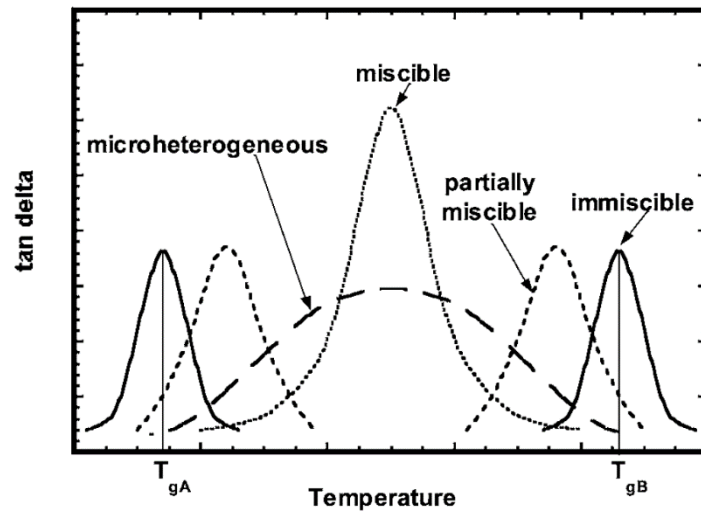


Figure I.22: Evolution of $\tan \delta$ vs Temperature for various types of polymer blends, figure reproduced from (Robeson, 2007)

I.2.3.2.2. Evaluation of the mechanical properties

The second parameter that must be considered is the mechanical properties of the blends in comparison with unblended constituents. The development of toughened polymers through blending is of great interest when one polymer such as PHBV is stiff and brittle. The use of a ductile material is expected to improve the toughness of the overall material. The mechanical properties can be characterized through tensile or Charpy impact test, which will give the stress-strain behavior and the toughness/impact strength, respectively. Miscible blends often show an enhancement in modulus and strength over unblended constituents due to specific interactions between both polymers. It could also be possible to find a positive synergistic effect on mechanical properties between immiscible blends but often exhibit poor tensile strength and impact strength (Robeson, 2007).

For immiscible blends, various models can be employed to predict the resulting mechanical properties. Elastic modulus can be modeled with the Reuss (parallel resistances), Voigt (serial resistances):

| | | |
|--|-------------------------------------|---------|
| | $E^n = \phi_1 E_1^n + \phi_2 E_2^n$ | Eq. I.5 |
|--|-------------------------------------|---------|

where E_1 and E_2 are the elastic modulus of phase 1 and 2, ϕ_1 and ϕ_2 the volume fraction of phase 1 and phase 2, and exponent n characterizes the type of model with $n=1$ (Parallel or Reuss model) or $n=-1$ (Series or Voigt model)

Chapter I

Another model which combines parallel and series models has been developed by Kolarik (Kolarik, 1996) and called the equivalent box model (EBM).

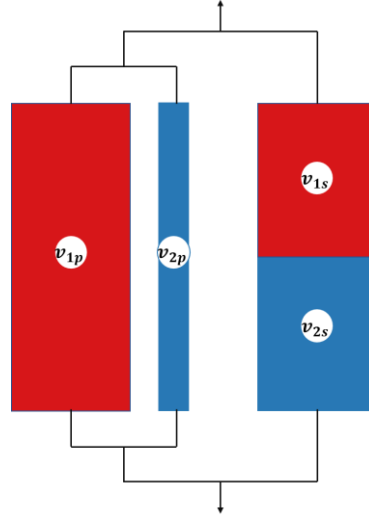


Figure I.23: Schematic representation of an equivalent box model (EBM) for a binary blend

EBM involves two-volume fractions, one acting in parallel and the other one in series (Figure I.23). (Kolarik, 1996) The EBM model is a two-parameter model, as of four-volume fraction v_{ij} , only two are independent (Phua, Pegoretti, Araujo, & Ishak, 2015). The fractions are linked as follows:

$$\begin{aligned} v_p &= v_{1p} + v_{2p} & v_s &= v_{1s} + v_{2s} \\ v_1 &= v_{1p} + v_{1s} & v_2 &= v_{2p} + v_{2s} \end{aligned} \quad \text{Eq. I.6}$$

$$v_1 + v_2 = v_p + v_s = 1$$

where v_p and v_s are the total volume fractions of the parallel branch and series branch, respectively.

The tensile moduli of the parallel (E_p) and series (E_s) branches of the EBM reads:

$$E_p = \frac{E_1 v_{1p} + E_2 v_{2p}}{v_p} \quad E_s = \frac{v_s}{\frac{v_{1s}}{E_1} + \frac{v_{2s}}{E_2}} \quad \text{Eq. I.7}$$

where E_1 and E_2 are the Young's moduli of phases 1 and 2, respectively.

The resulting tensile modulus of two components blend (E_b) is then given as the sum $E_p v_p + E_s v_s$ (Kolarik, 1996):

$$E_b = E_1 v_{1p} + E_2 v_{2p} + v_s^2 \left(\frac{v_{1s}}{E_1} + \frac{v_{2s}}{E_2} \right) \quad \text{Eq. I.8}$$

The main issue comes from the evaluation of v_{ij} . From percolation theory, (De Gennes, 1976) the contribution of one component is negligible and gives:

$$E_{1b} = E_0 (v_1 - v_{1cr})^q \quad \text{Eq. I.9}$$

Chapter I

where E_0 is a constant, q is the critical exponent, which assumes a value of 11/6 for a three-dimensional lattice (De Gennes, 1976).

From experimental results (De Gennes, 1976; Lyngaae-Jorgensen, Kuta, Sondergaard, & Poulsen, 1993), it has been shown that Eq. I.9 can plausibly fit the experimental data for blends in the range $v_{1cr} < v_1 < 1$ (where $E_1 \gg E_2$) so that the modulus of the neat component 1 can be expressed as follows:

$$E_1 = E_0(v_1 - v_{1cr})^{q_1} \quad \text{Eq. I.10}$$

Which gives:

$$E_{1b} = E_1[v_1 - v_{1cr}]/(1 - v_{1cr})^{q_1} \quad \text{Eq. I.11}$$

Based on the percolation theory, where the assumption that the contribution of the second component can be negligible when $E_1 \gg E_2$, the contribution $E_2 v_{2p}$ of component 2, which is coupled in parallel, and the contribution of the whole series branch to the EBM's modulus are negligible compared to the contribution of the $E_1 v_{1p}$ of component 1. Consequently, $E_1 v_{1p}$ (or $E_2 v_{2p}$ for $E_2 \gg E_1$) can be set equal to the apparent modulus E_{1b} (or E_{2b} for $E_2 \gg E_1$) where:

$$E_{1b} = E_1 v_{1p} \quad E_{2b} = E_2 v_{2p} \quad \text{Eq. I.12}$$

Hence, combining Eq. I.10 and Eq. I.11 gives:

$$v_{1p} = \left[\frac{v_1 - v_{1cr}}{(1 - v_{1cr})} \right]^{q_1} \quad v_{2p} = \left[\frac{v_2 - v_{2cr}}{(1 - v_{2cr})} \right]^{q_2} \quad \text{Eq. I.13}$$

In the marginal zone, *i.e.* $0 < v_1 < v_{1cr}$ (or $0 < v_2 < v_{2cr}$), it can be set for the minority component that $v_{1p}=0$ and $v_{1s}=v_1$ (or $v_{2p}=0$ and $v_{2s}=v_2$).

For discrete domains of spherical form, the percolation threshold can be set to $v_{1cr} = v_{2cr} = 0.156$. (Kolarik, 1996; L. A. Utracki, 1991) Most experimental values of q are located in the interval 1.6-2 so that $q = 1.8$ can be used as an average value. (Phua et al., 2015)

Moreover, the strength can be estimated from Eq. I.14 (Kolařík, 1996)

$$S_b = S_1 v_{1p} + S_2 v_{2p} + A S_2 v_s \quad \text{Eq. I.14}$$

Where $S_1 > S_2$, S_1 and S_2 are the strength of phase 1 and 2, respectively. While A can be identified as level of interfacial bonding.

Chapter I

Two limiting values of S_b can be identified with lower and upper bound where $A=0$ or 1 depending on the level of interfacial adhesion, either very weak or strong enough to transmit the acting stress between constituents. Consequently, for $A=0$, the series branch does not contribute and resulting S_b is equal to the sum of contributions of the parallel element. While for $A=1$, contribution of series branch is added to that of the parallel branch. (Kolarik, 1996; Phua et al., 2015)

I.2.3.3. Formulation and blending of PHAs with polyesters and PLA

I.2.3.3.1. Design of PHBV and PBSA with biodegradable polyesters

Different studies were already published describing the efficiency of the melt blending strategy to improve the mechanical performance of PHBV. In particular, the blending of PHAs with poly(lactide), PLA, has received strong interest because of commercial applications of PLA. Blends were tested for the biomedical field (He et al., 2014; Shabna, Saranya, Malathi, Shenbagarathai, & Madhavan, 2014), for mulch films (Dharmalingam et al., 2015), for textiles (Szuman, Krucinska, Bogun, & Draczynski, 2016), and technical applications such as packaging (Boufarguine, Guinault, Miquelard-Garnier, & Sollogoub, 2013; Martelli et al., 2012; Tri, Domenek, Guinault, & Sollogoub, 2013; I. Zembouai et al., 2014). The interest of using immiscible blends between PLA and PHB or PHBV is that the PHA can accelerate crystallization kinetics of PLA (Tri et al., 2013) and increase the elongation at break typically up to 40 % (T. Gerard, Budtova, Podshivalov, & Bronnikov, 2014; Modi, Koelling, & Vodovotz, 2013). Ternary blends of PLA, PHBV, and PBS afforded a good stiffness-toughness balance by improving the toughness and flexibility of PLA (K. Zhang, Mohanty, & Misra, 2012). The failure mode changed from brittle fracture of the neat PLA to ductile behavior. In that study, there was partial miscibility between PHBV and PLA but limited compatibility of both polymers with PBSA. The authors suggested that the optimum performances were obtained for a composition PHBV/PLA/PBSA of 60/30/10 (K. Zhang et al., 2012). (Phua et al., 2015) studied the blends of PHBV and PBS obtained from melt-blending. They found that despite that both polymers were immiscible, the moduli of the PBS/PHBV blends were significantly enhanced compared to that of the neat PBS. While the elongation at break of the blends was higher than the value of neat PHB, blending could mitigate their less desirable properties.

I.2.3.3.2. Compatibilization of PHBV and PBSA-based blends

To overcome the negative effects induced by immiscible polymer blends, compatibilization is usually used to improve the mechanical properties due to enhanced interfacial adhesion, which helps stress transfer across the interface. Moreover, the morphology will tend to structures with decreased nodule size by preventing coalescence between particles, as illustrated in Figure I.24. Immiscible polymer blends can be compatibilized either by *ex-situ*/non-reactive or *in-situ*/reactive compatibilization strategies.

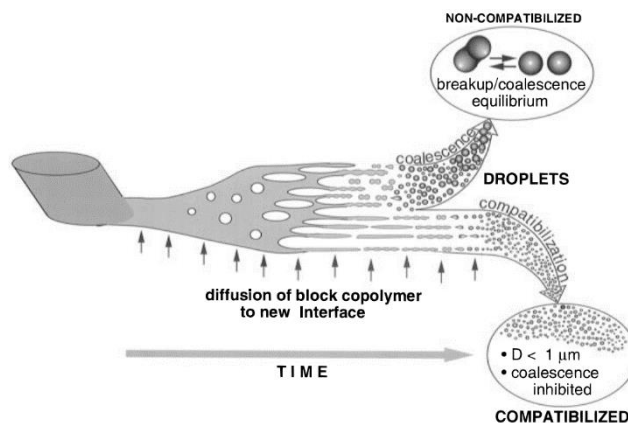


Figure I.24: Schematic of morphology development during melt blending. As pellets or powder of the minor phase soften, layers peel off. These stretch out into sheets which break up into fibers and then droplets from (Macosko et al., 1996)

Ex-situ compatibilization can be obtained by the use of a block copolymer based on the fact that one block can be miscible with one blended component, while the second block will be miscible with the second one. *Ex-situ* compatibilization involves the synthesis of the copolymer with proper functionality and melt-blending of the copolymer with the immiscible blend (Muthuraj, Misra, & Mohanty, 2018). For example, (B. Zhang, Sun, Bian, Li, & Chen, 2017) prepared poly(L-lactide)/poly(butylene succinate) (PLLA/PBS) blends via melt-mixing with a di-block, PBS(25%)-PLLA block copolymer, and a chain extender triarm block copolymer (PLLA-*block*-poly(glycidyl methacrylates))₃ (PLLA-*b*-PGMA)₃. They found that with copolymerization and *in-situ* reactive compatibilization, PLLA/PBS/PBS-PLLA/(PLLA-*b*-PGMA)₃ blends not only improved the toughness but also improved the melt strength. The mechanism is schematically illustrated in Figure I.25.

Chapter I

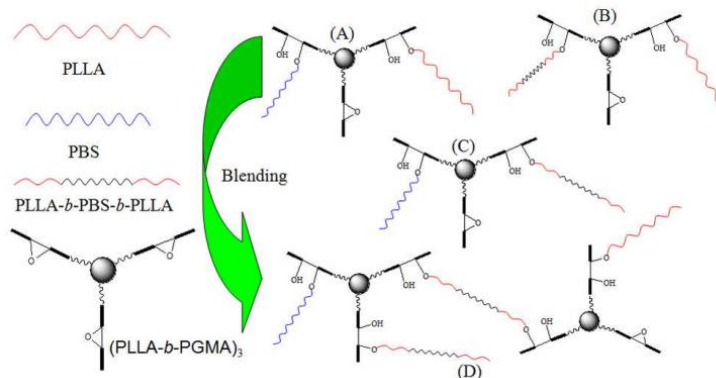


Figure I.25: Schematic illustrations of *in situ* reactive blending of PBS-PLLA, PLLA, PBS in the melt in the presence of (PLLA-*b*-PGMA)₃: (A) represents PBS-*g*-(PLLA-*b*-PGMA)₃-*g*-PLLA copolymer; (B) represents (PBS-PLLA)-*g*-(PLLA-*b*-PGMA)₃-*g*-PLLA copolymer; (C) represents (PBS-PLLA)-*g*-(PLLA-*b*-PGMA)₃-*g*-PBS copolymer; (D) represents PBS-*g*-(PLLA-*b*-PGMA)₃-*g*-(PBS-PLLA)-*g*-(PLLA-*b*-PGMA)₃-*g*-PLLA copolymer. PLLA-*b*-PBS-*b*-PLLA represents PBS-PLLA, *g* represents graft from (B. Zhang et al., 2017)

The second strategy to compatibilize immiscible blends uses *in-situ* compatibilization. This method uses a component that contains a reactive functional group (i.e., anhydride, epoxy, etc.) that will react with blend constituents. Reactive compatibilization can use (i) trans-reactions, (ii) reactive formation of graft or lightly crosslinked copolymer, or (iii) ionically bonded structures, for example. The conditions for reactive processing require that: (i) sufficient dispersive and distributive mixing, (ii) presence of a reactive functionality, (iii) sufficient reaction rate, (iv) stability of the formed chemical structures, and (v) stability of the morphology (Leszek A. Utracki, 2002).

From literature, several studies on *in-situ* compatibilization between biodegradable polymer blends have been selected and results are gathered in Table I.3. The following table reports on the thermo-mechanical properties of PHBV or PBSA based blend with biodegradable polyester in presence of either a chain extender or an organic peroxide.

The addition of chain extenders, which are low-molecular-weight multifunctional compounds, can be useful. The chain extension reaction can maintain or increase the molecular weight of the polymers by reconnecting the chains. Therefore, this strategy can enhance the thermo-mechanical properties and particularly the melt strength. (Eslami & Kamal, 2013a) have melt-blended PLA with PBSA with a ratio 70:30 with and without a multifunctional chain extender (CESA). They have shown that the blends containing chain extender exhibited strong melt strain-hardening behavior, whereas the blends without CESA showed weak strain-hardening. Adding PBSA enhanced the ductility of the blend, but CESA was not affecting the modulus and elongation at break. Pure PLA exhibited a strain at break of less than 10% while the blend PLA/PBSA 70/30 an elongation at break up to 250%.

Chapter I

1 **Table I.3: Thermo-mechanical properties of PHBV or PBSA based blend with biodegradable polyester in presence or an organic peroxide**

| Sample | Blend Ratio | Compatibilizer content | Process | Tg(°C) | Tm (°C) | Xc (%) | E (GPa) | Strain at break (%) | Stress at break (MPa) | Impact strength (kJ/m ²) | Ref. | | | | | | |
|---------------|-------------|------------------------|-------------------------|----------------------------|---------------------------|--------|----------|---------------------|-----------------------|--------------------------------------|--|-----------|-------|------|------|------|---------|
| P3(HB-co-3HV) | | | Injection moulding | N/A | 167 | 62.3 | 2.624 | 32.2 | 3.5 | | (Corre et al., 2012) | | | | | | |
| PLA/PBSA | 70/30 | dry blend | Batch mixer | n.d | | | 2 | 250 | 45 | | (Eslami & Kamal, 2013a) | | | | | | |
| | | 2 wt% CESA | | | | | 2 | 225 | 40 | | | | | | | | |
| PLA/PBSA | 90/10 | dry blend | Batch mixer | <i>T_{cc}</i> (°C) | <i>T_m</i> (°C) | 24.30 | 3.3* | 50* | 1100* | 21.5±2.1 | (Ojijo & Ray, 2015) | | | | | | |
| | | 0.3 wt% Joncryl | | 59.2 | 117.6 | | | | | | | 148.5 | 23.33 | 2.9* | 140* | 100* | 6.2±0.4 |
| | | 0.6 wt% Joncryl | | 58.5 | 117.5 | | | | | | | 148.0 | 16.66 | 2.8* | 120* | 95* | 6.4±0.3 |
| | | 1 wt% Joncryl | | 59.3 | 122.0 | | | | | | | 148.1 | 15.30 | 2.6* | 135* | 90* | 7.2±1.1 |
| | 80/20 | dry blend | | 58.9 | 115.5 | 146.1 | 23.90 | 3.7* | 90* | 120* | | 12.8±0.5 | | | | | |
| | | 0.3 wt% | | 58.7 | 119.3 | 149.1 | 20.19 | 3.1* | 195* | 100* | | 13.7±3.8 | | | | | |
| | | 0.6 wt% | | 58.4 | 120.5 | 147.8 | 14.77 | 2.7* | 180* | 92.5* | | 20.5±8.7 | | | | | |
| | | 1 wt% | | 58.5 | 121.6 | 146.9 | 15.61 | 2.2* | 200* | 77.5* | | 13.3±7.7 | | | | | |
| | 70/30 | dry blend | | 59.1 | 117.7 | 145.8 | 23.27 | 3.4* | 40* | 127.5* | | 13±1.3 | | | | | |
| | | 0.3 wt% | | 58.6 | 120.2 | 149.0 | 18.23 | 3.3* | 160* | 107.5* | | 18.2±4.0 | | | | | |
| | | 0.6 wt% | | 58.8 | 118.6 | 146.0 | 18.51 | 3* | 150* | 100* | | 20.2±3.3 | | | | | |
| | | 1 wt% | | 58.5 | 121.0 | 148.1 | 17.38 | 2.4* | 180* | 90* | | 19.2±3.0 | | | | | |
| | 60/40 | dry blend | | 59.2 | 111.6 | 144.7 | 19.41 | 3.4* | 30* | 127.5* | | 9.8±0.4 | | | | | |
| | | 0.3 wt% | | 57.7 | 122.2 | 149.2 | 19.22 | 3* | 70* | 115* | | 22.8±2.7 | | | | | |
| | | 0.6 wt% | | 58.8 | 120.1 | 147.4 | 12.35 | 2.7* | 140* | 95* | | 38.4±11.9 | | | | | |
| | | 1 wt% | | 58.5 | 122.4 | 146.8 | 15.57 | 2.4* | 150* | 80* | | 34.7±4.8 | | | | | |
| PHBV/PBS | 80/20 | 0 wt% DCP | Batch mixer | n.d | n.d | n.d | n.d | 8 | 25 | 2.8 | (P. M. Ma, D. G. Hristova-Bogaerds, P. J. Lemstra, Y. Zhang, & S. F. Wang, 2012) | | | | | | |
| | | 0.2 wt% DCP | | | | | | 200 | 29 | 3 | | | | | | | |
| | | 0.5 wt% DCP | | | | | | 400 | 28 | 5 | | | | | | | |
| | | 1 wt% DCP | | | | | | 350 | 27 | 5.5 | | | | | | | |
| PHB/PBS | 80/20 | 0 wt% DCP | TSE+ Injection moulding | n.d | n.d | n.d | n.d | 2 | 37 | 1.5 | | | | | | | |
| | | 0.5 wt% DCP | | | | | | 4 | 40 | 3.5 | | | | | | | |
| | 0 wt% | 2 | | | | | | 33 | 3 | | | | | | | | |
| | 0.5 wt% | 11 | | | | | | 38 | 4 | | | | | | | | |
| | 0 wt% | 4 | | | | | | 34 | 3 | | | | | | | | |
| | 0.5 wt% | 15 | | | | | | 37 | 5.5 | | | | | | | | |

2

Chapter I

| Sample | Blend Ratio | Compatibilizer content | | Process | Tg(°C) | Tm (°C) | | Xc (%) | | E (GPa) | Strain at break (%) | Stress at break (MPa) | Impact strength (kJ/m ²) | Ref. | |
|-----------------------------|----------------|------------------------|------------|-------------------------------|--------------|----------------------------|-------|-------------|------------|--------------|---------------------|-----------------------|--|--------------------------------------|---------------|
| | | | | | | | | | | | | | | | |
| PHBV/PBAT/ENR | 50/35/15 | 0 wt% DCP | | Micro TSE+ Micro injection | n.d | 148.1 | 166.3 | 24 | | 0.4 | 350 | 13 | Non break | (K. Zhang, Misra, & Mohanty, 2014) | |
| | | 0.3 wt% DCP | | | n.d | 146.4 | 165.8 | 25.5 | | 0.37 | 325 | 16 | Non break | | |
| PHBV/PCL | 80/20 | 0 phr | | Micro TSE+ injection | n.d | See article (DSC curve) | | PHBV | PCL | 2.984± 0.256 | 6.7±1.1 | 37.3± 0.9 | 28± 2.8 J/m | (Zytner, Wu, Misra, & Mohanty, 2020) | |
| | | 77.2 (0.9) | 28.7 (0.4) | | | | | | | | | | | | |
| | | 78.2 (1) | 29.8 (0.8) | | 3.114± 0.145 | | | 6± 0.8 | 39.2± 0.8 | | | | | | 25.4± 2.6 J/m |
| | | 77.6 (0.8) | 28.9 (1.2) | | 3.114± 0.260 | | | 5.3± 1 | 37.2± 1.6 | | | | | | 22.4± 2.2 J/m |
| | | 77.1 (3.5) | 28.5 (3.2) | | 2.358± 0.107 | | | 15.2± 1.6 | 38.9± 0.3 | | | | | | 26.1± 3.3 J/m |
| | | 71.8 (1.2) | 32.1 (1.4) | | 2.121± 0.101 | | | 25.3± 7.8 | 36.6± 0.9 | | | | | | 35.9± 6.1 J/m |
| | | 71.5 (0.6) | 33.1 (1.3) | 2.029 ±0.057 | 15.0± 4.1 | 26.9± 4.5 J/m | | | | | | | | | |
| Internal layer | External layer | PHB content (%) | | | | | | | | | MD/TD | | Tear resistance (N/μm) (PHB side/PBAT side) | | |
| PHB+ DCP | PBAT | 42.5-45 | 0.2 wt% | Film blowing | n.d | n.d | n.d | n.d | 0.6 | 800/3 | n.d | 0.04/0.05 | (Teixeira et al., 2020) | | |
| PHB/PBAT+ CE ⁽¹⁾ | | 52.5-55 | 2 phr | | n.d | n.d | n.d | n.d | 0.7 | 100/800 | n.d | 0.075/0.08 | | | |
| 90/10 | | 50-52.5 | | | n.d | n.d | n.d | n.d | 0.8 | 20/3 | n.d | 0.07/0.105 | | | |

3 n.d.: non determined ; * : determined from graphics; ⁽¹⁾ CE: Multifunctional epoxide styrene-acrylic oligomeric chain extender

Chapter I

(Ojijo & Ray, 2015) used a styrene-acrylic multifunctional oligomer chain extender named Joncryl® ADR 4368 to compatibilize PLA with PBSA. The reactive compatibilized blend showed improvement in impact strength with a critical Joncryl content of 0.6wt% compared to blends without chain extenders. The improved compatibility between both polymers was also confirmed by an increase in the elongation at break where PLA/PBSA 60/40 with 0.3 and 0.6wt% exhibited elongation of 201.4 and 178%, respectively, compared to only 6% for pure PLA.

Another effective way to improve the compatibility between immiscible polymers consists of using peroxide initiators. Dicumyl peroxide (DCP, (2,5-dimethyl-2,5-*tert*-butylperoxy) hexane) has been used in different immiscible biodegradable blends to compatibilize binary blends (Table I.3). DCP acts as a free radical initiator, which leads to the formation of crosslinked polymer blends by radical reaction. Combination of free radicals can also occur intra-domains which would lead the formation of branched/crosslinked neat polymer (intra-phase) and in some cases to degradation from chain scission (P. Ma, D. G. Hristova-Bogaerds, P. J. Lemstra, Y. Zhang, & S. Wang, 2012).

(P. Ma et al., 2012) compatibilized PHBV/PBS (80/20) *via* in-situ reactive extrusion using DCP as radical initiator and obtained already at a DCP content of 0.5 wt% improved mechanical properties. The morphology was much finer as shown Figure I.26. The strain-stress behavior changed from a brittle to a ductile behavior with an elongation at break increased from 8 to 400 %. This improvement was attributed to the formation of PHBV-*g*-PBS copolymer, which was assumed to be located at the interface between the polymers and thus act as a compatibilizer (P. Ma et al., 2012).

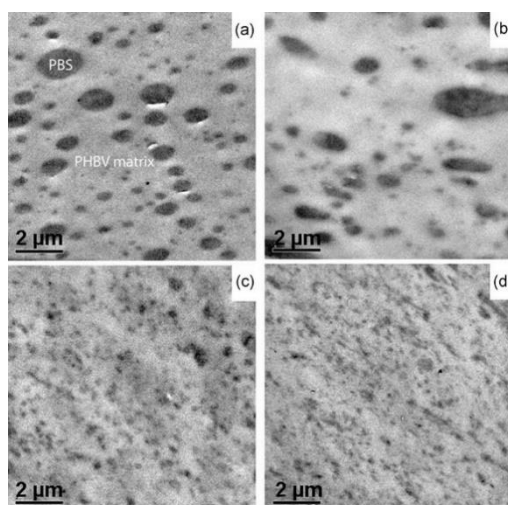


Figure I.26: TEM images of the PHBV/PBS (80/20) blends with DCP content of (a) 0, (b) 0.2, (c) 0.5, (d) 1.0wt% from (Ma, Hristova-Bogaerds et al. 2012)

Chapter I

(Ma et al., 2014) prepared also PLA/PBAT blends with DCP. The *in-situ* compatibilization conducted to a reduction in domain size of PBAT and an improvement in the interfacial adhesion. The mechanical properties were greatly improved with addition of DCP given that the elongation at break increased from 4 to 300 % for neat PLA and PLA/PBAT+ 0.1-0.2 phr (parts per hundred of resins) DCP, respectively. The impact toughness was also improved and reached a maximum of 110 J/m at the DCP content of 0.5 wt% compared to a value of 30 J/m for neat PLA.

(K. Zhang et al., 2014) designed a ternary blend of PHBV with PBAT and epoxidized natural rubber (ENR) using dicumyl peroxide as a reactive compatibilizer. The authors were able to improve the compatibility of PHBV with ENR and PBSA observed by a shift in $\tan \delta$ and improved impact strength.

(Wu, Misra, & Mohanty, 2019) were able to obtain a super toughened PLA material blended with PBAT and PBS through controlled reactive extrusion processing using a small amount of 2,5-bis(*tert*-butyl-peroxy)-2,5-dimethylhexane (Luperox® 101). A sharp brittle-ductile transition is observed when peroxide is added with increasing PBS and PBAT contents. The impact strength is increased ten times compared to uncompatibilized ternary blend, as shown in Figure I.27. Also, the incorporation of PBS and PBAT increased the elongation at break where the PLA/PBS/PBAT 40/40/20 blend reached a value of 167 %, which is much higher than pure PLA. However, a high DCP content decreased the strain at break given that the molecular chains are highly branched or cross-linked, limiting the chain movements. Also, the blends possess high melt elasticity, which was confirmed by an increase in storage moduli and a decrease in $\tan \delta$, revealing that some molecular networks are formed in their blends.

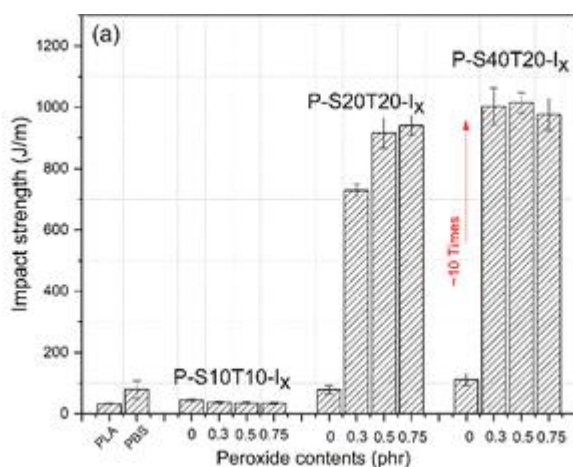


Figure I.27: Impact performance of the ternary blends where P: PLA/S: PBS/T: PBAT and I_x: peroxide content, figure modified from (Wu et al., 2019)

Chapter I

(Zytner et al., 2020) melt blended PHBV and PCL with blend ratio of 80/20 w/w in presence of both a free-radical initiator (under the trade name LUPEROX 101) and a cross-linking agent 1,3,5-tri-2-propenyl-1,3,5-triazine-1,4,6(1H,3H,5H)-trione (TAIC). The combination of peroxide and cross-linking agent led to an increase in elongation at break from 6 % to 25.3 % for PHBV/PCL 80/20 and PHBV/PCL/Peroxyde/TAIC 80/20/0.2phr/1phr, respectively. This improvement was accompanied by a decrease in elastic modulus from 3 GPa to 2.1 GPa while maintaining tensile strength of 37MPa for PHBV/PCL 80/20 and PHBV/PCL/Peroxyde/TAIC 80/20/0.2phr/1phr, respectively. The thermal properties were also modified with an increased PHBV crystallization temperature by 6 °C after the addition of both peroxide and TAIC while its crystallinity degree slightly decreased from 77.2 % to 71.8 %. The thermal, mechanical, and rheological properties were maximized with a peroxide content of 0.2 phr and 1 phr of TAIC since a higher content of cross-linker (3 phr) would lead to over cross-linking. This better compatibility between PHBV and PCL results from chain branching occurring on the “-CH₂” site of the backbone chains, leading to the formation of PHBV-PCL co-polymers, as shown in Figure I.28.

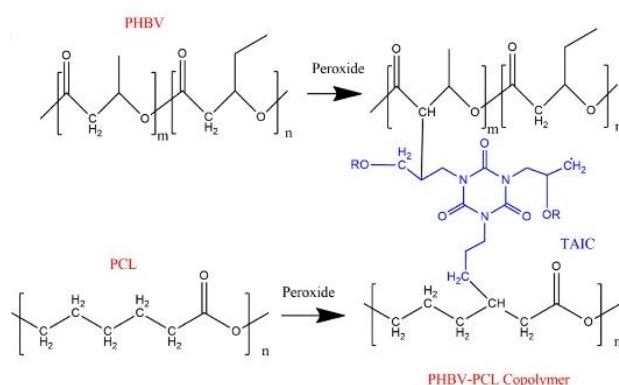


Figure I.28: Possible reaction mechanisms for co-polymer formation in the presence of peroxide and TAIC, figure from(Zytner et al., 2020)

(Teixeira et al., 2020) successfully produced PHBV-based film by film blowing in the presence of either dicumyle peroxide or a multifunctional epoxide styreneacrylic oligomeric chain extender (CE) in a co-extrusion process with PBAT as an external layer. The obtained films of PHBV/DCP+PBAT or PHBV/PBAT/CE+PBAT (internal+ external layers) displayed very good mechanical properties. In presence of DCP, films showed elongation at break as high as 400% in the machine direction (MD) while being at about 20% in the transverse direction (TD). While co-extruded bilayers films of PHB/PBAT+CE and PBAT as internal and external layers, respectively, showed tensile properties close to those displayed by PBAT, i.e., elongation at break of about 100% in MD and about 400% in TD.

Chapter I

Key points

Design of binary blends can be achieved by melt blending, which offers the ability to adjust the mechanical, thermal as well as rheological properties of polymer blends. Except in some rare cases, polymer blends are either immiscible or partially miscible and will develop a droplet-in-matrix structure or co-continuous phase structure depending on blend ratio. Final morphology results from an equilibrium between drop break-up and coalescence and therefore depends on viscosity ratio, interfacial tension, blend ratio, and processing conditions. The evaluation of the thermal and mechanical properties characterizes the level of miscibility between polymers.

- The brittleness of PHBV and its low melt strength imparts its ability to reach a large market size for flexible packaging. To increase the material performance of PHBV, the strategy of blending while preserving its bio-based and or biodegradable character can be achieved by mixing it with another polyester.
- The combination of the brittle material PHBV, with the highly ductile PBSA is potentially interesting for obtaining bio-based and biodegradable blends with improved processing and mechanical properties. PHBV/PBSA blends have never been investigated and are expected to broaden the thermal glass transition of PHBV-based blends thanks to its low T_g (-45 °C). They could enable to reach new market such as packaging of fresh, chilled and frozen food.
- However, despite the reported ability to balance the mechanical properties of PHBV, little improvements of the elongation at break have been observed. *In-situ* compatibilization can be used to improve the mechanical properties thanks to the enhancement of interfacial adhesion between both phases in binary blends. Organic peroxides are good candidates, including dicumyl peroxide or 2,5-bis(*tert*-butylperoxy)-2,5-dimethylhexane (Luperox 101). PHBV melt strength can be improved with the introduction of a free radical initiator resulting in increased length of macromolecular chain and apparition of a cross-linked network. Despite the *in-situ* compatibilization, the elongation at break is still low except when processed in co-extrusion film blowing.

To further improve the overall mechanical and thermal properties, *in-situ* compatibilization can be combined with the addition of plasticizers.

I.2.4. Plasticization

I.2.4.1. Principles of plasticizing

Plasticizers have been defined by the Council of the International Union of Pure and Applied Chemistry (IUPAC) as “a substance or material incorporated in a material (usually a plastic or elastomer) to increase its flexibility, workability or distensibility”. Plasticizers can be either internal or external. External plasticizers are low volatile substances that are added to polymers. The added substances interact with polymer chains but are not chemically linked to them, which

Chapter I

induces potential loss *via* evaporation or extraction. In contrast, internal plasticizers can be either co-polymerized or reacted with the original polymer (Vieira, da Silva, dos Santos, & Beppu, 2011). Both types of plasticizers are intended to tune the thermo-mechanical properties, including, e.g., depression of thermal glass temperature, change in melting temperature, change in viscosity, enhancement of flexibility (A Ruellan, Guinault, Sollogoub, Ducruet, & Domenek, 2015), a decrease of brittleness (Alexandre Ruellan et al., 2016).

The plasticization of polymers was first explained by two theories which were developed in parallel and described as the gel and the lubricity theory (Marcilla & Beltrán, 2012). These theories have been elaborated since the 1940's and attempted to explain the phenomena physically observed. The lubrication theory is credited to (Clark, 1941; Houwink, 1974; Kirkpatrick, 1940), and relies on the ability of the plasticizer to reduce intermolecular friction between the polymer molecules (Kirkpatrick, 1940). For (Kirkpatrick, 1940), the efficiency of plasticizing relies on the presence of specific chemical structure groups that afford points of mutual attraction with the polymer chains and leave an unattached portion. According to (Clark, 1941), the voids within the polymer chains are filled by the plasticizer, contributing to a lubrication effect. The Gel theory was introduced by (Aiken, Alfrey, Janssen, & Mark, 1947) in parallel, who postulated the existence of a three-dimensional gel network with great permanence within the plasticized polymer.

The study of plasticization relies on the ability to increase the free volume. Free volume comes from three principal sources (Platzer, 1982):

- motions of chain ends
- motions of side chains
- motions of the main chain.

The free volume of a polymer could be increased through several solutions:

- Increasing the number of end groups implies lower molecular weight
- Increasing the number or length which could be done *via* internal plasticization
- Increasing the chance for main chain movement by the inclusion of segments of low steric hindrance and low intermolecular attraction
- Introduction of a compatible external plasticizer that emphasizes motion through increased free volume

The efficiency of a plasticizer strongly relies on its compatibility with the polymer material. The best plasticizer is a high molecular mass molecule with good miscibility and a branched

structure; this brings large free volume and increases permeance inside the matrix. Compatibility with the target polymer needs to be ensured.

I.2.4.2.PHBV plasticizing

Several external plasticizers have been added within PHBV in the literature. The results are gathered in Table I.4. For PBSA, to our best of knowledge, no studies have been conducted on the incorporation of an external plasticizer.

(Brunel, Pachekoski, Dalmolin, & Agnelli, 2014) blended PHBV with epoxidized cottonseed oil and a fatty acid-based compound Licowax® as a plasticizing and nucleating agent, respectively. The study of both compounds shows that all additive formulations showed lower stress at rupture, lower elastic modulus, and higher strain at break (Table I.4). The lowest content of compounds (5 wt% and 0.1 wt% of plasticizing and nucleating agent, respectively) showed the best results. Hence, the elastic modulus, the strain at break, and stress at break were improved with values changed from 2 GPa to 1.3 GPa, from 4.6 to 8.5 %, and from 31.7 to 27.3 MPa, respectively. A change in thermal glass transition temperature T_g was observed with a shift towards lower temperature from 2.6 to -7.8°C . Both melting and cold crystallization temperatures were decreased. Finally, a change in crystalline degree was observed with a change from 46.3 to 38.1 %.

In another study by (Choi & Park, 2004), PHBV-6HV% was melt-mixed with different plasticizers, i.e., soybean oil (SO), epoxidized soybean oil (ESO), dibutyl phthalate (DBP), and triethyl citrate (TEC) with a polymer/plasticizer ratio of 80/20 w/w. The authors generated a classification based on the thermal and mechanical properties. Hence, from both thermal and mechanical properties, triethyl citrate appears to be the most suitable plasticizer since a significant shift in T_g towards lower temperature and a shift in T_m and ΔH_m was observed. While for mechanical properties, the elongation at break of PHBV blended with either ESO, DBP or TEC were improved and showed higher values compared to neat PHBV. According to the ranking erected by the authors, the effectiveness of TEC to tune the thermo-mechanical properties was followed by dibutyl phthalate, epoxidized soybean oil, and finally, soybean oil. (Correa et al., 2012) used acetyl tributyl citrate as plasticizer in blends with PHBV-18%HV as well as organo-modified montmorillonite as nanofiller. Incorporating 10 wt% of ATBC resulted in a significant decrease of PHBV's T_g by more than 10°C , which decreased from 1 to -13°C . Moreover, stiffness was lowered after the addition of ATBC with a decrease in elastic modulus of 300 MPa.

Chapter I

Table I.4: Thermo-mechanical properties of PHBV plasticized with polymeric external plasticizers

| Sample | Plasticizer content | Process | Tg(°C) | Tm (°C) | | ΔH_m (J/g) | Xc (%) | mW (g.mol ⁻¹) | E (GPa) | Strain at break (%) | Stress at break (MPa) | Ref. | |
|-----------------------|---------------------|-------------------|--------|----------|----------|--------------------|--------|---------------------------|-----------|---------------------|-----------------------|---|----|
| | | | | Tm1 (°C) | Tm2 (°C) | | | | | | | | |
| PHBV-18HV | | TSE | 1 | 139 | 162 | 32 | 29 | 100 | 1.08±0.03 | | 24.9±0.2 ^a | (Correa et al., 2012)) | |
| PHBV-18HV /10wt% ATBC | 10 wt% | | -13 | 132 | 157 | 38 | 39 | 180 | 0.73±0.01 | | 15.4±0.1 ^a | | |
| PHBV | | TSE and hot press | 3 | 168 | | 82 | 66 | 219 | 2.7 | 1.8 | 35 | (Martino, Berthet, Angellier-Coussy, & Gontard, 2015) | |
| PHBV/GTA | 5wt% | | | | [] | | [] | [] | [] | 1.6 | 4.3 | | 27 |
| | 10wt% | | -8 | 166 | | 89 | 67 | 226 | 1.1 | 5.3 | 23 | | |
| | 20wt% | | | | | | | | 0.9 | 4.2 | 17 | | |
| PHBV/ATBC | 5wt% | | | | | | | | | 1.7 | 3.8 | | 27 |
| | 10wt% | | -14 | 164 | | 86 | 68 | 227 | 1.2 | 6.4 | 24 | | |
| | 20wt% | | | | | | | | 1.1 | 4 | 19 | | |
| PHBV/PEG-400 | 5wt% | | | | | | 91 | 67 | 164 | 1.4 | 4.9 | | 25 |
| | 10wt% | | -12 | 164 | | | | | | 1.2 | 5.9 | | 24 |
| PHBV/PEG-1000 | 5wt% | | | | | | | | | 2.1 | 3.9 | | 35 |
| | 10wt% | | | | 166 | | 87 | 64 | 348 | 1.7 | 4.4 | | 30 |
| PHBV/PEG-4000 | 5wt% | | | | | | [] | [] | [] | 1.7 | 3.5 | | 27 |
| | 10wt% | | | | 168 | | 85 | 65 | 405 | 1.5 | 4.6 | | 24 |
| | 20wt% | | | | | | | | | 1.1 | 3.8 | | 17 |
| PHBV | | TSE and injection | 2.6 | 155 | 169 | | 46.3 | | 2.0±0.04 | 4.6±0.4 | 31.7±0.5 | (Brunel et al., 2014) | |
| PHBV+0.1wt% NA | 5wt% ECO | | -7.8 | 152 | 165 | | 38.1 | | 1.3±0.01 | 8.5±0.4 | 27.3±0.1 | | |
| | 7wt% ECO | | -9.3 | 150 | 164 | | 44.7 | | 1.3±0.03 | 7.1±0.4 | 24.9±0.1 | | |
| | 10wt% ECO | | -10.1 | 150 | 163 | | 37.1 | | 1.3±0.04 | 6.6±0.3 | 22.6±0.2 | | |
| PHBV+0.3wt% NA | 5wt% ECO | | -6.4 | 154 | 167 | | 36.8 | | 1.4±0.05 | 6.6±1.9 | 25.7±1.8 | | |
| | 7wt% ECO | | -9.1 | 150 | 164 | | 35.8 | | 1.4±0.02 | 6.3±0.3 | 24.3±0.2 | | |
| | 10wt% ECO | | -8.9 | 150 | 164 | | 37.6 | | 1.3±0.04 | 6.3±0.2 | 23.0±0.2 | | |
| PHBV+0.5wt% NA | 5wt% ECO | | -8.4 | 153 | 165 | [] | 39.3 | | 1.5±0.04 | 6.0±0.3 | 25.8±0.4 | | |
| | 7wt% ECO | | -8.6 | 152 | 165 | [] | 37.3 | | 1.5±0.08 | 5.9±0.5 | 24.4±0.2 | | |
| | 10wt% ECO | | -8.6 | 151 | 165 | [] | 36.1 | | 1.3±0.03 | 5.8±0.4 | 24.0±10.1 | | |

Chapter I

| Sample | Plasticizer content | Process | Tg(°C) | Tm (°C) | ΔH_m (J/g) | Xc (%) | mW (g.mol ⁻¹) | E (GPa) | Strain at break (%) | Stress at break (MPa) | Ref. |
|--------|-------------------------------|-----------------|--------|---------|--------------------|--------|---------------------------|---------|---------------------|-----------------------|---------------------|
| PHBV | | Solvent Casting | -6.6 | 161 | 65.9 | □ | | 0.25 | 5 | 46 ^b | (Choi & Park, 2004) |
| | 20 wt% Soybean oil | | -3.4 | 161.6 | 64.5 | □ | | 0.06 | 2,6 ^b | 38 | |
| | 20 wt% epoxidized soybean oil | | -19 | 159.5 | 61.6 | □ | | 0.17 | 6.8 ^b | 27 | |
| | 20 wt% dibutyl phtalate | | -28.5 | 152.7 | 59.1 | □ | | 0.14 | 9,8 | 15 | |
| | 20 wt% triethyl citrate | | -30 | 144.4 | 53 | □ | | 0.14 | 10 | 16 | |

^a: Stress at yield

^b: estimation from the graph

ECO: Epoxidized Cottonseed oil

NA: Nucleating agent

Chapter I

These results were further confirmed by Martino et al. 2015. The authors compared different plasticizers and different percentages (5, 10, and 20 wt%) on the ability to tune the thermo-mechanical properties using ATBC, glycerol triacetate (GTA), and polyethylene glycol (PEG) with three different molecular weights, i.e., 400, 1000 and 4000g.mol⁻¹. The apolar substance ATBC had the highest affinity towards PHBV. All three plasticizers had the ability to increase the mobility of polymer chains in the amorphous phase with a significant decrease of PHBV's Tg. Meanwhile, the crystallinity degree of PHBV blends did not change with melting enthalpy, which remained stable upon the type of plasticizer compared to neat PHBV (Table I.4).

Key points

The use of an external plasticizer in combination with PHBV is intended to tune the thermo-mechanical properties. Complying with food contact materials regulation, the addition of ATBC, a branched molecule exhibiting high permanence, in the PHBV matrix has shown positive results towards the modification of its thermo-mechanical properties.

Designing *in-situ* compatibilized PHBV/PBSA blends with the addition of ATBC as an external plasticizer is a highly novel and innovative approach to the design of new biodegradable blends. These new bio-based and biodegradable polymers are expected to fulfill the market demand. The ability to be processed through film blowing extrusion is of great importance to achieve a broad spectrum of applications, including flexible packaging for fresh, chilled and frozen food .

I.2.5. Safety of formulated biobased and biodegradable Food Contact Materials

I.2.5.1. General principles and binding regulations

US legislation The biological origin of the polymer or its ability to be degraded by microorganisms does not preclude the obligation of testing the suitability of the proposed material for food contact. According to section 201(s) of the FD&C Act (FEDERAL FOOD, DRUG, AND COSMETIC ACT, last revision June 24, 2019), possible contaminants originating from food contact materials (food contact substances are defined specifically in section 401(s) of the FD&C Act) are called indirect additives and correspond to any substance, which may reasonably become a component or otherwise affect the characteristics of any food. Substances that are generally recognized by experts, qualified by scientific training and experience, to be safe under the conditions of its intended use are exempted. With this respect, incorporating food components into the packaging material as filler, plasticizer, adhesive, or

Chapter I

antioxidant could be exempted from any restriction and preferable to the use of alternative synthetic substances. However, because a pesticide chemical residue in or on raw agricultural material or processed food requires can be present, the safety of agricultural or forestry by-products should always be established. Scientific procedures include the use of data (analytical, calculations, simulations, or other scientific studies), and methods, whether published or unpublished, as well as the methods to evaluate the toxicology and the chronic exposure of consumers. In short, if it is impossible in the present state of scientific knowledge to establish with complete certainty the absolute harmlessness of the use of any by-product, a safety assessment should be carried out. In determining safety, the possible ingestion of the substances originating from the considered by-products must be considered and its cumulative effect of the substance in the diet, considering any chemically or pharmacologically related substance or substances in such diet.

EU legislation The EU framework is built on very similar foundations (safety requirements for the manufacturing, processing, and distribution of food contact materials), but with different conditions of application. General safety requirements lay down by Regulation (EC) No 1935/2004) apply to any of the seventeen groups of materials identified by the EU Commission, and for which specific measures exist already or could be applied in the future (see Annex I of Regulation 1935/2004/EC). As a general rule, all food contact materials and articles should be manufactured in compliance with good manufacturing practice (further defined in Regulation (EC) No 2023/2006), so that, under normal and foreseeable conditions of use, they do not transfer their constituents to food in quantities that could endanger human health, bring about an unacceptable change in the composition of the food, or a deterioration of its organoleptic characteristics. Such rules do not exist yet for materials incorporating by-products originating from agriculture or food production. They are aimed at strengthening the self-assessment and responsibility of the manufacturers, processors, and distributors of food contact materials and components.

The concept of specific measures is essential in the EU legal system as it encourages the harmonization at EU level generally towards the highest standard among all member states. The adoption of such specific measures lies with the European Commission, which may adopt such measures but is not obliged to do so. In most cases, specific measures are adopted via the “regulatory procedure with scrutiny” in which the European Parliament plays a scrutiny role. Without being exhaustive, the specific measures include the list of authorized substances (positive list), purity standards and special conditions of use for positively listed substances,

Chapter I

specific and/or overall limits on the migration of certain constituents into the food, basic rules for checking compliance with the harmonized rules, authorization procedure for substances not yet in the positive list. In short, what is not accepted should not be used without submitting a dossier at the European Food Safety Authority (EFSA) and a positive opinion of the authority. As a general rule, EFSA has six months to issue its opinion as to whether, under the intended conditions of use of the material or article in which it is used, the substance complies with the general safety requirements of the framework Regulation 1935/2004/EC. If the opinion is favorable, EFSA will publish an opinion including the designation of the substance and its specifications, recommendations or restrictions of use, an assessment of the analytical method, and/or calculation method used for risk assessment. From 2004 to 2015, EFSA has evaluated 348 substances (Karamfilova & Sacher, 2016).

Specific measures and specific migration limits in the EU The level of harmonization at the EU level is far from complete. Specific measures exist only for plastics and recycled plastics, ceramics, regenerated cellulose film, active and intelligent packaging. For other groups of materials such as rubbers, silicones, textiles, paper and board, printing inks, adhesives, coatings and varnishes, waxes, and wood, such measures may exist at the national level. The principles of safety assessment for plastic materials used alone or in multilayers are summarized in Figure I.29. For accepting a new substance, the level of the studies depends on the expected level of migration, that is to say, on the level of mass transfer to the food in contact. Once the substance is accepted, the level of migration must be lower than the overall migration limit ($60 \text{ mg}\cdot\text{kg}^{-1}$ or $10 \text{ mg}\cdot\text{dm}^{-2}$) and the eventual specific migration limit (SML). The value of the SML is inferred from toxicological data and a conservative chronic exposure scenario for an adult of 60 kg ingesting 1 kg of food packed in 6 dm^2 . SML can be verified by migration testing or by migration modeling (Zhu, Nguyen, & Vitrac 2019).

Overall migration limits (OML) in the EU OML provide a global assessment of the inertia of food contact materials by assessing the total amount of non-volatile substances transferrable to the food. OML testing is achieved out by weighting the packaging before and after packaging. The test conditions for evaluating the overall migration limits are reported in Table I.5. The methodology is not sufficiently accurate to be related to specific migration limits, and the standard conditions (OM1..OM7) are not any more related to time and temperature conditions used to determined SML. The overall migration limit for plastics is $60 \text{ mg}\cdot\text{kg}^{-1}$ for children or infants and can be replaced by the limit of $10 \text{ mg}\cdot\text{dm}^{-2}$ in other cases.

Chapter I

Sensorial evaluation

The risk of deterioration of organoleptic characteristics needs to be verified, in particular, for bio-sourced and biodegradable components of the food packaging. The risk of aging, hydrolysis, and interactions with food are particularly high at all stages of its processing, storage, and final use. No specific guidance has been proposed to perform sensorial tests, but it is recommended to perform the evaluation on the food in worst-case conditions rather than on food simulants. The tests should be carried out in a way to detect off-flavors, bad taste, or odors. Triangular tests are the most used by the industry (two samples are identical) as they enable the evaluator to identify easily false positives.

Chapter I

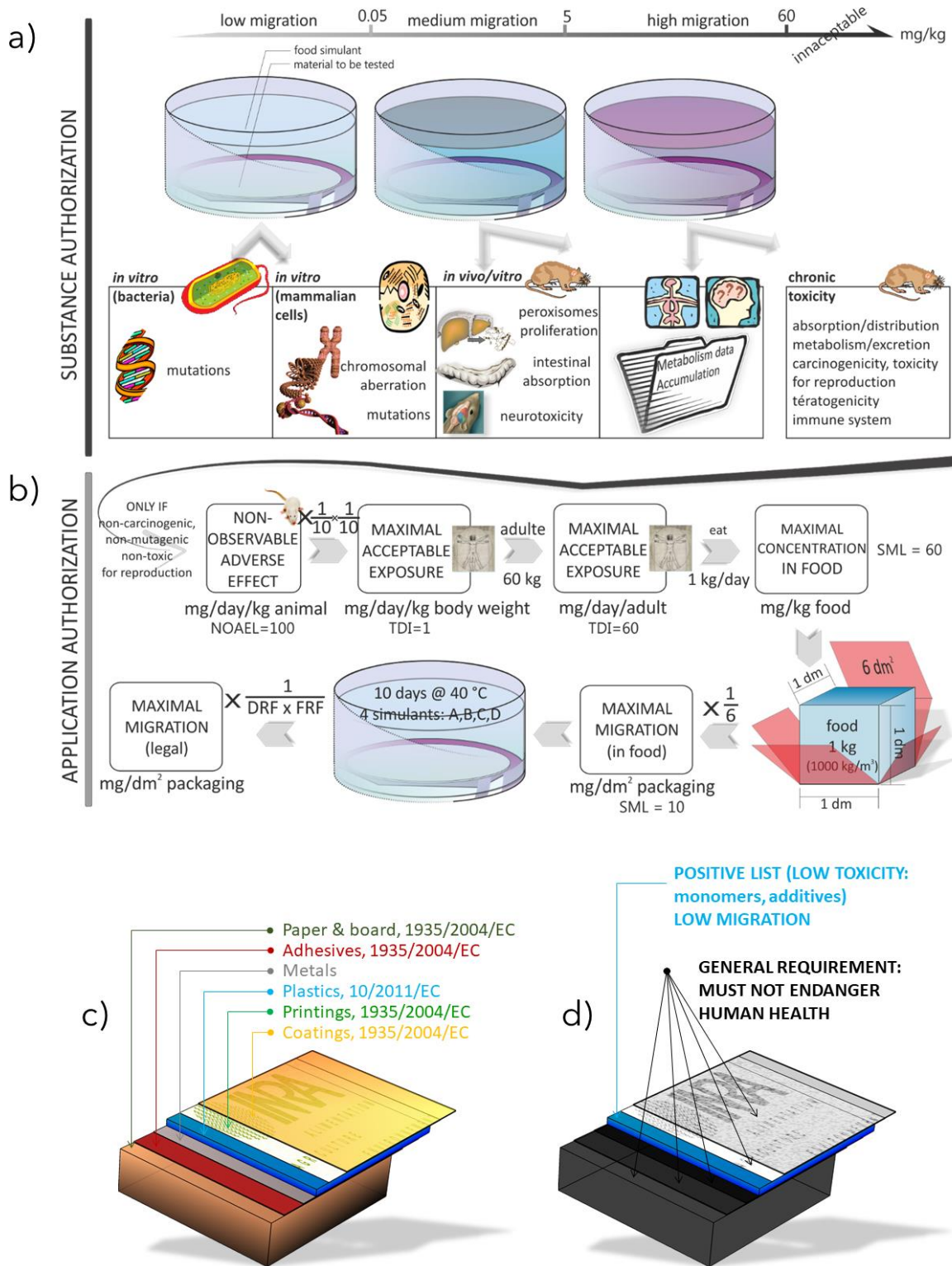


Figure I.29: Principles of safety assessment applied in EU (a) for the authorization of new substances, (b) for the verification of specific migration limits, (c-d) principles in multimaterials (here a laminate intended to be in contact with food). DFR = Simulant D

Chapter I

Table I.5: Test conditions for evaluating overall migration limits

| Test code | Food contact conditions | Test conditions |
|-----------|---|---|
| OM1 | Any food contact at frozen and refrigerated conditions | 10 days at 20 °C |
| OM2 | Any long-term storage at room temperature or below, including heating up to 70 °C for up to 2 h, or heating up to 100 °C for up to 15 min. | 10 days at 40 °C |
| OM3 | Any contact conditions that include heating up to 70 °C for up to 2 h, or up to 100 °C for up to 15 min, which are not followed by long-term room or refrigerated temperature storage | 2 h at 70°C |
| OM4 | High-temperature applications for all food simulants at temperature up to 100 °C | 1 h at 100°C |
| OM5 | High-temperature applications up to 121 °C | 2 h at 100 °C or at reflux or alternatively 1 h at 121 °C |
| OM6 | Any food contact conditions with food simulants A, B, or C, at temperatures exceeding 40 °C | 4 h at 100 °C or at reflux |
| OM7 | High-temperature applications with fatty foods exceeding the conditions of OM5 | 2 h at 175 °C |
| OM8 | High-temperature applications without storage as alternative to OM1, OM3, OM4, OM5, and OM6 | Food simulant E for 2 h at 175 °C and food simulant D2 for 2 h at 100 °C |
| OM9 | High-temperature applications with long-term storage as alternative to OM1, OM3, OM4, OM5, and OM6 | Food simulant E for 2 h at 175 °C and food simulant D2 for 10 days at 40 °C |

Food simulants: A (10% ethanol), simulant B (3% acetic acid), simulant C (20% ethanol), simulant D1 (50% ethanol), and simulant D2 (vegetable oil).

I.2.5.2. What is acceptable according to EU rules for thermoplastics

Though it has been constructed initially for synthetic substances, Regulation (EC) No 10/2011 for thermoplastics evolved progressively to integrate bio-sourced additives, monomers, and more recently, polymers obtained by fermentation. Criteria of purity prevail, and currently, the concept of GRAS (generically recognized as safe substances) does not hold. For plastics obtained by microbial fermentation recovered with or without subsequent solvent extraction, it is stated that “potential health risk may occur from the migration of non- or incompletely reacted starting substances, intermediates or by-products of the fermentation process. In this case, the final product should be risk assessed and authorized before its use in the manufacture of plastic materials and article”. Among the 885 positively listed initial substances, 314 additives or monomers can be obtained by fermentation, but only one polymer (3-hydroxybutyrate-co-3-

Chapter I

hydroxyvalerate, copolymer, *i.e.* PHBV) has been authorized. Current authorization requires this polymer to be produced by the controlled fermentation of *C. necator* (formerly *Alcaligenes eutrophus*) (strain H16 NCIMB 10442) with mixtures of glucose and propanoic acid as carbon sources.

In the general case and without prior authorization, by-products and bioproducts could be used in finished products under the same conditions, which have been accepted in general terms for recycled material. Materials or articles could incorporate non-listed substances when they are present behind a plastic functional barrier, preventing them from migrating in detectable amounts. The limit of detection is set to $0.01 \text{ mg}\cdot\text{kg}^{-1}$, and it excludes any mutagenic, genotoxic or reprotoxic substance as well as aggregates or molecular systems intermediate between dispersed solutes and nanoparticles. It is finally emphasized that other specific measures are not yet adopted at the EU level, and the complete requirements for multi-materials and multilayer materials and articles should be verified on a case basis for each member state, based on their own national provisions.

I.3.Objectives and approach

I.3.1.General objectives

The main objective of the present thesis is **to design a bio-based and biodegradable packaging with food contact ability which suits for packaging of frozen French fries.** Beyond the storage conditions that will strongly impact the thermo-mechanical properties of PHBV-based film. The design of packaging must also take into account the manufacturing process of the film and the temperature environments to which the package will be subjected as shown in Figure I.30.

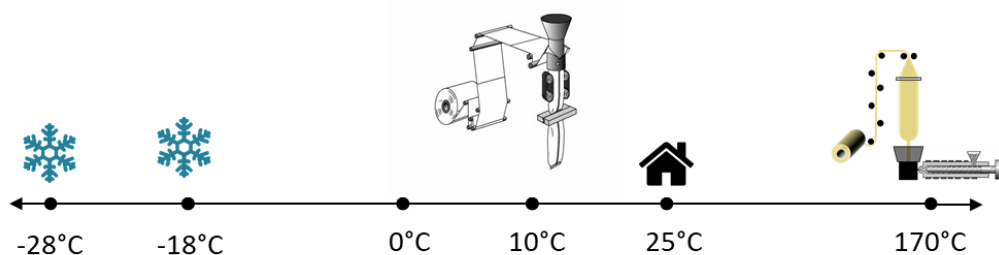


Figure I.30: Example of the different environments that the packaging will be subjected over the whole manufacturing process in the case of frozen food

Chapter I

From a technical point of view, PHBV misses sufficient mechanical performances for flexible packaging in that it has high stiffness and brittleness. Furthermore, it cannot be processed using conventional film blowing techniques because of low elongational viscosity and melt strength. A conventional strategy to improve thermomechanical properties of brittle material consists of blending it with a ductile material. A biodegradable aliphatic polyester with a low T_g (-45°C), poly(butylene succinate-co-adipate) (PBSA) was chosen to increase the ductility of the material.

I.3.2. Specific objectives

1. **Development of PHBV-based blends** that can be used for packaging of frozen food with a maximum of PHBV content: Characterization and observation of the interactions between biodegradable polyesters
2. **Evaluation of the processing ability of PHBV with film blowing technology:** Bringing good processing ability of PHBV thanks to better extensional viscosity based on interfacial compatibility

Chapter II
**Materials, methods and
implementation processes**

II.1. Materials

II.1.1. Materials

Commercial PHBV (reference PHI 002) containing 3 mole percent of hydroxyvalerate (HV) – according to technical datasheet – and PBSA (reference PBE 001) were purchased from NaturePlast (France). Their thermo-mechanical properties were collected from datasheet and summarized in Table II.1.

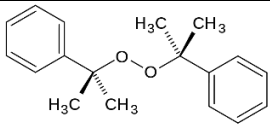
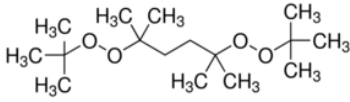
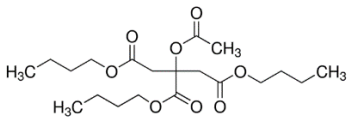
Table II.1 : Thermo-mechanical properties collected from Data Sheet

| Name | Grade | Density | MFI (g/10min) | Melting T°(°C) | Stress at break (MPa) | ε at break (%) | Young modulus (MPa) | Charpy impact (kJ/m ²) |
|------|-----------|---------|----------------------|-------------------|-----------------------------|-------------------|---------------------------|--|
| PHBV | Injection | 1,23 | 5-10 | 170-176 | 39,6 | 3,2 | 4200 | 5 |
| PBSA | Extrusion | 1,24 | 4-5 | 88 | 22 | 360 | 290 | NB |

II.1.2. Additives

Dicumyl peroxide was purchased from ACROS and used as received. Luperox® was kindly provided by ARKEMA, and Acetyl Tributyl Citrate was purchased from Sigma-Aldrich and used as received Table II.2.

Table II.2: Chemical formula and molar mass of used additives within the present study

| Additives | Chemical formula | Molar Mass (g/mol) |
|-------------------------|---|--------------------|
| Dicumyl peroxide |  | 270.37 |
| Luperox® 101 |  | 290.5 |
| Acetyl Tributyl Citrate |  | 402.48 |

II.2.Experimental methods

II.2.1.Polymers Drying

Before being subjected to melt mixing, all the polymer materials were dried at 70 °C under vacuum for at least six hours. Drying prevented premature degradation because of hydrolytic degradation.

Before being subjected to twin-screw extrusion at the pilot-scale, PHBV and PBSA were dried using a SOMOS dryer with a capacity of 60 L. To ensure optimal drying of the pellets according to data sheets, determination of the residual humidity (ppm) at different times was evaluated. It was done using a Hydrotracer Aboni FMX™ and results are shown in Figure II.1.

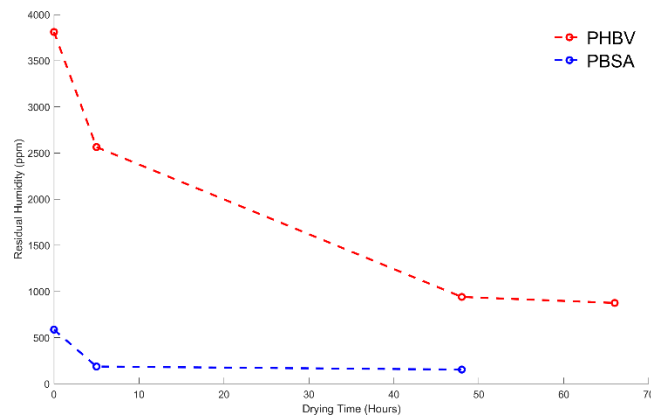


Figure II.1: Residual Humidity of PHBV and PBSA as a function of drying time

II.2.2.Internal Mixer

II.2.2.1.Internal mixer description

A Batch mixer, SCAMEX Rheoscam (France) was used all along with the present study. The internal mixer is equipped with a chamber of 100 cm³ and controlled with three heat resistance located on either side of the mixing chamber. Two roller rotors allow the material to be fed in the machine while a piston closes the mixing chamber. The batch mixer is based on the triptych: temperature, rotational speed, and residence time. These three parameters are independent, and each of them plays a role in obtaining a homogeneous bulk material at the end. First, the temperature should be high enough to allow the melt of the polymer while taking into account thermal degradation. During mixing, thermal degradation may appear because of the high shear

Chapter II

rate, which will cause heat release. Shearing is induced by the rotational speed of blades. Finally, residence time should be long enough to allow good mixing during blending.



Source: www.scamex.fr (visited on 09/14/2020)

Figure II.2: Picture of a SCAMEX batch mixer

II.2.2.2. Optimization of the experimental protocol

Previous to conduct experiments on PHBV/PBSA blends, a preliminary study was done to find the suitable parameters to ensure good mixing. Hence, the methodology followed is described and summarized in Table II.3.

Table II.3: Preliminary experimental procedures of mixing for PHBV/PBSA blends using a batch mixer

| | Mass (g) | | Protocol | Time (min) | Temperature (°C) | Rotational speed (rpm) | Final aspect |
|-----------------|----------|----|----------|------------|------------------|------------------------|------------------------------|
| Neat PHBV | 100 | | One-shot | 8 | 180 | 50 | Highly compact |
| Neat PBSA* | 100 | | One shot | 8 | 180 | 50 | Very low viscosity |
| PHBV/PBSA 50/50 | PHBV | 50 | One-shot | 9 | 180 | 50 | Lot of unmelted PHBV pellets |
| | PBSA | 50 | | | | | |
| PHBV/PBSA 50/50 | PHBV | 50 | One-shot | 9 | 180 | 90 | Lot of unmelted PHBV pellets |
| | PBSA | 50 | | | | | |

Chapter II

| | | | | | | | |
|----------------------------|------|----|---|---|-----|----|--|
| PHBV/PBSA 50/50 | PHBV | 50 | 1. PHBV:50g + PBSA: 10g → 4' of mixing: let PHBV melt while having an amount high enough to allow mixing in the chamber 2. Introduction of PBSA: 40g | 9 | 180 | 90 | Presence of unmelted PHBV pellets <u>Hypothesis:</u> Low volume in mixing chamber and/or too low T° |
| | PBSA | 50 | | | | | |
| PHBV/PBSA 50/50 | PHBV | 65 | 1. PHBV :65g+ PBSA : 10g → 6' of mixing 2. Introduction of PBSA: 55g → 3' of mixing | 9 | 190 | 90 | Homogeneous but mass maybe too high: presence of recirculation area |
| | PBSA | 65 | | | | | |
| PHBV/PBSA 50/50 | PHBV | 60 | 3. PHBV :60g+ PBSA : 10g → 6' of mixing Introduction of PBSA: 50g → 3' of mixing | 9 | 190 | 90 | Homogeneous and no sign of degradation |
| | PBSA | 60 | | | | | |

*First grade of PBSA used: Highly degraded which induced a very low viscosity in the internal mixer.

The first batches were dedicated to pure polymers to take the machine in hand and determine the right mixing parameters . Experiments conducted on PHBV/PBSA 50/50 blends helped to set the minimum of 70 g in the cavity. The methodology developed is based on a two steps introduction. First PHBV was introduced and let mix for 6 minutes since the torque was stabilized enough. Then, PBSA was introduced in a second phase based on the fact that it has a low melting temperature, i.e. $T_m=88^{\circ}\text{C}$ ($T_{\text{process}} = T_m+100^{\circ}\text{C}$). In case an amount of PHBV lower than 70 g was introduced bulk materials were found partly unmelted.

It has to be noticed that a content of 120 g was introduced in the batch mixer for the first part of the thesis (PHBV/PBSA blends). After several discussions with polymer processing experts and based on the literature, a content representing 70 wt% of the maximum capacity was used. Based on the densities of the used polymers, i.e., 1.24, a content of 93 g was used.

Chapter II

II.2.2.2.1. Physical blends of PHBV/PBSA

PHBV/PBSA blends were prepared using an internal mixer at 190 °C at 90 rpm for 9 min. First, PHBV was introduced in the mixing chamber for 6 min to allow its melting. After, PBSA pellets were introduced and mixed for another 3 min. Different ratios of PHBV/PBSA were prepared to evaluate the effect of blend ratio on the thermo-mechanical properties. The compositions of the PHBV/PBSA blends are as follows: 100/0, 70/30, 50/50, 30/70, 0/100. The used quantities are specified in Table II.4. The blended materials were finally processed by thermo-compression molding at 180 °C and 150 bars (SCAMEX 15T, France).

Table II.4: Experimental protocol for physical blends of PHBV/PBSA prepared with batch mixer

| PHBV/PBSA | PHBV content | PBSA content | Protocol |
|--------------|--------------|--------------|--|
| 100/0 | 120g | 0 | 1. PHBV : 120g → 9 min of mixing |
| 70/30 | 84 | 36 | 1. PHBV :84g→ 6 min of mixing 2. Introduction of PBSA: 36g → 3 min of mixing |
| 50/50 | 60 | 60 | 1. PHBV :60g+ PBSA : 10g → 6 min of mixing 2. Introduction of PBSA: 50g → 3 min of mixing |
| 30/70 | 36 | 84 | 1. PHBV :36g+ PBSA: 34g→ 6 min of mixing 2. Introduction of PBSA: 50g → 3 min of mixing |
| 0/100 | 0 | 120 | PBSA : 120g → 9 min of mixing |

II.2.2.2.2. Compatibilized PHBV/PBSA blends with dicumyl peroxide

Crosslinked PHBV with 0, 0.02, 0.1, 0.5 and 1.0 wt% DCP contents and compatibilized PHBV/PBSA blends with DCP contents of 0, 0.02, 0.1, 0.5, and 1.0 phr (parts per hundred) were melt-blended in a mixing chamber of an internal mixer SCAMEX Rheoscam (France) at 190 °C and 90 rpm for 9 min. First, PHBV was introduced in the mixing chamber for 6 min to allow its melting. After, PBSA pellets and DCP were introduced and mixed for 3 mins. The used quantities are specified in Table II.5. The blended materials were finally processed by thermo-compression molding at 180 °C and 150 bar (SCAMEX 15T, France).

Chapter II

Table II.5: Experimental protocol for compatibilized PHBV/PBSA with dicumyl peroxide prepared with batch mixer:

| Materials | Content of DCP | Quantity of DCP |
|----------------------|----------------|-----------------|
| PHBV/PBSA 70/30 w/w% | 0.02phr | 18,6mg |
| | 0.1 phr | 93mg |
| | 0.2 phr | 186mg |
| | 1phr | 930mg |

II.2.2.2.3. Plasticizing of PHBV/PBSA/DCP with Acetyl Tributyl Citrate (ATBC)

The strategy adopted was to keep a constant mass of 93 g for the PHBV/PBSA mixture, which was the filling quantity of the mixing chamber required to ensure mixing. The mass of ATBC was calculated to match the appropriate ratio in the mixture.

Plasticized PHBV/PBSA/DCP blends with Acetyl Tributyl Citrate (ATBC) were prepared using an internal mixer at 190 °C at 90 rpm for 9 min. First, PHBV was introduced in the mixing chamber for 3 min to allow its melting. Then, ATBC was introduced in the mixing chamber and mixed for 3 min. After reaching 6 min, PBSA pellets and DCP were introduced and mixed for another 3 min. The used quantities are specified in Table II.6. The blended materials were finally processed by thermo-compression molding at 180 °C and 150 bar (SCAMEX 15T, France).

Table II.6: Experimental protocol for compatibilized PHBV/PBSA with dicumyl peroxide and ATBC prepared with batch mixer:

| Materials | Content of ATBC | Quantity of ATBC |
|----------------------------------|-----------------|------------------|
| PHBV/PBSA 70/30 w/w% +0.1phr DCP | 5wt% | 4.9gr |
| | 10wt% | 10.3gr |
| | 15wt% | 16.4gr |
| | 20wt% | 23.2gr |

II.2.2.2.4. Alternative organic peroxide

Following the previous experiments, the mass of PHBV/PBSA was set to 93 g. For blends including ATBC, its content was then adjusted to reach a concentration of 10 wt%. Since LUPEROX is used as an alternative to DCP, the parameters of batch mixing remained unchanged.

Chapter II

Formulations containing LUPEROX were prepared using an internal mixer at 190 °C at 90 rpm for 9 min. For more clarity, the following methods were followed depending on the introduction of either ATBC or ATBC/TAIC in the PHBV/PBSA/LUPEROX blends:

PHBV/PBSA 70/30 w/w% +Xphr LUPEROX:

First, PHBV was introduced in the mixing chamber for 6 min to allow its melting. After, PBSA pellets and LUPEROX were introduced and mixed for 3 min. The following formulations were done:

- PHBV/PBSA 70/30 w/w% +0.1phr LUPEROX
- PHBV/PBSA 70/30 w/w% +0.2phr LUPEROX

PHBV/PBSA/ATBC 63/27/10 w/w% +Xphr LUPEROX:

First, PHBV was introduced in the mixing chamber for 3 min to allow its melting. Then, ATBC was introduced in the mixing chamber for 3 min. After reaching 6 min, PBSA pellets and LUPEROX were introduced and mixed for another 3 min. The following formulations were done:

- PHBV/PBSA/ATBC 63/27/10 w/w% +0.1phr LUPEROX
- PHBV/PBSA/ATBC 63/27/10 w/w% +0.2phr LUPEROX

II.2.3. Thermo-compression molding

II.2.3.1. Experimental protocol

After melt mixing, bulk materials were further cut in pellets and further dried at 70 °C for at least 4 h. Then, pellets were placed at the center of the thermo-controlled plateau. A mass of 4 g was used to obtain a film while aluminum foils of 200 µm were used to control the thickness of samples as shown in Figure II.3. First, pellets were pre-melt for 3 min before being subjected to 80 bar and 150 bar for 1 min each, as shown in Figure II.4. The final thickness of the sample was measured.

Chapter II

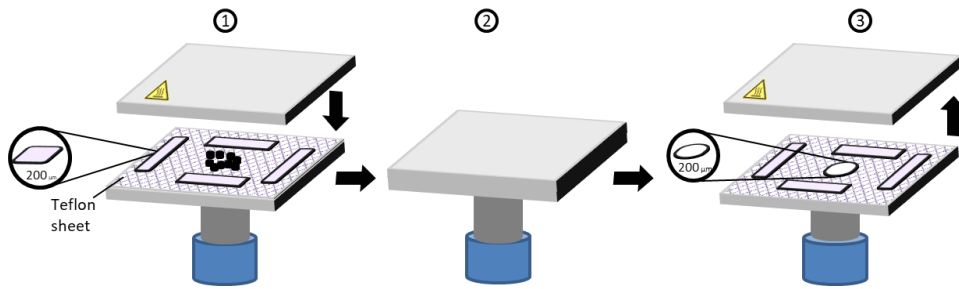


Figure II.3: Schematic representation of thermo-compression molding machine

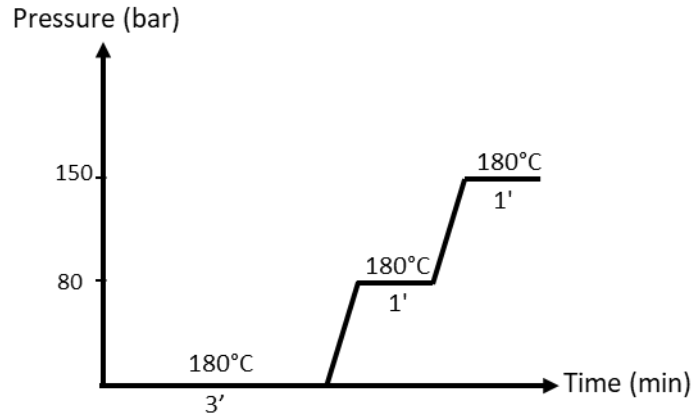


Figure II.4: Experimental protocol for compression molding

II.2.4. Twin-screw extrusion at lab scale

The experiments were realized at CTCPA-Bourg en Bresse (France).

Twin-screw extrusion was used to prepare PHBV/PBSA blends in the presence of dicumyl peroxide with the purpose of preparing masterbatches of compatibilized PHBV/PBSA blends. Prior to compounding *via* twin-screw extrusion process, pellets were dried for at least 24 h at 60 °C under vacuum.

For convenient work and since the extrusion campaign took place at CTCPA Bourg-en-Bresse, the drying process was carried out at AgroParisTech, and dried pellets were sealed in plastic bags in batches of 200 g. At CTCPA, the pellets were once again placed in a ventilated oven at 60 °C to minimize moisture content for at least 24 h.

Preliminary experimental tests on the PHBV/PBSA 70/30 blend were carried out in order to define the right setting to ensure good mixing before following the defined experimental plan. The twin-screw profile is sketched in Figure II.5.

Chapter II

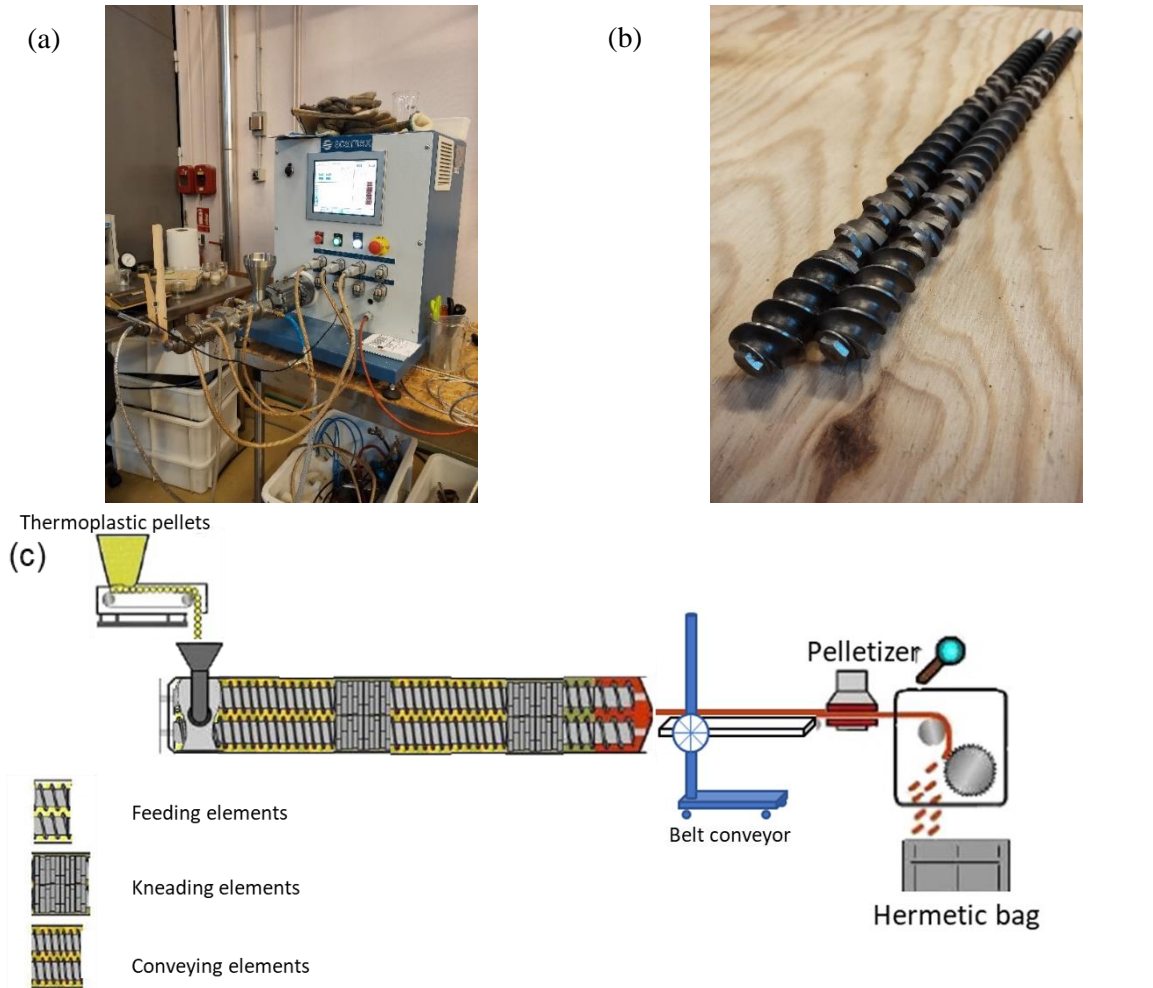


Figure II.5: (a) Twin-screw extruder scamex Rheoscam ... D, (b) twin-screw profile, (c) schematic representation of the twin-screw profile

II.2.4.1. Experimental protocol

Compatibilized PHBV/PBSA 70/30 blends with DCP contents of 0, 0.1, and 0.2 phr were first compounded using a twin-screw extrusion process with a screw diameter of 18 mm and a length-to-diameter of 16 L/D. The screw profile is depicted in Figure II.5(c) and is composed of three conveying zones and two shearing zones. The barrel comprises three independent temperature control for each barrel segment. The addition of DCP was carried out by dry-mixing to reach the proper amount of compatibilizer. The twin-screw extruder temperature zones were set to 175/185/155 °C from hopper to die, and screw speed was maintained at 20 rpm. The experimental design is detailed in Table II.7.

Table II.7: Compounding experimental design of compatibilized PHBV/PBSA blends with dicumyl peroxide

| Samples | Batch mass (g) | Rotational speed (rpm) | Temperature (°C) | | |
|---------|----------------|------------------------|------------------|--------|--------|
| | | | Zone 1 | Zone 2 | Zone 3 |
| | | | | | |

Chapter II

| | | | | | |
|--------------|-------------|----|-----|-----|-----|
| 70/30 | 35+15 | 20 | 175 | 185 | 155 |
| 70/30+0.1phr | 35+15+0.05g | | | | |
| 70/30+0.2phr | 35+15+0.1g | | | | |

II.2.5. Blown film extrusion at lab scale

Single screw extrusion, which was used a conveying element, was mounted prior to the film blowing module and equipped with a screw whose specifications with a diameter of 20 and a length-to-diameter of 11 (SCAMEX, France).

Blown film extrusion was conducted using a blown film head presented in Figure II.7. Set temperature profile and the experimental design is detailed in Table II.8.

Table II.8: Blown-film experimental design of compatibilized PHBV/PBSA blends with dicumyl peroxide

| | Drawing speed | Screw speed (rpm) | Zone 1 (°C) | Zone 2 (°C) | Zone 3 (°C) | Zone 4 (°C) |
|--------------|---------------|-------------------|-------------|-------------|-------------|-------------|
| 70/30 | -21 | 50 | 165 | 170 | 170 | 160 |
| 70/30+0.1phr | -21 | 50 | 165 | 170 | 170 | 160 |
| 70/30+0.2phr | -21 | 50 | 165 | 170 | 170 | 160 |

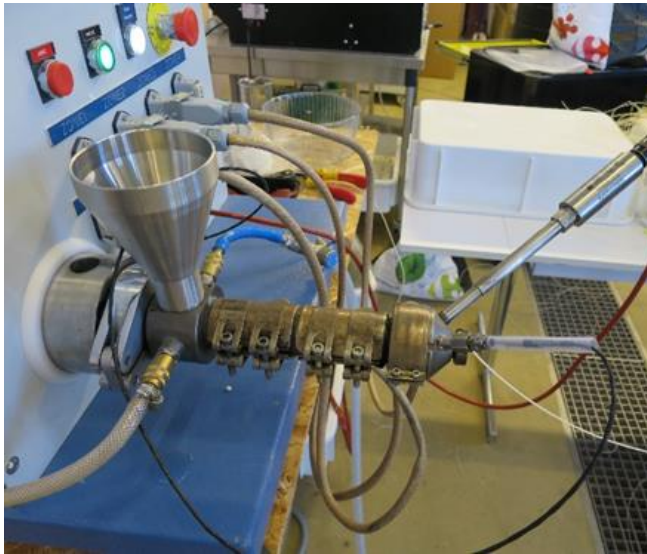


Figure II.6: Single screw extrudeur SCAMEX Rheoscam 20mm 11D

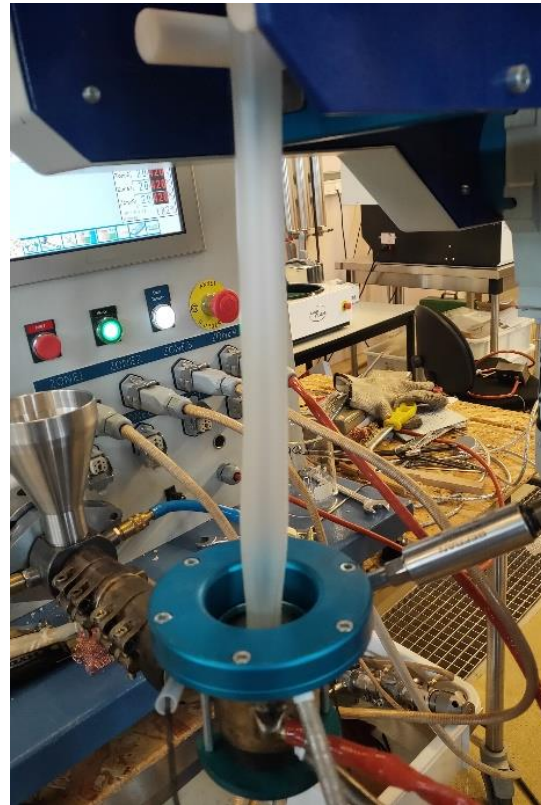


Figure II.7: Assembly of the single-screw machine with film blowing module

II.2.6. Twin-screw extrusion at semi-pilot scale

The experiments were realized at PIMM, Arts et Métiers, Paris (France).

II.2.6.1. Drying

Before being subjected to twin screw extrusion at pilot scale, PHBV and PBSA pellets were dried using a SOMOS dryer with a capacity of 60 L. The drying conditions were set at 60 °C for at least 24 h.

II.2.6.2. Twin-screw extrusion

Compounding of PHBV/PBSA blends was carried out using a twin-screw extrusion process with a screw length to diameter of 32/16 L/D (Thermo Haake Ptw 16-40D). The screw profile is depicted in Figure II.8 and is composed of 3 conveying zones and two shearing zones. The barrel comprises seven independent temperature control for each barrel segment. In the present study, the used configuration was co-rotating, intermeshing, and interpenetrated screws.

Chapter II

Finally, at the exit of the die, the rod was cooled on a conveyor belt and pelletized before being sealed in hermetic bags.

Since degradation of PHBV is a well-known phenomenon and to minimize it, we shortened the screw by introducing pellets in the first mixing zone (Figure II.8).

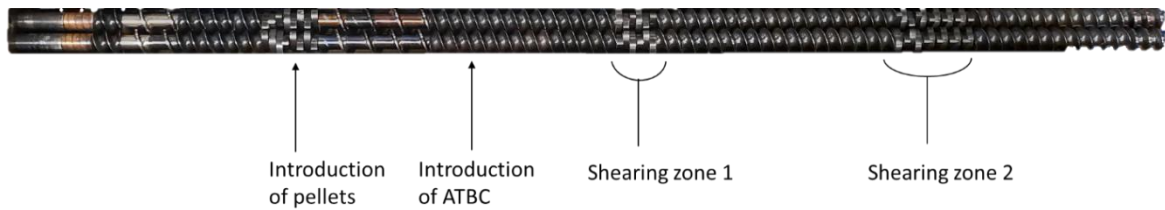


Figure II.8: Screw profile for production of PHBV/PBSA masterbatch

For the preparation of plasticized PHBV/PBSA blends with ATBC, the initial configuration was slightly modified. Introduction of ATBC was carried out using a dispensing pump ISMATEC® REGLO-Z (Cole-Parmer GmbH, Germany). Schematic representation of the twin-screw extrusion line is shown in Figure II.9.

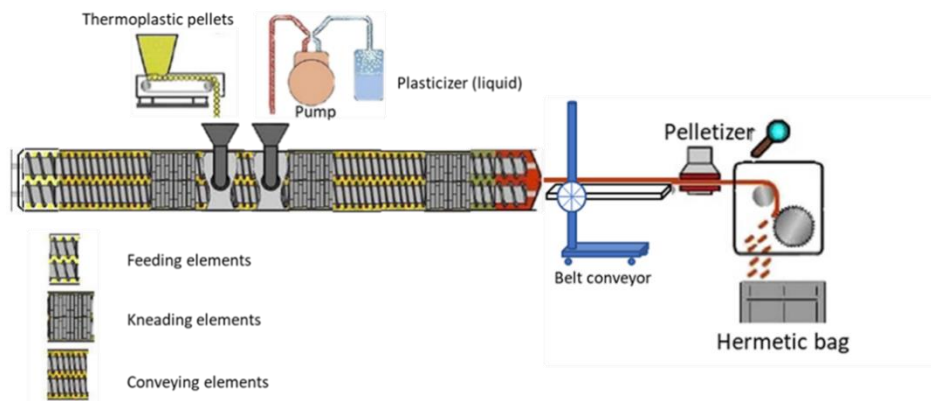


Figure II.9: Schematic representation of the twin-screw extrusion line 16D. L/D=32:1

II.2.6.3. Experimental protocol

Dried pellets of PHBV/PBSA were hand mixed in the proper amount to get a ratio 70:30 w/w. Pellets were introduced into the 3rd segment of the barrel as described above. In the present study, a pellet dosing unit was used to adjust the mass flow rate according to the torque. To maximize mixing, a target torque value would be between 50 % and 70 % since filling of the barrel at 100 % will not improve mixing conditions. For all samples, the screw speed was set at 300 rpm.

Chapter II

In the case of plasticized PHBV/PBSA blends, ATBC was introduced in the 4th segment of the barrel in a drip-feed manner. The pump speed was set at a value of 2 to reach the proper amount of ATBC since speed 1 of the pump, gives a flow rate of 0.85 cm³/min. ATBC was introduced a weight rate target of 53.4 gr/h. The temperature profile was set as follow:

- Barrel: Zone 1/2/3/4/5/6: 20°C/20°C/130°C/170°C/170°C+ Die: 170°C
- Screw speed: 300 rpm

Zone 1 and Zone 2 were set at 20 °C since PBSA has a low melting temperature and was found to melt very fast. As a result, at higher temperatures, a plug would form at the entrance of the barrel and led to numerous issues. The following segment temperatures were set to allow melting of PHBV, considering that PHBV degrades rapidly upon temperature, and shearing would induce internal heat. The rod produced was cooled by means of an airflow generated by compressed air and conveyed towards the pelletizer (SCAMEX, France) thanks to a conveyor belt.

The experimental parameters are detailed in Table II.9:

Table II.9: : Compounding experimental design of compatibilized PHBV/PBSA blends at semi- pilot scale

| Materials | Screw speed | Flow rate | Production quantity |
|--|---------------|----------------|----------------------------|
| <i>PHBV/PBSA 70/30+ 0.2phr LUPEROX</i> | <i>300rpm</i> | <i>800gr/h</i> | <i>About 5kg/batch</i> |
| <i>PHBV/PBSA/ATBC 63/27/10+ 0.2phr LUPEROX</i> | | <i>1.2kg/h</i> | |

II.2.7. Blown film extrusion at semi-pilot scale

PHBV/PBSA blends, after being prepared by twin screw extrusion process, the formulations were shaped by film blowing extrusion (Figure II.10).



Figure II.10: Film blowing machine MAPRE/COLLIN

II.2.7.1. Description

II.2.7.1.1. Screw

Single screw extrusion was mounted prior to film blowing module and equipped with a screw having length-to-diameter of 25:20 L/D (SCAMEX Rheoscam, France). Single screw brings two functions:

- Melting of pellets thanks to a barrel with seven independent temperature controls
- Conveying function thanks to the friction between the screw, the polymer, and the barrel

Chapter II

II.2.7.1.2.Die

Film blowing was conducted on the single-layer film blowing extrusion module MAPRE/COLLIN. Several parts are comprised within this module and will be presented in the following section.

First, to ensure that the material is properly conveyed from the single screw to the squaring hear, a crimp collar was used, as shown in Figure II.11(a). To further improve the quality of the melt, a filter holder was placed at the junction between both parts. It makes it possible to have filters of a specific mesh size, as shown in Figure II.11(b). It ensures the filtering of impurities, increases the pressure at the end of the screw, and regulates the flow of the material.

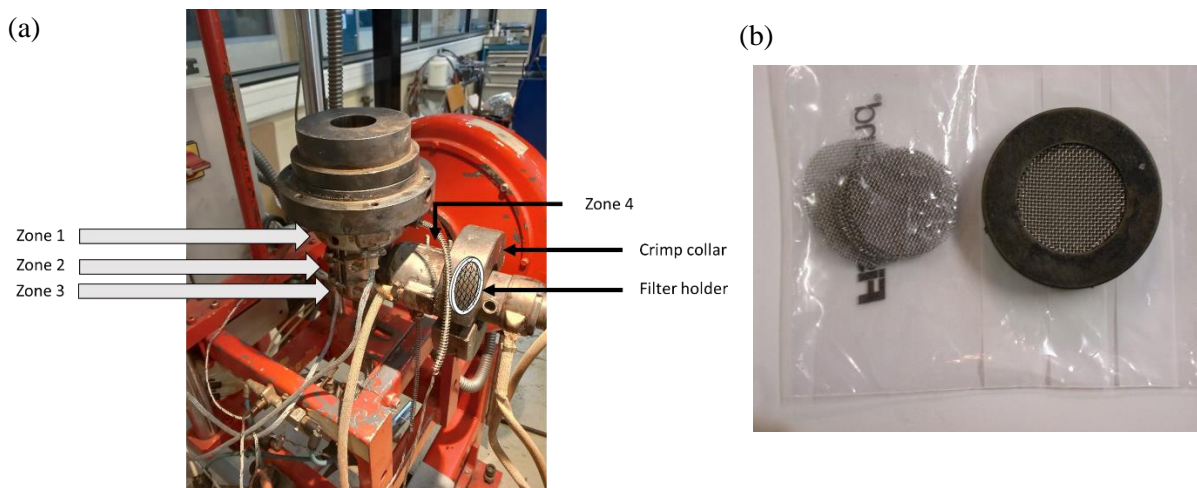


Figure II.11: (a) Overview of the film blowing extrusion module and (b) view of the filter holder and 450µm filters

Regarding the film blowing die, the extruder head is fixed at a right angle to the axis of the extruder barrel and allows to inflate the bubble thanks to its configuration, as shown in Figure II.12. In the present study, the die geometry was the spiral mandrel geometry. Regarding temperature regulations, the die head could be heated by four independent heating collars to precisely control the temperature of the material and were located as shown in Figure II.11(a).

The die head had the followed specifications:

Diameter of the punch: 50mm

Die-gap: 0.8mm

These data are essential to calculate the Blow Up Ratio (BUR) and the Draw Down Ratio (TUR) via Eq. II.1 & Eq. II.2:

Blow Up Ratio

$$\text{Blow Up Ratio (BUR)} = \frac{R}{R_0}, \quad \text{Eq. II.1}$$

Chapter II

where R and R_o are the final radius of the duct and punch radius, respectively.

Draw down ratio (DDR)

$$\text{Draw down ratio (DDR)} = (\text{Die gap}/\text{Film thickness})/\text{BUR} . \quad \text{Eq. II.2}$$

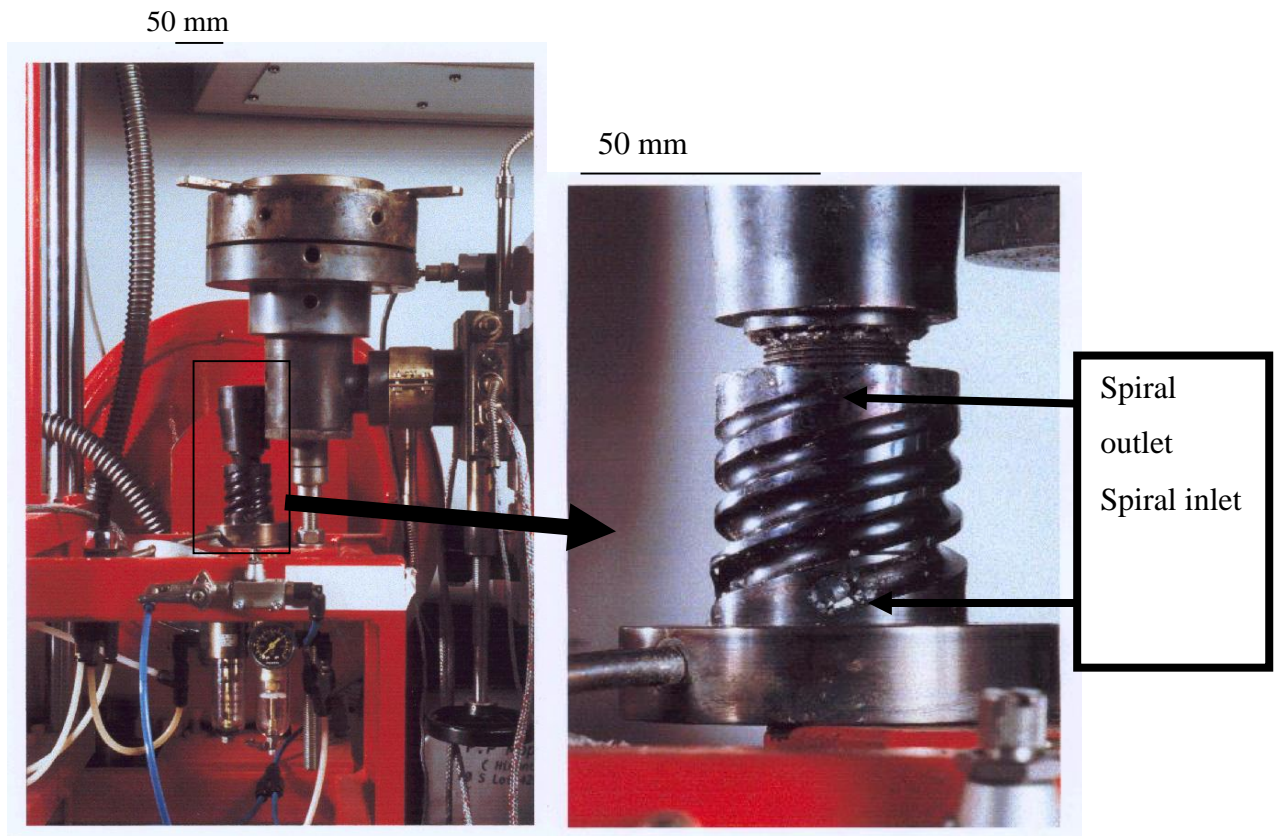


Figure II.12: Images of the die head and the spiral mandrel with the magnification of the spiral showing one inlet and one outlet, images kindly provided by Alain Guinault Ph.D. Thesis with modifications

II.2.7.1.3. Cooling

The cooling system plays an essential role in the bubble behavior. In the present study, the cooling system is shown in Figure II.13. It consists of a ring-air flow where the flow is directly rejected onto the outer side of the bubble to lick its surface. For our case, the temperature of the rejected airflow was not controlled but could be assumed to be around 20 °C since the experiment took place in a large ventilated area. The airflow rate can be tuned by tightening the

Chapter II

ring, which will greatly impact the bubble behavior, as shown in Figure II.14. Moreover, an iris ring was used with the purpose to stabilize the bubble better.

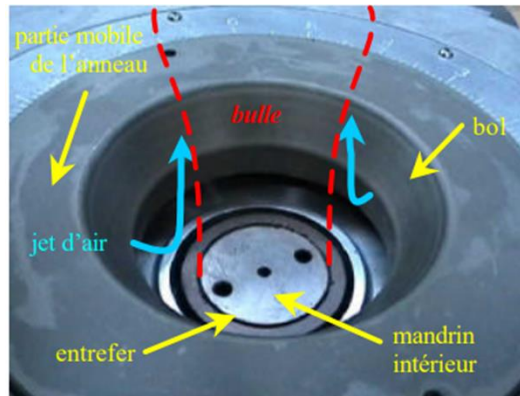


Figure II.13: Die outlet and blowing ring configuration (extracted from (Laffargue, 2003))

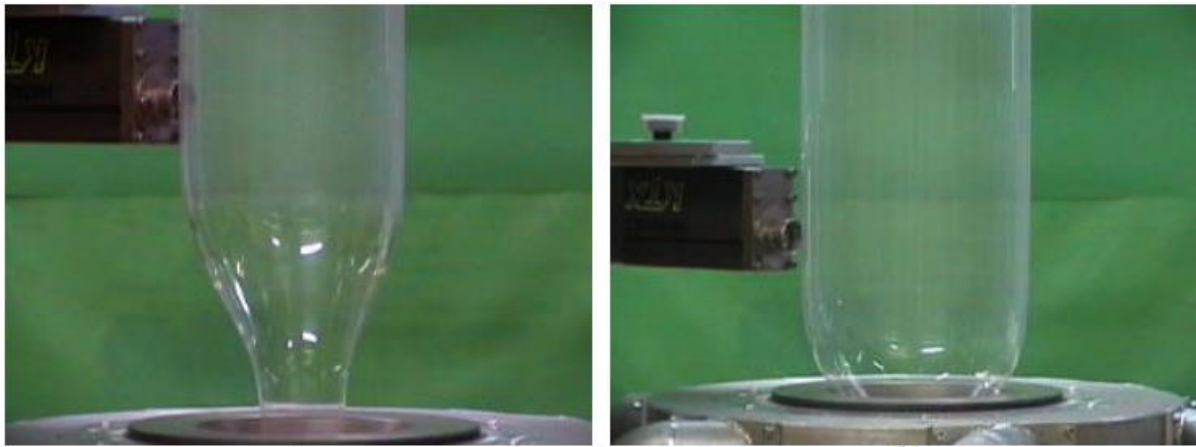


Figure II.14: Example of bubble shape depending on (a) low cooling rate and (b) high cooling rate, images extracted from (Laffargue, 2003)

II.2.7.2. Experimental design

After twin-screw extrusion of about 15kg, pellets were once again dried before being processed. Thanks to small-scale experiments, it was known that PHBV/PBSA 70/30 had the ability to be blown. Therefore and prior processing compatibilized and plasticized PHBV/PBSA formulations, we managed to set the temperature profile on the dry blend. The temperature profile chosen was as follows:

- Barrel: Zone 1/2/3/4/5/6/7: 140°C/160°C/170°C/170°C/180°C/180°C/170°C
- Die: Zone 1/2/3/4 : 170°C/165°C/165°C/165°C
- Screw speed: 30 rpm

This temperature profile was used for all three formulations.

Chapter II

Synoptic table of materials, equipment, implementation processes and characterizations used

| Study | Polymers | Additives | Implementation process | Samples | Characterization |
|---|----------------------------------|-------------------|--|---------|---|
| PHBV/PBSA dry blend Chapter III | PHBV : PHI 002 PBSA : PBE 001 | | Batch Mixer Thermocompression molding | Films | Process monitoring Dynamic Mechanical Analysis (DMA) Thermogravimetric analysis Differential Scanning Calorimetry <ul style="list-style-type: none"> • Non isothermal Crystallization • Non isothermal Crystallization kinetics • Isothermal Crystallization kinetics Scanning Electron Microscopy <ul style="list-style-type: none"> • Cryo-fracture Tensile test: Ambient T° Rheology: SAOS |
| Compatibilized PHBV/PBSA blend with DCP Chapter IV | PHBV : PHI 002 PBSA : PBE 001 | Dicumyle Peroxide | Batch Mixer Thermocompression molding | Films | Process monitoring Gel content Differential Scanning Calorimetry <ul style="list-style-type: none"> • Non isothermal Crystallization Tensile test: Ambient T° Scanning Electron Microscopy <ul style="list-style-type: none"> • Cryo-fracture • After tensile test Rheology: SAOS FTIR Melt Flow index |

Chapter II

| | | | | | |
|---|----------------------------------|--|--|--------------------------------------|--|
| Scale-Up of compatibilized PHBV/PBSA with addition of DCP Chapter IV | PHBV : PHI 002 PBSA : PBE 001 | Dicumyle Peroxide | Twin-screw extrusion Film blowing module Thermocompression molding | Films Thick sheets (4mm thick) | Gel content Differential Scanning Calorimetry Tensile test: <ul style="list-style-type: none"> • Ambient T° • Frozen T° Rheology: SAOS Charpy unnotched test Packaging Aging <ul style="list-style-type: none"> • Tensile test • Melt Flow index |
| Plasticized PHBV/PBSA blend with DCP and ATBC Chapter V | PHBV : PHI 002 PBSA : PBE 001 | Dicumyle Peroxide Acetyl Tributyl Citrate | Batch Mixer Thermocompression molding | Films | Process Monitoring Gel Fraction Differential Scanning Calorimetry Tensile test: Ambient T° Scanning Electron Microscopy: After tensile test |
| Alternative compatibilization of PHBV/PBSA blend with Luperox and ATBC Chapter V | PHBV : PHI 002 PBSA : PBE 001 | LUPEROX® 101E Acetyl Tributyl Citrate | Batch Mixer Thermocompression molding | Films | Process monitoring Gel content Differential Scanning Calorimetry Tensile test: Ambient T° |
| Scale-Up PHBV/PBSA/ATBC+Luperox Chapter V | PHBV : PHI 002 PBSA : PBE 001 | LUPEROX® 101E Acetyl Tributyl Citrate | Twin-screw extrusion Single screw extrusion+ film blowing module Thermocompression molding | Films | Differential Scanning Calorimetry Tensile test: <ul style="list-style-type: none"> • Ambient T° • Frozen T° Scanning Electron Microscopy: After tensile test Rheology: SAOS |

Chapter II

| | | | | | |
|--|--|--|--|--|--|
| | | | | | Aging: <ul style="list-style-type: none">• Frozen conditions |
|--|--|--|--|--|--|

II.3.Characterization methods

II.3.1.Scanning Electron Microscopy (SEM)

The morphology was studied by an Environmental Scanning Electronic Microscopy (ESEM, FEI Quanta 200) with an accelerated voltage of 12 kV. Compatibilized and non-compatibilized PHBV/PBSA +DCP samples were cryo-fractured using liquid nitrogen followed by selective dissolution of the PBSA phase by tetrahydrofuran at room temperature for at least one hour. Finally, the cryo-fractured samples were sputter-coated with a thin gold layer (Sputter coater Emitech K550), and snapshots were taken on the cryo-fracture edge of the sample.

II.3.2.Thermo-gravimetric analysis (TGA)

The thermal stability of the blends was assessed by Thermo-Gravimetric Analysis (TGA, Q500, TA Instruments). The experiment was performed from +25°C to +450°C in high-resolution mode under nitrogen atmosphere. The applied heating rate imposed the decomposition rate of the sample. The analyzes were carried out on ca. 10 mg samples.

II.3.3.Differential scanning calorimetry (DSC)

Thermal properties of blends were assessed by Differential Scanning Calorimetry, DSC, (DSC1, Mettler Toledo, Switzerland) according to two complementary temperature programs shown in Figure 10. All measurements were used under nitrogen atmosphere (flowrate 50 mL/min) with five to ten milligrams of materials sealed in 40 μ L aluminum pans. Calibration was carried out with Indium and Zinc standards. All measurements were duplicated.

Program I (Figure II.15) was used to measure melting and crystallization peaks and, secondly, the glass transition temperature. Samples were heated from -80 °C to 200 °C with a heating rate of 10 °C/min and held for 3 min at 200 °C, then cooled down to -80 °C at -10 °C/min and held for 5 min at -80 °C, and subsequently heated to 200 °C at 10° C/min. The glass transition temperature was measured by quenching the sample from 200 °C to -10 °C for 60 min to physically age PHBV, and subsequently cooled down to -40 °C for 10 min and heated to 60 °C at 10 °C/min. A cycle was done down quenching to -60 °C for 60 min to physically age PBSA,

Chapter II

cooling to -80 °C for 10 min, and heating to 60 °C. The crystallinity of each polymer $\{\chi_i\}_{i=PHBV,PBSA}$ was determined from the endotherm $\Delta H_{m,i}$ as:

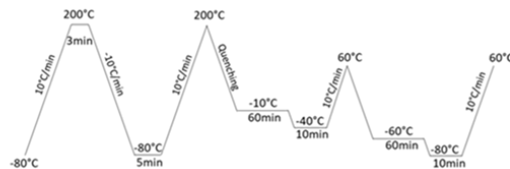
$$\chi_i = \frac{\Delta H_{m,i} - \Delta H_{cc,i}}{w_i \Delta H_{m,i}^0} \quad \text{Eq. II.3}$$

where w_i the weight content of the corresponding polymer, $\Delta H_{cc,i}$ the cold crystallization enthalpy and $\Delta H_{m,i}^0$ the melting enthalpy of a 100 % crystalline material with pure PHBV (146 J/g), (Corre et al., 2012) and PBSA (113.4 J/g) (Charlon et al., 2016).

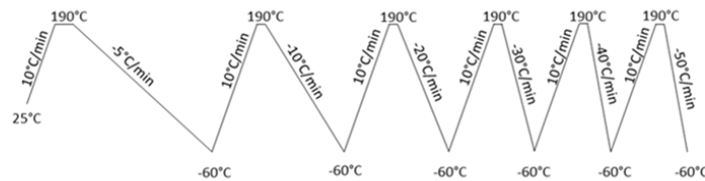
Program II (Figure II.15) was used to analyze the non-isothermal crystallization of PHBV and PBSA. Samples were heated up to 190 °C at 10 °C/min, annealed for 3 min to erase any thermal history in the sample, and cooled down to -60 °C. Crystallization temperatures (T_c) and exotherms (ΔH_c) were measured at cooling rates -5, -10, -20, -30, -40 and -50 °C/min.

Program III, (Figure II.15), monitored crystallization kinetics at different temperatures. Samples were quenched down to the desired crystallization temperature from the melt: 120 °C, 110 °C, 100 °C and 90 °C. Crystallization kinetics were recorded isothermally until equilibrium. Corresponding melting temperatures were analyzed during heating to 190 °C at 10 °C/min.

Program I: Determination T_m, T_c and T_g



Program II : Non-isothermal crystallization kinetic



Program III

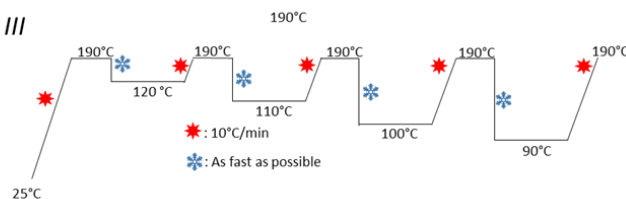


Figure II.15: Schematic representation of the different DSC protocols

II.3.4. Dynamic mechanical analysis (DMA)

Viscoelastic behavior of blends was characterized at 1 Hz and a stretch ratio of 0.1 % with a dynamic mechanical analyzer (model Tritec 2000 DMA, Triton Technology Ltd., UK). A temperature scan was performed from -60 °C to 190 °C at a heating rate of 2 °C/min on samples cut from thermocompression molded sheets (length = 10.25 mm, width = 5 mm) and pre-tension set to -0.75 N.

II.3.5. Mechanical properties

II.3.5.1. Tensile test

Tensile tests were carried under both ambient and freezer (-20 °C) conditions. For ambient conditions, tensile properties were measured using a texture analyzer (model TAHD, Stable Micro Systems, UK) equipped with pneumatic grips with a 5 mm/min crosshead speed. For freezing conditions (-20°C), tensile tests were performed on a Zwick Z010. The dumbbell-shaped samples of type 5 with a target thickness of 200 µm were cut from the compression-molded sheets for the tensile test. Thickness was an average of 5 measurements measured with a micrometer. At least five samples were tested for each ratio.

II.3.5.2. Impact test

Charpy impact tests were assessed according to ISO 179, using a Zwick B5113.300 impact tester. Pendulums of 1 and 4 J were used for PHBV-based blends and PBSA, respectively. At least five samples were tested for each ratio.

II.3.6. Rheological properties

II.3.6.1. Melt Flow Index (MFI)

Melt flow index (MFI) experiments were conducted following ISO 1133 (MFI 4106, Zwick, Germany). The samples were extruded through a die under a constant load of 2.16 kg at 190 °C. The melt flow index is expressed as the mass passing through the die during 10 minutes (g/10 min).

Chapter II

II.3.6.2. Small-amplitude oscillatory shear (SAOS)

Rheology measurements in melt state were performed with a stress-controlled rheometer (MCR 302, Anton Paar, Graz, Austria) using a disk-shaped specimen. A parallel-plate geometry with a gap set between 750 and 800 μm at 185 $^{\circ}\text{C}$. Dynamic frequency sweep experiments were performed from 0.01 to 100Hz in the linear visco-elastic region with a strain of 0.01%.

II.3.7. Gel content

Compatibilized PHBV/PBSA 70/30 blends with DCP contents of 0, 0.02, 0.1, 0.2, and 1.0 phr were first milled (Model Retsch MM400, Germany). Two successive Soxhlet extraction were performed to extract the two polymers PHBV and PBSA, independently. Chloroform is a suitable solvent for PBSA and PHBV, but not for the cross-linked network. Besides that THF is a suitable solvent only for PBSA. The extraction of PBSA in boiling tetrahydrofuran (THF) for one day followed by extraction of PHBV in boiling chloroform for two consecutive days. The gel fraction was calculated following :

$$gel\ wt.\ \% = \frac{m_1}{m_0} \cdot 100\% \quad \text{Eq. II.4}$$

where m_0 is the original weight of samples and m_1 is the weight of dry residues obtained after extraction

II.3.8. Fourier transform infrared spectroscopy (FTIR)

The Fourier transform infrared (FTIR) spectra were performed on a Pekin-Elmer FT-IR Frontier using an attenuated total reflectance (ATR) module. Measurements were recorded by absorption (A) between 4000 to 650 cm^{-1} with a resolution of 4 cm^{-1} .

II.3.9. Aging test: long time storage at -20 $^{\circ}\text{C}$

Blown film bags were filled with parfried frozen French fries and stored at -20 $^{\circ}\text{C}$ before being tested at different stages over a long period (Figure II.16).

Chapter II

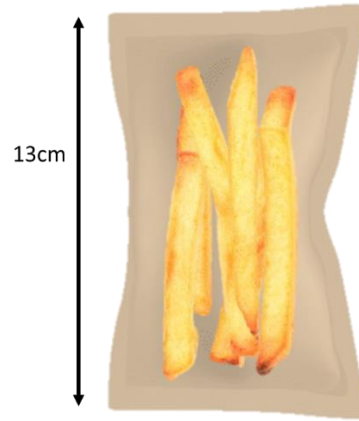


Figure II.16: Schematic representation of hot sealed bags filled with frozen French fries

Chapter III

**Characterization of new bio-based
and biodegradable polymer blend:
Application to poly(3-
hydroxybutyrate-co-3-
hydroxyvalerate) / poly(butylene-co-
succinate-co-adipate) blends**

Benjamin Le Delliou¹, Olivier Vitrac¹, Mickael Castro², Stephane Bruzaud², , Sandra Domenek^{1,}*

¹UMR 0782 SayFood Paris-Saclay Food and Bioproduct Engineering Research Unit, INRAE, AgroParisTech, Université Paris-Saclay, 91300, Massy France

² Smart Plastics Group, Université de Bretagne Sud, UMR CNRS 6027, IRDL, 56100 Lorient, France;

Keywords: blends, PHBV, PBSA, mechanical properties

III.1. Abstract

Melt blending of poly(3-hydroxybutyrate-co-3-hydroxyvalerate) and poly(butylene-co-succinate-co-adipate) is investigated by means of batch mixer at different weight ratios (100:0, 70:30, 50:50, 30:70 and 0:100). PHBV and PBSA are immiscible. PBSA formed small nodules in PHBV, while PHBV formed large inclusions in PBSA. In 50/50 wt% mixture, a co-continuous structure is obtained. The crystallization rate of PHBV and PBSA increase in the blends, most probably due to mutual nucleation, except at the later stages, where PHBV crystallization rates slowed down in nodules and in the co-continuous structure. The mechanical properties are successfully modeled with the EBM model, including parallel and serial resistances, and show that the rigidity of the material can be modulated using PBSA. The elongation at break is, however, governed by PHBV featuring brittle fracture even in case PBSA is the continuous phase, and the analysis of the stress at break shows that the fracture can be ascribed to debonding at the interfaces.

III.2.Introduction

Polymers are largely used in short-lived products, such as food packaging or single-use containers, because they are low-cost, light-weight, easy to process, flexible over an extensive range of temperatures. Their service life is thus much shorter than their total lifetime, which leads to persistent environmental pollution if collection and end-of-life are not managed adequately (Verghese et al., 2015). One means to prevent persistent pollution is to substitute commonly used polymers by biodegradable and compostable materials with satisfying performance.

Polyhydroxyalkanoates (PHAs) are biobased thermoplastic polyesters that are biodegradable even in the marine environment but have poor mechanical performance and are difficult to process. They are synthesized as carbon and energy storage compounds by numerous microorganisms when macronutrients such as oxygen, nitrogen, or phosphorus are limited, but a carbon source is present (Laycock et al., 2014). Today, the main commercial polymers are short-chain-length PHAs, represented by poly(3-hydroxybutyrate), PHB, and copolymer poly(3-hydroxybutyrate-co-3-hydroxyvalerate), PHBV (Deroiné et al., 2014; Laycock et al., 2014). Their glass transition temperature (T_g) ranges between 0 and 5 °C. The isotacticity of PHBV results in stiff and brittle materials with an elongation at break below 5 % and a stress at break between 30 and 40 MPa (Anjum et al., 2016). PHBV has, besides, a very narrow processing window and degrades rapidly upon melting. Its low shear viscosity and elastic melt strength impede its processing by extrusion-blowing (Cunha et al., 2015). To increase the material performance of PHBV, the strategy of blending with other polymers was already proposed. In the perspective of preserving the biodegradability and/or the biosourced character of the mixture, binary blends have been studied with polylactic acid (PLA) (Boufarguine et al., 2013; Idris Zembouai et al., 2013; M. Zhang & Thomas, 2011), polybutylene adipate-co-

Chapter III

terephthalate (PBAT) (Bittmann, Bouza, Barral, Castro-Lopez, & Dopico-Garcia, 2015; Cunha et al., 2015), polybutylene succinate (PBS) (Phua et al., 2015). Improved stiffness-toughness balance and possibilities of tuning mechanical properties have been notably shown with ternary blends based on PLA, PHBV, and PBS (K. Zhang et al., 2012). Poly(butylene-co-succinate-co-adipate) (PBSA) is an alternative to PBS for developing polymer blends with increased ductility, with an elongation at break up to 400 % (Xu & Guo, 2010). It is a biodegradable polymer that can be partially or fully biobased (Salomez et al., 2019). The higher elongation at break and its lower T_g (-45 °C) make PBSA superior to PBS. In addition, the lower crystallinity of PBSA compared to its counterpart, *i.e.* PBSA, accelerates its biodegradation (Tserki et al., 2006). Polyester blends of PBSA and PLA have already been studied at ambient temperature and relative humidity (Nofar et al., 2017; Ojijo, Sinha Ray, & Sadiku, 2012). Authors reported on immiscibility between both constituents, formation of small nodules of PBSA in PLA, a reduction in tensile modulus from about 2.7 GPa (neat PLA) to 1 GPa (PLA/PBSA 50/50) and a moderate improvement of the elongation at break, up to $\epsilon=6.5$ % for PLA/PBSA 70/30 (Ojijo et al., 2012). While great attention has been devoted through extensive characterization of PHBV in literature, reports on PBSA are rare. The combination of the brittle material PHBV, and the highly ductile PBSA is potentially interesting for obtaining bio-based and biodegradable blends with improved processing and mechanical properties.

The present study presents a detailed rheological, morphological, thermal, and mechanical characterization of PHBV/PBSA blends. The impact of the blend composition and structure on viscosity, crystallinity, and tensile modulus was quantified and interpreted using known models, such as mixing rules, Avrami-Jerziony analysis for non-isothermal crystallization, and Equivalent Box Model (EBM) model for tensile strength of blends.

III.3.Experimental Section

III.3.1.Materials

Commercial PHBV (reference PHI 002) containing 3 mol-% of hydroxyvalerate (HV) – according to technical datasheet – and PBSA (reference PBE 001) were purchased from NaturePlast (France). Polymers were dried at 70 °C under vacuum for at least six hours before use.

III.3.2.Processing of PHBV and PBSA blends and sheets

PHBV and PBSA were blended at molten state within an internal mixer (model Rheoscam, Scamex, France) at 190 °C at 90 rpm for 9 min. PHBV was firstly introduced in the mixing chamber for 6 min to allow its melting. PBSA pellets were subsequently introduced and mixed for additional 3 min. Blended materials were finally processed by thermo-compression molding at 180 °C and 150 bar (thermoccompression press model 15 T, Scamex, France). Typical torque curves of recorded during mixing are presented in the supporting information S1. Pellets initially pre-melt for 3 min were compressed successively to 80 and 150 bar for 1 min each. Aluminum foils of 200 µm were used to control the sample thickness. Thermomechanical properties were tested on five blend ratios PHBV:PBSA: 100:0, 70:30, 50:50, 30:70, 0:100 w% (weight percent).

III.3.3.Characterization Methods

III.3.3.1.Thermal characterization

Thermal properties of blends were assessed by Differential Scanning Calorimetry, DSC (DSC1, Mettler Toledo, Switzerland) according to two complementary temperature programs shown in

Chapter III

Figure III.1. All measurements were used under nitrogen atmosphere (flowrate 50 mL/min) with five to ten milligrams of materials sealed in 40 μ L aluminum pans. Calibration was carried out with Indium and Zinc standards. All measurements were duplicated.

The program I (Figure 1) was used to measure melting and crystallization peaks and, secondly, the glass transition temperature. Samples were heated from -80 $^{\circ}$ C to 200 $^{\circ}$ C at 10 $^{\circ}$ C/min and held for 3 min at 200 $^{\circ}$ C, then cooled down to -80 $^{\circ}$ C at -10 $^{\circ}$ C/min and held for 5 min at -80 $^{\circ}$ C, and subsequently heated to 200 $^{\circ}$ C at 10 $^{\circ}$ C/min. The glass transition temperature was measured by quenching the sample from 200 $^{\circ}$ C to -10 $^{\circ}$ C for 60 min to physically age PHBV, then cooling down to -40 $^{\circ}$ C for 10 min and heating to 60 $^{\circ}$ C at 10 $^{\circ}$ C/min. A cycle was done down quenching to -60 $^{\circ}$ C for 60 min to physically age PBSA, cooling to -80 $^{\circ}$ C for 10 min, and heating to 60 $^{\circ}$ C. The crystallinity of each polymer $\{\chi_i\}_{i=PHBV,PBSA}$ was determined from the endotherm $\Delta H_{m,i}$ as:

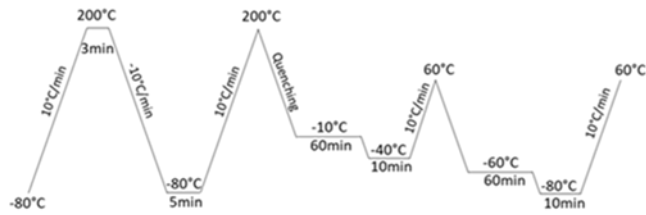
$$\chi_i = \frac{\Delta H_{m,i} - \Delta H_{cc,i}}{w_i \Delta H_{m,i}^0} \quad \text{Eq. III.1}$$

where w_i the weight content of the corresponding polymer, $\Delta H_{cc,i}$ the cold crystallization enthalpy, and $\Delta H_{m,i}^0$ the melting enthalpy of a 100 % crystalline material with pure PHBV (146 J/g) (Corre et al., 2012), and PBSA (113.4 J/g) (Charlon et al., 2016).

Program II (Figure 10) was used to analyze the non-isothermal crystallization of PHBV and PBSA. Samples were heated up to 190 $^{\circ}$ C at 10 $^{\circ}$ C/min, annealed for 3 min to erase any thermal history in the sample, and cooled down to -60 $^{\circ}$ C. Crystallization temperatures (T_c) and exotherms (ΔH_c) were measured at cooling rates -5, -10, -20, -30, -40 and -50 $^{\circ}$ C/min.

Chapter III

Program I: Determination T_m , T_c and T_g



Program II : Non-isothermal crystallization kinetic

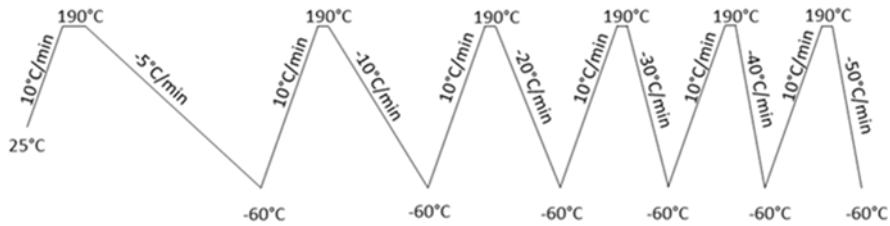


Figure III.1 : Schematic representation of the different DSC protocols

III.3.3.2. Scanning Electron Microscopy

The PHBV/PBSA blend morphology was observed by an Environmental Scanning Electronic Microscopy (model FEI Quanta 200, FEI Company, USA) with an accelerated voltage of 12 kV. Cryo-fractured samples were subjected to the selective dissolution of the PBSA phase by tetrahydrofuran (THF) at room temperature for at least one hour. Selective dissolution of PBSA was carried out in THF but only for ratios 70:30 and 50:50. For higher PBSA content, the treatment was not carried out because the sample integrity was not conserved. Samples were finally sputter-coated with a thin gold layer (model Sputter coater Emitech K550, Emitech, UK) and imaged from their cryo-fracture edges.

III.3.3.3. Rheological properties

Rheological properties were measured at molten state on 25 mm disk-shaped specimens placed within a stress-controlled rheometer (model MCR 302, Anton Paar, Graz, Austria). A parallel-

Chapter III

plate geometry with a gap set at 750-800 μm . All dynamic frequency sweep experiments were carried out at 185°C. Dynamic frequency sweep experiments were performed varying from 0.01 to 100 Hz in the linear viscoelastic region.

III.3.3.4. Mechanical properties

Tensile properties were measured using a texture analyzer (model TAHD, Stable Micro Systems, UK) equipped with pneumatic grips with a 5 mm/min crosshead speed. Two hundred micrometer thick dumbbell-shaped samples of type V were cut from our compression-molded sheets and used for tensile testing. Sample thickness was averaged from five measurements with a caliper. At least five samples were tested for each blend composition.

III.3.3.5. Dynamic mechanical properties

Viscoelastic behavior of blends was characterized at 1 Hz and a stretch ratio of 0.1 % with a dynamic mechanical analyzer (model Triton 2000 DMA, Triton Technology Ltd., UK). A temperature scan was performed from -60 °C to 190 °C at a heating rate of 2 °C/min on samples cut from thermocompression molded sheets (length = 10.25 mm, width = 5 mm).

III.4. Results and Discussion

III.4.1. Rheological properties

The viscoelastic properties of neat PHBV, PBSA, and PHBV/PBSA blends were analyzed with dynamic frequency sweep experiments from high to low frequencies, as shown in Figure III.2(a,b).

(a)

Chapter III

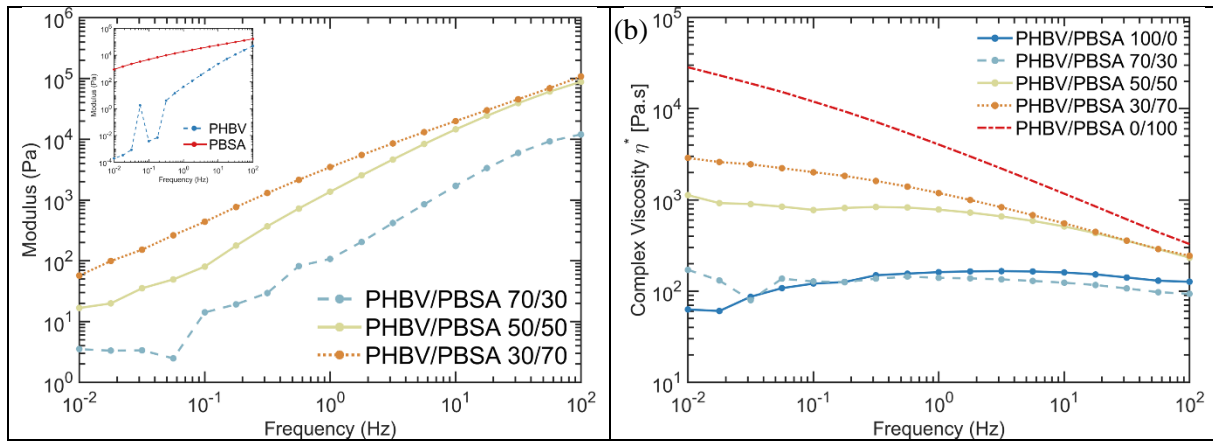


Figure III.2 : Mechanical spectrum of (a) storage modulus and (b) complex viscosity for neat PHBV, PBSA (inset in (a)), and PHBV/PBSA blends at 185°C after batch mixing. Data were recorded starting with high frequencies.

The insert in Figure 1a shows that PBSA featured typical terminal flow behavior with a terminal slope close to 2. PHBV showed a strong drop in modulus at 0.3 Hz caused by the thermal degradation of PHBV. For confirmation, an isothermal dynamic time sweep test of PHBV available in the supplementary information S3. PHBV degrades indeed quickly above its melting temperature (Weinmann & Bonten, 2019). Storage modulus (G') of PHBV/PBSA blends were between the neat polymers' values and increasing with PBSA content. Complex viscosity spectra (Figure 1b) evidenced that neat PHBV had Newtonian flow behavior in the observed frequency range while PBSA showed frequency dependent behavior. The change from PBSA dominated viscosity to PHBV dominated behavior was observed for blends with a concentration of PHBV equal to or higher than 50 wt%. This behavior revealed an inversion of the continuous flowing phase.

The flow of blends is characterized by the ratio of their viscosities, the capillary number, and the ratio of viscous to surface forces (Grace†, 1982). The ratio of viscosity respectively to the continuous phase, λ , predicts possible morphologies of two immiscible polymers and the critical capillary number when shear forces overcome surface tension. Based upon the spectra of complex viscosity and shear stresses between 30 and 100 Hz, ratios of shear viscosities

Chapter III

η_{PBSA}/η_{PHBV} (for PHBV as theoretical continuous phase) and η_{PHBV}/η_{PBSA} (for PBSA as theoretical continuous phase) were evaluated to 3.6-2.8 and 0.2-0.1, respectively. Large $\lambda_{\eta_{PBSA}/PHBV}$ values are indicative for high difficulty of dispersion of PBSA in PHBV as small droplets, whereas small droplets of PHBV in PBSA because of low $\lambda_{\eta_{PHBV}/PBSA}$ was very probable. The complex viscosity of PHBV-PBSA mixtures (η_{mix}^*) was calculated via a semi-logarithmic mixing rule (L. A. Utracki, 1991):

$$\log \eta_{mix}^* = w_{PBSA} \log \eta_{PBSA}^* + (1 - w_{PBSA}) \log \eta_{PHBV}^* \quad \text{Eq. III.2}$$

Predictions shown in Figure III.3 at different frequencies were in good agreement with experiments at PBSA concentration above 50 wt%, where small PHBV droplets were predicted. Phase separation was the likely cause of the deviation observed for 30 wt% PBSA, where large droplets were predicted.

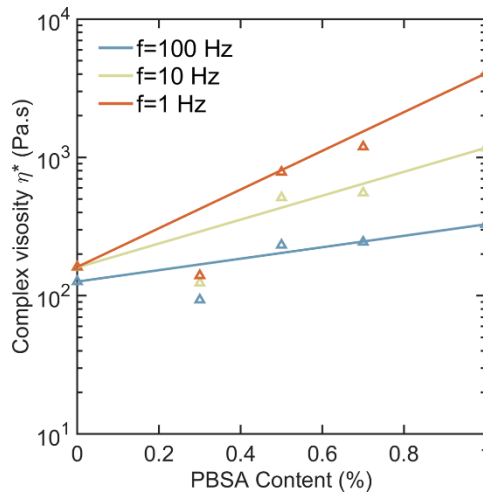


Figure III.3 : Complex viscosity as a function of PBSA content. The solid line represents the values calculated from the mixing rule .

III.4.2. Morphology of PHBV/PBSA blends

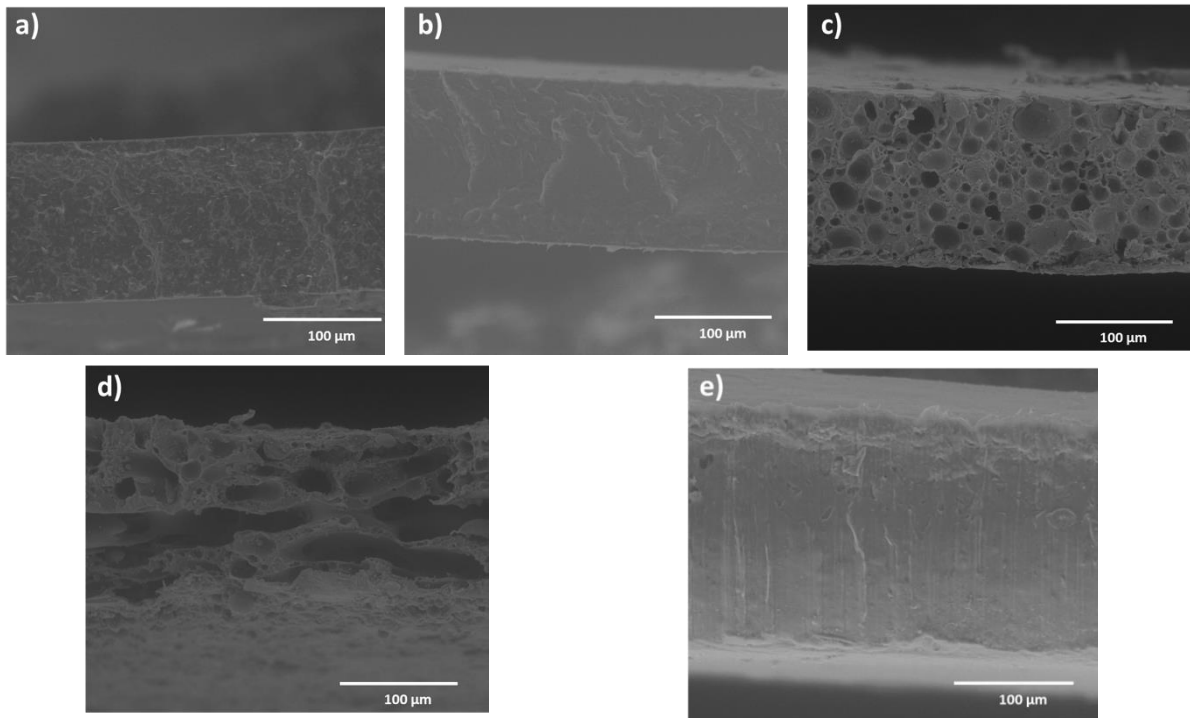


Figure III.4 : SEM images of cryo-fractured neat PHBV, PBSA and PHBV/PBSA blends: (a) neat PHBV, (b) neat PBSA, (c) 70/30, (d) 50/50, (e) 30/70

The morphology of blends after melt-mixing and thermo-compression was observed on cryo-fractured samples by SEM (Figure 3(a-e)). Neat PBSA showed a smooth surface (Figure III.4(b)), whereas neat PHBV presented a rugous surface (Figure III.4(a)) with fractured crystallites and white items identified as inorganic fillers (Idris Zembouai et al., 2013). Phase separation was detected in PHBV/PBSA as expected from the rheological analysis. Figure III.4(c) shows large PBSA droplets dispersed in PHBV for 70:30 PHBV/PBSA blend. For the 50:50 PHBV/PBSA blend, a co-continuous morphology was apparently observed. Further increase in PBSA content led to a phase inversion, with small droplets of PHBV in PBSA as expected from viscosity ratios. The developed morphologies of PHBV/PBSA were typical of immiscible blends.

III.4.3. Thermal properties of PHBV/PBSA blends

III.4.3.1. Melting behavior

Melting temperatures of neat PHBV and PBSA and of their blends were analyzed by DSC via protocol I (Figure III.5). Two distinct melting points (T_m) were identified at 174 °C and 86 °C for neat PHBV and PBSA, respectively. No change in melting temperature was observed in binary blends. Details are reported in Table III.1. Exothermic cold crystallization of PBSA was observed at $T_{CC} \approx -5$ °C. Cold crystallization due to incomplete crystallization of the copolymer PBS₅₉A₄₁ has been already described by Debuissy et al. (Debuissy, Pollet, & Avérous, 2017).

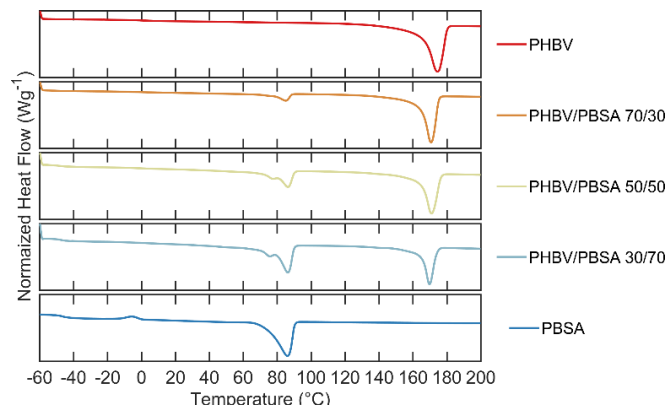


Figure III.5 : DSC curves of neat PHBV, neat PBSA and PHBV/PBSA blends recorded in the second heating scan following the protocol I

Table III.1 : Thermal properties of PHBV/PBSA blends evaluated by DSC from the second heating and cooling scans

| Samples | T_m (°C) | | T_c (°C) | | χ (%) | | T_g (°C) | |
|---------|------------|------|------------|------|------------|---------------------|------------|-----------|
| | PHBV | PBSA | PHBV | PBSA | PHBV | PBSA | PHBV | PBSA |
| 100/0 | 171±3 | n.d | 122± 1 | n.d | 68±1 | n.d | 2.4±0.4 | n.d |
| 70/30 | 169±2 | 86±2 | 117±1 | 50±1 | 67±2 | 33±5 | -1.5±0.1 | -48.6±2.3 |
| 50/50 | 169±2 | 87±1 | 116±2 | 49±5 | 61±1 | 39±6 | -3.1±0.8 | -47±1.3 |
| 30/70 | 169±1 | 87±1 | 114±5 | 47±5 | 67±6 | 43±2 | -3.3±0.3 | -46.4±2 |
| 0/100 | n.d | 88±3 | n.d | 38±3 | n.d | 45±4 ⁽¹⁾ | n.d | -45.9±1.6 |

⁽¹⁾ For calculation of PBSA crystallinity degree, cold crystallization was retrieved from melting enthalpy

III.4.3.2. Glass transition in the amorphous phase

Conventional heating scans are often not sensitive enough to reveal the relaxation of the amorphous phase of PHBV, because it accounts for a small quantity of the sample. The sensitivity problem is even greater in blends where the percentage of amorphous PHBV in the sample is still lower. Therefore a physical aging treatment of PHBV or PBSA was applied to reveal the T_g using the enthalpy of relaxation peak. DSC thermograms presented in Figure III.6(a,b) show typical thermograms; the quantified data are given in Table 1. Two separate T_g were identified in PHBV/PBSA blends. The presence of two distinct T_g is consistent with the observation of a nodular blend structure due to immiscibility, but the shift of the T_g of PHBV from 2 to -3 °C might indicate some level of compatibility.

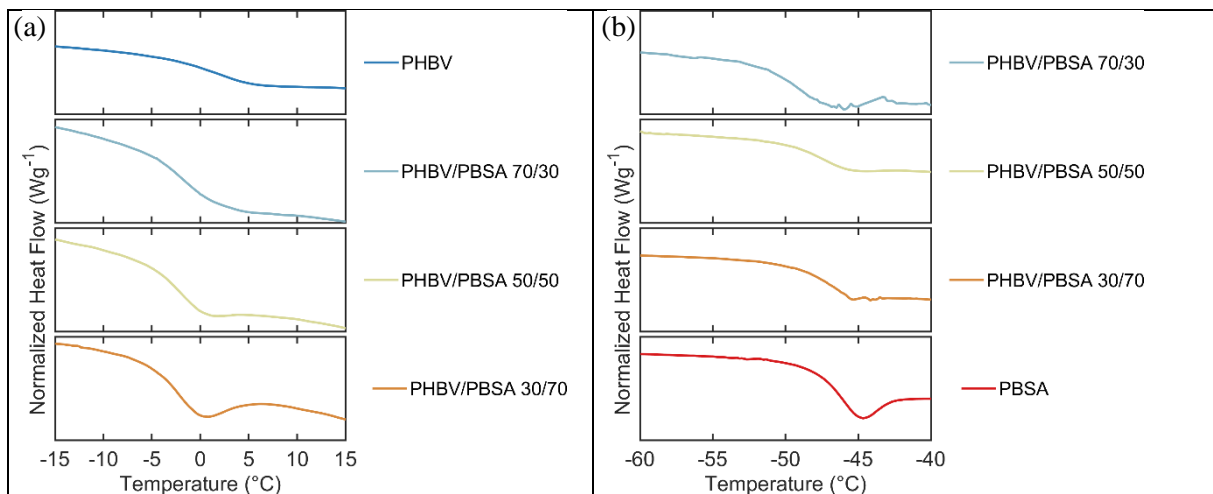


Figure III.6 : DSC curves of neat PHBV, neat PBSA and PHBV/PBSA blends aged at (a) -10°C and (b) -40°C

III.4.3.3. Non isothermal crystallization kinetics of PHBV/PBSA blends

Crystallization kinetics of PHBV/PBS blends were studied using non-isothermal crystallization (program II, Figure III.1). As shown in Figure 6, the crystallization peak temperature (T_c) of

Chapter III

PHBV shifted towards lower temperature, which suggests that the addition of PBSA slowed down the crystallization process of PHBV, while an increase in PBSA crystallization temperature with the addition of PHBV was observed. The quantification of the non-isothermal crystallization kinetics of the blends was carried out using the Avrami-Jeziorny method and Liu & Mo's model (Avrami, 1939, 1940, 1941; T. Liu, Mo, Wang, & Zhang, 1997). Both models are presented in the supplementary information S5.

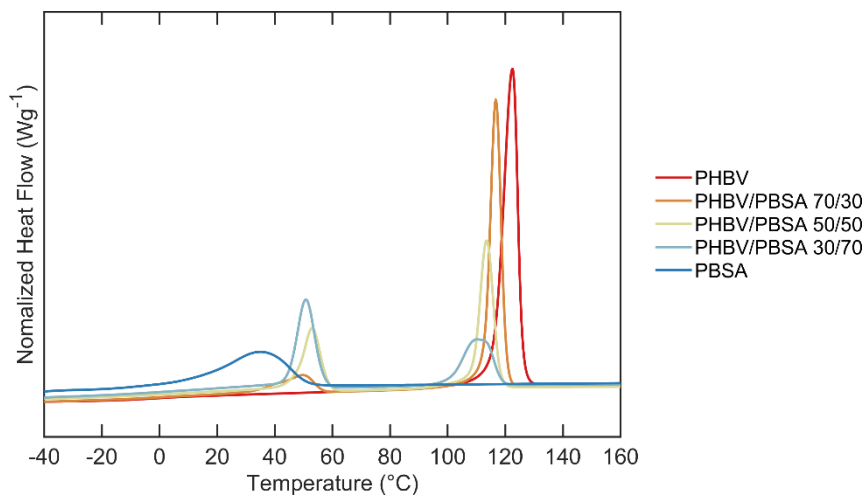


Figure III.7: Non-isothermal crystallization of neat PHBV, neat PBSA, and PHBV/PBSA blends recorded during cooling at $-10\text{ }^{\circ}\text{C}/\text{min}$ (protocol II)

The relative degree of crystallinity versus time for PHBV/PBSA blends showed a sigmoidal profile with a linear part between 0.2 and 0.6 % relative crystallinity (data available in supplementary information). The Avrami-Jeziorny analysis of non-isothermal crystallization kinetics was carried out within this range, and the double logarithmic form, for PHBV and PBSA, is shown in supplementary information S5. All obtained values for Avrami constants n_a , k_a and k_c are gathered in a synoptic table available in supplementary information S5. The crystallization peak temperature T_c and half time of crystallization $t_{1/2}$ calculated with the help of the Avrami-Jeziorny constants are presented in Table III.2. The $t_{1/2}$ of the blends was smaller than that of the neat polymers. Closer observation of the values shows that $t_{1/2}$ (PHBV)

Chapter III

decreased with increasing PBSA content. The minimum was obtained in blends containing small PBSA nodules (PHBV/PBSA 70/30) (see Figure III.4). There might have been a nucleating effect of the matrix on the nodule surfaces. PHBV also acted as a nucleating agent for PBSA, which allowed crystallization of PBSA at cooling rates higher than 30 °C/min.

Table III.2 : Avrami–Jeziorny parameters during nonisothermal crystallization of neat PHV, neat PBSA, and PHBV/PBSA blends

| Samples | Cooling | PHBV | | PBSA | |
|-----------------|---------|------------|-----------------|------------|-----------------|
| | | T_c (°C) | $t_{1/2}$ (min) | T_c (°C) | $t_{1/2}$ (min) |
| PHBV | 5 | 127.7 | 1.18 | n.d | n.d |
| | 10 | 123.8 | 0.93 | n.d | n.d |
| | 20 | 119.2 | 0.83 | n.d | n.d |
| | 30 | 114.5 | 0.84 | n.d | n.d |
| | 40 | 114.2 | 0.83 | n.d | n.d |
| | 50 | 111.2 | 0.88 | n.d | n.d |
| PBSA | 5 | n.d | n.d | 38.2 | 1.16 |
| | 10 | n.d | n.d | 29.3 | 0.94 |
| | 20 | n.d | n.d | 19.8 | 0.80 |
| | 30 | n.d | n.d | 23.2 | 0.77 |
| | 40 | n.d | n.d | - | - |
| | 50 | n.d | n.d | - | - |
| PHBV/PBSA 70/30 | 5 | 123 | 1.03 | 58.9 | 0.96 |
| | 10 | 118.8 | 0.90 | 54 | 0.85 |
| | 20 | 113.9 | 0.87 | 48.6 | 0.80 |
| | 30 | 110.5 | 0.85 | 45.3 | 0.78 |
| | 40 | 108.5 | 0.85 | 39.7 | 0.77 |
| | 50 | 105.3 | 0.84 | 28.7 | 0.77 |
| PHBV/PBSA 50/50 | 5 | 120.9 | 1.09 | 59 | 0.99 |

Chapter III

| | | | | | |
|-----------------|----|-------|------|------|------|
| | 10 | 116.4 | 0.90 | 54.4 | 0.86 |
| | 20 | 106.9 | 0.86 | 43.9 | 0.81 |
| | 30 | 111.5 | 0.80 | 48.7 | 0.80 |
| | 40 | 104.4 | 0.80 | 38.4 | 0.79 |
| | 50 | 101.2 | 0.82 | 26.2 | 0.79 |
| PHBV/PBSA 30/70 | 5 | 120.1 | 1.06 | 55.5 | 1.03 |
| | 10 | 115.6 | 0.86 | 49.9 | 0.88 |
| | 20 | 110 | 0.84 | 43 | 0.83 |
| | 30 | 104.6 | 0.77 | 34 | 0.82 |
| | 40 | 101.4 | 0.78 | 26.5 | 0.80 |
| | 50 | 98.4 | 0.77 | 11.3 | 0.80 |

To go further in the kinetic analysis of the present study, the model developed by Liu et al. 1997 was investigated (T. Liu et al., 1997). This model is characterized by two parameters, $F(T)$ and m (ratio of Avrami and Ozawa exponents). $F(T)$ represents the difficulty of the crystallization process because it denotes the required cooling rate to achieve a given degree of crystallinity. The $\log \alpha$ vs $\log t$ was plotted and obtained results are available in supplementary information S5. Both parameters, m and $F(T)$ were obtained from the slope and the intercept of the as-defined linear portion of $\log \alpha$ versus $\log t$, respectively. The results obtained are gathered in Table III.3 and show that for both phases, $F(T)$ increased with the increase of the relative degree of crystallinity, a behavior generally observed because crystallization slows down at high crystallinity degrees. Comparison of blends shows that the PHBV phase was much more sensitive to the blend morphology at the same level of crystallinity. The PHBV crystallization in blends was facilitated at the lower degrees of crystallinity, notwithstanding the morphology. Introduction of low amount of PBSA as small nodules in PHBV resulted in the lowest $F(T)$ values. The latter stages of crystallization showed, on the contrary, increase of $F(T)$. In blends with co-continuous structure, $F(T)$ reached a maximum at 80 % degree of crystallinity. The

Chapter III

$F(T)$ of PHBV dispersed inside of PBSA was also higher than the blank. These morphologies seemed to hinder the PHBV crystallization at the later stages. On the contrary, all $F(T)$ values of PBSA in blends were lowered than the blank. The introduction of PHBV in PBSA facilitated the crystallization by possibly inducing a nucleation effect since it reflects the difficulty of the crystallization process (H. Li, Lu, Yang, & Hu, 2015).

Table III.3 : Liu parameters during nonisothermal crystallization of neat PHBV, neat PBSA and PHBV/PBSA blends

| | $\chi(t)(\%)$ | PHBV | | | PBSA | | |
|--------------------|---------------|------|--------|-------|------|--------|-------|
| | | m | $F(T)$ | R^2 | m | $F(T)$ | R^2 |
| Neat PHBV | 20 | 0.92 | 10.11 | 0.97 | n.d | n.d | n.d |
| | 40 | 0.97 | 12.87 | 0.97 | n.d | n.d | n.d |
| | 60 | 1.04 | 15.88 | 0.98 | n.d | n.d | n.d |
| | 80 | 1.01 | 22.61 | 0.97 | n.d | n.d | n.d |
| Neat PBSA | 20 | n.d | n.d | n.d | 1.02 | 14.39 | 0.92 |
| | 40 | n.d | n.d | n.d | 1.1 | 27.51 | 0.92 |
| | 60 | n.d | n.d | n.d | 1.18 | 43.78 | 0.91 |
| | 80 | n.d | n.d | n.d | 1.21 | 63.79 | 0.91 |
| PHBV/PBSA 70/30 | 20 | 1.26 | 6.2 | 0.99 | 1.34 | 4.72 | 0.99 |
| | 40 | 1.31 | 8.56 | 1 | 1.45 | 9.67 | 0.99 |
| | 60 | 1.44 | 11.12 | 0.99 | 1.51 | 14.96 | 0.99 |
| | 80 | 1.51 | 20.21 | 1 | 1.48 | 23.65 | 0.99 |
| PHBV/PBSA 50/50 | 20 | 1.17 | 8.61 | 0.99 | 1.4 | 5.26 | 0.99 |
| | 40 | 1.26 | 12.42 | 0.99 | 1.53 | 10.25 | 0.99 |
| | 60 | 1.44 | 18.48 | 1 | 1.6 | 15.77 | 0.98 |
| | 80 | 1.49 | 34.64 | 0.99 | 1.59 | 26.25 | 0.98 |
| PHBV/PBSA 30/70 | 20 | 1.13 | 7.7 | 0.93 | 1.46 | 6.86 | 0.99 |
| | 40 | 1.12 | 13.61 | 0.9 | 1.63 | 13.45 | 1 |
| | 60 | 1.1 | 20.59 | 0.85 | 1.68 | 20.43 | 0.99 |
| | 80 | 1.1 | 29.73 | 0.83 | 1.65 | 32.99 | 0.99 |

III.4.3.4. Mechanical properties of PHBV/PBSA blends

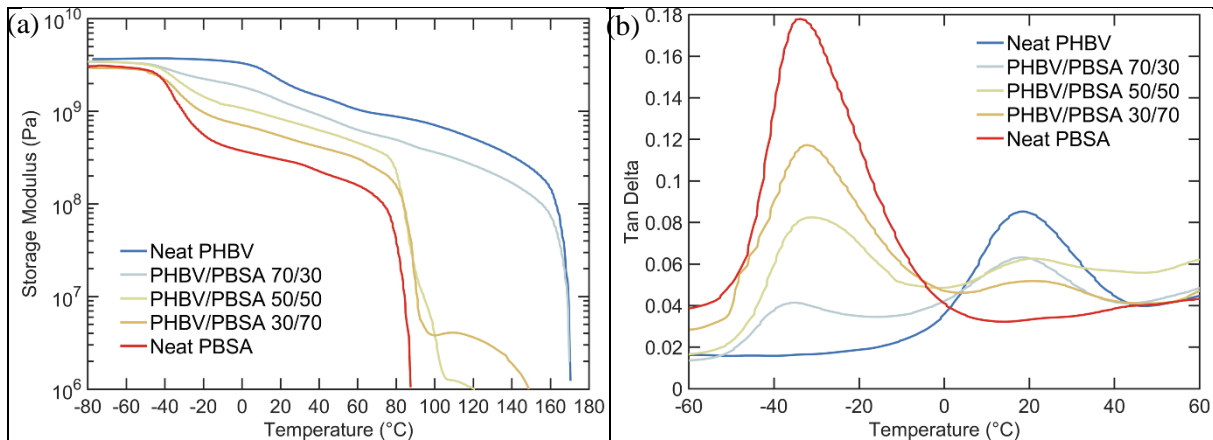


Figure III.8 : Evolution of (a) the elastic modulus and (b) $\tan\delta$ as function of Temperature for neat PHBV, neat PBSA and PHBV/PBSA blends

Figure III.8(a) shows the evolution of the elastic modulus (E') as a function of temperature ranging from -60 °C to 180 °C. PHBV featured, as expected a higher storage modulus values over the whole temperature range than PBSA. The addition of PHBV to PBSA increased the height of the rubbery plateau modulus but had a moderate impact on the increase of the flow temperature of PBSA. Even in the co-continuous blend, the material flowed below 100 °C. In the case of PHBV being the continuous phase, the decrease of the rubbery moduli of the nodular blends with respect to PHBV was observed without change in flow behavior. Table III.4 highlights E' values at relevant service temperatures, i.e., at room temperature (20 °C) and in freezer conditions (-20 °C). Figure III.8 (b) shows the evolution of $\tan \delta$ as a function of temperature ranging from -60 °C to 60 °C, which can be attributed to the dynamic glass transition temperature T_a determined as the maximum value of the peaks (T_a values are available in in supplementary information S6). Two distinct relaxation temperatures were identified and consistent of the immiscibility of PHBV and PBSA similar to previous observations from DSC.

Chapter III

Table III.4 : Determination of Storage Modulus E' and Mechanical properties of PHBV/PBSA blends obtained from DMA and tensile test measurements. respectively

| Samples | Storage Modulus (MPa) from DMA | | Tensile properties | | |
|---------|-----------------------------------|------|-------------------------|-----------------------------|----------------------------|
| | -20°C | 20°C | Young modulus* (MPa) | Stress at yield (MPa) | Elongation at break (%) |
| 100/0 | 3625 | 2153 | 3485±63 | 22±2 | 0.98±0.1 |
| 70/30 | 2247 | 1297 | 2227±108 | 19±2.5 | 1.48±0.4 |
| 50/50 | 1438 | 829 | 1360±125 | 12±1.9 | 1.48±0.2 |
| 30/70 | 966 | 543 | 833±147 | 12±1.6 | 3.1±0.8 |
| 0/100 | 553 | 303 | 332±8 | 15±1.4 | 134.8±48 |

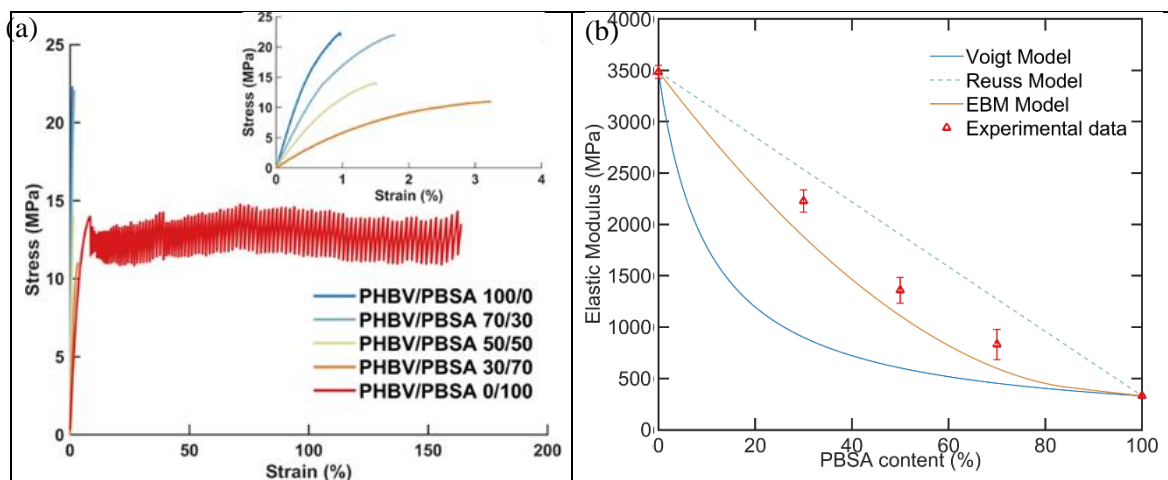


Figure III.9 : (a) Typical stress-strain curves of tensile test of PHBV/PBSA blends except neat PBSA and (b) Evolution of the elastic modulus of PHBV/PBSA blends depending on PBSA content (Tensile test measurements)

The mechanical properties of the PHBV-based blends were assessed with tensile tests and typical stress-strain curves, as well as the evolution of the elastic modulus with PBSA content are shown in Figure III.9(a) and Figure III.9(b), respectively. Typical fragile behavior was observed for neat PHBV with low elongation at break. Several authors have already discussed that the brittle behavior of PHBV can be caused by i) the cold crystallization of the amorphous phase at ambient temperature, ii) glass transition temperature close to room temperature, and iii) radial or circumferential cracks potentially contained in spherulites of PHBV with low content of 3HV (Barham & Keller, 1986; El-Hadi et al., 2002). The existence of these cracks is supposed to be caused by the difference in the thermal expansion coefficients of the material

Chapter III

along the radius and the circumference of crystallites, which generates drastic internal stresses (Laycock et al., 2014).

PBSA featured ductile behavior with high elongation at break. Stress-oscillation of pure PBSA was observed. The occurrence of stress-oscillation was reported for poly(butylene succinate) due to alternating regions of highly oriented crystalline zones and micro cavities due to crazing and voiding (C. Y. Wan et al., 2018; T. Wan, Zhang, Liao, & Du, 2015). It generated alternating transparent/opaque bands as shown in Figure III.10(a), and video of the phenomenon is available in supplementary information S7.

Table III.4 reports the tensile properties of PHBV, PBSA, and its blends. The apparent Young modulus was in accordance with the E' values at room temperature. The increase of the PBSA content lowered the stress at break. The obtained evolution of the elongation at break was disappointing. Even when the ductile polymer PBSA made the continuous phase, the samples broke at 3 % elongation. Apparently, although there might be some interfacial compatibility between PBSA and PHBV, an efficient stress transfer between both phases could not be achieved. To understand the result, the data were modeled with the Reuss (parallel resistances), Voigt (serial resistances):

$$E^n = \phi_1 E_1^n + \phi_2 E_2^n \quad \text{Eq. III.3}$$

where E_1 and E_2 are the elastic modulus of phase 1 and 2, ϕ_1 and ϕ_2 the volume fraction of phase 1 and phase 2, and exponent n characterizes the type of model with $n=1$ (Parallel or Reuss model) or $n=-1$ (Series or Voigt model)

The data were also modeled with the Equivalent Box Model (EBM), which is detailed in supplementary information S8 (Kolarik, 1996). Based on the percolation theory, critical volume fractions were set to $v_{1cr} = v_{2cr} = 0.16$ (De Gennes, 1976).

Chapter III

The resulting tensile modulus of two components blend (E_b) is given as the sum $E_p v_p + E_s v_s$ (Kolarik, 1996):

$$E_b = E_1 v_{1p} + E_2 v_{2p} + v_s^2 / \left(\frac{v_{1s}}{E_1} + \frac{v_{2s}}{E_2} \right) \quad \text{Eq. III.4}$$

where E_1 and E_2 are the Young's moduli of phases 1 and 2 and $v_{i,p}$ and $v_{i,s}$ are the total volume fractions of the parallel branch and series branch, respectively.

Prediction of strength can be modeled as follows (Kolařík, 1996):

$$S_b = S_1 v_{1p} + S_2 v_{2p} + AS_2 v_s \quad \text{Eq. III.5}$$

Where $S_1 > S_2$ and S_1 and S_2 are the strengths of phase 1 and 2, respectively. While A can be identified as a level of interfacial bonding.

The comparison of the experimental results with the different models (Figure III.10(b)) shows that the evolution of the Young modulus (E) with increasing PBSA content in the blends was fairly well captured by the EBM model using the universal parameters. This observation further confirmed the immiscibility between both components, similarly to PHBV/PBS blends (Phua et al., 2015). From Figure III.10(b), the experimental data on σ (PHBV/PBSA 70/30) which are more sensitive to interfacial adhesion. EBM predictive model can indicate if the interfacial adhesion is strong ($A=1$) or weak ($A=0$), as explained in detail in supplementary information S8. The results showed that a low adhesion factor (A) needs to be assumed to describe the behavior of the blends at high PBSA content. The strain at break was at any composition lower than the strain at break of the stronger polymer, PHBV, which shows that the materials fractured by debonding at the interface.

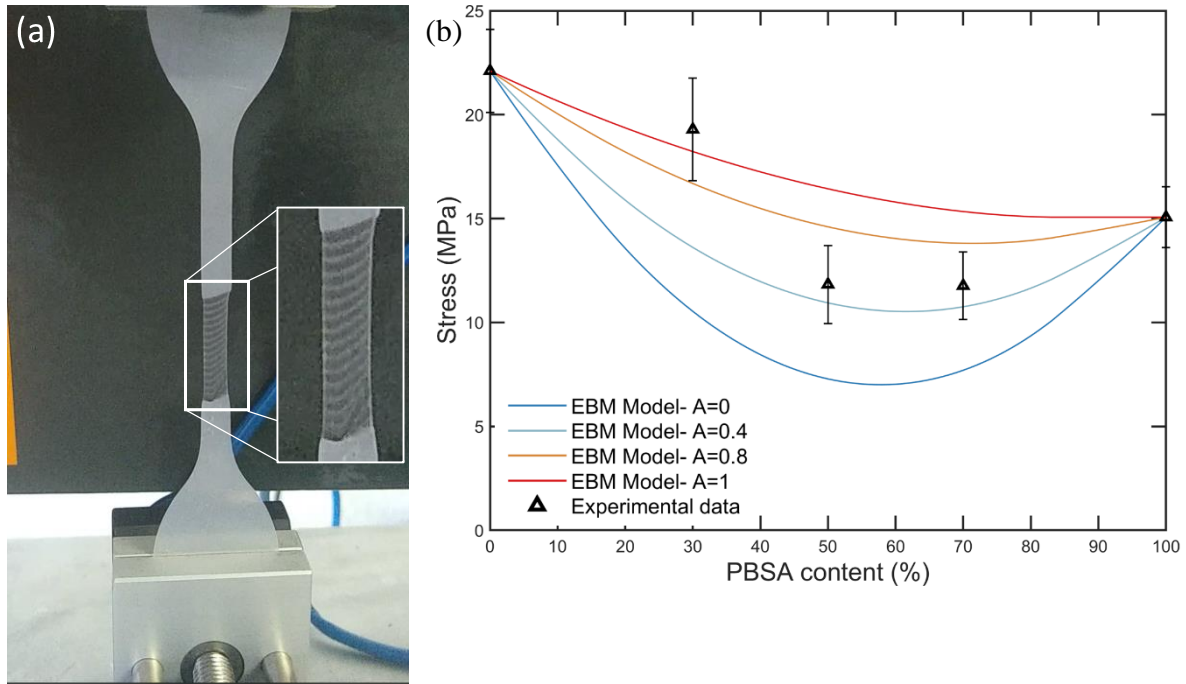


Figure III.10 : (a) Stress-oscillation of PBSA samples during tensile testing and (b) Evolution of the tensile stress of PHBV/PBSA blends with representation of EBM model at different level of interfacial adhesion (A)

III.5.Conclusion

This study presents a detailed investigation of thermo-mechanical and rheological properties of PHBV/PBSA blends prepared by batch mixing. PHBV and PBSA were immiscible. As predicted by the viscosity ratio between the polymers and confirmed by SEM observation, PBSA formed small nodules in PHBV, while PHBV formed large inclusions in PBSA. A co-continuous blend morphology was observed in 50/50 PHBV/PBSA blends. The investigation of the crystallization kinetics showed that the crystallization rate of PHBV and PBSA increased in the blends, most probably due to mutual nucleation. However, the crystallization rates observed at high PHBV crystallinity were slowed down when PHBV was dispersed in large nodules in PBSA or blends had co-continuous structure. The mechanical properties were successfully modeled with the EBM model, including parallel and serial resistances, and showed that the rigidity of the material could be modulated using PBSA. However, the

Chapter III

elongation at break was governed by PHBV featuring brittle fracture even in case PBSA was the continuous phase, in accordance with a model of serial resistances. The analysis of the adhesion factor showed that there was most likely debonding at the interfaces. In conclusion, PHBV/PBSA blends have improved melt viscosity and accelerated crystallization kinetics, but for successful improving mechanical properties, compatibilizers will be necessary.

Supporting Information

Thermal, mechanical and rheological properties of binary poly(3-hydroxybutyrate-co-3-hydroxyvalerate) / poly(butylene-co-succinate-co-adipate) blends

Benjamin Le Delliou¹, Mickael Castro², Stephane Bruzard², Olivier Vitrac¹, Sandra Domenek^{1,*}

¹UMR 0782 SayFood Paris-Saclay Food and Bioproduct Engineering Research Unit, INRAE, AgroParisTech, Université Paris-Saclay, 91300, Massy France

² Smart Plastics Group, Université de Bretagne Sud, UMR CNRS 6027, IRDL, 56100 Lorient, France;

Corresponding author : Sandra Domenek, UMR SayFood
sandra.domenek@agroparistech.fr

S.1. Internal mixing of PHBV/PBSA blends

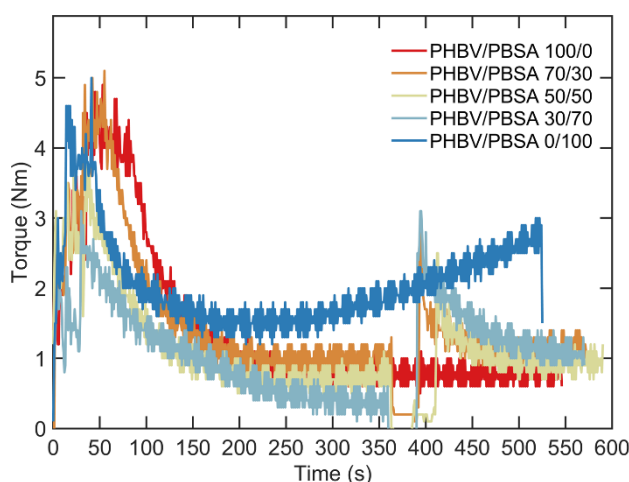


Figure S 1: Evolution of torque during melt mixing of PHBV/PBSA blends

PHBV/PBSA blend behavior during mixing was assessed by monitoring the torque evolution over time for five PBSA ratios, as shown in Figure S 1. During the first 300 s, pure PHBV exhibited an exponential torque decay down to a plateau below 1 N·m controlled by its viscosity at molten state. After melting, PHBV/PBSA blend showed stable torque at ca. 1 N·m independent of PBSA content. Comparatively, the torque of pure PBSA was twice higher due to its higher melt viscosity.

S.2. Thermo-gravimetric analysis of PHBV/PBSA blends

The thermal stability of the blends was assessed by Thermo-Gravimetric Analysis (TGA, Q500, TA Instruments). The experiment was performed from +25 °C to +450 °C in a high-resolution mode where the heating rate is controlled by the decomposition rate of the sample. An average weight of 10 mg was used each time.

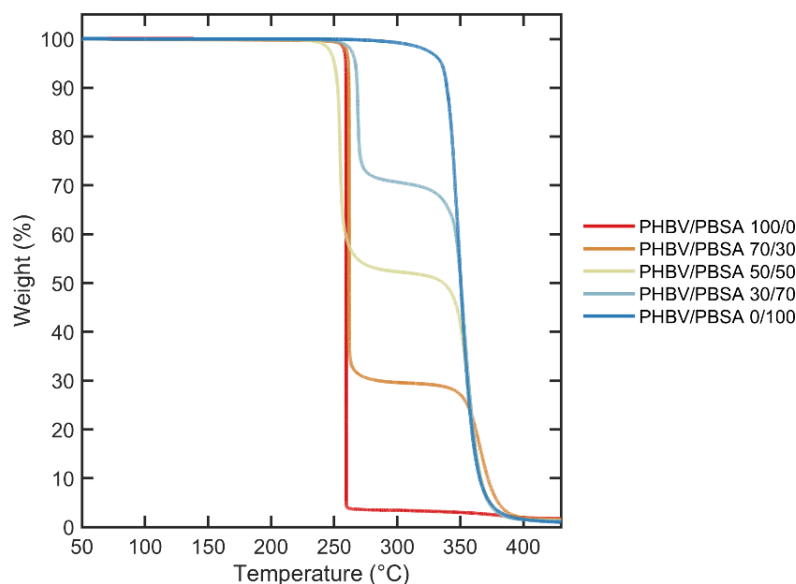


Figure S 2: Thermogravimetric analysis of neat PHBV, neat PBSA, and PHBV/PBSA blends

The thermo-gravimetric analysis was used to confirm the weight ratio of PBSA in the PHBV/PBSA blends. In fact, PHBV and PBSA have two different degradation temperatures, which were used to confirm the initial ratio of PBSA phase in the blend, as shown in Figure S 2. Secondly, thermo-gravimetric analysis was used to study the thermal stability of the blends depending on the PBSA content added. Both PHBV and PBSA show a single-step decomposition. PHBV degrades at about 250 °C and presents a high degradation rate, while PBSA degrades at a temperature of about 350 °C with slower kinetics. PHBV/PBSA blend curves present two degradation steps where the first step is correlated to the degradation of the PHBV phase and the second one at higher temperature to the PBSA phase.

S.3. Thermal stability of PHBV

The thermal stability of PHBV was assessed following a dynamic time sweep test during one h at 0.1 % and 1 Hz. As shown in Figure S 3, after 20 min, the complex viscosity dropped by decade from 1238 Pa.s to 92 Pa.s. PHBV undergoes rapid thermal degradation showing poor thermal stability. This behavior was expected given the very narrow processing window of PHBV and was already observed by Gerard (Thibaut Gerard & Budtova, 2012);

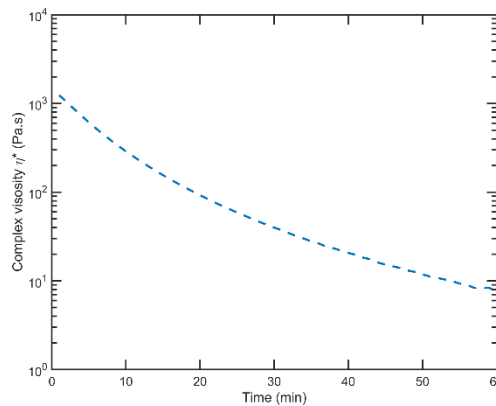


Figure S 3: Study of the thermal stability of PHBV with evolution the complex viscosity in time at strain 0.1 %, frequency 1 Hz and $T= 185$ °C

S.4. Determination of the equilibrium melting temperature

$$T_m^0$$

Program III, Figure S 4, monitored crystallization kinetics at different temperatures. Samples were quenched down to the desired crystallization temperature from the melt: 120 °C, 110 °C, 100 °C, and 90 °C. Crystallization kinetics were recorded isothermally until equilibrium. Corresponding melting temperatures were analyzed during heating to 190 °C at 10 °C/min.

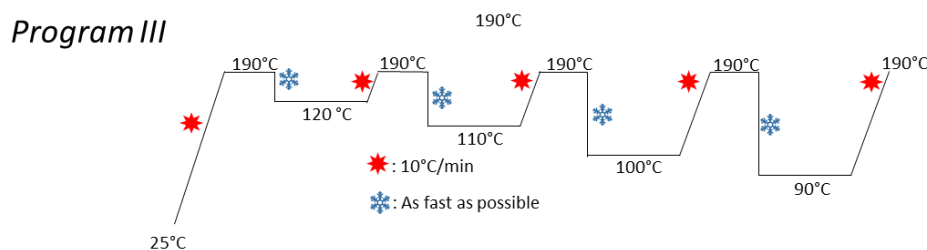


Figure S 4.: Schematic representation of DSC protocol of Program III

The equilibrium melting temperature T_m^0 of PHBV in blends was determined by following the Hoffman-Weeks (H-W) method (Hoffman & Weeks, 1962) after heating the crystallized

Chapter III

samples at 10 °C/min. Collected melting temperatures T_m were plotted against crystallization temperatures, as shown in Figure S 5. The evolution is extrapolated linearly until intercepting the line $T_m = T_c$ which identifies the condition $T_m = T_m^0$. The obtained values with H-W method are gathered in Table S1. For neat PHBV, T_m^0 was found equal to 175 °C in agreement with the previous determination of 178 °C \pm 5 °C reported with PHBV-3HV% (ENMAT Y1000, TianAn Biopolymer, China) (Puente, Esposito, Chivrac, & Dargent, 2013). T_m^0 values in PHBV/PBSA blends were similar, except for PHBV/PBSA 30/70, whose value shifted to 182 °C.

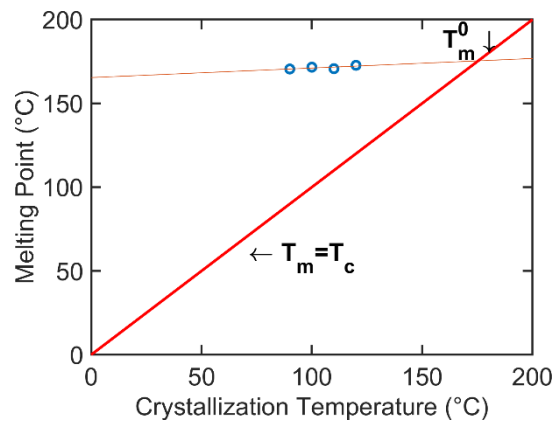


Figure S 5: Determination of equilibrium melting temperature from isothermal crystallization kinetics, example shown for neat PHBV sample

Table S1. Equilibrium melting temperature from isothermal crystallization kinetics

| Samples | | T_m^0 (°C) |
|-----------|-------|--------------|
| PHBV/PBSA | 100/0 | 175 |
| | 70/30 | 175 |
| | 50/50 | 174 |
| | 30/70 | 182 |
| | 0/100 | n.d |

S.5. Avrami-Jeziorny analysis of non-isothermal crystallization kinetics

The relative crystallinity degree (χ), as a function of temperature (T), is calculated from the energy released over the nonisothermal crystallization process using the running integral of the crystallization enthalpy recorded by DSC. It is defined as:

Chapter III

$$\frac{\int_{T_0}^T \left(\frac{dH_c}{dT}\right) dT}{\int_{T_0}^{T_\infty} (dH_c/dT) dT}, \quad \text{Eq. III.6}$$

where T_0 and T represent the onset and end of crystallization temperature, respectively and dH_c is the measured enthalpy of crystallization for an infinitesimal temperature range dT .

Since it can be considered that the difference between the sample temperature and DSC furnace is negligible, then the relative crystallinity versus time can be obtained from Eq. III.7, where α is the cooling rate ($^{\circ}\text{C}/\text{min}$) and t represents time (min):

$$t = \frac{T_0 - T}{\alpha}, \quad \text{Eq. III.7}$$

The relative degree of crystallinity versus time for PHBV/PBSA blends is represented in Figure S 6(a) and Figure S 6(b) for PHBV and PBSA phase, respectively. All curves showed a sigmoidal profile with a linear part between 0.2 and 0.6 % relative crystallinity. The Avrami-Jeziorny analysis of non-isothermal crystallization kinetics was carried out within this range.

All obtained values for Avrami constants n_a , k_a and k_c are gathered in Table S2.

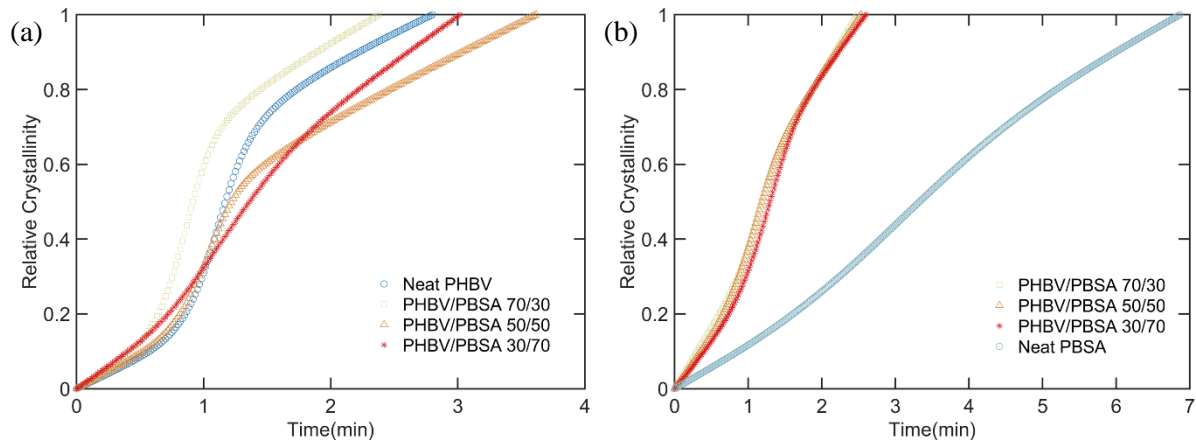


Figure S 6: Variation of relative crystallinity versus crystallization time for PHBV/PBSA blend ratios related to a) PHBV phase and b) PBSA phase for non-isothermal crystallization at $10^{\circ}\text{C}/\text{min}$

The study of the crystallization kinetics was conducted using the most common model to describe the overall isothermal crystallization that is the Avrami model (Avrami, 1939, 1940, 1941). It relates on the relative crystallinity as a function of time following Eq. III.8:

$$\chi(t) = 1 - \exp(-k_a t^{n_a}) \in [0,1] \quad \text{Eq. III.8}$$

By taking the double logarithmic form of Equation S3, then it can be transformed into Eq. III.9 :

$$\log(-\ln(1 - \chi(t))) = \log k_a + n_a \log t, \quad \text{Eq. III.9}$$

where k_a is the Avrami crystallization rate constant and n_a the Avrami exponent gives information about nucleating and growth geometry.

Chapter III

Both Avrami parameters, n_a and k_a , can be obtained from the slope and intercept of the as-defined linear portion of $\log(-\ln(1-X(T)))$ versus $\log t$, respectively (Figure S 7 (a,b)).

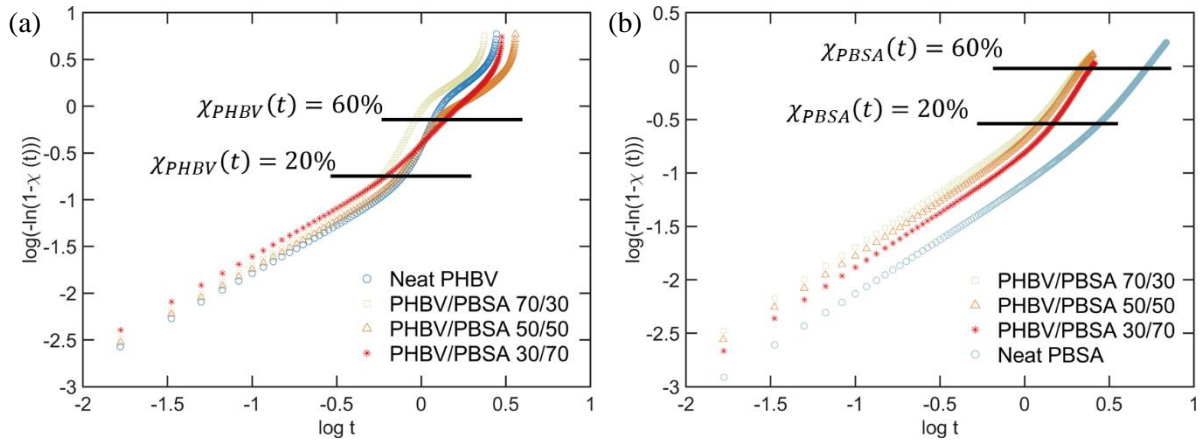


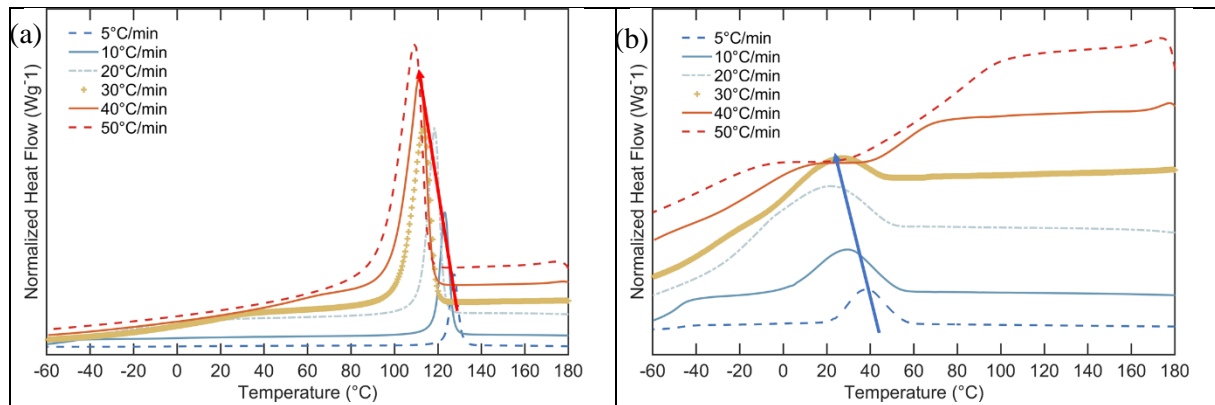
Figure S 7: Plots of $\log(-\ln(1-X(T)))$ versus $\log t$ for non isothermal crystallization at $10^\circ\text{C}/\text{min}$ for PHBV/PBSA blend with a) PHBV phase and b) PBSA phase

Given the non-isothermal conditions and based on Jeziorny recommendations, the value k_a should be corrected by taking into account the cooling rate as introduced in Eq. III.10 (Jeziorny, 1978):

$$\log k_c = \frac{\log k_a}{\alpha} \quad \text{Eq. III.10}$$

From the fitted Avrami-Jeziorny parameters, the half time of crystallization $t_{1/2,c}$ can be estimated according to Eq. III.11:

$$t_{1/2,c} = \left(\frac{\ln 2}{k_c} \right)^{1/n_a} \quad \text{Eq. III.11}$$



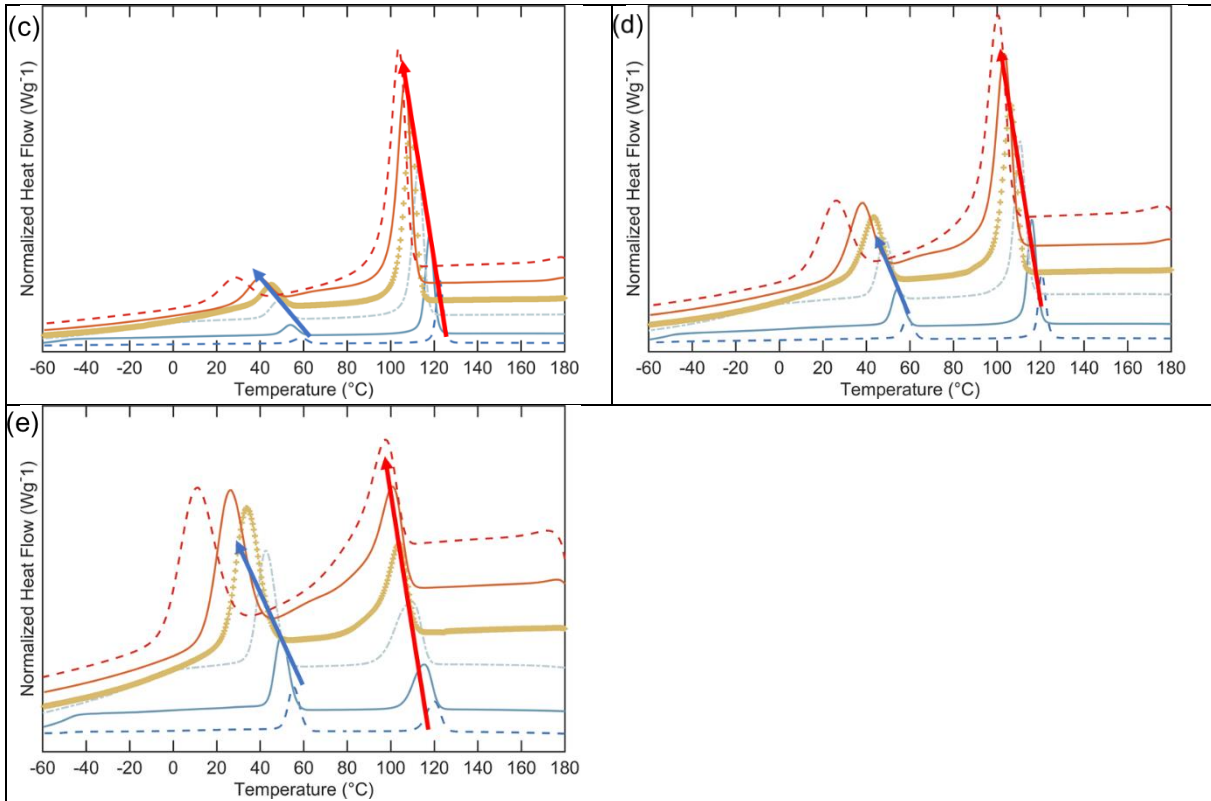


Figure S 8: DSC curves for non-isothermal crystallization at various cooling rate of (a) neat PHBV, (b) neat PBSA and PHBV/PBSA blends, i.e. (c) 70/30, (d) 50/50, (e) 30/70

For both phases, the rate constant k_c increased from 5 °C/min to 20 °C/min while no change was observed for a higher cooling rate with a value close to unity. Evaluation of n_a brings information on the type of homogeneous or heterogeneous nucleation. In non-isothermal crystallization kinetic studies, n_a values can be used to compare systems. A decrease in n_a of PHBV was observed with the incorporation of PBSA, indicating a diminishing of the dimension of crystallization. The $F(T)$ values of PBSA phase remained stable.

Chapter III

Table S2. Avrami–Jeziorny parameters during nonisothermal crystallization of neat PHV, neat PBSA and PHBV/PBSA blends

| Materials | Cooling | n | Ka | Kc | n | Ka | Kc |
|------------------------|---------|-----|------|-----|-----|------|-----|
| PHBV | 5 | 4.6 | 0 | 0.3 | n.d | n.d | n.d |
| | 10 | 3.7 | 0.38 | 0.9 | n.d | n.d | n.d |
| | 20 | 2.1 | 1.14 | 1 | n.d | n.d | n.d |
| | 30 | 2.4 | 4.91 | 1.1 | n.d | n.d | n.d |
| | 40 | 2.2 | 7.63 | 1.1 | n.d | n.d | n.d |
| PBSA | 50 | 3.6 | 33.2 | 1.1 | n.d | n.d | n.d |
| | 5 | n.d | n.d | n.d | 1.8 | 0.04 | 0.5 |
| | 10 | n.d | n.d | n.d | 1.5 | 0.06 | 0.8 |
| | 20 | n.d | n.d | n.d | 1.5 | 0.2 | 0.9 |
| | 30 | n.d | n.d | n.d | 1.3 | 0.7 | 1 |
| PHBV: PBSA 70/30 | 40 | n.d | n.d | n.d | - | - | - |
| | 50 | n.d | n.d | n.d | - | - | - |
| | 5 | 3.7 | 0.1 | 0.6 | 1.9 | 0.2 | 0.7 |
| | 10 | 3.2 | 0.91 | 1 | 1.4 | 0.3 | 0.9 |
| | 20 | 3 | 3.25 | 1.1 | 1.7 | 1.5 | 1 |
| PHBV: PBSA 50/50 | 30 | 2.6 | 6.41 | 1.1 | 1.6 | 2.1 | 1 |
| | 40 | 2.5 | 9.18 | 1.1 | 1.5 | 2.3 | 1 |
| | 50 | 2.3 | 10.3 | 1.1 | 1.5 | 2.6 | 1 |
| | 5 | 3.5 | 0.03 | 0.5 | 2.1 | 0.2 | 0.7 |
| | 10 | 2.5 | 0.4 | 0.9 | 1.5 | 0.2 | 0.9 |
| PHBV: PBSA 30/70 | 20 | 2.6 | 1.29 | 1 | 1.9 | 1.4 | 1 |
| | 30 | 1.7 | 1.78 | 1 | 1.8 | 1.9 | 1 |
| | 40 | 1.8 | 2.33 | 1 | 1.7 | 2.2 | 1 |
| | 50 | 2 | 3.77 | 1 | 1.6 | 2.5 | 1 |
| | 5 | 1.6 | 0.1 | 0.6 | 2.3 | 0.1 | 0.7 |
| PHBV: PBSA 30/70 | 10 | 1.8 | 0.4 | 0.9 | 1.4 | 0.2 | 0.8 |
| | 20 | 2 | 2.5 | 1 | 2 | 0.9 | 1 |
| | 30 | 1.5 | 1.3 | 1 | 1.9 | 1.3 | 1 |
| | 40 | 1.5 | 1.7 | 1 | 1.8 | 1.8 | 1 |
| | 50 | 1.4 | 1.9 | 1 | 1.7 | 2 | 1 |

Chapter III

To go further in the kinetic analysis of the present study, the model developed by Liu et al. (T. Liu et al., 1997), was investigated. Liu's model combines the Avrami and Ozawa model (Ozawa, 1971), which was developed by Ozawa et al. (Ozawa, 1971), from the Avrami equation. The degree of conversion at temperature T amounts to Eq. III.12:

$$\chi(T) = 1 - \exp\left(-\frac{k_0}{\alpha^{n_0}}\right), \quad \text{Eq. III.12}$$

where k_0 and n_0 are the Ozawa rate constant and exponent, respectively, and α the constant cooling rate. Then by taking the double logarithmic form of Equation S7, then it can be transformed into Eq. III.13:

$$\log(-\ln(1 - \chi(T))) = \log k_0 - m_0 \log \alpha, \quad \text{Eq. III.13}$$

where m is the ratio of the Ozawa and the Avrami exponent ($m = n_a/m_o$).

The Liu and Mo model is defined as the combination of the double logarithmic form of the Avrami and Ozawa (T. Liu et al., 1997), which gives Eq. III.14:

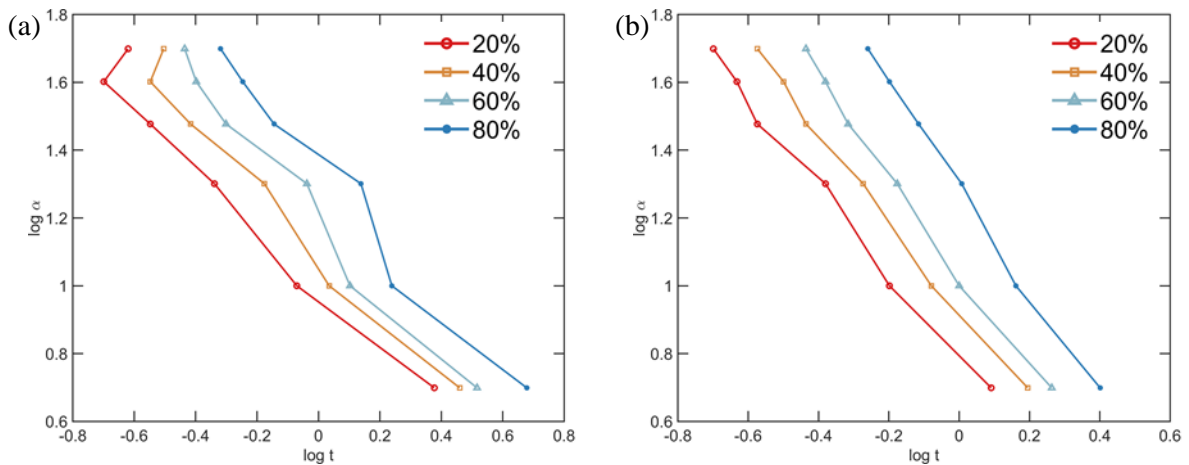
$$\log k_a - n_a \log t = \log k_0 - m_0 \log \alpha, \quad \text{Eq. III.14}$$

and rewritten as Eq. III.15:

$$\log \alpha = \log F(T) - m \log t, \quad \text{Eq. III.15}$$

where $F(T) = [(k_0/k_c)^{\frac{1}{n_0}}]$ and as previously said m is the ratio of the Ozawa and the Avrami exponent ($m = n_a/m_o$).

The $\log \alpha$ vs $\log t$ was plotted, and obtained results are available in Figure S 9(a-d) and Figure S 10(a-d) for PHBV and PBSA phases, respectively.



Chapter III

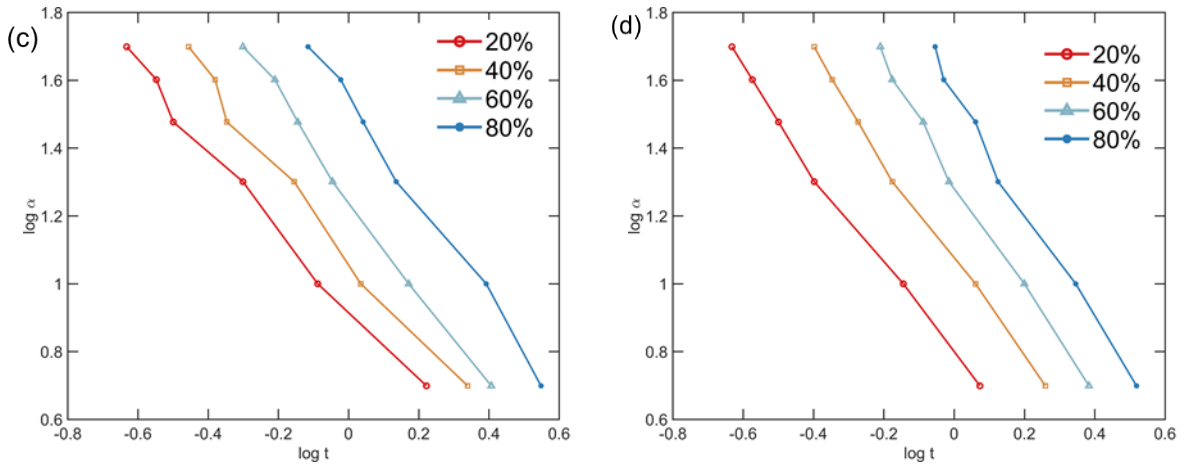


Figure S 9: Plots of $\log \alpha$ versus $\log t$ for non-isothermal crystallization for PHBV-phase of (a) Neat PHBV, (b) PHBV/PBSA 70/30, (c) PHBV/PBSA 50/50, (d) PHBV/PBSA 30/70

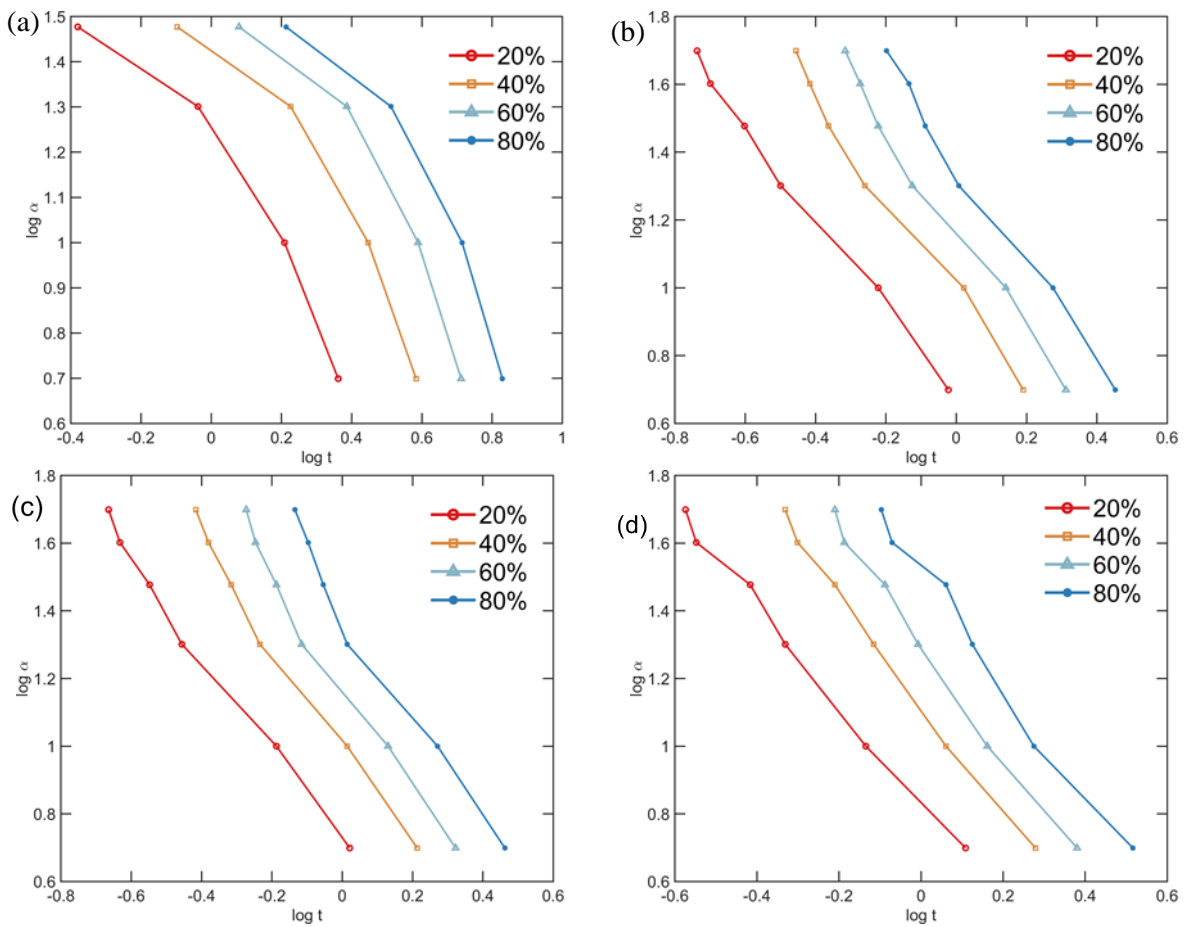


Figure S 10: Plots of $\log \alpha$ versus $\log t$ for non-isothermal crystallization for PBSA-phase of (a) Neat PBSA, (b) PHBV/PBSA 70/30, (c) PHBV/PBSA 50/50, (d) PHBV/PBSA 30/70

S.6. Dynamic mechanical analysis

Table S3. Determination of Storage Modulus E' and T_α values of PHBV/PBSA blends obtained from DMA

| Samples | | $T_\alpha^{(1)}$ | |
|-----------|-------|------------------|------|
| | | PHBV | PBSA |
| PHBV/PBSA | 100/0 | 19.6 | n.d |
| | 70/30 | 19.5 | -35 |
| | 50/50 | 21.7 | -33 |
| | 30/70 | 23.8 | -33 |
| | 0/100 | n.d | -35 |

⁽¹⁾ Determined as the maximum value of the $\tan \delta$ peaks

The dynamic glass transition temperature determined as the maximum value of the $\tan \delta$ peaks is reported in Table S3. As expected, two distinct relaxation temperatures were observed because of the immiscibility of PHBV and PBSA, which is coherent with previous observations from DSC. The T_α attributed to PHBV and PBSA could reasonably be described as stable since no significant shift towards lower and higher temperatures was observed for PHBV and PBSA phase, respectively. Hence, this result brings further confirmation that PHBV and PBSA components are both immiscible.

S.7. Equivalent box model

In the present study, the prediction of the elastic modulus was monitored using the Equivalent Box Model (EBM). The effective elasticity modulus was framed by the Reuss (parallel resistances), Voigt (serial resistances) models:

$$E^n = \phi_1 E_1^n + \phi_2 E_2^n \quad \text{Eq. III.16}$$

where E_1 and E_2 are the elastic modulus of phase 1 and 2, ϕ_1 and ϕ_2 the volume fraction of phase 1 and phase 2, and exponent n characterizes the type of model with $n=1$ (Parallel or Reuss model), $n=-1$ (Series or Voigt model)

Chapter III

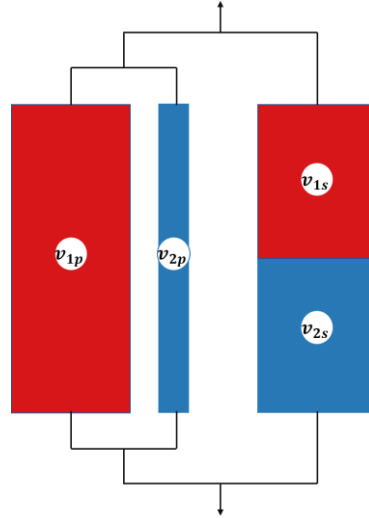


Figure S 11: Schematic representation of an equivalent box model (EBM) for a binary blend

More complex models can be required since the representation of the mechanical properties with simple parallel or series models cannot be accurately used. The equivalent box model (EBM) relates on the existence of two volume fractions where a volume fraction that acts in parallel and a volume fraction that acts in series (Figure S 11) (Kolarik, 1996). The EBM model is a two-parameter model, as of four volume fraction v_{ij} , only two are independent (Phua et al., 2015). The fractions are linked as follows:

$$\begin{aligned} v_p &= v_{1p} + v_{2p} & v_s &= v_{1s} + v_{2s} \\ v_1 &= v_{1p} + v_{1s} & v_2 &= v_{2p} + v_{2s} \\ v_1 + v_2 &= v_p + v_s = 1 \end{aligned} \quad \text{Eq. III.17}$$

where v_p and v_s are the total volume fractions of the parallel branch and series branch, respectively.

The tensile moduli of the parallel (E_p) and series (E_s) branches of the EBM can be expressed by the following equations:

$$E_p = \frac{E_1 v_{1p} + E_2 v_{2p}}{v_p} \quad E_s = \frac{v_s}{\frac{v_{1s}}{E_1} + \frac{v_{2s}}{E_2}} \quad \text{Eq. III.18}$$

where E_1 and E_2 are the Young's moduli of phases 1 and 2, respectively.

The resulting tensile modulus of two components blend (E_b) is then given as the sum $E_p v_p + E_s v_s$ (Kolarik, 1996):

$$E_b = E_1 v_{1p} + E_2 v_{2p} + v_s^2 \left(\frac{v_{1s}}{E_1} + \frac{v_{2s}}{E_2} \right) \quad \text{Eq. III.19}$$

The main issue comes from the evaluation of v_{ij} . From percolation theory (De Gennes, 1976), the contribution of one component is negligible and gives:

$$E_{1b} = E_0 (v_1 - v_{1cr})^q \quad \text{Eq. III.20}$$

Chapter III

where E_0 is a constant, q is the critical exponent, which assumes a value of 11/6 for a three-dimensional lattice (De Gennes, 1976).

From experimental results (De Gennes, 1976; Lyngaae-Jorgensen et al., 1993), it has been shown that Equation S15 can plausibly fit the experimental data for blends in the range $v_{1cr} < v_1 < 1$ (where $E_1 \gg E_2$) so that the modulus of the neat component 1 can be expressed as follows:

$$E_1 = E_0(v_1 - v_{1cr})^{q1}, \quad \text{Eq. III.21}$$

which gives:

$$E_{1b} = E_1[v_1 - v_{1cr}]/(1 - v_{1cr})^{q1}. \quad \text{Eq. III.22}$$

Based on the percolation theory, where the assumption that the contribution of the second component can be negligible when $E_1 \gg E_2$, the contribution E_2v_{2p} of component 2, which is coupled in parallel, and the contribution of the whole series branch to the modulus of the EBM are negligible in comparison with the contribution the $E_1 v_{1p}$ of component 1. Consequently, $E_1 v_{1p}$ (or $E_2 v_{2p}$ for $E_2 \gg E_1$) can be set equal to the apparent modulus E_{1b} (or E_{2b} for $E_2 \gg E_1$) where:

$$E_{1b} = E_1 v_{1p} \quad E_{2b} = E_2 v_{2p}. \quad \text{Eq. III.23}$$

Hence, combining Eq. III.22 and Eq. III.23 gives:

$$v_{1p} = \left[\frac{v_1 - v_{1cr}}{(1 - v_{1cr})} \right]^{q1} \quad v_{2p} = \left[\frac{v_2 - v_{2cr}}{(1 - v_{2cr})} \right]^{q2}. \quad \text{Eq. III.24}$$

In the marginal zone, *i.e.* $0 < v_1 < v_{1cr}$ (or $0 < v_2 < v_{2cr}$), it can be set for the minority component that $v_{1p}=0$ and $v_{1s}=v_1$ (or $v_{2p}=0$ and $v_{2s}=v_2$).

For discrete domains of spherical form, the percolation threshold can be set to $v_{1cr} = v_{2cr} = 0.156$ (Kolarik, 1996; L. A. Utracki, 1991). Most experimental values of q are located in the interval 1.6-2 so that $q = 1.8$ can be used as an average value (Phua et al., 2015).

Moreover, prediction of strength can be modeled from Eq. III.25 (Kolařík, 1996):

$$S_b = S_1 v_{1p} + S_2 v_{2p} + AS_2 v_s, \quad \text{Eq. III.25}$$

where $S_1 > S_2$, S_1 and S_2 are the strength of phases 1 and 2, respectively. While A can be identified as the level of interfacial bonding.

Chapter III

Two limiting value of S_b can be identified with lower and upper bound where $A= 0$ or 1 depending on the level of interfacial adhesion, either very weak or strong enough to transmit the acting stress between constituents. Consequently, for $A=0$, series branch does not contribute and resulting S_b is equal to the sum of contributions of the parallel element. While for $A=1$, the contribution of the series branch is added to that of the parallel branch (Kolarik, 1996; Phua et al., 2015).

Chapter III

Chapter IV

In-situ compatibilization of binary poly(3-hydroxybutyrate-co-3- hydroxyvalerate) / poly(butylene-co- succinate-co-adipate) blends using free radical initiator: Batch-mixer to film blowing of PHBV-based for food packaging

Benjamin Le Delliou¹, Olivier Vitrac¹, Patrice Dole², Sandra Domenek^{1,*}

¹*UMR 0782 SayFood Paris-Saclay Food and Bioproduct Engineering Research Unit, INRAE, AgroParisTech, Université Paris-Saclay, 91300, Massy France*

²*CTCPA Centre Technique de la Conservation des Produits Agricoles, Bourg-En-Bresse, France*

IV.1. Abstract

In-situ compatibilization of poly(3-hydroxybutyrate-co-3-hydroxyvalerate) and poly(butylene-co-succinate-co-adipate) with dicumyl peroxide (DCP) as free radical initiator is investigated by means of batch mixer followed by film blowing extrusion trials. The reactive extrusion leads to a reduction of PBSA particle size, melt flow index, and increased gel content. The rheological properties highlight in the low-frequency range the change from Newtonian to the apparition of a frequency dependent behavior. At the optimal DCP of 0.1 phr, the compatibilized blend featured improved film blowing ability with PHBV content of 70 wt %. The mechanical properties under freezer conditions displayed improved interfacial compatibility with maximum stress increased by a factor of 2 and higher than neat PHBV. The elongation at break is, however, governed by PHBV featuring brittle fracture despite the presence of stretched fibers after tensile testing.

IV.1.1. Introduction

Over the last decades, great attention has been paid towards the sustainability of polymers for food contact application due to the serious environmental impact exhibited from petro-based and non-biodegradable plastics. Polymers exhibit numerous advantages since they are low-cost, light-weight, and easy to process, but the depletion of the natural resources and environmental ask to rethink how plastics must be used. Packaging is the major use of plastics. A major sustainable strategy consists of redesigning food packaging with bio-based and biodegradable polymers while reducing the weight of used plastics. Their thermo-mechanical performance still needs to be optimized to meet the specifications.

Polyhydroxyalkanoates (PHAs) are thermoplastic polyesters produced as carbon and energy storage compounds in the presence of excess carbon and limited nutrients such as oxygen, nitrogen or phosphorus (Laycock et al., 2014). Short-chain-length PHAs, mainly represented by poly(3-hydroxybutyrate) P(3HB) and the copolymer poly(3-hydroxybutyrate-co-3-hydroxyvalerate)P(3HB-co-3HV) are already commercially available. These polyesters meet the two most important requirements: bio-based and biodegradable even in aqueous environments (Deroine, Cesar, Le Duigou, Davies, & Bruzard, 2015; Laycock et al., 2014). PHBV production is possible using carbon sources coming from waste or byproducts of

Chapter IV

agriculture and food industries (Elain et al., 2016; Kumar et al., 2016; Lemechko et al., 2019; Verlinden et al., 2011) which would further fit into circular economy because local food wastes could be used to produce food containers. PHBV is however a stiff and brittle, a highly crystalline polymer with low thermal stability and a narrow processing window. Typical elongation at break is below 5 % and stress at break between 30 and 40 MPa. It is rubbery at room temperature, featuring a glass transition temperature (T_g) ranging between 0 and 5 °C. Its main drawback for use as a packaging material is its brittleness (Anjum et al., 2016).

To overcome these drawbacks, one strategy that can be adopted is based on physical melt-blending. Great attention has been paid to PHBV-based blends with other biodegradable polymers such as polylactic acid (PLA) (Boufarguine et al., 2013; I. Zembouai et al., 2014; M. Zhang & Thomas, 2011), polybutylene adipate-co-terephthalate (PBAT) (Bittmann et al., 2015; Cunha et al., 2015), polybutylene succinate (PBS) (Phua et al., 2015). In our previous study (Chapter III), the characteristics of blends of poly(3-hydroxybutyrate-co-3-hydroxyvalerate) / poly(butylene-co-succinate-co-adipate) (PBSA) prepared by batch mixing were analyzed. PBSA was used as the second polymer because it is partially biobased and biodegradable. It features high elongation at break (> 200 %) and low T_g (-45 °C). The two components were found to be immiscible. The blends had a nodular morphology at low PBSA contents. The mechanical properties were found to be mainly driven by brittleness of PHBV with an elongation at break as low as 3 %, even a PBSA content of 70 wt %. The analysis of the stress at break showed that the rupture was most probably located at the PHBV/PBSA interfaces because it was in all cases lower than the stress at break of pure PHBV.

In-situ compatibilization can be used to improve the mechanical properties thanks to the enhancement of interfacial adhesion between both phases in binary blends. It relies on the use of a third component containing a functional group (i.e., anhydride, epoxy, etc.) which will react with blend constituents (Leszek A. Utracki, 2002).

Extensive research has been conducted on *in-situ* compatibilization of binary blend poly(lactic acid) and PBSA using chain extenders (Eslami & Kamal, 2013a; Lascano, Quiles-Carrillo, Balart, Boronat, & Montanes, 2019; Mirzadeh, Ghasemi, Mahrous, & Kamal, 2015; Ojijo, Sinha Ray, & Sadiku, 2013). (Eslami & Kamal, 2013a) used a multifunctional chain extender (CESA) and have shown that the blends containing chain extender exhibited strong melt strain-hardening behavior, whereas the blends without CESA showed weak strain-hardening. Adding PBSA enhanced the ductility of the blend, but CESA was not affecting the modulus and elongation at break. The use of an epoxy styrene-acrylic oligomer (ESAO) as a chain extender was also investigated (Lascano et al., 2019). As evidenced from tensile properties, addition of

Chapter IV

0.5 phr ESAO increased elongation at break by a factor 4 up to 121.2 % with decreased elastic modulus and tensile strength.

Compatibilization of PHBV with other biodegradable polyesters was mostly carried out using dicumyl peroxide (DCP), a free radical initiator. Examples are the compatibilizing of PHBV with PLA (Dong et al., 2013), PBAT/ epoxidized natural rubber (ENR) (K. Zhang et al., 2014) or PBS (Chikh, Benhamida, Kaci, Pillin, & Bruzaud, 2016; P. Ma et al., 2012). Free radicals can be generated on PHBV and on the second polyester chain via a hydrogen abstraction in the presence of DCP, which acts as a free radical initiator (Ma et al., 2014). As a result, cross-linking between both components can be obtained by combining macro-free radicals. This is of great interest since it is supposed to increase length of the macromolecular chain and its branching degree, thereby increasing the elongation viscosity, melt strength and thus allowing blown-film molding (Teixeira et al., 2020). However, the DCP concentration needs to be optimized because it can also lead to chain degradation.

For example, (P. Ma et al., 2012) compatibilized PHBV/PBS (80/20) involving in-situ reactive extrusion using DCP (0.5 wt%). The authors found that, reactive extrusion drastically improved the elongation at break from 8 to 400 % for non-aged samples. This improvement was attributed to the formation of PHBV-*g*-PBS copolymer, which was assumed to be located at the interface between the polymers and thus act as a compatibilizer (P. Ma et al., 2012). However, this result may be put into perspective since it has been discussed in the literature (T. Gerard et al., 2014) that blends (PLA/PHBV) with low content of PHBV was strongly subjected to aging process. After two days, injected samples showed an elongation at break as high as 200 %, but the performance decreased to a few % after one month of aging. The long-term performance of the materials of (P. Ma et al., 2012) may have been overestimated.

The film blowing extrusion process is one of the most used processing tools to produce flexible polymer films, but this technique requires high melt strength and extensional viscosity, while PHBV exhibits low shear viscosity and elastic melt strength (Cunha et al., 2016). Very few studies are reporting successful film blowing of PHBV blends (Cunha et al., 2016; Jandas et al., 2013; S. Sun et al., 2017; Teixeira et al., 2020). Film blowing of PLA/PHB with the addition of maleic anhydride as a reactive compatibilizer was successfully achieved (Jandas et al., 2013). The best results were obtained for PLA/PHB/MA 70/30/7 with an elongation at break as high as 540 % resulting from maleic anhydride acting as bridging unit among PLA and PHB macromolecules through dipole-dipole or inter-molecular hydrogen bonding. Blends of hydroxypropyl di-starch phosphate (HPDSP) and poly(3-hydroxybutyrate-co-4-hydroxybutyrate) (P3H4HB) were analyzed by (S. Sun et al., 2017). Although successful film

Chapter IV

blowing, a large decrease in elongation at break from 73.5 to 24.8 % in machine direction was found when PHA was added at 36 wt%, because of a lack of compatibility. (Cunha et al., 2016) produced PHBV/PBAT films by film blowing using either a blend structure or a co-extruded multilayer structure. The films exhibited elongation at a break of 8-14 %, while was 11-19 % for a PHBV/PBAT multilayer with PHBV outside and 358-539 % for PBAT/PHBV with PBAT as the external layer. In another study focusing on PHBV/PBAT, (Teixeira et al., 2020) successfully produced co-extruded PHBV/PBAT films using DCP or a multifunctional epoxide styreneacrylic oligomeric chain extender (CE) with PBAT as external layer. The elongation at break as high as 400 % in the machine direction (MD) and about 20 % in the transverse direction (TD). The production of bilayer films relies on adhesion between layers. Moreover, the inner and outer layer must be in equivalent quantity to ensure integrity while being processed. As a consequence, the total concentration of PHBV in the films is limited around 50 wt%. To maximize the PHBV content the blending strategy needs to be used.

Building on our previous work, we developed PHBV/PBSA blends compatibilized with DCP and investigated the morphological rheological, thermal, mechanical characteristics and processability. The formulation was optimized using melt blending, and the film blowing extrusion, campaign was conducted. Blown films were then tested in a service situation, corresponding to packaging conditions of frozen food.

IV.2. Materials and Methods

IV.2.1. Experimental protocols

IV.2.1.1. Materials

Commercial PHBV (PHI 002) containing 3 mole percent of hydroxyvalerate (HV) – according to technical datasheet – and PBSA (PBE 001) were purchased from NaturePlast (France). Polymers were dried at 70 °C under vacuum for at least six hours before use. Dicumyl peroxide was purchased from ACROS and used as received.

Chapter IV

IV.2.1.2. Compatibilized polymer blends

IV.2.1.2.1. Batch mixer

Compatibilized PHBV/PBSA 70/30 blends with DCP contents of 0, 0.02, 0.1, 0.2, and 1.0 phr (parts per hundred of resin on a weight basis, meaning that 0.02 phr correspond to 100 g blend + 0.02 g DCP) were melt-blended in the internal mixer SCAMEX Rheoscam (France) at 190 °C at 90 rpm for 9 min. PHBV was pre-melted for 6 minutes. Then, PBSA pellets mixed with DCP were introduced and mixed for 3 minutes. The blended materials were finally processed by thermo-compression molding (SCAMEX 15T, France). Pellets were pre-melted for 3 min before being subjected to 80 bars, then 150 bars for 1 min each. Aluminum foils of 200 µm were used to control the thickness of samples. The final thickness was further measured with a caliper before characterization.

IV.2.1.2.2. Compounding by twin-screw extrusion (TSE)

Compatibilized PHBV/PBSA 70/30 blends with DCP contents of 0, 0.1, and 0.2 phr were compounded using a lab-scale twin-screw extrusion process with a screw diameter of 18 mm and a length-to-diameter of 16 L/D (SCAMEX, France) using the dry-mix technique. The pellets of both polymers and DCP were first hand mixed and introduced in the hopper. The twin-screw extruder temperature zones were set to 175/185/155°C from hopper to die, and screw speed was maintained at 20 rpm.

IV.2.1.2.3. Film blowing extrusion

Film blowing was conducted on compatibilized PHBV/PBSA 70/30 with varying amounts of DCP. Single-screw specifications were a diameter of 20 mm and a L/D of 11 equipped with a lab-scale film blowing module (SCAMEX, France). The temperature profile was set to 165/170/170/160 °C from hopper to die and screw speed was maintained at 50 rpm. The film blowing parameters are summarized in Table IV.1.

Table IV.1: Film blowing parameters

| Film blowing parameters | Values | | |
|-------------------------|-----------------|---------------------------------|---------------------------------|
| | PHBV/PBSA 70/30 | PHBV/PBSA 70/30+ 0.1 phr DCP | PHBV/PBSA 70/30+ 0.2 phr DCP |

Chapter IV

| | | | |
|-----------------------|--------------------|--------------------|--------------------|
| Die diameter | 19 mm | | |
| Die gap | 1 mm | | |
| Film thickness | 95 ± 9 μm | 122 ± 30 μm | 221 ± 36 μm |
| Blow up Ratio (BUR) | 1.7 | 2.6 | 1.3 |
| Draw down ratio (DDR) | 6.2 ⁽¹⁾ | 3.2 ⁽¹⁾ | 3.5 ⁽¹⁾ |

⁽¹⁾ Based on the average value of film thickness

The Blow Up Ratio (BUR) and Draw Down Ratio (DDR) were calculated using Eq. IV.1 and Eq. IV.2:

$$\text{Blow Up Ratio (BUR)} = \frac{R}{R_o}, \quad \text{Eq. IV.1}$$

$$\text{Draw down ratio (DDR)} = (\text{Die gap}/\text{Film thickness})/\text{BUR}, \quad \text{Eq. IV.2}$$

where R and R_o are the duct and punch radius, respectively.

IV.2.2.Characterization

IV.2.2.1.Thermal characterization

Thermal properties of blends were measured by DSC (DSC1, Mettler Toledo, Switzerland) with the temperature program shown in Figure IV.1. All measurements were done under nitrogen atmosphere (flow rate 50 mL/min) with 5 to 10 mg of materials sealed in 40 μL aluminum pans. Calibration was carried out with Indium and Zinc standards. All measurements were duplicated. The first cooling and second heating scan (Figure IV.1) served to measure the melting and crystallization enthalpy. The glass transition temperature of PHBV was measured at the 3rd heating scan after physical aging of either PHBV at -10 °C and the Tg of PBSA at the 4th heating scan after physical aging at -60 °C.

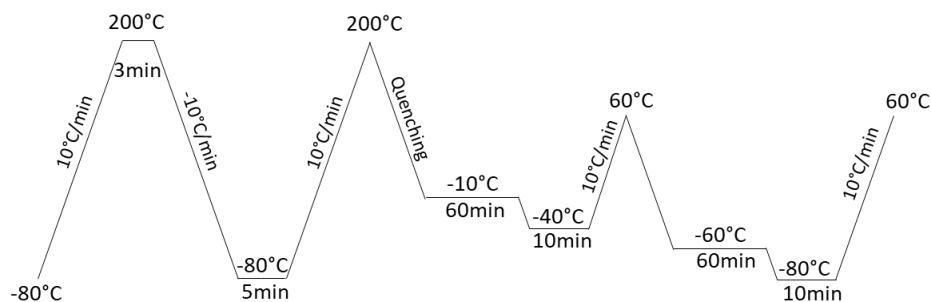


Figure IV.1 : Differential scanning calorimetry measurement protocol

Chapter IV

The crystallinity degree of each polymer $\{\chi_i\}_{i=PHBV,PBSA}$ was determined from the endotherm $\Delta H_{m,i}$ as:

$$\chi_i = \frac{\Delta H_{m,i} - \Delta H_{cc,i}}{w_i \Delta H_{m,i}^0}, \quad \text{Eq. IV.3}$$

where w_i the weight content of the corresponding polymer, $\Delta H_{cc,i}$ the cold crystallization enthalpy, and $\Delta H_{m,i}^0$ the melting enthalpy of a 100 % crystalline material with pure PHBV (146 J/g, from Corre et al. (2012)) and PBSA (113.4 J/g, from Charlon et al. (2016)).

IV.2.2.2. Scanning Electron Microscopy

The morphology of the PHBV/PBSA blends was studied by an Environmental Scanning Electronic Microscopy (ESEM, FEI Quanta 200) with an accelerated voltage of 12kV. First, the samples were cryo-fractured using liquid nitrogen followed by selective dissolution of the PBSA phase by tetrahydrofuran at room temperature for at least one hour. Finally, the cryo-fractured samples were sputter-coated with a thin gold layer (Sputter coater Emitech K550), and snapshots were taken on the cryo-fracture edge of the sample.

IV.2.2.3. Rheological properties

Melt flow index (MFI) experiments were conducted according to ISO 1133 (MFI 4106, Zwick, Germany). The samples were extruded through a die under a constant load of 2.16 kg at 190 °C. The melt flow index is expressed as the mass passing through the die during a period of 10 minutes (g/10min).

Rheology measurements in melt state were performed with a stress-controlled rheometer (MCR 302, Anton Paar, Graz, Austria) using a disk-shaped specimen. A parallel-plate geometry with a gap set between 750 and 800µm at 185°C. Dynamic frequency sweep experiments were performed from 0.01 to 100Hz in the linear viscoelastic region.

Chapter IV

IV.2.2.4. Mechanical properties

Because of large thickness inhomogeneities in blown film samples, all mechanical tests were carried out on compression-molded specimens obtained in a thermal press (SCAMEX 15T, France). Pellets were pre-melted for 3 min before being subjected to 80 bars then 150 bars for 1 min each. Aluminum foils of 200 μm were used to control the thickness of samples. Dumbbell-shaped samples of type 5 with a target thickness of 200 μm were cut from the compression-molded sheets. Thickness was an average of 5 measurements measured with a caliper. At least five samples were tested for each blend formulation.

Tensile tests were carried under both ambient and freezer (-20 °C) temperature. At ambient temperature, tensile properties were measured using a texture analyzer (model TAHD, Stable Micro Systems, UK) equipped with pneumatic grips with a 5 mm/min crosshead speed. At freezer temperature (-20°C), tensile tests were performed on a Zwick Z010 (Zwick, Ulm, Germany).

Un-notched Charpy impact tests were assessed according to ISO 179, using a Zwick B5113.300 impact tester. Two Pendulums of 1 and 4 J were used for PHBV-based blends and PBSA, respectively. At least five samples were tested for each ratio.

IV.2.2.5. Gel content

Compatibilized PHBV/PBSA 70/30 blends with DCP contents of 0, 0.02, 0.1, 0.2, and 1.0 phr were first milled (Model Retsch MM400, Germany). Two successive Soxhlet extraction were performed to independently extract the two polymers PHBV and PBSA. Chloroform is a suitable solvent for PBSA and PHBV, but not for the cross-linked network. Besides that THF is a suitable solvent only for PBSA. The extraction of PBSA extraction in boiling THF tetrahydrofuran for one day followed by extraction of PHBV in boiling chloroform for two consecutive days. The gel fraction was calculated as follows :

$$gel\ wt.\ \% = \frac{m_1}{m_0} \cdot 100\% \quad \text{Eq. IV.4}$$

where m_0 is the original weight of samples and m_1 is the weight of dry residues obtained after extraction

Chapter IV

IV.2.2.6. Fourier transform infrared spectroscopy (FTIR)

The Fourier transform infrared (FTIR) spectra were performed on a Pekin-Elmer FT-IR Frontier using an attenuated total reflectance (ATR) module. Measurements were recorded by absorption (A) between 4000 to 650 cm^{-1} with a resolution of 4 cm^{-1} .

IV.2.2.7. Physical Aging in contact fatty food at -20°C

Physical aging was carried out on PHBV-based bags upon various storage time at -20°C and in contact with fatty food. First, the obtained films were cut with a length of 13 cm and thermo-sealed manually from one side using a vacuum packing machine with sealing conditions of 0.8 s (Model C200, Multivac, Germany). Then, bags were filled with frozen French fries with a quantity of about 25 g before being sealed on the other side. Finally, samples were placed in a freezer with a temperature of -20°C for various periods. Before being subjected to tensile tests, samples were thawed and placed at 25°C , RH=50% for a minimum of 24 h.

IV.3. Results and Discussion

IV.3.1. Batch mixing processability: effect of dicumyl peroxide content

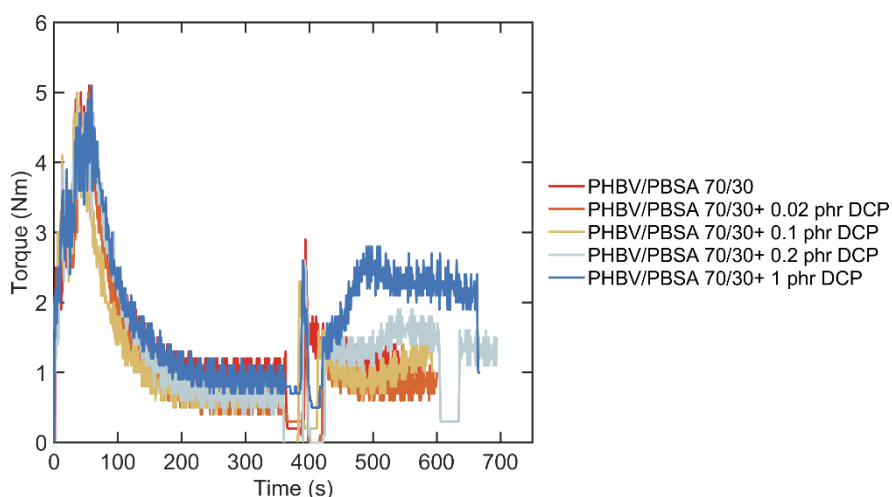


Figure IV.2: Measurement of torque over time during melt mixing of compatibilized PHBV/PBSA blends at constant weight ratio 70/30 with different content of dicumyl peroxide

Figure IV.2 shows the evolution of the torque measured in the mixing chamber during melt-blending. PHBV was melt-blended with PBSA at a fixed ratio of 70/30 while the amount of dicumyl peroxide was varied from 0.02 to 1 phr. The torque decreased gradually which results

Chapter IV

from the melt of PHBV pellets. After the introduction of both PBSA and DCP, a change in torque was observed depending on free-radical initiator content. Hence, for DCP content of 0, 0.02 and 0.1, no torque variation was detected. However, for DCP content higher than 0.2 phr, a large torque increase in torque appeared with maximum peaks at 550 s and 500 s for DCP content of 0.2 and 1 phr DCP, respectively. This significant increase was attributed to the cross-linking reaction between PHBV and PBSA, as already reported in the literature (Fei et al., 2004).

IV.3.2. Fourier transform infrared spectroscopy (FTIR)

FTIR spectra in ATR mode were recorded to investigate the chemical modifications of neat PHBV, neat PBSA, and PHBV/PBSA/DCP blends after reactive extrusion. Figure IV.3(a) shows the absorption spectrum of neat PHBV. The absorption band at 2975 cm^{-1} is attributed to the crystalline phase's C-H stretching vibration (Wang, Chen, Chen, Pan, & Xu, 2010). The absorption bands at 2932 and 1451 cm^{-1} are attributed to -CH stretching of -CH₂ and -CH₃, respectively (Kennouche et al., 2016). The sharp band at 1719 cm^{-1} refers to the stretching mode of C=O of the highly crystalline phase of PHBV, while the shoulder at 1740 cm^{-1} refers to C=O in the amorphous region (Padermshoke et al., 2004). Absorption bands at 1275 , 1261 and 1227 cm^{-1} can be assigned to the C-O-C stretching modes of the crystalline parts (Buzarovska & Grozdanov, 2009). The band at 1180 cm^{-1} is assigned to amorphous of C-O-C stretching band (Kennouche et al., 2016). For neat PBSA, the band at 2946 cm^{-1} is attributed to C-H stretching. In the region 1650 - 1750 cm^{-1} , *i.e.*, at 1721 and 1713 cm^{-1} , these are assigned to C=O stretching of the ester group (Cai, Qi, Xu, Guo, & Huang, 2019). The peaks at 1313 and 1334 cm^{-1} may arise from carboxyl acid C-O stretching of the degradation products of PBSA (H.-S. Kim, Kim, Lee, & Choi, 2006). The observed band at 1154 cm^{-1} and 1047 cm^{-1} can be assigned to C-O-C and C-O stretching, respectively (Cai et al., 2019).

The FTIR spectra of PHBV/PBSA blends as a function of DCP content zoomed in the region 1800 - 1600 cm^{-1} and 1500 - 700 cm^{-1} are displayed in Figure IV.3(b) and Figure IV.3(c), respectively. Inspection showed that no band shift or evidence of a new chemical bond observed after the introduction of PBSA and DCP in PHBV, probably because of a lack of sensitivity, making nearly impossible to sample rare events.

Chapter IV

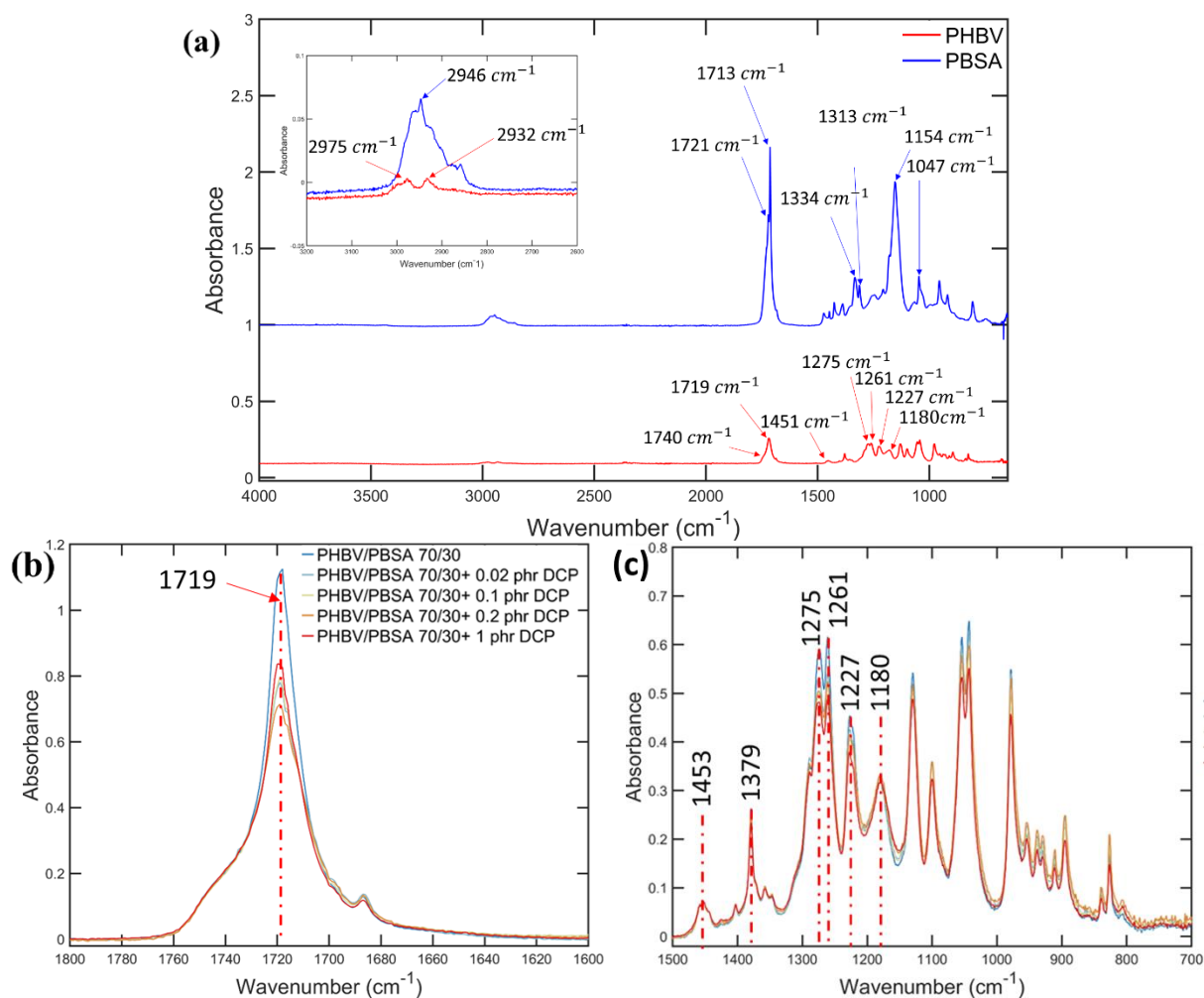


Figure IV.3: FTIR spectra of a) neat PHBV and neat PBSA in the region 4000-650 cm^{-1} and PHBV/PBSA/DCP blends in the region b) 1800-1600 cm^{-1} and c) 1500-700 cm^{-1}

IV.3.3. Gel content and melt flow index

The crosslinking reaction introduced by DCP was monitored by measuring the gel content and the MFI of the blends. The collected values are reported in Table IV.2. The results highlighted that both neat components have a considerable difference in MFI and simple mixing of PHBV and PBSA at a weight ratio of 70/30 gives an intermediate MFI following an additive rule. The introduction of 0.1 phr DCP decreased the MFI dramatically with a drop from 67 to 22 g/10min. Further increase of DCP content yielded no change. The gel content (Table IV.2) obtained from the batch mixer increased with DCP content and can be related to crosslinking reaction leading to PHBV-g-PBSA as proposed by (Ma et al. 2012) on PHBV/PBS blends. The decomposition of organic peroxides generates a cascade of free radicals, which may recombine with polymer macro-radicals. Very high amounts of DCP could break polymer chains, as suggested by the decreased value at ca. 1 phr DCP. Compared to batch mixing, samples after

Chapter IV

twin screw extrusion (TSE) and film blowing displayed lower MFI and gel content values. The lower value of MFI could result from the lower MFI value of neat PHBV, and highlighted the variability between PHBV batches. On the one hand, the depression of gel content can result from the lower cross-linking reaction between PHBV and PBSA in reactive extrusion due to slightly lower residence time in twin screw extrusion than in the batch mixer.

On the other hand, further reduction of gel content after film blowing can result from the chain scission due to the second thermal treatment. It is worth noticing that TSE produced samples with much higher variability. Apparently, the dry-blend technique and the small scale of the twin-screw extruder lead to high inhomogeneity of crosslinking points within samples.

Table IV.2: Melt Flow Index and Gel content of PHBV/PBSA with varying content of DCP as function of implementation process

| Samples | Melt Flow Index (g/10min) | | Gel content (%) | | |
|--------------------------|---------------------------|---------|-----------------|--------|--------------|
| | Batch Mixer | TSE | Batch Mixer | TSE | Film blowing |
| Neat PHBV ⁽¹⁾ | 90±3 | 30± 1 | n.d | n.d | n.d |
| Neat PBSA ⁽¹⁾ | 2.5±0.1 | 2.5±0.7 | | | |
| 70/30 | 67±2 | 45±1 | | | |
| 0.02 phr | n.d | n.d | 8±6 | | |
| 0.1 phr | 22±1 | 13±1 | 9± 4 | 16± 1 | 7 |
| 0.2phr | 21±1 | 17±1 | 36± 4 | 28± 12 | 11 |
| 1 phr | 20±1 | | 24± 2 | n.d | n.d |

⁽¹⁾ MFI values of raw pellets

IV.3.4.Rheological measurements

The rheological properties were evaluated in regard to the evolution of the complex viscosity η^* of non-compatible and compatibilized PHBV-based compounds of batch mixing and twin screw extrusion blends in Figure IV.4a and Figure IV.4b, respectively. Figure IV.4a shows a large change in complex viscosity between 0.1 and 0.2 phr DCP. Batch mixer samples show that below 0.1 phr DCP, the complex viscosity almost equal to that of the neat PHBV and the PHBV/PBSA blend. For DCP contents larger than 0.1 phr, an increase of two orders of magnitude at low frequencies is found, and frequency dependent behavior appeared. These characteristics are typical of polymer systems with long-chain branched structures (Eslami & Kamal, 2013a; Tian, Yu, & Zhou, 2006). The complex viscosity curves constantly rose at low frequencies, which revealed very high zero shear viscosity due to the high gel content. Comparison of the complex viscosity η^* between the batch mixer and twin-screw extrusion showed minor differences (graph not shown here). A deviation in the low-frequency range was

Chapter IV

observed between both extrusion techniques while exhibiting the same trend. Complex viscosity η^* of compatibilized blends displayed higher values from batch mixing than extrusion. It was interpreted as a lower cross-linking between PHBV and PBSA. Thus, free radical generation and recombination would be slightly impacted (Mirzadeh et al., 2015). This is further suggested from lower gel content between twin-screw extrusion and batch mixer. The comparison of the rheological properties between both techniques further confirmed that the lab-scale extrusion process, *i.e.*, batch mixer, is a useful tool where resulting properties can be transposable to scale-up. The combination of blending between PHBV and PBSA and the addition of dicumyl peroxide contributed to improving the melt strength, which is positive for its ability to be processed through blown film molding.

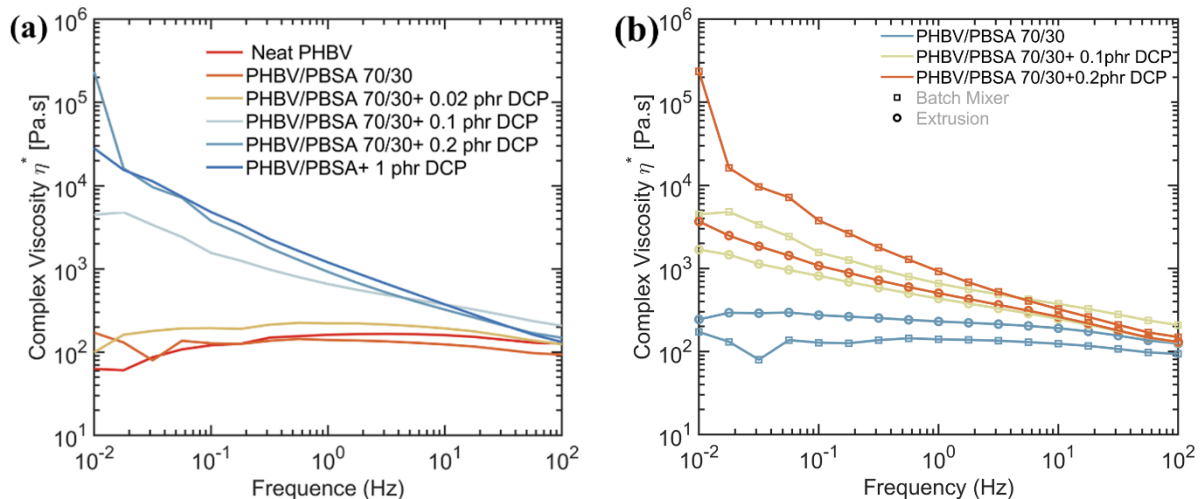


Figure IV.4: Evolution of the complex viscosity as a function of frequencies resulting from (a) batch mixing and (b) selected formulation from twin-screw extrusion of PHBV/PBSA with varying content of DCP at 185°C

Cole-Cole plots (out-of-phase component η'' versus in-phase component of the complex viscosity η') were plotted and are shown in Figure IV.5. The Cole-Cole plot is sensitive to the phase structures in polymer blends (Wu et al., 2019). Not compatibilized and compatibilized (0.02phr DCP) PHBV/PBSA blends show a semicircular shape. Passing a threshold value of 0.1 phr DCP, the Cole-Cole plots derived from circular shape with an almost linear evolution in log-log scale, which indicates a long relaxation time at low frequencies characteristic of long-chain branched structure (Eslami & Kamal, 2013a).

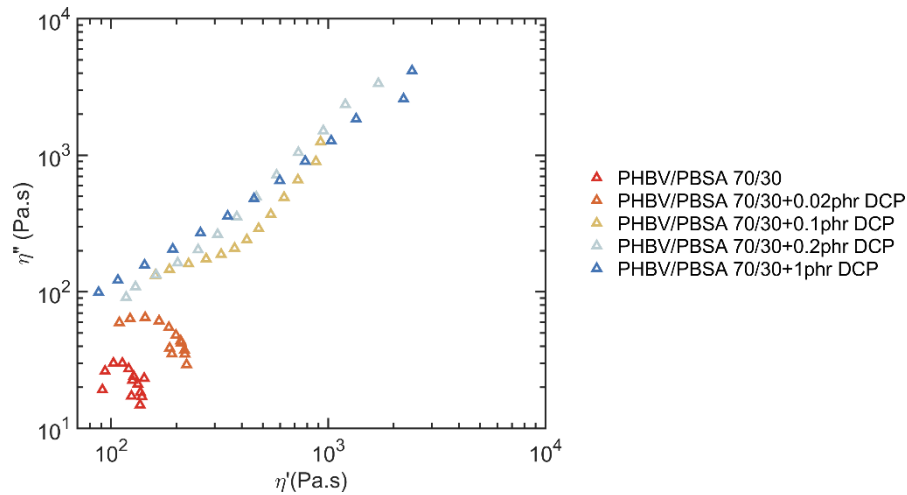


Figure IV.5: Cole-Cole plots of PHBV/PBSA 70/30 and the compatibilized PHBV/PBSA blends with dicumyl peroxyde from 0.02 to 1phr (batch mixer)

IV.3.5. Scanning Electron Microscopy

Developed morphologies resulting from melt blending of PHBV/PBSA 70/30 in the presence of dicumyl peroxyde were observed by SEM (Figure IV.6(a-d)). Figure IV.6(a) shows large PBSA droplets dispersed in PHBV for 70/30 PHBV/PBSA. The introduction of DCP led to a change in morphology with a decrease in the size of PBSA nodules. At 0.02 phr DCP the domain size decreased from about 10 μm in diameter down to 3.8 μm with a large dispersion in nodule sizes within the sample. At DCP content, the SEM resolution was not sufficient to distinguish nodules. The morphology in polymer blends results from an equilibrium between droplet break up and coalescence. As seen, rheological measurements showed a change in melt behavior. This reduction in domain size can be attributed to compatibilization by crosslinking of PHBV and PBSA at the interface or reduced the interfacial tension between both polymers because of the formation of PHBV-g-PBSA fragments. Both mechanisms would prevent coalescence (Macosko et al., 1996).

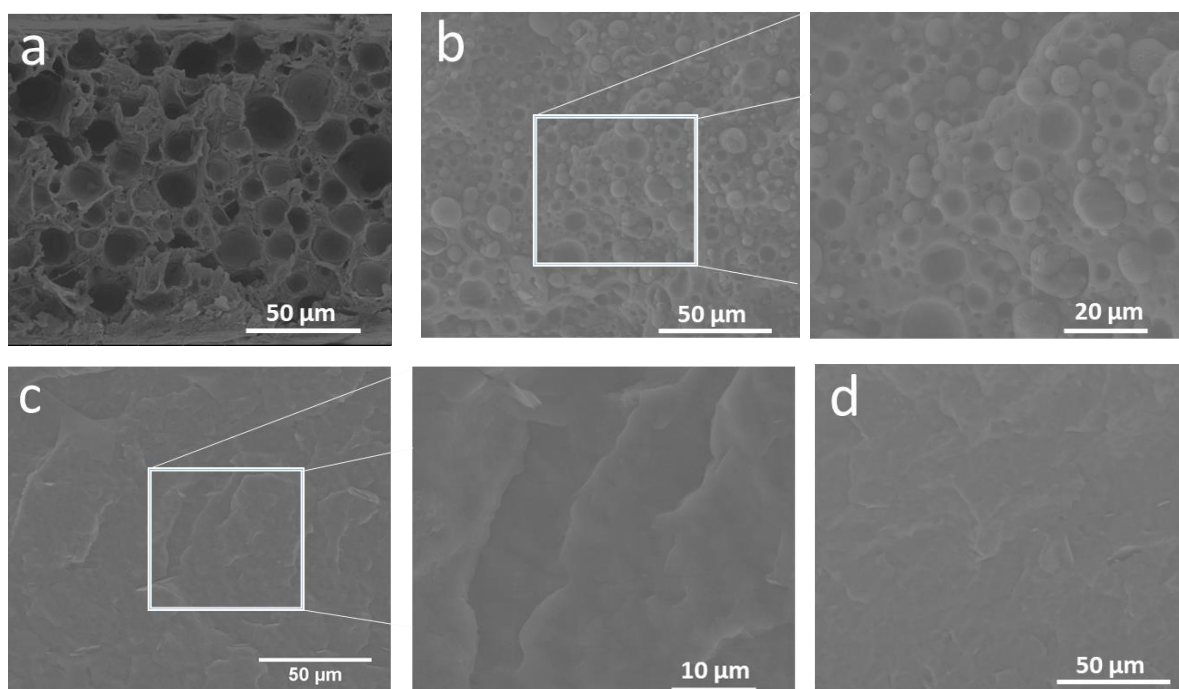


Figure IV.6: SEM images of cryo-fractured surfaces of compatibilized PHBV/PBSA blends(batch mixer) with different DCP content, (a) 0 phr, (b)0.02 phr, (c) 0.1 phr and (d)0.2 phr

IV.3.6. Thermal properties

Different scanning calorimetry techniques were used to study the effect of DCP on the thermal properties of PHBV/PBSA blends, and the results are summarized in Table IV.3. No change in melting temperature was observed up to a DCP content of 0.2 phr in the PHBV or PBSA phase. However, a decrease in T_m of 5 °C and 8°C for PHBV and PBSA was noticed at a DCP content of 1 phr. The depression of T_m may arise from the thermal degradation of both phases and/or was caused by the chain scission peroxy radicals (Immirzi, Malinconico, Orsello, Portofino, & Volpe, 1999), as suggested by the decreasing gel content (Table IV.2).

Two distinct T_g were identified within non-compatibilized and compatibilized PHBV/PBSA blends. DCP did not shift the T_g of either PHBV or PBSA phase towards lower or higher temperatures than non-compatibilized PHBV/PBSA. The glass transition region broadened at 1 phr DCP, which might indicate macromolecular chain scission.

Chapter IV

Table IV.3: Thermal properties of neat PHBV, PHBV/PBSA 70/30 and compatibilized PHBV/PBSA blends with different content of dicumyl peroxide evaluated by DSC from the second heating scan and ageing method

| Samples | T _m (°C) | | T _c (°C) | | χ (%) | | T _g (°C) | | |
|-------------|---------------------|-------|---------------------|--------|-------|------|---------------------|----------|-----------|
| | PHBV | PBSA | PHBV | PBSA | PHBV | PBSA | PHBV | PBSA | |
| Batch Mixer | Neat PHBV | 171±3 | n.d | 122± 1 | n.d | 68±1 | n.d | 2.4±0.4 | n.d |
| | Neat PBSA | n.d | 88±3 | n.d | 38±3 | n.d | 45±4 ⁽¹⁾ | n.d | -45.9±1.6 |
| | 70/30 | 169±2 | 86±2 | 117±1 | 50±1 | 67±2 | 33±5 | -1.5±0.1 | -48.6±2 |
| | 0.02 phr | 169±1 | 85±1 | 118±1 | 53±4 | 66±0 | 28±0 | -1.3±0.1 | -49.6±0.5 |
| | 0.1 phr | 169±1 | 85±1 | 117±1 | 54±1 | 63±2 | 29±5 | -1.1±0.7 | -48.9±1.3 |
| | 0.2phr | 168±1 | 83±1 | 118±1 | 54±1 | 67±2 | 22±9 | -1.3±1.1 | -48.7±0.9 |
| | 1 phr | 163±1 | 75±1 | 118±1 | 51±1 | 64±0 | 21±1 | -2.0±1.6 | -48.1±1.3 |
| TSE | 70/30 | 170±1 | 86±1 | 119±1 | 56±1 | 72±7 | 32±1 | -1.1±0.7 | -49.6±0.5 |
| | 0.1 phr | 169±1 | 80±1 | 117±1 | 57±1 | 64±1 | 32±1 | -0.9±0.4 | -48.1±0.2 |
| | 0.2 phr | 169±1 | 83±1 | 118±1 | 56±1 | 69±1 | 24±3 | -0.5±0.2 | -48.7±0.7 |

IV.3.7.Mechanical properties

The mechanical properties were evaluated by means of tensile tests, and results are presented in Table IV.4. As already reported in our earlier work (Chapter III), the melt mixing of PHBV with PBSA did not allow gains in elongation at break and decreased the break strength below the value of PHBV because of rupture at the interface. The maximum stress of the compatibilized PHBV/PBSA blends at 0.02, and 0.1 phr increased to reach the value of the PHBV blank, which can be ascribed to successful compatibilization. At higher DCP quantities, it decreased again, indicating that the DCP quantity was too high and yielded degradation. All blends displayed brittle behavior with an elongation at break as low as 2 % and largely driven by PHBV and high brittleness. Several authors have already discussed that the brittle behavior of PHBV can be caused by i) the cold crystallization of the amorphous phase at ambient temperature, ii) glass transition temperature close to room temperature, and iii) radial or circumferential cracks potentially contained in spherulites of PHBV with low content of 3HV (Barham & Keller, 1986; El-Hadi et al., 2002). For higher free radical initiator content, *i.e.*, above 0.2 phr, a decreased value of elongation at break is evidenced, which can be related to macromolecular chain degradation and resulting in gel points which can act as defects and lead to premature fracture.

Chapter IV

Table IV.4: Mechanical properties of PHBV/PBSA blends with varying content of DCP obtained from tensile test measurements

| Samples | | Young modulus (MPa) | Maximum stress (MPa) | Elongation at break (%) | Impact Strength (kJ.m ⁻²) |
|--------------------|-----------|------------------------|-------------------------|----------------------------|--|
| Batch Mixer | Neat PHBV | 3485±63 | 22±2 | 0.98±0.1 | 2.0±0.6 |
| | Neat PBSA | 332±8 | 15±1.4 | 134.8±48 | 32.4±4.1 |
| | 70/30 | 2227±108 | 19±2 | 1.5±0.4 | |
| | 0.02 phr | 2222± 96 | 20±2 | 1.4±0.2 | |
| | 0.1 phr | 1973± 124 | 21± 3 | 1.9±0.2 | n.d |
| | 0.2phr | 1879± 234 | 19± 6 | 1.9±0.5 | |
| | 1 phr | 1742±295 | 13±3 | 1±0.1 | |
| TSE ⁽¹⁾ | 70/30 | 1807±79 | 15±3 | 1.6±1.4 | n.d |
| | 0.1 phr | 1703±138 | 17±4 | 2.0±0.5 | 2.8±0.3 |
| | 0.2 phr | 1713±81 | 17±2 | 2.1±0.4 | 6.8±0.2 |

(1) Samples were thermo-compression molded

The study investigate in more detail the fracture mechanism, the cross-sections of the fractured samples were analyzed using SEM observations (Figure IV.8(a-e)). at different localization identified as position A and B (Figure IV.7). Samples of uncompatibilized and very low DCP content at 0.02 phr, Figure IV.8(a,b), show a rough surface with clear debonding at the PBSA / PHBV interface. Introduction of dicumyl peroxide, up to 1 phr, changed the fracture morphology. For samples with 0.1 and 0.2 phr DCP, Figure IV.8(c/location A) and Figure IV.8(d/location B), respectively, matrix yielding was observed revealed by stretched fibers. As DCP content increased, the fibrils got longer. This type of morphology was already reported for *in-situ* compatibilized PLA/PBAT blends in the presence of DCP (Ma et al., 2014). DCP concentration of 1 phr (Figure IV.8(e/location A)) led to a denser structure with less elongated fibrils, which is consistent with the decrease of the elongation at break (Table IV.4).

Chapter IV

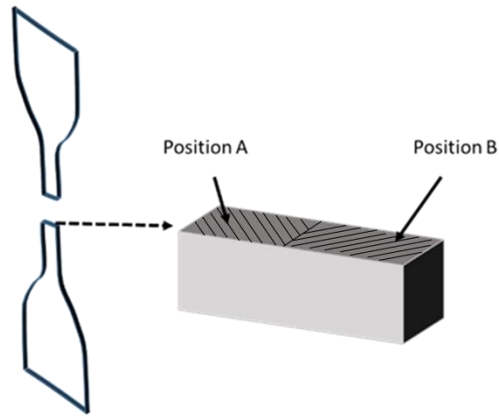
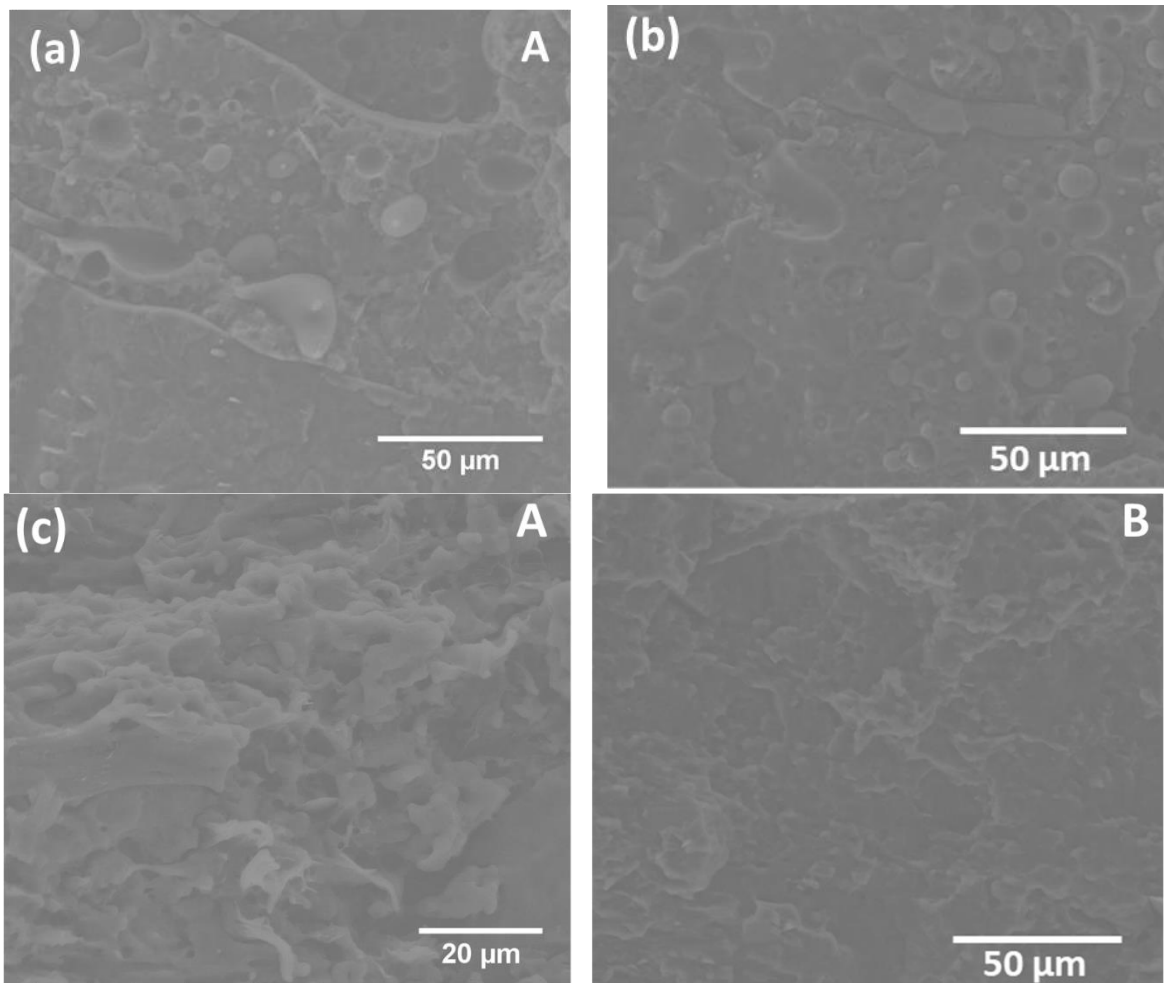


Figure IV.7 : Schematic illustration of the location of the observations on the SEM samples after failure of the tensile test



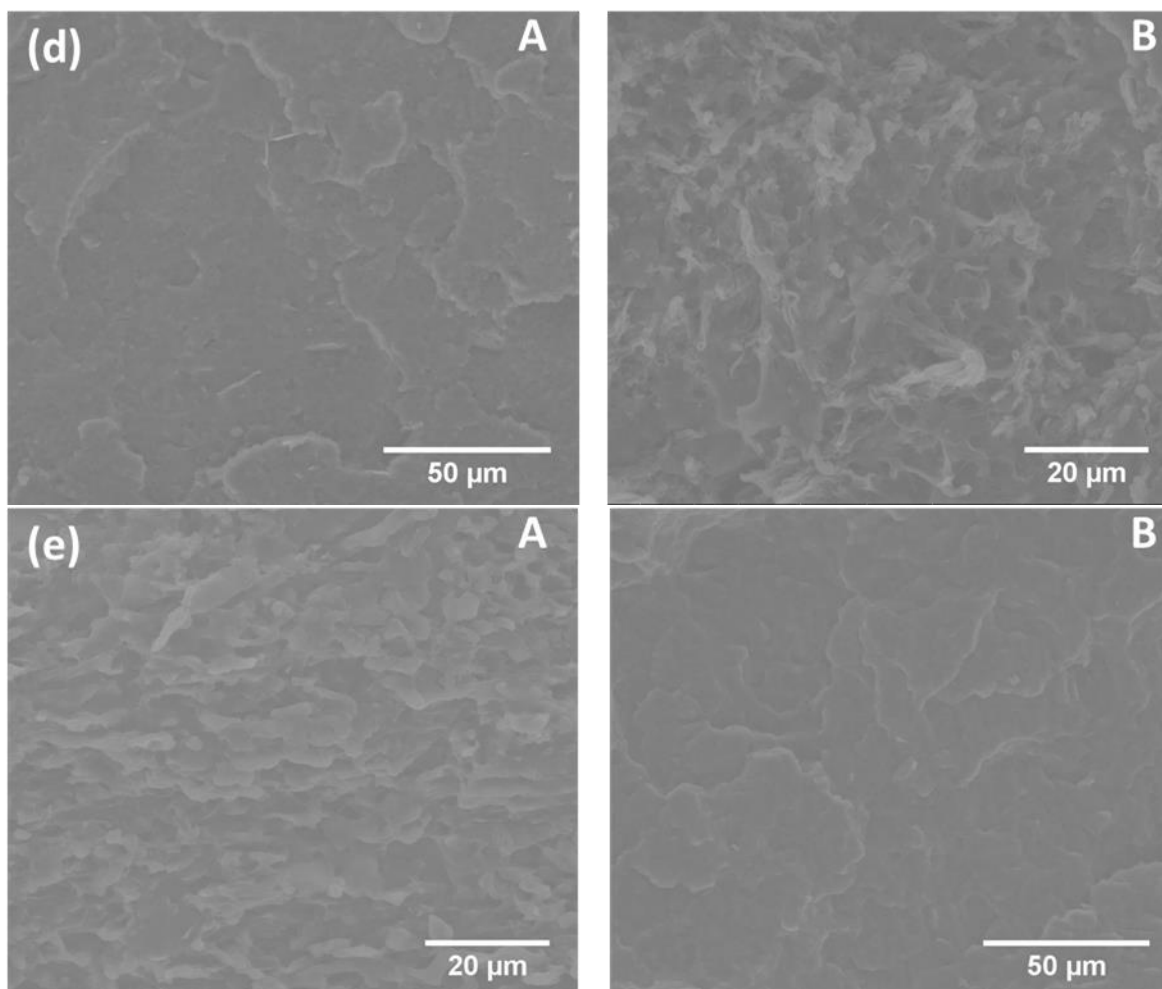


Figure IV.8: SEM images of the cross-section after tensile test of compatibilized PHBV/PBSA blends with different DCP content, (a) 0 phr, (b) 0.02 phr, (c) 0.1 phr, (d) 0.2 phr and (e) 1 phr at different localization within sample marked as A and B

IV.4. Film-blowing of *in-situ* compatibilized PHBV/PBSA blends

Figure IV.9 illustrates the ability of the blend containing 0, 0.1, and 0.2 phr DCP to be processed by film blowing. Introduction of PBSA with content as low as 30 wt% provided enough melt strength making film blowing possible. The main drawback of the dry blend was that the bubble was found to be difficult to stabilize and showed a tendency to exhibit draw resonance. Addition of DCP at ca. 0.1 phr, further improved the melt strength and added extensional viscosity by displaying greater film blowing stability as assessed from the greater blow-up ratio (BUR) achieved in comparison of the dry blend (Table IV.1). However, the ability of blown film was found limited for formulation containing 0.2 phr DCP which showed white aggregates (inset *Figure IV.9*) and less extensibility, which could be caused by the too high cross-linking

Chapter IV

network. These particles were found to act as defect points and did not allow the film to blow correctly.

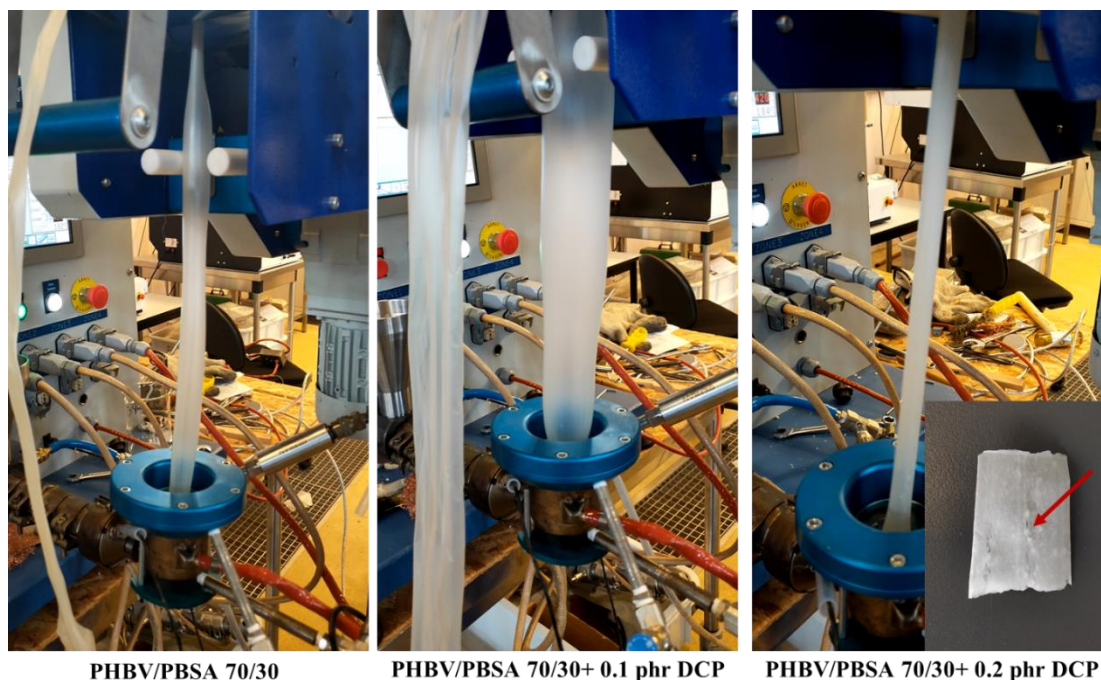


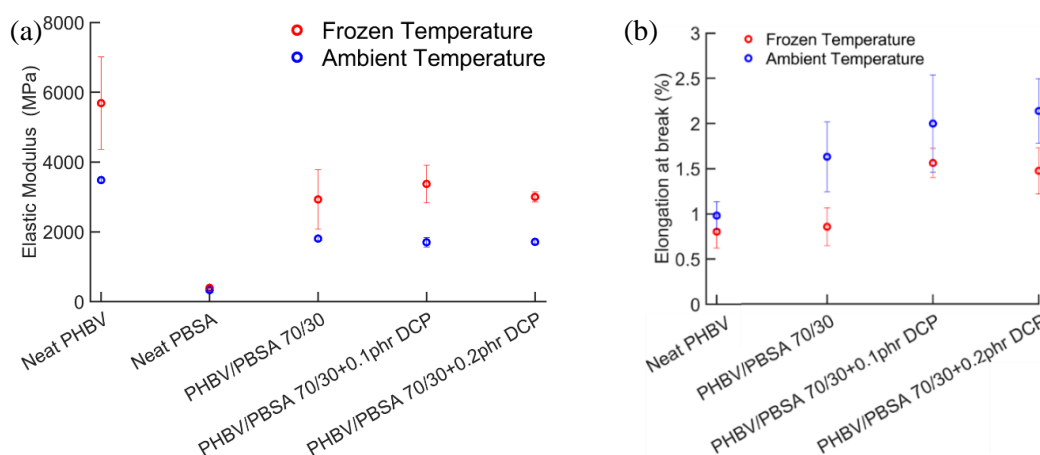
Figure IV.9: Film blowing of PHBV/PBSA with addition of dicumyl peroxide (DCP) resulting from in-situ reactive extrusion

In-situ compatibilization was obviously positive for the processability of the PHBV/PBSA blends, because of the large decrease of the melt flow index as well as the increase of gel content (Table IV.2). PHBV was already found to be sensitive to free-radical grafting with modified PHB blend in the presence of dicumyl peroxide resulting from higher chain branching (Fei et al., 2004), increased strain hardening (D'Haene, Remsen, & Asrar, 1999; Kolahchi & Kontopoulou, 2015), and better processability compared to neat PHBV (Teixeira et al., 2020). For PBSA, to the best of knowledge, no studies have been conducted on the incorporation of organic peroxide. Its counterpart, polybutylene succinate (PBS), also displayed enhanced viscosity with the incorporation of DCP (D. J. Kim et al., 2001; G. Li et al., 2013). Incorporation of DCP in PBS resulted in chemical cross-linking with increased gel content with the increase of DCP content. The complex viscosity of cured PBS increased ten folds compared with that of pure PBS with the addition of 6 phr of DCP (G. Li et al., 2013).

IV.4.1. Tensile properties under ambient and frozen conditions

The mechanical properties of blends produced by TSE were evaluated by means of tensile and Charpy impact tests. Different temperatures, *i.e.* ambient and freezer conditions, were assessed to evaluate the potential of PHBV-based film to be used for packaging dry, chilled, and frozen food. The tensile properties and Charpy impact test under ambient conditions were evaluated and compared with batch mixer samples (Table IV.4). Impact strength improvement with addition of DCP was limited and increased on a limited extent at a DCP content of 0.2 phr. Comparison of the tensile performances between the batch mixer and TSE showed good agreement in maximum stress and elongation at break. Only the elastic modulus was decreased by about 19%.

Evolution of the elastic modulus as a function of experimental temperature and DCP content was evaluated (Figure IV.10(a,b)). The introduction of 30 wt % of PBSA in the PHBV matrix contributes largely to reducing the stiffness of the PHBV-based blend at ca. $-20\text{ }^{\circ}\text{C}$ with a decrease of about 2.5 GPa between neat PHBV and PHBV/PBSA 70/30. The effect of DCP on the elastic modulus is limited since all PHBV/PBSA blends showed an increase of about 1.3 GPa between conditions. However, elongation at break and maximum stress were positively impacted, and both reached a maximum at 0.1 phr DCP. The maximum stress of PHBV/PBSA with 0.1 phr DCP shows an increase by a factor two compared to non-compatible PHBV/PBSA and a value greater than PHBV blank (Figure IV.4(c)). This higher cohesion was interpreted as an improved interfacial compatibility between PHBV and PBSA phases.



Chapter IV

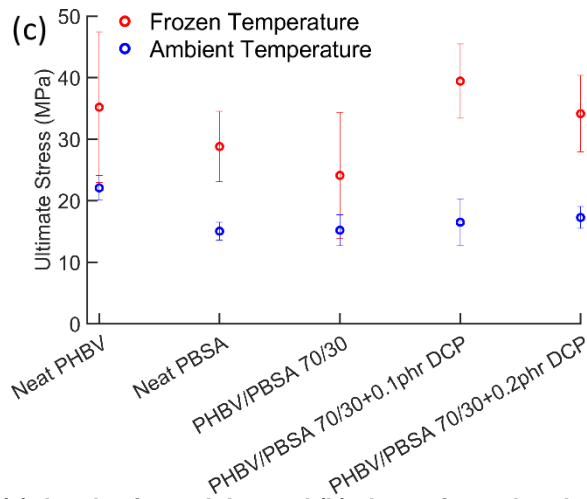


Figure IV.10: Evolution of (a) the elastic modulus and (b) elongation at break and (c) stress at break of the different PHBV/PBSA blends in the presence of dicumyl peroxyde with varying experimental temperatures (Tensile test measurements), ⁽¹⁾Elastic Modulus and stress at break values for neat PHBV and neat PBSA were directly from pellets

IV.4.2. Aging in food contact

Blown PHBV/PBSA (0.1 phr DCP) films were tested as flexible packaging for frozen food. Frozen foods, possibly fatty (parfried or fried products, ice cream, etc.), are subjected to long-time storage at low temperature, *i.e.*, -20°C , and are in permanent contact with the film. Here the film was filled with frozen French fries, hot sealed and stored at -20°C . The hot sealing was possible, making it possible to obtain a plastic bag filled with frozen fatty food products (Figure IV.11). No evidence of delamination was observed over time on the sealing line.



Figure IV.11: Hot sealed film of PHBV/PBSA + 0.1phr DCP filled with frozen French fries

Figure IV.12 (a,b) shows the elastic modulus and elongation evolution at break over time. PHBV-based blend shows a tendency of embrittlement within the first two weeks before reaching a stable state. The maximum loss of elongation at break ca. 20% was reached during the first two weeks. These observations were in good agreement with previously reported

Chapter IV

results, showing stabilization of mechanical properties after 15 days of aging (Corre et al., 2012; Deroiné et al., 2014). Secondary crystallization after processing was the dominant cause (de Koning & Lemstra, 1993). Similar observations at ambient conditions were made with a loss of about 22 % from 1.4 to 1.1 % in elongation at break after one year (Deroiné et al., 2014). Despite the severe storage conditions, *i.e.*, -20°C and saturated humidity, mechanical properties were not impacted because PHBV was already glassy and very brittle. Embrittlement due to physical aging has no additional effect.

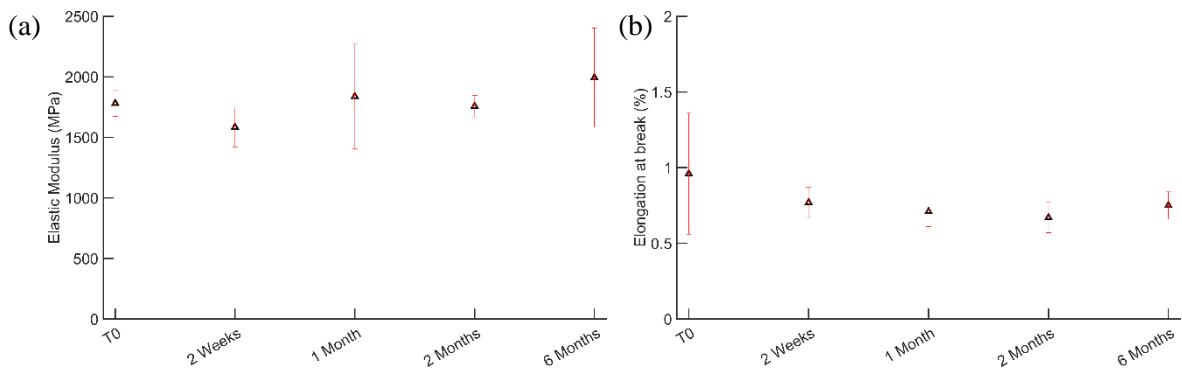


Figure IV.12: Evolution of (a) the elastic modulus and (b) the elongation at break of PHBV/PBSA 70/3+ 0.1 phr DCP in contact with frozen French fries after being stored at -20°C over various period of time (Tensile test measurements)

IV.5. Conclusion

This study investigates the *in-situ* compatibilization of PHBV/PBSA blends at a weight ratio of 70:30 with the introduction of dicumyl peroxide in reactive extrusion. Batch mixing was subsequently followed by film blowing trials and successfully demonstrated its ability to be blown at a PHBV content of 70 wt%. Addition of DCP induced reaction mechanism between PHBV and PBSA leading to the formation of cross-linked PHBV-g-PBSA structure as confirmed from the evolution of melt flow index, gel content, and change in morphologies. Reactive extrusion was found to have a positive impact on the rheological properties. The results of the linear viscoelastic measurement highlighted a change from Newtonian to the apparition of a frequency dependent behavior at low frequencies. Film blowing processability of PHBV was positively impacted with improved melt strength. The results of tensile testing showed that the elastic modulus was decreased with the addition of DCP. The elongation at break over an extensive temperature range between -20 °C and 20°C displayed comparable values, while the introduction of DCP led to limited improvement in ductility.

Chapter IV

Chapter V

Part I: Improvement of the thermo- mechanical properties of PHBV- based blend through plasticization using Acetyl Tributyl Citrate

V.1.Introduction

Poly(3-hydroxybutyrate-*co*-3-hydroxyvalerate) (PHBV) exhibits high brittleness and is described as the results of glass temperature (T_g) close to room temperature, secondary crystallization of the amorphous phase, and the presence of inter-spherulitic cracks (El-Hadi et al., 2002). In our previous studies (Chapter III & Chapter IV), melt blending of PHBV and poly(butylene-*co*-succinate-*co*-adipate) (PBSA) followed by *in-situ* compatibilization with dicumyl peroxide (DCP) were conducted. Film blowing of *in-situ* compatibilized PHBV-based film was successfully conducted. Optimal performances were reached with DCP content of 0.1 phr with the change of the rheological behavior in the low-frequency range from Newtonian to the apparition of frequency dependent behavior. Mechanical properties showed decreased stiffness, improved tensile strength but still show a lack in elongation at break with early rupture.

The addition of a plasticizer is a widely used strategy to enhance the elongation at break of PHBV-based through plasticization via increased free volume in the amorphous phase (Alexandre Ruellan, Ducruet, & Domenek, 2015). Several plasticizers have been studied in PHBV, including Licowax® (Brunel et al., 2014), soybean oil (SO), epoxidized soybean oil (ESO), dibutyl phthalate (DBP), and triethyl citrate (TEC) (Choi & Park, 2004), Polyethylene glycol (Martino et al., 2015) and acetyltributyl citrate (ATBC) (Correa et al., 2012). (Correa et al., 2012) used ATBC as a plasticizer in blend with PHBV-18%HV as well as organo-modified montmorillonite as nanofiller. The incorporation of 10 wt% of ATBC resulted in a significant decrease of glass transition temperature (T_g) of PHBV by more than 10 °C and reduced stiffness. These results were further confirmed by (Martino et al., 2015), who compared several external plasticizers using ATBC, glycerol triacetate (GTA), and PEG. The apolar substance ATBC had the highest affinity with PHBV with the depression of T_g , reduction of elastic modulus, and slight modification of the elongation at break. Moreover, ATBC is authorized for food contact according to European regulation (EC) 10/2011.

In the present work, the effect of the addition of ATBC on the thermal and mechanical properties of the *in-situ* compatibilized PHBV/PBSA blend with different content was assessed at the laboratory scale using a batch mixer. The work aimed to investigate the optimum quantity of ATBC in PHBV-based blend before scale-up using film blowing process for packaging film production.

V.2. Materials and Methods

V.2.1.1. Materials

Commercial PHBV (reference PHI 002) containing 3 mole percent of hydroxyvalerate (HV) – according to technical datasheet – and PBSA (reference PBE 001) were purchased from NaturePlast (France). Polymers were dried at 70 °C under vacuum for at least six hours before use. Dicumyl peroxide (DCP) was purchased from ACROS, Acetyl Tributyl Citrate (ATBC) was purchased from Sigma-Aldrich and used as received.

V.2.1.2. Sample preparation using a batch mixer

The basis formulation PHBV/PBSA with a ratio of 70/30 wt/wt and 0.1 phr (parts per hundred of resin on a weight basis) DCP was used. The amount of PHBV/PBSA and DCP were fixed, and the mass of ATBC was calculated to match the appropriate ratio in the mixture. The individual formulations are presented in Table V.1.

Plasticized PHBV/PBSA/DCP blends with ATBC were prepared using an internal mixer at 190 °C at 90 rpm for 9 min. First, PHBV was introduced in the mixing chamber for 3 min to allow its melting. Then, ATBC was introduced in the mixing chamber for 3 min. After 6 min of mixing, PBSA pellets and DCP were introduced, and the blend was mixed for another 3 min. The blended materials were finally molded by thermo-compression in foils thanks to a thermal press (SCAMEX 15T, France). First, pellets were pre-melt for 3 min before being subjected successively to 80 and 150 bar for 1 min each. Aluminum foils of 200 µm were used to control the thickness of samples. The final thickness was measured with a caliper.

Table V.1: Formulations and nomenclature

| Sample | Formulations | | | |
|----------------------|----------------|----------------|------------|----------|
| | PHBV (wt %) | PBSA (wt %) | DCP* | ATBC (%) |
| PHBV/PBSA+DCP | 70 | 30 | 0.1 phr | - |
| PHBV/PBSA/ATBC5+DCP | 66.5 | 28.5 | | 5 |
| PHBV/PBSA/ATBC10+DCP | 63 | 27 | | 10 |
| PHBV/PBSA/ATBC15+DCP | 59.5 | 25.5 | | 15 |
| PHBV/PBSA/ATBC20+DCP | 56 | 24 | | 20 |

*based on the quantity of PHBV/PBSA blend

V.2.1.3.Characterization techniques

V.2.1.3.1.Thermal properties

Thermal properties of blends were assessed by DSC (DSC1, Mettler Toledo, Switzerland) according to the program shown in Figure V.1. All measurements were used under nitrogen atmosphere (flow rate 50 mL/min) with 5 to 10 mg of materials sealed in 40 μ L aluminum pans. Calibration was carried out with Indium and Zinc standards. The first cooling and second heating scan served to measure the crystallization and melting enthalpy. The glass transition temperature of PHBV was measured at the 3rd heating scan after physical aging of either PHBV at -10 °C and the T_g of PBSA at the 4th heating scan after physical aging at -60 °C.

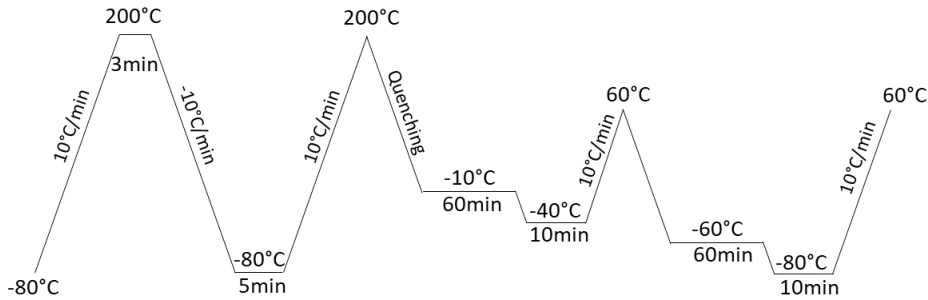


Figure V.1 : Differential scanning calorimetry measurement protocol

The crystallinity degree of each polymer $\{\chi_i\}_{i=PHBV,PBSA}$ was determined from the endotherm

$\Delta H_{m,i}$ as:

$$\chi_i = \frac{\Delta H_{m,i} - \Delta H_{cc,i}}{w_i \Delta H_{m,i}^0}, \tag{Eq. V.1}$$

where w_i the weight content of the corresponding polymer; $\Delta H_{cc,i}$ the cold crystallization enthalpy and $\Delta H_{m,i}^0$ the melting enthalpy of a 100 % crystalline material with pure PHBV (146 J/g, from Corre et al. (2012)) and PBSA (113.4 J/g , from Charlon et al. (2016)).

V.2.1.3.2.Mechanical properties

Tensile properties were measured using a texture analyzer (model TAHD, Stable Micro Systems, UK) equipped with pneumatic grips with a 5 mm/min crosshead speed. Two hundred

Chapter V

micrometer thick dumbbell-shaped samples of type 5 were cut from our compression-molded sheets and used for tensile testing. Sample thickness was averaged from five measurements with a caliper. At least ten samples were tested for each blend composition.

V.2.1.3.3. Scanning Electron Microscopy

After failure from tensile tests, the morphology of the plasticized PHBV-based blends was observed with an Environmental Scanning Electronic Microscopy (model FEI Quanta 200, FEI Company, USA) with an accelerated voltage of 12 kV. Samples were sputter-coated with a thin gold layer (model Sputter coater Emitech K550, Emitech, UK) and imaged from their edges.

V.2.1.4. Gel content

Plasticized PHBV/PBSA/ATBC+ 0.1 phr DCP blends with ATBC contents of 0, 5, 10, 15 and 20 wt% were first milled (Model Retsch MM400, Germany). Two successive Soxhlet extraction were performed to extract the two polymers PHBV and PBSA, independently. Chloroform is a good solvent for PBSA and PHBV but not for the cross-linked network. Besides, THF is a good solvent only for PBSA. The extraction of PBSA extraction in boiling THF tetrahydrofuran for one day followed by extraction of PHBV in boiling chloroform for two consecutive days. The gel fraction was calculated as follows :

$$gel\ wt.\ \% = \frac{m_1}{m_0} \cdot 100\%, \quad \text{Eq. V.2}$$

where m_0 is the original weight of samples and m_1 is the weight of dry residues obtained after extraction

V.3. Results and discussion

V.3.1. Batch mixing processability: effect of ATBC content

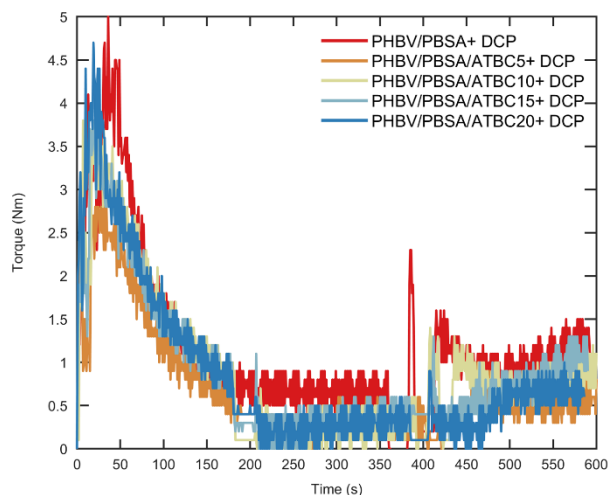


Figure V.2: Measurement of torque over time during melt mixing of plasticized and unplasticized PHBV/PBSA/ATBC+ DCP with different ATBC content

Figure V.2 shows the evolution of the torque measured in the mixing chamber during melt blending of PHBV and PBSA with DCP and ATBC as free radical initiator and plasticizer, respectively. After introducing ATBC at 200 s, the torque decreased compared to unplasticized blends, resulting from the introduction of a low viscous compound. After introducing PBSA and DCP, a significant torque increase was monitored and interpreted as the cross-linking reaction between PHBV and PBSA (Chapter IV) during 100 s between 500 s and 600 s and decreased with ATBC content. For ATBC content lower than 20 wt %, maximum torque was reached at about 575 s against 525 s with 20 wt % ATBC.

V.3.2. Gel content

The cross-linking reaction between PHBV and PBSA was measured by the gel fraction as a function of ATBC content. The increase of ATBC up to 10 wt % led to decreased gel content and reached a minimum value for 10 wt % ATBC. However, passing a threshold value of 10 wt % ATBC the gel content was increased and reached a maximum of 20 wt % ATBC. The presence of gel content can be related to crosslinking reaction, as proposed by (P. Ma et al., 2012). Therefore, despite the addition of ATBC, the reaction mechanism leading to PHBV-g-PBSA was still promoted but to a limited extend for low content of ATBC, i.e., 5 and 10 wt %.

Table V.2: Gel content of plasticized and unplasticized PHBV-based blends with varying ATBC content

| Samples | Gel content (%) |
|----------------------|-----------------|
| PHBV/PBSA+DCP | 9± 4 |
| PHBV/PBSA/ATBC5+DCP | 8± 1 |
| PHBV/PBSA/ATBC10+DCP | 4.7±1 |
| PHBV/PBSA/ATBC15+DCP | 11±4 |
| PHBV/PBSA/ATBC20+DCP | 13±3 |

V.3.3. Thermal properties

Differential scanning calorimetry was used to study the effect of ATBC on the thermal properties of *in-situ* compatibilized PHBV/PBSA blends, as shown in Figure V.3(a,b). DSC results are reported in Table V.3. Regarding the evolution of the melting behavior, a double melting endotherm with two melting temperatures T_{m1} and T_{m2} was observed. The DSC curve of PHBV/PBSA/ATBC10+DCP show a double crystallization peak in the PHBV phase and located between T_c of unplasticized blend and PHBV/PBSA/ATBC15+DCP. The double melting peaks account for the appearance of two forms of crystallites with different perfection, where T_{m1} is related to less well-crystallized PHBV (Correa et al., 2012). This phenomenon was also observed in PBSA crystals. T_{m1} is shifted by 10 °C towards cooler temperatures at 10 wt % ATBC. Further increase in additive content did not lead to further depression of melting peaks. Moreover, ATBC had a positive effect on the crystallinity degree of PBSA, which increased from 29 to about 40 % with 20 wt % ATBC. The higher polymer mobility promotes crystallization and might have caused its increase in the amorphous phase of PBSA.

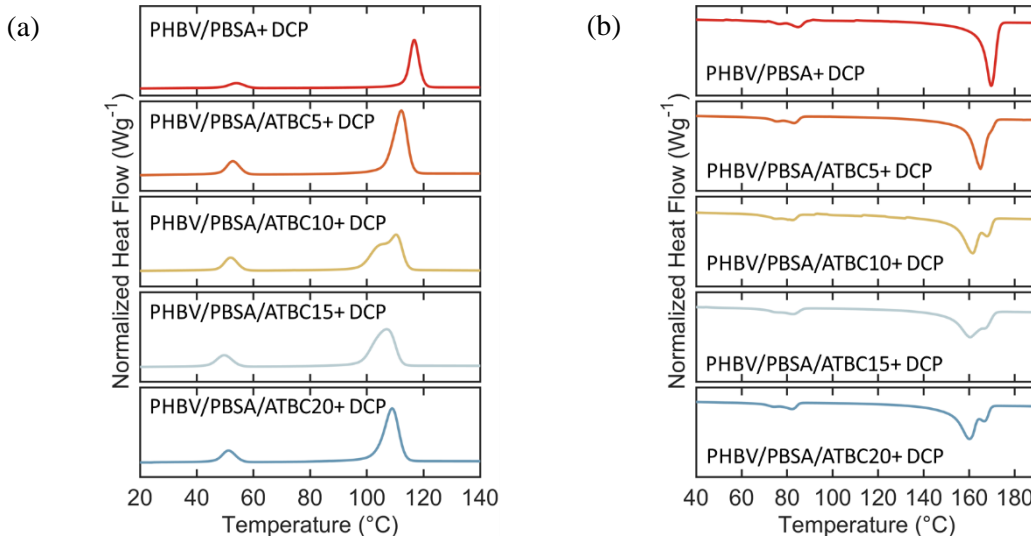


Figure V.3: Different scanning calorimetry curves of (a) cooling curves and (b) melting behavior resulting from 2nd heating scan of the plasticized PHBV/PBSA blends with varying ATBC content of 0, 5, 10, 15 and 20 wt %

V.3.4. Relaxation of the amorphous phase

The glass transition temperature of PBSA and PHBV upon inclusion of 5 to 20 wt% ATBC is shown in Figure V.4(a,b). As expected, two distinct T_g were identified and decreased because of the action of the plasticizer. It suggests that the addition of ATBC led to its distribution in both phases. However, when the ATBC concentration was increased, no further change in T_g was observed except for PBSA.

The prediction of T_g as a function of ATBC can be estimated by the empirical Fox equation:

$$\frac{1}{T_{g,i}} = \frac{w_{1,i}}{T_{g1,i}} + \frac{1-w_{1,i}}{T_{g2}}, \quad \text{Eq. V.2}$$

where $T_{g1,i}$ is the glass temperature of PHBV or PBSA phase, T_{g2} is the glass temperature of ATBC, while $w_{1,i}$ is the weight fraction of $i = PHBV, PBSA$.

As plotted in Figure V.4(a), the T_g value of PBSA followed the Fox equation remarkably with a slight deviation at 15 wt %. These observations supported the good miscibility of the studied mixtures PBSA/ATBC. However, for PHBV phase, as shown in Figure V.4(b), there is a leveling off of the T_g at about -4 °C. This phenomenon is mostly related to the low miscibility of ATBC within PHBV phase for concentrations higher than 5 wt %. (Martino et al., 2015) observed a T_g at -14 °C with the introduction of 10 wt % ATBC in PHBV and intersects well with the Fox equation as shown in Figure V.4(b). Therefore, ATBC preferentially solubilizes in the PBSA phase due to miscibility ATBC/PBSA in the investigated range.

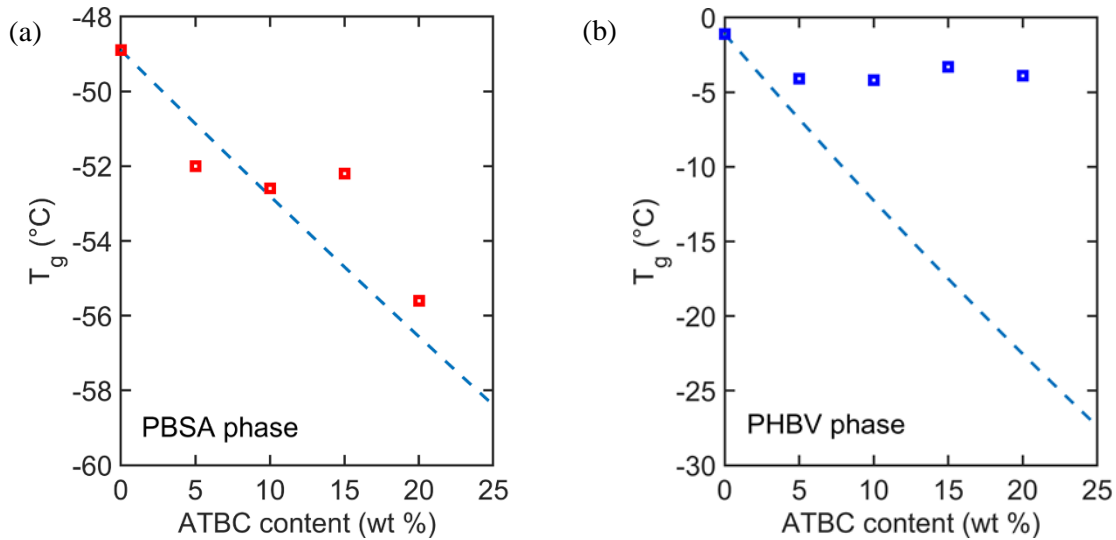


Figure V.4: Glass transition temperature of the two distinct PHBV and PBSA phases as a function of ATBC with (a) PBSA/ATBC and (b) PHBV/ATBC (DSC measurements). Experimental results (empty symbols) and Fox equation (dashed line)

Table V.3: Thermal properties of plasticized PHBV/PBSA blends evaluated by DSC from the second heating and cooling scans

| Samples | T_m (°C) | | | | χ (%) | | T_c (°C) | | T_g (°C) | |
|----------------------|------------|----------|----------|----------|------------|------|------------|--------|------------|-----------|
| | PHBV | | PBSA | | PHBV | PBSA | PHBV | PBSA | PHBV | PBSA |
| | T_{m1} | T_{m2} | T_{m1} | T_{m2} | | | | | | |
| PHBV/PBSA+DCP | 169±1 | | 85±1 | | 63±2 | 29±5 | 117±0.2 | 54±0.2 | -1.1±0.7 | -48.9±1.3 |
| PHBV/PBSA/ATBC5+DCP | 165 | | 76 | 82 | 61 | 31 | 113 | 53 | -4.1 | -52 |
| PHBV/PBSA/ATBC10+DCP | 161 | 168 | 75 | | 63 | 35 | 111 | 52 | -4.2 | -52.6 |
| PHBV/PBSA/ATBC15+DCP | 160 | 167 | 76 | | 62 | 45 | 107 | 50 | -3.3 | -52.2 |
| PHBV/PBSA/ATBC20+DCP | 160 | 166 | 74 | | 70 | 41 | 109 | 51 | -3.9 | -55.6 |

V.3.5. Tensile properties of plasticized PHBV-based blends

Evidenced stiffness and brittleness of PHBV hampers its ability to be used as flexible food packaging. Blend mixing of PHBV and PBSA followed by *in-situ* compatibilization using DCP has been conducted. The processing conditions lowered the elastic modulus but were insufficient to increase the elongation at break (Chapitre IV) significantly. Changes in the

Chapter V

mechanical behavior of PHBV/PBSA+DCP blends upon inclusion of ATBC are presented in Figure V.5(a,b), and the values are gathered in Table V.4. The external plasticizer lowered the stiffness in that it reduced the Young modulus (Figure V.5(a)). A plateau modulus close to 700 MPa was reached at higher content of ATBC. This corroborates well with the results found from the relaxation of the amorphous phase where T_g was not lowered beyond an ATBC content of 10 wt %. However, maximum stress was found to decrease with increased ATBC content and reached a minimum value of 8 MPa. Figure V.5(b) shows that the elongation at break could be slightly improved to a maximum value of 2.9 %. The obtained results displayed the same tendency as plasticized PHBV with ATBC in literature. The work conducted by (Martino et al., 2015) showed that the introduction of 10 wt % of ATBC in PHBV-3HV led to the decrease of Young modulus from 2.7 GPa to 1.2 GPa as well as a decrease in tensile strength from 35 to 24 MPa. In the present work, obtained values of PHBV/PBSA/ATBC10+ DCP were very close to that of PHBV-18HV/10 wt % ATBC (Correa et al., 2012). The authors showed that Young modulus and tensile strength were decreased from 1080 to 730 MPa and from 24.9 to 15.4 MPa after plasticization, respectively. According to the comparison with other studies and gel content, the interface between PHBV and PBSA was optimum for an ATBC content of 10 wt %.

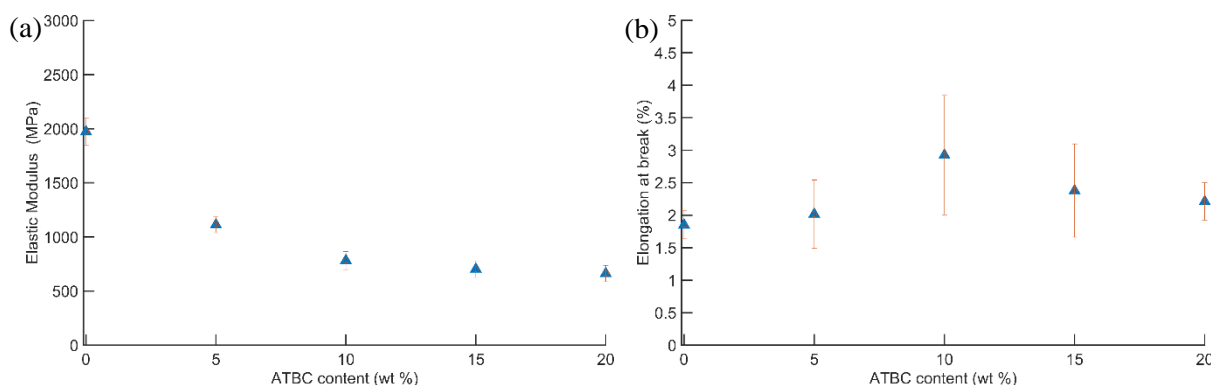


Figure V.5: Experimental mechanical properties of the plasticized PHBV/PBSA blends with evolution of (a) elastic modulus and (b) elongation at break with varying ATBC content of 0, 5, 10, 15 wt %

Despite that the improvement in ductility is very limited, changes in the fracture surface of the samples were observed using SEM (Figure V.6(a-e)). As already observed in the previous section (Chapter IV) addition of 0.1phr DCP resulted in morphological changes with the apparition of stretched fibers. This type of morphology was already reported for *in-situ* compatibilized PLA/PBAT blends in the presence of DCP (Ma et al., 2014). For very low contents of ATBC, i.e., 5 wt%, the tensile fracture surface showed similar morphology compared to the unplasticized blend. The inclusion of 10 wt % ATBC led to the apparition of

Chapter V

long stretched filaments (Figure V.6(c)). Further increase of ATBC up to 20 wt % accounted for a morphology with shorter elongated fibers (Figure V.6(d,e)). These tensile fracture surfaces corroborated well the tensile properties since matrix yielding was evidence for 10 wt % ATBC while it showed the maximum elongation at break.

Table V.4: Mechanical properties of plasticized PHBV/PBSA blends obtained from tensile test measurements

| Materials | Young modulus (MPa) | Maximum stress (MPa) | Elongation at break (%) |
|----------------------|---------------------|----------------------|-------------------------|
| PHBV/PBSA+DCP | 1973± 124 | 21± 3 | 1.9±0.2 |
| PHBV/PBSA/ATBC5+DCP | 1114±73 | 12±2 | 2±0.5 |
| PHBV/PBSA/ATBC10+DCP | 783± 83 | 11± 2 | 2.9± 0.9 |
| PHBV/PBSA/ATBC15+DCP | 703± 77 | 9±2 | 2.4± 0.7 |
| PHBV/PBSA/ATBC20+DCP | 663± 75 | 8±1 | 2.2± 0.3 |

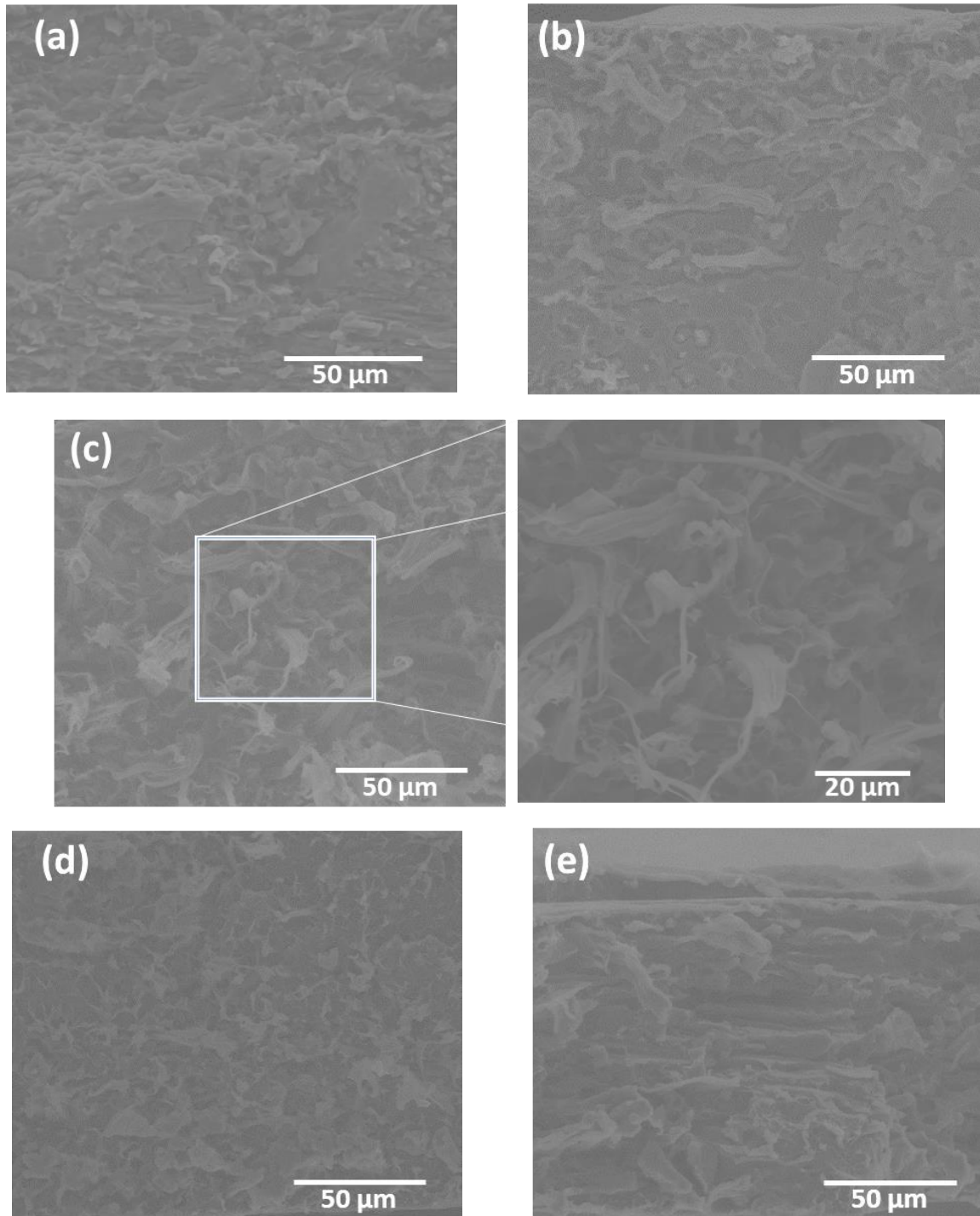


Figure V.6: SEM images of the cross-section after tensile test of unplasticized and plasticized PHBV/PBSA/ATBC+DCP with ATBC content of a) 0 wt %, b) 5 wt %, c) 10 wt %, d) 15 wt %, e) 20 wt %

V.4. Conclusion

The matrix yielding was limited compared to externally plasticized composites. Where elongated fibers reveal matrix yielding. Despite that, and as already discussed in the literature, the improvement of the mechanical properties of PHBV through the addition of an external

Chapter V

plasticizer remains difficult. PHBV has very high crystallinity content and even blended with another ductile polyester; the overall crystallinity remains high. As a consequence, and since plasticizer acts on the amorphous phase, the plasticizing effect remains limited (Martino et al., 2015).

Chapter V

Chapter V:
**Part II: Design of poly(3-
hydroxybutyrate-co-3-
hydroxyvalerate)-based flexible
packaging for frozen food: from
batch-mixer to film blowing**

V.5.Introduction

Packaging food safety compliance is of high importance since the present study designed bio-based and biodegradable flexible food packaging to come into contact with fatty food. The use of dicumyl peroxide (DCP) as a compatibilizer between immiscible binary blends was tested by several authors (Dong et al., 2013; P. Ma et al., 2012; Teixeira et al., 2020; K. Zhang et al., 2014). A change in the European regulation will occur from September 2022. Dicumyl peroxide (DCP, CAS 80-43-3) will be categorized reprotoxic, “Reproductive toxicity 1B”. Therefore, it cannot be used in the future in Food Contact Materials. An alternative peroxide compliant with the European regulations (EC) 10/2011 and (EC) 1935/2004 needed to be found. LUPEROX® 101E was selected as the best option. This organic peroxide is listed as a polymerization aid and, therefore, not specifically regulated. As a result, it may be present in the plastic layers intended to come into contact with foodstuffs according to Article 6(4)(b) and Article 19 of regulation 10/2011/EC. The present study reports the capacity of LUPEROX® 101E to replace DCP in *in-situ* compatibilization of PHBV, and PBSA plasticized or not with Acetyl Tributyl Citrate (ATBC).

The previous sections of this thesis have reported the adopted strategy to modify the rheological and thermal properties, including binary mixture, the addition of the reactive compatibilizer DCP, and the use of the external plasticizer ATBC. Reactive extrusion in the presence of DCP resulted in a change in the rheological behavior, and as a key result, film blowing of PHBV/PBSA blends at the lab scale was demonstrated. Final properties showed reduced stiffness under both ambient and freezer conditions compared to neat PHBV and stable thermo-mechanical properties over long-time storage under freezing conditions in contact with fatty food. The fragile behavior of the formulation evidenced by its poor elongation at break limits its potential use for flexible food packaging. A workaround was suggested by adding an external plasticizer ATBC to the blend to decrease PHBV-based blend rigidity further. Best results were obtained for 10 wt % ATBC with decreased stiffness and slight improvement in elongation at break. Thermal properties were modified with depression of T_m , T_c and T_g in both phases, i.e. PHBV and PBSA. T_g evolution fitted with the Fox equations predicted a deviation for ATBC content higher than 5 wt%, supporting the assumption of phase separation. By contrast, the good fitting of T_g values of PBSA/ATBC mixtures confirmed their good miscibility.

LUPEROX® 101E is expected to induce at least the same improvements as those observed with DCP in the PHBV/PBSA mixture in terms of rheological and thermo-mechanical

Chapter V

properties. Preliminary tests suggested to test two contents at 0.1 and 0.2 phr LUPEROX® 101E. Since the introduction of an external plasticizer induced changes in the final properties, a fixed content of ATBC at 10 wt % was applied in all experiments.

The present study reports first on the thermo-mechanical properties obtained from a batch-mixer, where great attention was devoted to the capacity of LUPEROX® to replace DCP. Finally, film-blowing trials were conducted to support the industrial processing of PHBV-based blends for flexible food packaging.

V.6. Materials and Methods

V.6.1. Materials

Commercial PHBV (reference PHI 002) containing 3 mole percent of hydroxyvalerate (HV) – according to technical datasheet – and PBSA (reference PBE 001) were purchased from NaturePlast (France). Polymers were dried at 70 °C under vacuum for at least six hours before use. Luperox® 101E was supplied by ARKEMA, Dicumyl peroxide (DCP) was purchased from ACROS, and Acetyl Tributyl Citrate was purchased from Sigma-Aldrich and used as received.

V.6.2. Batch mixer

The plasticized and unplasticized blends of PHBV/PBSA 70/30 in the presence of Luperox® were mixed at 190 °C and 90 rpm for 9 min. For unplasticized blends, PHBV/PBSA with the addition of Luperox® at ca. 0.1 and 0.2 phr (parts per hundred of resin on a weight basis) were first prepared. First, PHBV was pre-melted for 6 min, then PBSA pellets mixed with Luperox® were introduced and mixed for 3 min. For plasticized blends, PHBV/PBSA was mixed with ATBC, resulting in weight ratios PHBV/PBSA/ATBC 63/27/10. Formulations with 0.1 and 0.2 phr Luperox® were prepared. The quantity of Luperox® was related to the amount of PHBV/PBSA blend. For plasticized blends, PHBV was introduced in the mixing chamber for three min to allow its melting. Then, ATBC was introduced in the mixing chamber and mixed for three extra min. After 6 min, PBSA pellets and Luperox® were introduced and mixed for another 3 min.

Thermo-compression molding (SCAMEX 15T, France) was used to obtain foils. First, pellets were pre-melted for 3 min without pressure before being subjected successively to 80 and 150

bar, for 1 min each. Aluminum foils of 200 μm were used to control the thickness of samples. The final thickness was measured with a micrometer.

V.6.3. Compounding using twin screw extrusion

Compounding of plasticized and unplasticized PHBV/PBSA blends with Luperox® contents 0.2 phr was carried out using a twin-screw extrusion process with a screw length-to-diameter ratio of 32/16 L/D (Thermo Haake Ptw 16-40D). In the present study, the used configuration was co-rotating, intermeshing, and interpenetrated screws. At the exit of the die, the rod was cooled on a conveyor belt and pelletized before being sealed in a hermetic bag. The temperature profile was as follows:

- Barrel: Zone 1/2/3/4/5/6: 20°C/20°C/130°C/170°C/170°C+ Die: 170°C
- Screw speed: 300 rpm.

V.6.4. Film blowing extrusion

A single screw extrusion equipped with a screw having a length-to-diameter ratio of 25/20 L/D (SCAMEX Rheoscam, France) was used. Film blowing was realized using the film blowing extrusion module MAPRE/COOLIN (France). The film blowing parameters are gathered in Table V.1. The temperature profile was as follows:

- Barrel: Zone 1/2/3/4/5/6/7: 140°C/160°C/170°C/170°C/180°C/180°C/170°C
- Die: Zone 1/2/3/4 : 170°C/165°C/165°C/165°C
- Screw speed: 30 rpm.

Table V.1: Film blowing parameters

| Film blowing parameters | Values | |
|-------------------------|-----------------------------------|---|
| | PHBV/PBSA 70/30 + 0.2 phr Luperox | PHBV/PBSA/ATBC 63/27/10 + 0.2 phr Luperox |
| Die diameter | 50 mm | |
| Die gap | 0.8 mm | |
| Film thickness | 77±11 μm | 88±11 μm |
| Blow up Ratio (BUR) | 2.4 | 3.8 |
| Draw down ratio (DDR) | 4.3 ⁽¹⁾ | 2.4 ⁽¹⁾ |

⁽¹⁾Based on the average value of film thickness

The Blow Up Ratio and Draw down ratio are given by Eq. V.1 and Eq. V.2, respectively:

$$\text{Blow Up Ratio (BUR)} = \frac{R}{R_o} \quad \text{Eq. V.1}$$

Chapter V

Draw down ratio (DDR) = (Die gap/Film thickness)/BUR , Eq. V.2
 where R and R_o are the final radius of the duct and punch radius.

V.6.5.Characterization techniques

V.6.5.1.Thermal characterization

Thermal properties of blends were assessed by DSC (DSC1, Mettler Toledo, Switzerland) according to the program shown in Figure V.1. All measurements were used under nitrogen atmosphere (flow rate 50 mL/min) with 5 to 10 mg of materials sealed in 40 μ L aluminum pans. Calibration was carried out with Indium and Zinc standards. The first cooling and second heating scan served to measure the crystallization and melting enthalpy. The T_g of PHBV was measured at the 3rd heating scan after physical aging of either PHBV at -10 °C and the T_g of PBSA at the 4th heating scan after physical aging at -60 °C.

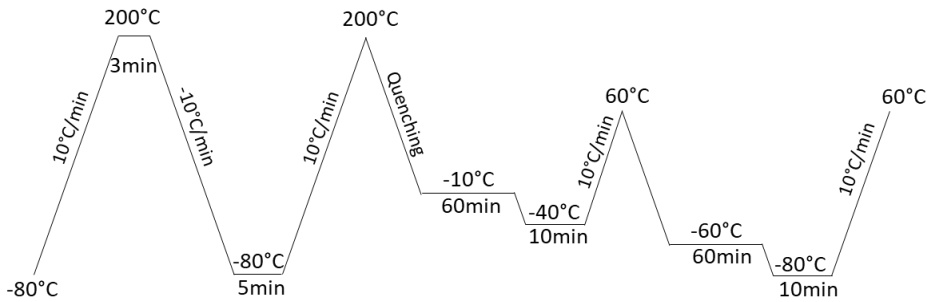


Figure V. 1 : Differential scanning calorimetry measurement protocol

The crystallinity degree of each polymer $\{\chi_i\}_{i=PHBV,PBSA}$ was determined from the endotherm

$\Delta H_{m,i}$ as:

$$\chi_i = \frac{\Delta H_{m,i} - \Delta H_{cc,i}}{w_i \Delta H_{m,i}^0}, \quad \text{Eq. V.3}$$

where w_i the weight content of the corresponding polymer; $\Delta H_{cc,i}$ the cold crystallization enthalpy and $\Delta H_{m,i}^0$ the melting enthalpy of a 100 % crystalline material with pure PHBV (146 J/g, from (Corre et al., 2012)) and PBSA (113.4 J/g , from (Charlon et al. (2016))).

V.6.5.2. Scanning Electron Microscopy

The morphology of the PHBV/PBSA blends was studied by an Environmental Scanning Electronic Microscopy (ESEM, FEI Quanta 200) with an accelerated voltage of 12 kV. Prior to observation, the samples were sputter-coated with a thin gold layer (Sputter coater Emitech K550).

V.6.5.3. Rheological properties

Rheology measurements in melt state were performed with a stress-controlled rheometer (MCR 302, Anton Paar, Graz, Austria) using a disk-shaped specimen. A parallel-plate geometry with a gap set between 750 and 800 μm at 185 $^{\circ}\text{C}$. Dynamic frequency sweep experiments were performed from 0.01 to 100 Hz in the linear viscoelastic region.

V.6.5.4. Mechanical properties

Tensile tests were carried under both ambient and freezer (-20 $^{\circ}\text{C}$) conditions. For ambient conditions, tensile properties were measured using a texture analyzer (model TAHD, Stable Micro Systems, UK) equipped with pneumatic grips with a 5 mm/min crosshead speed. For frozen conditions (-20 $^{\circ}\text{C}$), tensile tests were performed on a Zwick Z010. The dumbbell-shaped samples of type 5 with a target thickness of 200 μm were cut from the compression-molded sheets for tensile test. Thickness was an average of 5 measurements measured with a micrometer. At least five samples were tested for each ratio.

Charpy notched impact tests were assessed according to ISO 179, using a Zwick B5113.300 impact tester. Pendulums of 1 and 4 J were used for PHBV-based blends and PBSA, respectively. At least five samples were tested for each ratio.

V.6.5.5. Gel content

Plasticized and unplasticized PHBV/PBSA/ATBC+ 0.2 phr Luperox[®] were first milled (Model Retsch MM400, Germany). Two successive Soxhlet extraction were performed to independently extract the two polymers PHBV and PBSA. Chloroform is a suitable solvent for PBSA and PHBV, but not for the cross-linked network. Besides that THF is a good solvent only for PBSA. The extraction of PBSA extraction in boiling THF tetrahydrofuran for one day

Chapter V

followed by extraction of PHBV in boiling chloroform for two consecutive days. The gel fraction was calculated as follow :

$$gel\ wt.\ \% = \frac{m_1}{m_0} \cdot 100\%, \quad \text{Eq. V.4}$$

where m_0 is the original weight of samples and m_1 is the weight of dry residues obtained after extraction

V.6.5.6. Aging

Physical aging was carried out on PHBV-based bags upon various storage times at $-20\text{ }^\circ\text{C}$ and in contact with fatty food. First, the obtained films were cut with a length of about 30 cm and thermo-sealed manually from one side using a vacuum packing machine with sealing conditions of 0.8 s (Model C200, Multivac, Germany). Then, bags were filled with frozen French fries with a quantity of about 625 g before being sealed on the other side. Finally, samples were placed in a freezer with a temperature of $-20\text{ }^\circ\text{C}$ for various periods. Before being subjected to DSC and tensile tests, samples were thawed and placed at $25\text{ }^\circ\text{C}$, RH=50 % for 24 h at least.

V.7. Results and Discussion

V.7.1. Batch mixing processability: effect of ATBC content

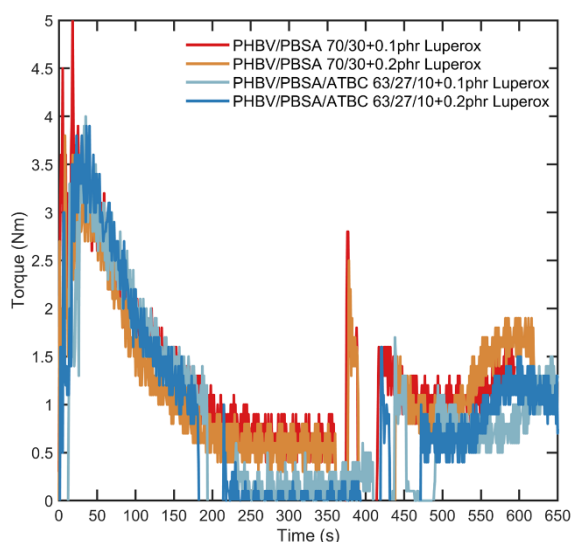


Figure V.2: Torque evolution with time during melt mixing of PHBV/PBSA blend with or without the addition of ATBC and as a function of Luperox® content, i.e. 0.1 and 0.2 phr

Chapter V

Figure V.2 shows the evolution of the torque measured in the mixing chamber during melt mixing of PHBV/PBSA blend as a function of Luperox® content with or without the addition of ATBC. After the introduction of PBSA and Luperox®, the curve showed an abrupt increase and was attributed to the cross-linking reaction between PHBV and PBSA similarly to our previous study (Chapter IV). The addition of a fixed content of ATBC, i.e., 10 wt %, led to the decrease of the torque when blended with PHBV due to its low viscosity. Despite the presence of ATBC, an increase in torque is still observed and reached a maximum at the early stage with 0.2 phr Luperox®. However, the torque showed a depression of the torque and may be attributed to partial degradation of polymer chains. Similar to the addition of DCP in PHBV/PBSA blends (Chapter IV), Luperox® was found to act as a cross-linking agent and led to the formation of PHBV-g-PBSA. Moreover, the addition of ATBC did not hinder the cross-linking reaction between PHBV and PBSA.

V.7.2. Gel content

The efficiency of cross-linking reaction between PHBV and PBSA with the addition of ATBC and Luperox® was measured as a function of gel content. Obtained values are given in Table V.2. A similar quantity of organic peroxide, i.e., 0.1 phr DCP and 0.1 Luperox®, led to an increase in gel content by a factor 2. The higher gel content can be attributed to a higher cross-linking reaction as proposed by (P. Ma et al., 2012). An increase in Luperox® content led to higher gel content due to the generation of more free radicals. Inclusion of 10 wt % ATBC combined with Luperox® was still subjected to cross-linking reaction as the gel content remained above plasticized and unplasticized PHBV/PBSA blends with the addition of DCP.

Table V.2: Gel content of plasticized and unplasticized PHBV/PBSA blends with varying content of Luperox® and compared with plasticized and unplasticized PHBV/PBSA/ATBC+ DCP

| Samples | Gel content (%) |
|--|-----------------|
| PHBV/PBSA+ 0.1 phr DCP ⁽¹⁾ | 9± 4 |
| PHBV/PBSA/ATBC 63/27/10 + 0.1 phr DCP ⁽¹⁾ | 4.7±1 |
| PHBV/PBSA 70/30 + 0.1 phr Luperox® | 20± 5 |
| PHBV/PBSA 70/30 + 0.2 phr Luperox® | 28± 2 |
| PHBV/PBSA/ATBC 63/27/10 + 0.1 phr Luperox® | 15 ±1 |
| PHBV/PBSA/ATBC 63/27/10 + 0.2 phr Luperox® | 19 ±1 |

⁽¹⁾ Gel content value extracted from (Chapter IV)

V.7.2.1. Evaluation of the thermal properties of PHBV/PBSA/Luperox® blends

Evaluation of the thermal properties of plasticized and unplasticized PHBV/PBSA blends with varying content of the organic peroxide Luperox® was assessed by means of DSC (Figure V.3(a,b)). DSC results are reported in Table V.3. As expected from previous results (Chapter IV), the introduction of Luperox® in the PHBV/PBSA mixture did not lead to changes in the thermal properties (Table V.3). However, the introduction of 10 wt % ATBC led to the depression of T_m , T_c , and T_g in both phases, *i.e.* PHBV and PBSA. This result was attributed to the increased free volume in the amorphous phase of PHBV and PBSA and resulted in higher chain mobility. The prediction T_g can be estimated by the empirical Fox equation:

$$\frac{1}{T_{g,i}} = \frac{w_{1,i}}{T_{g1,i}} + \frac{1-w_{1,i}}{T_{g2}}, \quad \text{Eq. V.2}$$

Based on the previous study (Chapter V, Part I), the obtained T_g of plasticized PHBV/PBSA/ATBC 63/27/10 with the addition of either Luperox® or DCP and based on Fox law showed phase separation of ATBC with PHBV for an ATBC content of 10 wt % while good miscibility of PBSA/ATBC was still promoted. Therefore, the replacement of the organic peroxide DCP with Luperox® did not interfere with the plasticization of PHBV/PBSA blend.

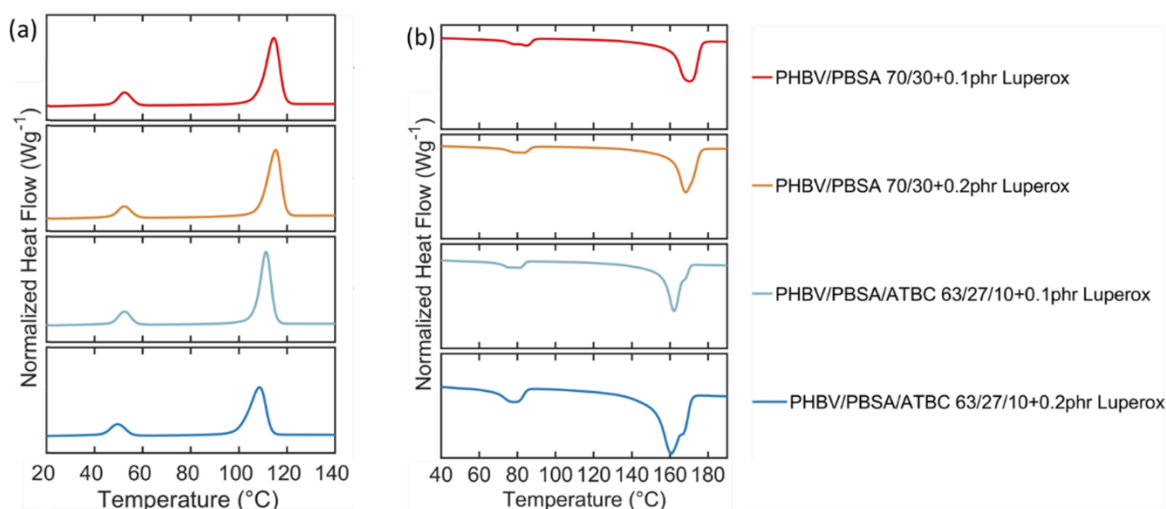


Figure V.3: Different scanning calorimetry curves of a) cooling curves and b) melting behavior resulting from 2nd heating scan of the plasticized and unplasticized PHBV/PBSA blends with varying content of Luperox®

Chapter V

Table V.3: Thermal properties of plasticized PHBV/PBSA/Luperox blends evaluated by DSC from the second heating and cooling scans

| Samples | T _m (°C) ⁽¹⁾ | | T _c (°C) ⁽¹⁾ | | χ (%) ⁽²⁾ | | T _g (°C) | |
|--|------------------------------------|------|------------------------------------|------|----------------------|------|---------------------|-----------|
| | PHBV | PBSA | PHBV | PBSA | PHBV | PBSA | PHBV | PBSA |
| PHBV/PBSA 70/30 | 169±2 | 86±2 | 117±1 | 50±1 | 67±2 | 33±5 | -1.5±0.1 | -48.6±2 |
| PHBV/PBSA 70/30 + 0.1 phr Luperox® | 170 | 85 | 115 | 52 | 63 | 38 | -1.3±0.1 | -47.1±0.1 |
| PHBV/PBSA 70/30 + 0.2 phr Luperox® | 169 | 83 | 116 | 52 | 61 | 35 | -0.8±0.1 | -48±0.8 |
| PHBV/PBSA/ATBC 63/27/10 + 0.1 phr Luperox® | 162 | 81 | 111 | 52 | 61 | 39 | -4.4±0.1 | -53.4±0.1 |
| PHBV/PBSA/ATBC 63/27/10 + 0.2 phr Luperox® | 160 | 78 | 109 | 50 | 57 | 40 | -2.8±0.4 | -52.9±0.6 |

⁽¹⁾ Standard deviation of 1 °C

⁽²⁾ Standard deviation of 1 %

V.7.2.2. Mechanical properties

The tensile properties results are gathered in Table V.4 and obtained values are compared with the mechanical properties of plasticized and unplasticized PHBV/PBSA/DCP blends.

The addition of either 0.1 or 0.2 phr of Luperox® in PHBV/PBSA blends achieved the same value of Young modulus and maximum stress. *In-situ* compatibilization of PHBV/PBSA blend with Luperox® showed similar activity as DCP. However, samples blended with Luperox® showed higher elongation at break than DCP and can be attributed to better interfacial adhesion as suggested from higher gel content Table V.2. Alike our previous work on plasticized PHBV/PBSA/ATBC +DCP (Chapter V, Part II), the inclusion of 10 wt % ATBC reduced stiffness as well as maximum stress. Optimum tensile properties were reached with Luperox® content of 0.2 phr with increased tensile strength and increased elongation at break compared to plasticized blends cross-linked with DCP.

Table V.4: Mechanical properties of plasticized and unplasticized PHBV/PBSA blends with addition of either DCP or Luperox obtained from batch mixer, results are obtained from tensile test measurements

| Samples | Young modulus (MPa) | Maximum stress (MPa) | Elongation at break (%) |
|--|---------------------|----------------------|-------------------------|
| Neat PHBV | 3485±63 | 22±2 | 0.98±0.1 |
| PHBV/PBSA 70/30 | 2227±108 | 19±2 | 1.5±0.4 |
| PHBV/PBSA 70/30 + 0.1 phr DCP | 1973 ±124 | 21±3 | 1.8±0.2 |
| PHBV/PBSA/ATBC 63/27/10 + 0.1 phr DCP | 783± 83 | 11± 2 | 2.9± 0.9 |
| PHBV/PBSA 70/30 + 0.1 phr Luperox® | 1968±146 | 18±3 | 1.5±0.3 |
| PHBV/PBSA 70/30 + 0.2 phr Luperox® | 1942±129 | 19±2 | 2.3±0.7 |
| PHBV/PBSA/ATBC 63/27/10 + 0.1 phr Luperox® | 942±62 | 11±3 | 2.5±0.9 |
| PHBV/PBSA/ATBC 63/27/10 + 0.2 phr Luperox® | 1001±140 | 14±2 | 4±1 |

Higher gel content, higher tensile strength, and higher elongation at break highlight the positive impact of Luperox® and can be attributed to improved interfacial adhesion between PHBV and PBSA. In conclusion, replacing DCP with Luperox® is a viable solution for *in-situ* compatibilization of PHBV/PBSA based on thermo-mechanical values and yields improvement in properties. The combination of Luperox® and ATBC appears as an excellent strategy to realize flexible PHBV-based films by film-blowing extrusion.

V.7.3.Scale-up

The transition from laboratory scale to large capacity production of PHBV-based blends for flexible food packaging is dependent on its ability to be processed through blown film extrusion. The film-blowing capacity was assessed on a semi-pilot scale. Two formulations were tested, i.e. PHBV/PBSA 70/30+ 0.2 phr Luperox® and PHBV/PBSA/ATBC 63/27/10 + 0.2 phr Luperox®.

Compounds of plasticized and unplasticized PHBV/PBSA+ Luperox® were prepared using twin-screw extrusion with the same temperature at 170 °C with a screw speed of 300 rpm. The temperature was adjusted since PBSA melts at relatively low temperature and zone 1 and 2 were decreased from 70 °C to 20 °C until pellets reached the first shearing zone. For plasticized compounds, despite the introduction of ATBC, the polymer rod was found unchanged and did not lead to a revision of the temperature profile. The mass outputs of plasticized and unplasticized were 0.8 kg.h⁻¹ and 1.2 kg.h⁻¹, respectively.

V.7.3.1. Melt viscosity of the plasticized PHBV/PBSA/Luperox blend

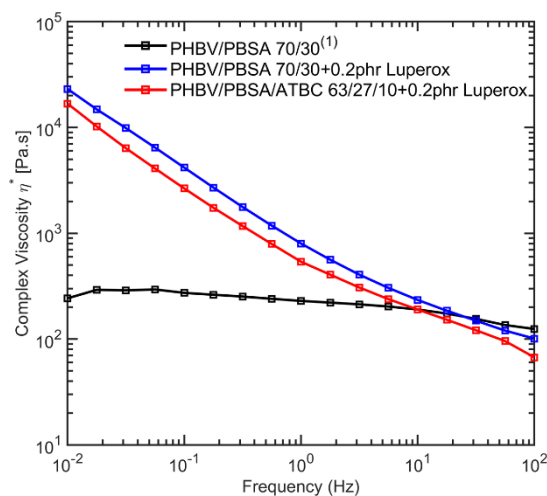


Figure V.4: Evolution of the complex viscosity as function of frequencies of plasticized and unplasticized PHBV/PBSA 70/30+ 0.2 phr Luperox at 185°C, ⁽¹⁾ values taken from previous work (Chapter IV)

Figure V.4 shows the evolution of the complex viscosity η^* of PHBV/PBSA 70/30, PHBV/PBSA 70/30+ 0.2 phr Luperox with and without ATBC as a function of frequency. Both *in-situ* compatibilized PHBV-based formulations displayed decreased viscosity with an increasing frequency by two orders of magnitude when compared to PHBV/PBSA 70/30 while no distinct sign of Newtonian plateau was observed and led to the apparition of a frequency dependent behavior. As already explained in previous work (Chapter IV), this behavior is characteristic of long-chain branching systems resulting from *in-situ* compatibilization of PHBV-*g*-PBSA with the introduction of Luperox® which acts as a free radical initiator (P. Ma et al., 2012; Tian et al., 2006; Zytner et al., 2020). The inclusion of 10 wt % ATBC led decrease of η^* but still exhibited frequency dependent behavior in the whole investigated frequency range. The lower η^* of the plasticized formulation can be attributed to the introduction of a low-viscous additive, *i.e.* ATBC. However and as supported by gel content, ATBC did not hindered cross-linking reaction.

V.7.3.2. Processability of plasticized and unplasticized PHBV/PBSA+Luperox®

Figure V.5 shows film blowing extrusion process of plasticized PHBV/PBSA/ATBC 63/27/10 with the addition of 0.2 phr Luperox®. While film blowing ability of PHBV/PBSA in the presence of dicumyl peroxide (DCP) was already demonstrated and discussed previously (Chapter IV), Unplasticized PHBV/PBSA/Luperox® blends could be blown but below a thickness of about 60 μm , the extruded film was found to be very sticky which irreparably caused inflation problems and instabilities (Figure V.5(a)). On the contrary, the film containing

Chapter V

10 wt % ATBC exhibited very stable bubbles and no sticking problems (Figure V.5(a)). Thus, ATBC acted as a processing aid by playing the role of lubricant agent. Film blowing trials demonstrated that a combination of *in-situ* reactive extrusion with Luperox® leading to partial cross-linking and addition of external plasticizer acting as a sliding agent (from processing view) leads to very good processability with a blow-up ratio (BUR) up to 3.8 and a PHBV content of 63 wt %. Other studies obtained a BUR and take-up ratio (TUR) of 2.5 and about 5 for PHBV/PBAT blends, respectively (Cunha et al., 2015). In another study, using the coextrusion process of bi-layered PHB-PBAT films, authors varied BUR and TUR between 1.8-2.1 and 7.1-13.9 for PHB content varying between 45 and 55 %.(Teixeira et al., 2020)

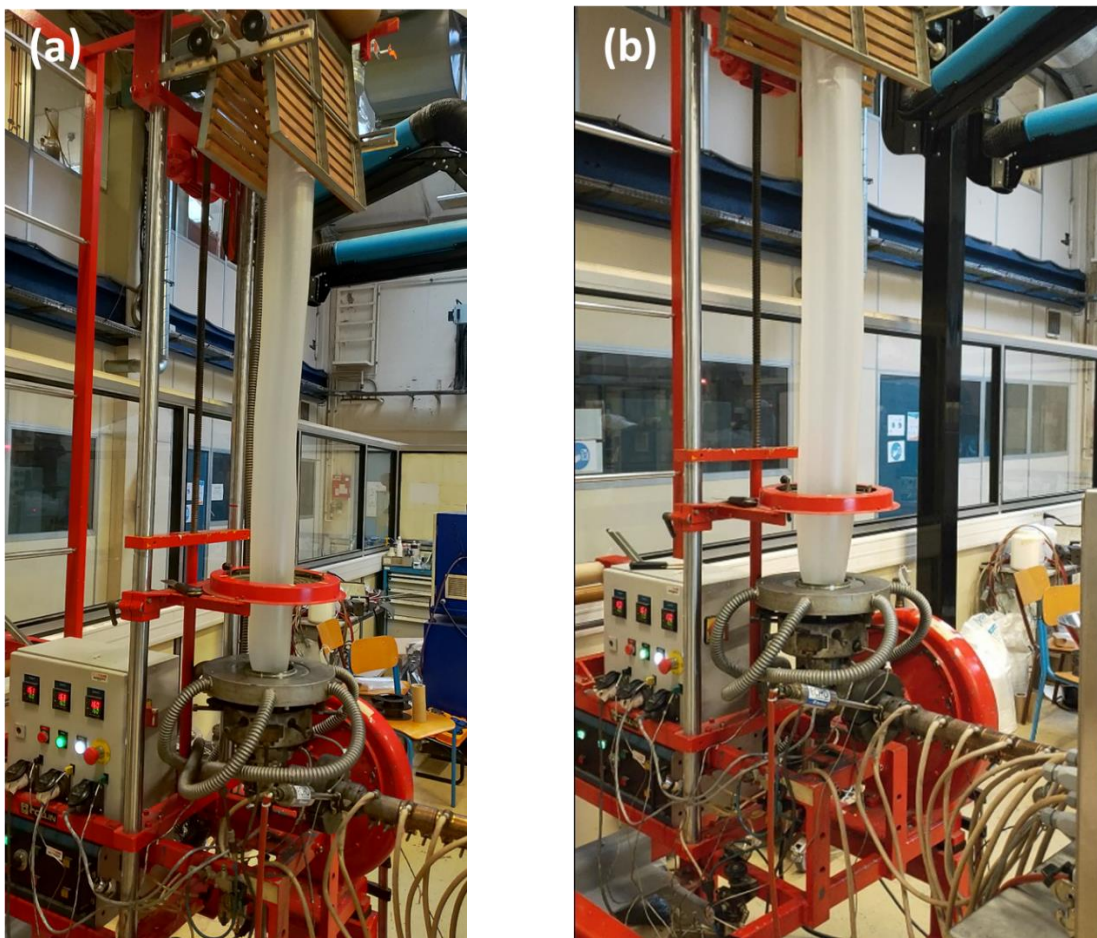


Figure V.5: Film blowing of a) unplasticized PHBV/PBSA 70/30+ 0.2 phr Luperox® with BUR of about 2.4 and b) plasticized PHBV/PBSA/ATBC 63/27/10+ 0.2 phr Luperox® with BUR of about 3.8, height of the blow film process is about 180 cm

V.7.3.3. Tensile test

Table V.5: Mechanical properties of plasticized and unplasticized PHBV/PBSA/Luperox blends obtained from tensile test measurements under both ambient and freezer conditions

| Samples | | Young modulus (MPa) | | Maximum stress (MPa) | | Elongation at break (%) | | Impact Strength (kJ.m ⁻²) ⁽⁴⁾ |
|--|---------------------------------|---------------------|----------|----------------------|--------|-------------------------|---------|--|
| | | 23 °C | -20 °C | 23 °C | -20 °C | 23 °C | -20 °C | 23 °C |
| 70/30 ⁽¹⁾ | | 1807±79 | 2929±852 | 15±3 | 24±10 | 1.6±1.4 | 0.9±0.2 | n.d |
| PHBV/PBSA 70/30 + 0.2 phr Luperox® | MD ⁽²⁾ | 2165±96 | 2408±888 | 18±2 | 43±6 | 1.8±0.4 | 1.6±0.3 | 3.6± 0.5 |
| | TD ⁽²⁾ | 2052±142 | n.d. | 11±4 | n.d. | 0.7±0.2 | n.d. | |
| PHBV/PBSA/ATBC 63/27/10 + 0.2 phr Luperox® | MD | 1115±94 | 1774±354 | 14±2 | 37±3 | 4.2±0.5 | 4.8±0.5 | 7.7± 0.5 |
| | TD | 1064±94 | 1731±412 | 11±2 | 29±3 | 2.5±0.7 | 2.3±0.4 | |
| | Aging : 3 months ⁽³⁾ | 986±145 | n.d. | 13±3 | n.d. | 4.9±0.9 | n.d. | n.d |

⁽¹⁾Values reproduced from (Chapter IV): Twin screw extrusion followed by thermo-compression molding, ⁽²⁾ MD: Machine direction, TD: Transverse direction, ⁽³⁾ Aged 3 months at -20 °C in contact with fatty food, ⁽⁴⁾ Measured from thermo-compressed samples

The mechanical properties of plasticized and unplasticized PHBV/PBSA blends with 0.2 phr Luperox® were evaluated by means of tensile and Charpy notched impact tests. The tensile properties were evaluated under ambient and freezer conditions, and obtained values are reported in Table V.5. Typical stress/strain curves are shown in Figure V.6, and it can be seen that the addition of ATBC led to a change from fragile to ductile behavior with the apparition of a short yielding. SEM images in Figure V.6(a,b) showed, in that case, long stretched filaments. Oscillation of the stress curves was observed for samples containing ca. 10 wt % ATBC during the tensile test at -20 °C. This phenomenon was related to a local change in

Chapter V

temperature during the test. The device is temperature-controlled by injecting nitrogen in the traction chamber.

As a consequence, the temperature varied periodically between -22 to -18 °C and impacted the tensile curves. The results showed that samples exhibited anisotropy in the machine and transverse directions. The Young modulus and the elongation at break were superior in the machine direction. This is expected since a preferential orientation of the macromolecular chains occurs in the melt state as a result of shear stress in the die and of stretching by means of pinch rolls during the film blowing (X. M. Zhang, Elkoun, Ajji, & Huneault, 2004). However, obtained values in machine direction were similar to those obtained from the batch mixer (Table V.5). The phenomena of anisotropy induced by film blowing were already observed for PHBV/PBAT blends (Cunha et al., 2015). The synergetic effect of *in-situ* compatibilization of PHBV/PBSA and plasticization reduced stiffness but also increased elongation at break by a factor two compared to unplasticized compound. Charpy notched impact tests showed improved toughness with the addition of ATBC and can be attributed to improved interfacial compatibility between PHBV and PBSA.

The evolution of the mechanical properties between ambient and freezing conditions (ca. $\Delta T \cong 40$ °C) showed that the decrease in temperature caused the increase of the elastic modulus and the maximum stress. This is expected as the decrease of temperature decreases chain mobility. Rare results of tensile properties at low temperatures are available in the literature. For example, PLA/PBAT blends had increased modulus at -25 °C with increased PLA content with a change in fracture behavior from ductile to brittle. On the contrary, higher content of PBAT led to higher elongation at break due to its less sensitivity to change in temperature ($T_g = -25$ °C) (Pietrosanto, Scarfato, Di Maio, Nobile, & Incarnato, 2020). However, in the present study, the elongation at break did not change; it was already very small, so that eventual differences were not observable. The addition of Luperox improved interfacial compatibility between PHBV and PBSA, while on the other side ATBC increased free volume within the amorphous phase and increased chain mobility resulting in higher elongation under ambient and freezer conditions.

Chapter V

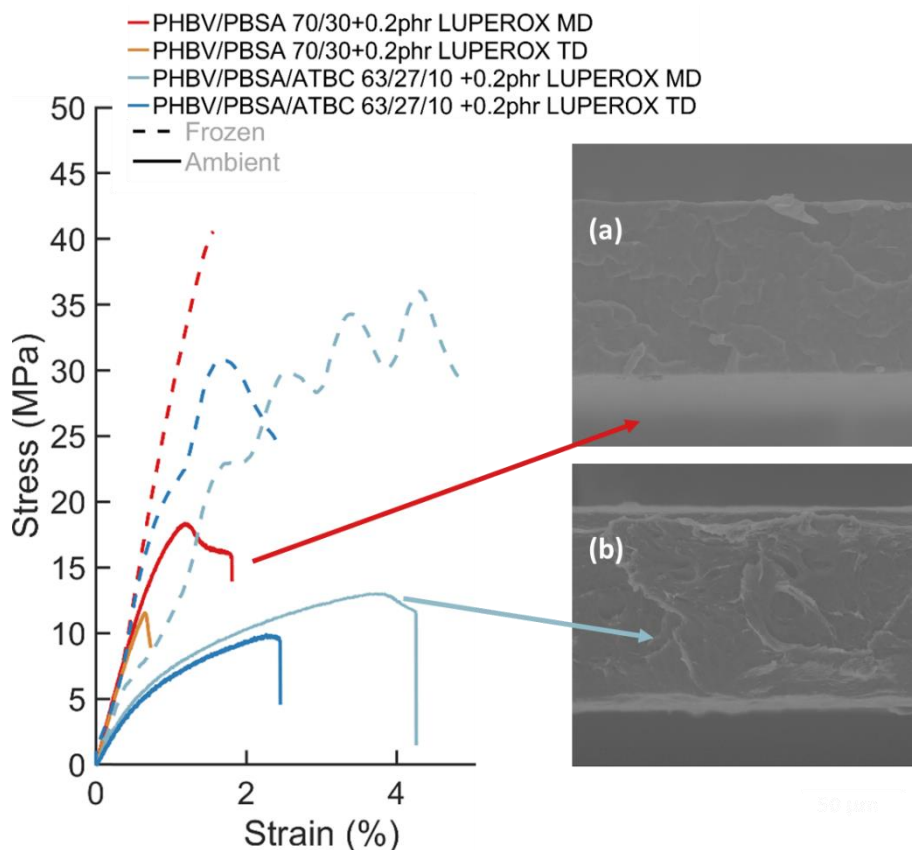


Figure V.6: Typical stress/strain curves of PHBV-based blends with addition of ATBC at 23 et -20 °C with inset of SEM images of the cross-section after tensile test (23 °C) of (a) unplasticized and (b) plasticized PHBV/PBSA/Luperox

From the present study, the best results were obtained from a formulation comprising ATBC. In fact, the addition of the external plasticizer to PHBV/PBSA+ 0.2 phr Luperox® blend resulted in improved processing ability and advantaged thermal and mechanical properties with reduced stiffness, increased elongation at break, and lower glass transition temperature. Consequently, the developed formulation could be used for flexible food packaging of frozen food. The mechanical properties of the films stored at -20 °C in contact with fatty food (French fries) were monitored for three months. The results are gathered in Table V.5. A comparative experiment with PHBV/PBSA 70/30 + 0.1 phr DCP was carried out. All formulations could be heat sealed using a vacuum packing machine (Figure V.7). After three months, the Young modulus, maximum stress, and elongation at break values were found to be stable over time.

Chapter V



Figure V.7: Hot sealed film of PHBV/PBSA/ATBC 63/27/10 + 0.2 phr luperox filled with 625 g of frozen French fries

V.8. Conclusion

The use of alternative organic peroxide, namely LUPEROX® 101E, combined with an external plasticizer, ATBC, for designing novel biobased and biodegradable blends was investigated. LUPEROX® 101E, as well as ATBC, may be present in the plastic layers of the plastic materials intended to come into contact with foodstuff. Combination of reactive extrusion and plasticization appeared as good candidates for improving the interfacial compatibility of PHBV/PBSA mixture while inducing plasticizing effect with the aim to improve thermal and mechanical properties. Luperox was efficient to induce *in-situ* compatibilization similarly to dicumyl peroxide while moderate improvement in ductility was evidenced. Large scale production of PHBV-based blend for flexible food packaging was demonstrated with synergic effect resulting from the combination of Luperox® and ATBC, which played a role of processing aid as demonstrated from the very good processability. Final application properties showed similar Young Modulus and elongation at break and increased maximum stress under freezer conditions. The finalized film could be handle either at 23 °C or -25 °C without falling apart and can be attributed to its increased flexibility over a large temperature range. This makes PHBV/PBSA/ATBC/Luperox blend a good candidate to be used in flexible film packaging of frozen food intended to be used in contact with fatty food.

Chapter V

Chapter VI

Valorization of potato peels and their constituents

VI.1.Introduction

Food industries generate a huge amount of by-products coming directly from their production units (ADEME, 2015). Potato is the world's fourth most important food crop after rice, wheat and maize, with an annual production of over 370 million tons (Mt) in 2019 (FAO, 2019). It is estimated that more than 50 % of the global potato production is consumed as processed food, including frozen products, dried flakes, prepared meals and potato starch (Sampaio et al., 2020). The process from raw potato to an end product involves generally tubers peeling where different techniques may be used such as abrasive or steam peeling. Potato peels are a by-product, which have a zero or negative value on the market. This means that it is sold as animal feed (Ncobela, Kanengoni, Hlatini, Thomas, & Chimonyo, 2017) or turned in biogas at the best. In this way, valorization of by-products in applications of higher values than animal feed is of economic interest.

The main objective of this study is to explore new routes for valorization of vegetable by-products such as potato peels in new bio-based and biodegradable materials. This objective fits with the circular economy strategy. Moreover the evaluation of the structural constituents and the measurement of the phenolic compounds of potato peels will allow to have a better understanding on the resulting properties of the developed materials and also explore new valorization ways of high-value added molecules, respectively.

A schematic representation was drawn as shown in Figure VI.1, to evidence the multiple routes that has been adopted in the present study towards new valorization of potato peels. First strategy is based on production of bio-based and biodegradable thermoplastic material from microbial fermentation. The implementation process for production of polyhydroxyalkanoates (PHAs) imparts the use of macronutrients for microbial growth. However, this process is highly expensive and imparts large scale production. One strategy to reduce overall cost states on the use of agri-food by-products or vegetable waste as fermentation substrate and already explored in literature and for more details report to (Chapter I). As shown in Figure VI.1, another possible way for valorization of potato by-products arises from its direct use for fabrication of bio-based and biodegradable products or valorization of high-value added extractible molecules present in potato peels. First, starch features thermoplastic character when blended with water and/or external plasticizer. Complementary, potato peels contain polymeric carbohydrates, including

Chapter VI

cellulose, hemicellulose, lignin, pectin and starch. This last, even present in minor fraction in potato peels compared to potato flesh, could allow film forming of potato peels.

Potato peels also contain high-value molecules such as phenolic compounds or glycoalkaloids (Katariina et al., 2015). These last could be a source of antioxidants molecules and find multiple applications in pharmaceutical or food for example (Jeddou et al., 2016; Rehman, Habib, & Shah, 2004).

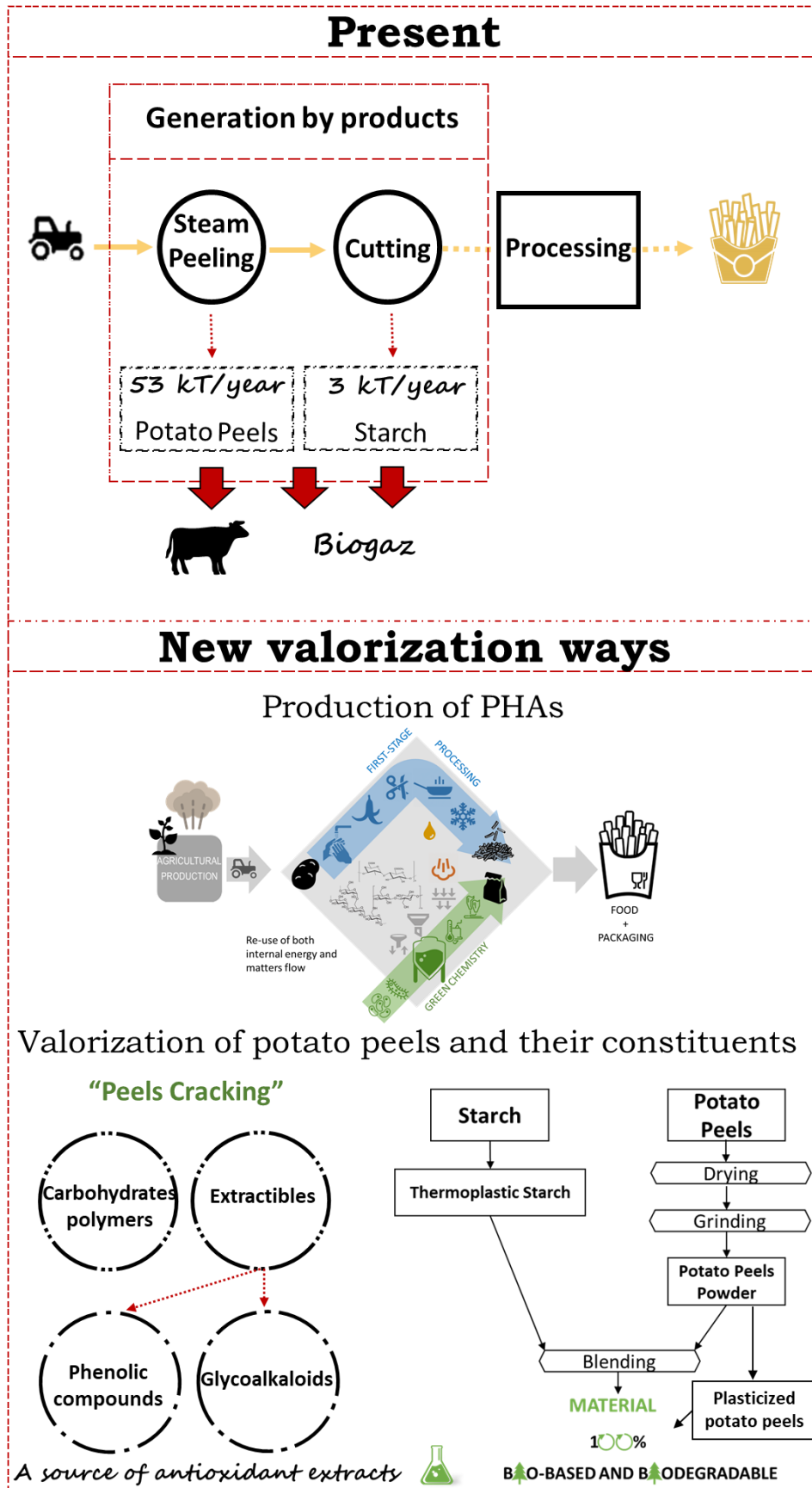


Figure VI.1: Principles of new ways of valorization of agri-food industries by-products in added value products

VI.2.Literature review on the valorization of potato peels and their constituents

Potato peel is a fibrous envelope around potato flesh, which is a loose tissue rich in starch. Depending on its state of preservation, the peel has a water content of 70 to 90 %. Main constituents of potato peels are carbohydrates which can be divided into two main categories, which are storage carbohydrates (starch) and structural polysaccharides (cellulose, hemicellulose, lignin, suberin, pectin) (Sheldon, 2014). In the present review, the main constituents of potato peels are described and molecules which have potentially high market value. Furthermore, the possibility to produce bio-based and biodegradable products is evaluated.

VI.2.1.Starch

Starch is one of the most abundant polysaccharide on the Earth, because it is the main carbon storage polymer of terrestrial plants. Starch is readily available and low cost. It is employed in many industries such as food industry, papermaking, packaging, mulch films. Main source of starch are cereals, such as wheat, maize, rice and tubers, such as potatoes and manioc (Buléon, Colonna, Planchot, & Ball, 1998). Starch is a semicrystalline polymer of glucose with two main structures, which are named amylose and amylopectin. The amylose content of potato starch amounts to 10-38 % depending tuber source (Hoover, 2001). Amylose is made of α -(1,4)-D-glycosidic bonds and due to its linearity, amylose chains arrange themselves into single or double helixes (Averous, 2004). On the contrary, amylopectin is a highly branched polymer with linear addition of glucose units with α -(1,4)-D-glycosidic bonds and branching occurring at α -(1,6) bonds for each 24-30 glucose repeating units (Figure VI.2) (Niranjana Prabhu & Prashantha, 2018).

Chapter VI

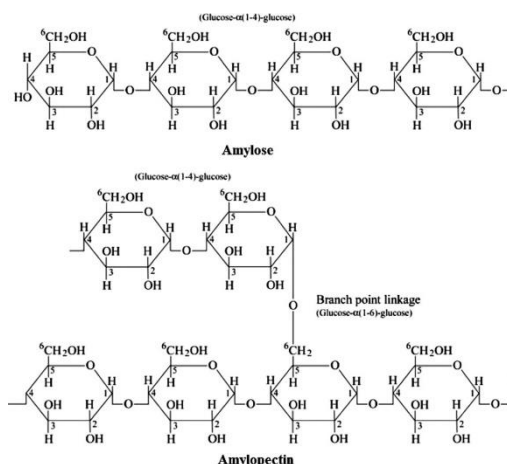


Figure VI.2: Chemical structure of amylose and amylopectin figure reproduced from (Niranjana Prabhu & Prashantha, 2018)

Native starch is hierarchically organized on four length scales (Figure VI.3) (Buléon et al., 1998; Waigh, Gidley, Komanshek, & Donald, 2000):

- Starch granule whose size ($\sim \mu\text{m}$) greatly depends on botanical source
- “Growth rings” that correspond to alternating ring structure of amorphous and semi-crystalline regions
- Lamellar structure within the crystalline shells which consists of alternating regions of amorphous and crystalline lamellae with a repeat distance of 9 -10 nm
- Molecular scale of monomers ($\sim \text{\AA}$)

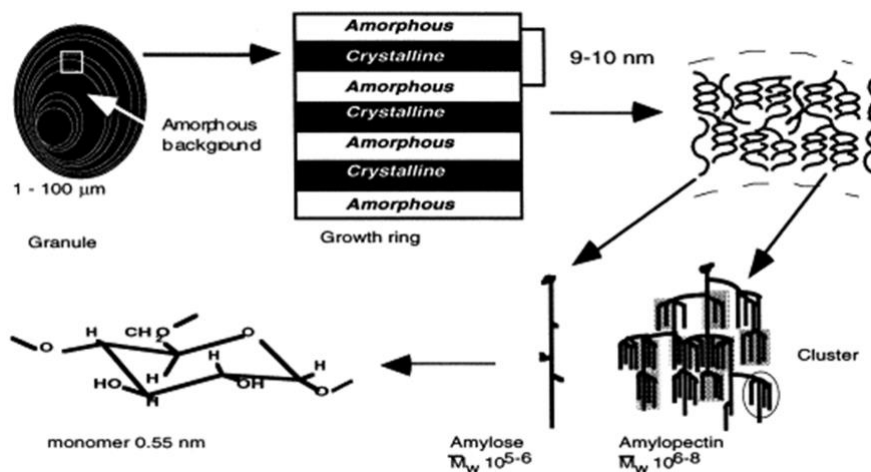


Figure VI.3: Schematic representation of starch granule ultrastructure, figure modified from (Buléon et al., 1998)

The transformation from native to thermoplastic starch (TPS) corresponds to gelatinization which means the disruption of the granule organization and crystals. The gelatinization process proceeds to be the combination of water and heat which will cause swelling and destruction of

Chapter VI

most of inter-macromolecular hydrogen links by dissolution (Avérous, 2004; Lai & Kokini, 1991). Introduction of water induces a change in melting behavior.

The fabrication of thermoplastic starch consist in the introduction of a non-volatile plasticizer, where its plasticizing effect strongly depends on its molecular mass to induce penetration and destruction of hydrogen bonds between the macromolecules (Avérous, 2004). Polyols and in particular glycerol appears as the most widely used external plasticizer (Rodriguez-Gonzalez, Ramsay, & Favis, 2004). Their ability to form hydrogen bonds with starch leads to depression of the melting temperature T_m . The phenomenon of anti-plasticization effect on TPS was evidenced for low amount of glycerol (< 12 wt %) where a decrease of elongation at break was observed (Figure VI.4) (Lourdin, Bizot, & Colonna, 1997).

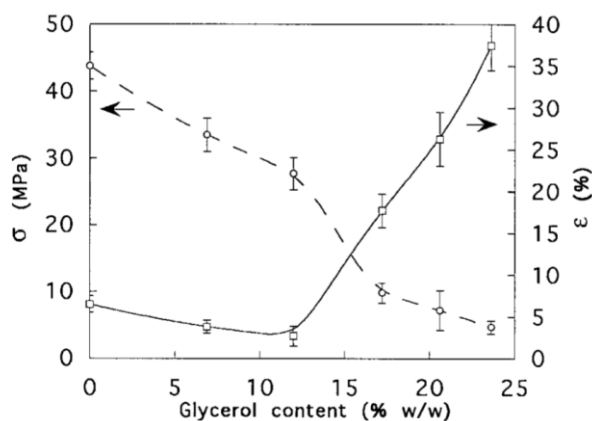


Figure VI.4: Evolution of the elongation and yield at break of potato starch films as function of glycerol content, figure reproduced from (Lourdin et al., 1997)

Thermoplastic starch can be processed either by solvent casting or extrusion. Solvent casting involves the gelatinization of native starch in excess water at temperature higher than gelatinization temperature. The solvent casting method is the easiest method to produce films at the laboratory scale. It consists in pouring the gelatinized starch in a Petri dish with anti-adherent surface and evaporation of the solvent, in most cases water. On a larger scale, melt processing by extrusion is however preferable, as it increases process productivity. The combination of thermal and mechanical energy inputs helps to produce thermoplastic starch and the film in a single processing step (Figure VI.5) (Avérous, 2004). Thermoplastic starch ages quickly because of cold-crystallization during storage, à process termed retrogradation (Van Soest & Knooren, 1997). The retrogradation can be slowed down by formulations or use of modified starches, which maintain their amorphous character.

Chapter VI

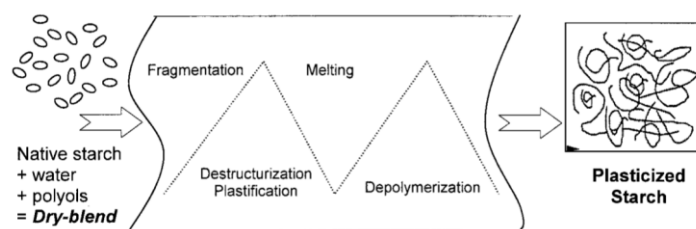


Figure VI.5: Schematic representation of starch process: from native to plasticized starch, figure reproduced from (Avérous, 2004)

VI.2.2. Cellulose

Cellulose is the most abundant biopolymer on earth, as it is the main structural constituent of terrestrial plants. In plants, it is organized as fibers, which are constituted of bundles of microfibrils with a diameter of 10-20 nm. One microfibril is several elementary fibrils. Cellulose microfibrils and elementary fibers are termed cellulose nanofibers (CNF) (Eichhorn et al., 2010). Cellulose is a semicrystalline polymer constituted of cellobiose units, which are two β -1,4-linked D-glucopyranose rings (Figure VI.6). Crystalline and amorphous zones are alternating in the cellulose fibers. Therefore, cellulose nanocrystals (CNC) can be extracted upon selective degradation of the amorphous zones. Those crystals are rigid nanorods. They are film-forming and give rise to materials with interesting optical and barrier properties. Cellulose nanocrystals derived from potato peel waste were successfully obtained. Authors submitted potato peels to alkali treatment using sodium hydroxide solution to eliminate lignin, hemicellulose and other extractibles. Then, bleaching using sodium chlorite was done followed by acid hydrolysis using sulfuric acid. CNC obtained from potato peels showed large distribution in size with average length of 410 ± 181 nm and diameter of 10 nm. Such CNC were then blended with solution of either starch or polyvinyl alcohol (PVA) in a solution casting process. Final films showed improved mechanical properties (Tensile modulus) with increased potato peels-CNC and showed its potential as reinforcing agent (Chen, Lawton, Thompson, & Liu, 2012).

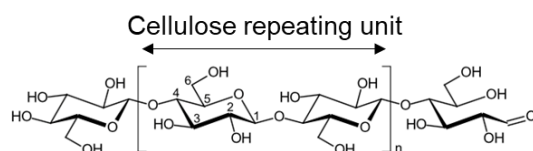


Figure VI.6: Cellulose repeating unit, figure adapted from (Nechyporchuk et al. 2016)

Chapter VI

Cellulose nanofibrils are obtained through a top-down strategy, where plant cell walls are subjected to a strong enough mechanical disintegration action such as high shearing forces to induce the defibrillation of the fiber and diminish the size. Three main technologies are being used for production of cellulose microfibrils (MFC) and listed as: homogenizer, grinder and microfluidizer (Nechyporchuk, Belgacem, & Bras, 2016). Such types of CNF can be addressed for preparation of nanopaper or CNF films. (Sehaqui, Liu, Zhou, & Berglund, 2010) adapted a papermaking production using a semiautomatic sheet former and obtained nanostructured films of CNF (Figure VI.7). CNF could also be used as reinforcing agent in polymeric systems. Cellulose microfibrils derived from potato tuber cells were reported to be effective reinforcements of gelatinized potato starch (Dufresne, Dupeyre, & Vignon, 2000; Dufresne & Vignon, 1998). The microfibrils were prepared by alkaline washing (sodium hydroxide), bleaching (sodium chlorite) and mechanically treated using homegenizer (15 passes). Cellulose microfibrils reinforced plasticized starch, but the strength of the material was strongly dependent on relative humidity (RH) conditions.

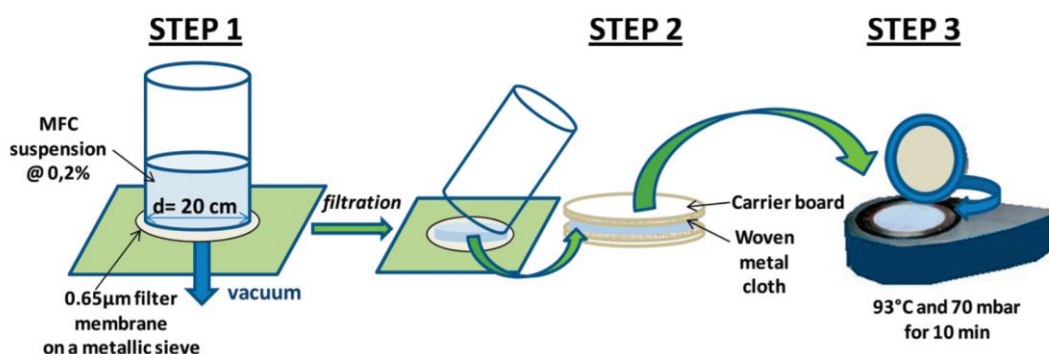


Figure VI.7: Experimental procedure of MFC films using a semiautomatic sheet former, figure reproduced from (Sehaqui et al., 2010)

VI.2.3.Hemicelluloses

Hemicellulose is a branched polymer made up of different sugars connecting the different parietal constituents. It includes all the parietal polysaccharides that are neither cellulosic nor pectin (Ralet, Buffet, Capron, & Guillon, 2016). Hemicellulose are complex polysaccharides that are soluble in alkaline solution but not in water. Hemicelluloses are a class homo- and heteropolymers that are mainly linked and composed of $\beta - (1 \rightarrow 4)$ -glucopyranose, mannopyranose or xylopyranose residues and called glucans, mannans, or xylans, respectively (Ralet et al., 2016; Scheller & Ulvskov, 2010).

VI.2.4.Pectins

Pectins are present in plant cell walls and are involved in various cell functions and plant processes (Ralet et al., 2016). They are defined as a hetero-polysaccharide that contain 1,4 – *linked* α -D- galactosyluronic acid (GalpA) composed of three major domains, homomagalacturonan (HG), type I rhamnogalaturonans (RG-I) and substituted galacturonans (SG) (Ridley, O'Neill, & Mohnen, 2001; Voragen, Coenen, Verhoef, & Schols, 2009).

- Homogalacturonan (HG) is a linear chain of GalpA residues in which some of the carboxyl groups are methyl esterified.
- Type I rhamnogalaturonans (RG-I) is a family of pectic polysaccharides that contain a backbone of the repeating disaccharide. Substituted galacturonans (SG) are a diverse group of polysaccharides that contain a backbone of linear 1,4 – *linked* α -D- GalpA which are listed as Type-II rhamnogalacturonan (RG-II), xylogalacturonans, apiogalacturonans.

VI.2.5.Lignin

Lignins are complex aromatic amorphous polymers (Figure VI.8) which accumulate in the plant walls during their construction (Pouteau, Dole, Cathala, Averous, & Boquillon, 2003). The three primary monomers are *p*-coumaryl, coniferyl, and synapil alcohols (Figure VI.9).

Kraft pulping process represent over 90 % of chemical paper process. The objective is to separate lignin to cellulose fibers and producing a suitable pulp for paper making (Chakar & Ragauskas, 2004). The chemical reactants designated as “white liquor”, an aqueous solution of sodium hydroxide and sodium sulfide, is used in the Kraft cook process. Delignification occurs with cleavage of α - and β -aryl-ether bonds (Gierer, 1980). Integrated in a biorefinery approach, the resulting black liquor, comprised of lignin and hemicelluloses, is then concentrated and used as fuel for production of electricity and steam. However, production of lignin exceeds the necessary needs and new ways of valorization of this renewable resource needs to be found such as lignin based polymers (Laurichesse & Avérous, 2014).

Chapter VI

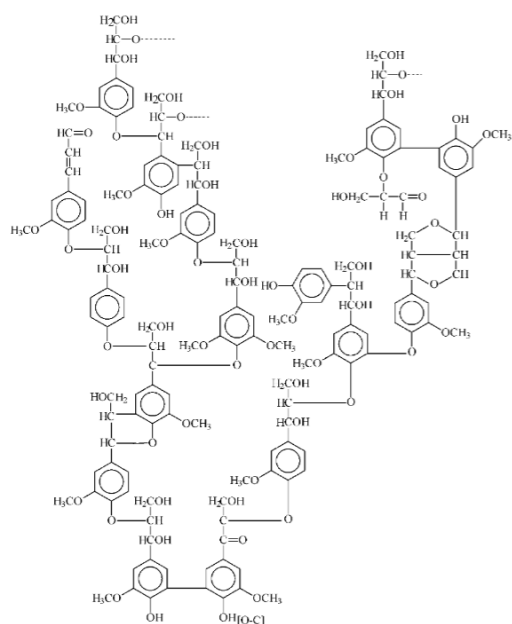


Figure VI.8: Schematic representation of lignin molecules (R. Sun, Lawther, & Banks, 1997)

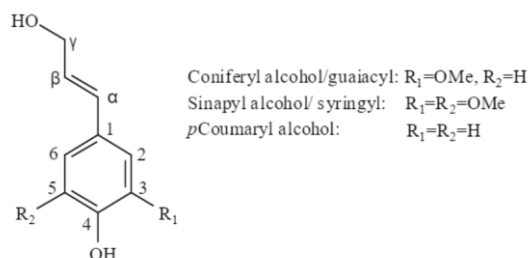


Figure VI.9: The three building blocks of lignin (Chakar & Ragauskas, 2004)

VI.2.6. Structural constituents of potato peels

Numerous studies focused on the characterization of polymer carbohydrates within potato peels. A selection is listed in Table VI.1. Large differences in chemical composition is depicted which strongly depends on potato variety as well as peeling method. As an example, potato peels studied by (Katariina et al., 2015) which were mechanically peeled had a starch content of 46 wt% on a dry weight. (Camire, Violette, Dougherty, & McLaughlin, 1997) used the industrial steam peeling process, which is more efficient. They found 25 wt% of starch on a dry weight.

Table VI.1: Chemical composition of potato peels

| Variety | Carbohydrates (%) | | | Protein/amino acids (%) | Ash (%) | Reference |
|-------------------|-------------------|-------------------------|----------------|-------------------------|---------------|---|
| | Starch | Nonstarch polyaccharide | Lignin/Suberin | | | |
| Red potato | 72 | | | 15.99 | 6.69 | (Elkahoui, Bartley, Yokoyama, & Friedman, 2018) |
| Gold potato | 70 | | | 14.17 | 9.12 | |
| Organic Russet | 76 | | | 11.98 | 7.32 | |
| Nonorganic Russet | 71 | | | 17.19 | 7.34 | Friedman, 2018) |
| Spunta | 88± 4.4 | | | 2.099± 0.105 | 0.906± 0.0006 | (Jeddou et al., 2016) |

Chapter VI

| | | | | | | |
|-----------------|------|------|------|-----|-----|--------------------------|
| Russet Burbank | 25 | 30 | 20 | 18 | 6 | (Camire et al., 1997) |
| n.d | 37 | 48 | n.d | 4 | 4 | (Mayer, 1998) |
| Nicolas variety | 46.2 | 26.6 | 7 | 6.4 | 2.8 | (Katariina et al., 2015) |
| Russet Burbank | 16.8 | 22.5 | 21.6 | n.d | 11 | (Liang & McDonald, 2014) |

VI.2.7. Biologically active compounds in potato peels of high value

Beyond the structural polymers that constitute potato peels, they also contain many valuable molecules that can be a source of high-value compounds for the food, pharmaceutical or cosmetic industries. Phenolic compounds and glycoalkaloids are of particular interest thanks to their antioxidant and antibacterial activities (Sánchez Maldonado, Mudge, Gänzle, & Schieber, 2014).

VI.2.7.1. Phenolic compounds

While an extensive list of phenolic compounds is present in potatoes, the most abundant phenolic component is the hydroxycinnamate derivative chlorogenic acid. It represents over 90 % of the phenolic compounds in potato peels. In lower quantity, caffeic, *p*-coumaric and ferulic acids can be found (Figure VI.10) (Schieber & Saldaña, 2009). Those molecules are potent natural antioxidants, which could replace synthetic compounds in food and pharmaceutical applications (Jeddou et al., 2016; Rehman et al., 2004).

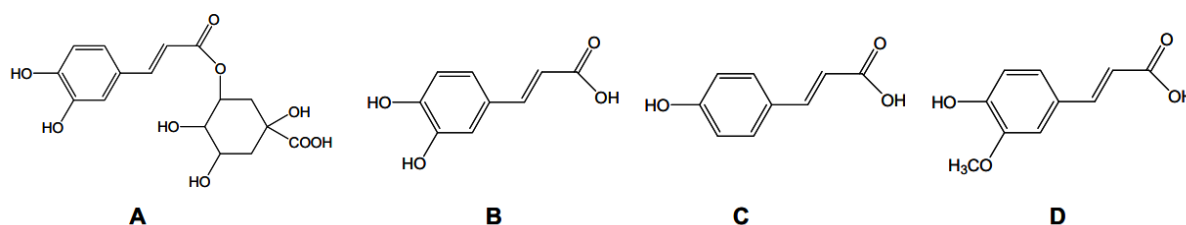


Figure VI.10: Chemical structure of hydroxycinnamic acids of A) chlorogenic acid, B) caffeic acid, C) *p*-coumaric acid, D) ferulic acid, figure modified from (Schieber & Saldaña, 2009)

VI.2.7.2. Glycoalkaloids

Potatoes are part of the Solanaceae family which are plants known to produce glycoalkaloids with α -chaconine and α -solanine. They are active against bacterial, fungal and insect attacks (Sampaio et al., 2020). If consumed in high concentrations, they can be toxic to human health with a recommended safety level below 20 mg/100 g (Knuthsen, Jensen, Schmidt, & Larsen, 2009). At lower concentration those molecules might be used as natural antimicrobials.

Potato peels are composed of numerous carbohydrate polymers which varies depending on its botanical origin but also on the peeling method since starch can vary from 15 wt % up to 45 % in chemical composition. Besides that, potato peels contain a great source of valuable molecules. The separation between structural constituents and antioxidant molecules present in the extractible fraction is of great interest towards the extraction and purification of phenolic compounds and glycoalkaloids (Figure VI.1). However, high added value substances, which may be extracted, can be assumed to be minor in terms of quantity. Therefore, it is interesting to look for applications of the structural constituents taking advantage of what is known from paper making and thermoplastic starch.

VI.2.8. Using potato peels in material applications

Investigations on the ability to transform edible vegetable waste into bioplastics and/or bio-based and biodegradable items has gained interest during the last decade.

From literature, turning vegetable waste in bio-based and biodegradable plastics using dissolution of biomass followed by solvent casting has been investigated. Notable recent studies by a group in Italy at 'Istituto Italiano di Tecnologia' (ITT) have addressed the direct transformation of agricultural or food by-products into bio-based and biodegradable plastics. (Bayer et al., 2014) turned vegetable wastes rich of cellulose, *such as* parsley, spinach stems, rice hulls, and cocoa pod husks in bio-based and biodegradable free-standing films. Dry vegetable powders were processed by dissolution in trifluoroacetic acid (TFA) and solvent-casting (Figure VI.11a). The obtained materials after dissolution resulted in amorphous of cellulose as depicted from X-ray diffraction spectroscopy (XRD). They displayed large difference in mechanical range. Mechanical properties were done at room temperature and 44 % RH. Parsley and spinach films had a strain at break amounting to 45 and 60 %. Cocoa, microcrystalline cellulose and rice films were less ductile (Figure VI.11b). Therefore, the resulting mechanical properties depended on the botanic origin and the composition in non-

Chapter VI

cellulosic constituents. However, authors did not discuss the effect of relative humidity on the mechanical properties. In fact, as evidenced from water absorption isotherms, water uptake between vegetables showed very large difference between 40 and 80 % RH and water is supposed to induce a plasticization effect as shown in evolution of T_g (Figure VI.11b).

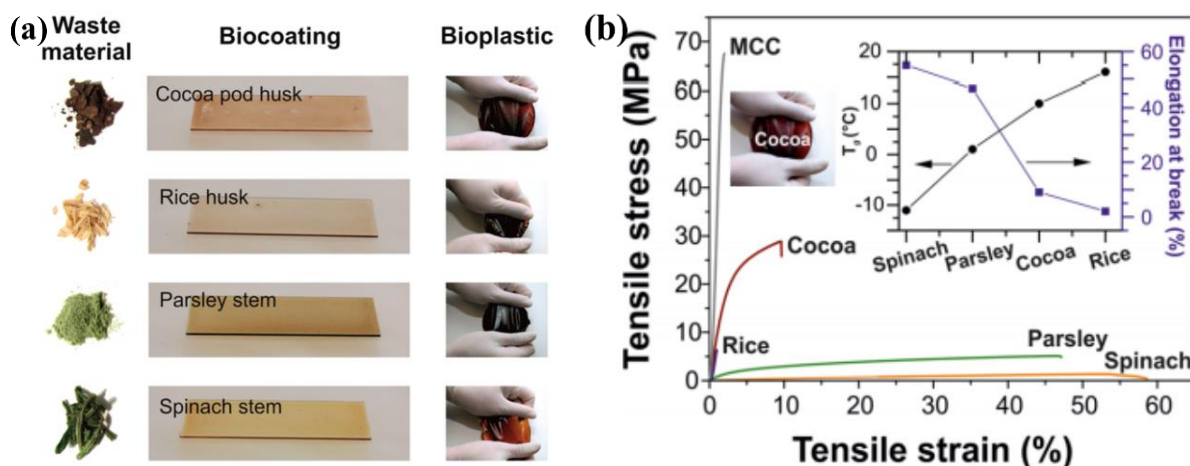


Figure VI.11: (a) Different edible plant wastes in diverse forms and (b) typical stress-strain curves for pure cellulose (MCC), spinach, parsley, cocoa and rice, images reproduced from (Bayer et al., 2014)

Following their previous research, (Giovanni Perotto et al., 2018) investigated the production of films with micronized powders of vegetable waste, *such as* carrot, radicchio, parsley and cauliflower avoiding the use of TFA. Similarly, vegetable powders were dispersed in concentrated HCl followed by solvent-casting. The obtained films as shown in Figure VI.12 were homogeneous and flexible and displayed elongation at break value at ca. 6 %. Compared to TFA-processed materials and despite the fact that samples were subjected to 100 % RH for 60 min, the water-based bioplastic films showed higher elastic modulus and lower ductility. From NMR results, authors found an increase in crystallinity degree after processing that can be attributed to the hydrolysis of amorphous fraction of cellulose. The cellulose nanocrystals are known to act as reinforcing agent (Chen et al., 2012). Consequently, mechanical properties were improved. Finally, food contact migration using Tenax® as a simulant for dry food was assessed and showed that all films displayed overall migration below the 10 mg/dm² set by 10/2011/EC.

Chapter VI

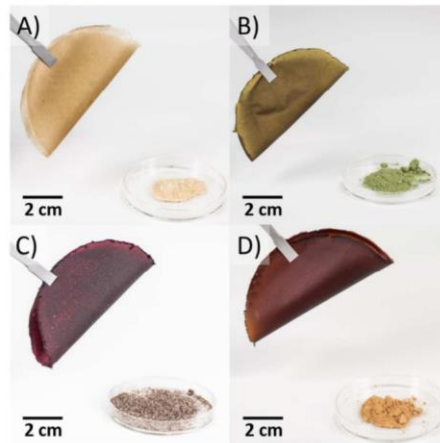


Figure VI.12: Images of bioplastic films of A) Carrot , B) Parsley, C Radicchio and, D) Cauliflower, image reproduced from (Giovanni Perotto et al., 2018)

More recently, (G. Perotto et al., 2020) converted carrot powder into a bioplastic film using formic acid instead of HCl and followed same protocol as previously (Giovanni Perotto et al., 2018). From NMR results, carrot films showed the same spectra as carrot treated with HCl while crystallinity degree was slightly lower with formic acid as a result of less hydrolysis of the amorphous fraction of cellulose. Moreover, presence of peaks characteristic of pectin and polyester were identified. The authors concluded that formic acid treatment was milder compared to HCl-process with reduced degree of crystallinity and presence of pectin and aliphatic polyester. The investigation of the mechanical properties as a function of RH evidenced its sensitivity to water uptake (Figure VI.13). This transition was correlated to the change in T_g where water induced plasticization. The plasticization effect was mostly related to pectins but also to the amorphous or hydrolyzed cellulose fractions. Obtained results evidence a transition from brittle to ductile behavior at a threshold of about 50 % RH. This behavior allowed, when submitted to moisture and in a reversible way, to obtain macroscopic objects with complex shapes that can be maintained after drying (G. Perotto et al., 2020).

Chapter VI

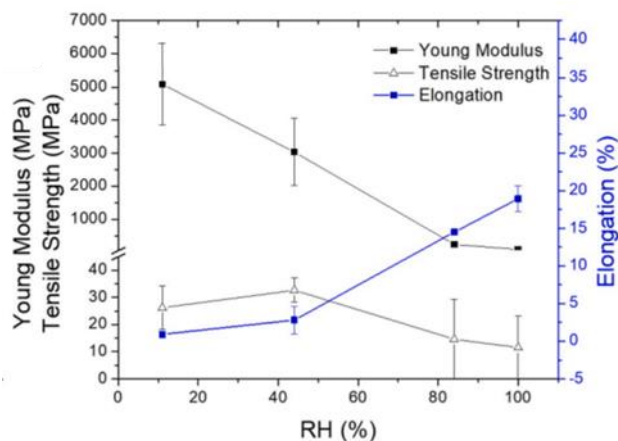


Figure VI.13 :Evolution the mechanical properties of carrot-based films as a function of relative humidity, figure reproduced and modified from (G. Perotto et al., 2020)

Based on another approach, valorization of vegetable waste comprising starch can be effective with the use of an external plasticizer. Based on the knowledge about TPS, potato peels which feature relative high amount of starch in combination with non-starch polysaccharides can be processed into bio-based and biodegradable films using gelatinization. Several studies showed that potato peels are film forming. Some mechanical properties for potato peel-based films are given in Table VI.2.

(Kang & Min, 2010) evaluated the production of potato peels film using high-pressure homogenization (HPH), irradiation or ultrasound treatment. The films formed by HPH exhibited the best integrity and smoothness when compared to irradiation and ultrasound process. The addition of glycerol as plasticizer was necessary to reduce polymer chain-to-chain hydrogen bonding and increase intermolecular spacing, which increased strain at break (Kang & Min, 2010). Using the same HPH-process, (Katariina et al., 2015) additional thermal treatment was positive for the film transparency because of complete gelatinization of starch. As shown in Table VI.2, for all samples the evolution of the mechanical properties, tensile strength and Young's modulus were decreased while strain a break increased as a function of glycerol content. With equal glycerol content, i.e. 30 wt % , (Katariina et al., 2015) had higher elongation at break and lower Young modulus. This difference in mechanical properties may arise from starch content since in both studies potatoes were hand peeled. Therefore, starch content may be very different between both studies. (Katariina et al., 2015) had a starch content up to 46 %. As a consequence sensibility of potato peels to glycerol may be impacted since thermoplastic starch is highly dependent on glycerol content (Lourdin et al., 1997).

Chapter VI

Table VI.2: Mechanical properties for potato peel-based films with addition of external plasticizer

| Samples | Plasticizer | Plasticizer amount (w/w of dried potato peels) | Tensile properties | | | | | | Reference |
|--------------------------------|-------------|--|------------------------|---------------------|---------------------|---------------------|-----------------------|------------------------|--------------------------|
| | | | Tensile strength (MPa) | | Strain at break (%) | | Young's modulus (GPa) | | |
| Potato peels (2 wt % solution) | Glycerol | 10 wt% | 29±5 | 38±3 ⁽¹⁾ | 2±0 | 3±0 ⁽¹⁾ | 1.9±0.1 | 1.8±0.1 ⁽¹⁾ | (Katariina et al., 2015) |
| | | 20 wt% | 25±1 | 25±2 ⁽¹⁾ | 4±0 | 6±1 ⁽¹⁾ | 1.2±0 | 1.1±0.1 ⁽¹⁾ | |
| | | 30 wt% | 14±2 | 13±1 ⁽¹⁾ | 11±2 | 10±1 ⁽¹⁾ | 0.5±0.2 | 0.6±0.1 ⁽¹⁾ | |
| Potato peels (3 wt % solution) | Glycerol | 30 wt% | 9.48± 1.24 | | 5.33± 2.05 | | 0.366 | | (Kang & Min, 2010) |
| | | 50 wt% | 3.99± 0.8 | | 14.35± 3.56 | | 0.0854 | | |

⁽¹⁾ High pressure homogenization+ Heat treatment

Besides the use of a solvent for dissolution of the biomass or the use of an external plasticizer for valorization of vegetables waste in bio-based and biodegradable films. Another approach gives rise to the transformation of vegetables waste in biodegradable items with very short life time. Such approach has been successfully done by (Wysocki, 2003), who processed wheat bran in edible items under the commercial name BIOTREM. The company has been able to make biodegradable moldings, in particular table utensils and packaging containers starting from wheat bran (Figure VI.14). Their patented process involves the use wheat bran under the form of powder, exposed to heat and compressive forces in a multipartite mold (Wysocki, 2003). The invention allows the design of items with various shapes and thickness (BIOTREM., 2016).



Figure VI.14: Schematic representation of BIOTREM technology, image reproduced from (BIOTREM., 2016)

Chapter VI

In conclusion, literature review reports on the ability to process by-products with currently zero value on the market to added-value materials. The structural constituents of potato peels have film forming ability either starch when submitted to heat or cellulose after amorphization as well as pectin. Besides that, potato peels represent a source of antioxidant molecules such as phenolic compounds and glycoalkaloids. Combination of both valorizations could allow the coupling of material and energy flow in a biorefinery approach. For a potato processor, by-products comprising potato peels and potato starch represent an important source of income with an annual quantity of over 53,000 tons and 3,000 tons of potato peels and starch, respectively. The present work has been divided in 3 different parts. First the biochemical characterization of potato peels was carried out by the quantification of the main constituents. Second, the potential extraction of high added value molecules such as phenolic compounds or glycoalkaloids was evaluated. Third, material applications of potato peels containing starch were investigated.

VI.3. Materials and methods

VI.3.1. Materials

Fresh potato peels and starch were kindly provided by McCain Alimentaire S.A.S. Potato peels were collected from the production line of Matougues. Separation of potato flesh and peel was done by exposing potato to steam in a pressure vessel under standard industry conditions. Exhaust of pressure separates both parts of potato and potato peels are collected in big bags. Collected peels had a dry content of about 90 % as measured from moisture analyzer (MA30, Sartorius) and were stored in the freezer at ca. -20 °C.

VI.3.2. Methods

VI.3.2.1. Wet milling and drying of potato peels

First, thawed potato peels were wet-milled in a grinder (Henzi Buaygeaud). Two drying methods were used. Freeze drying was carried out thanks to a (Christ Alpha (2-4 LD plus) equipments at -20 °C for 72 h. Air-drying was done in a Memmert Inc, Germany oven at 55 °C for at least 24 h. Then dried potato peels were grinded by means of a water-cooled mill ((IKA Analysenmühle A 10, Germany) for 2 min at a rotational speed of 25.000 rpm.

Chapter VI

VI.3.2.2. Biochemical analysis

Biochemical analysis of potato peels was assessed following work flow showed in Figure VI.15 and described in detail in following sections.

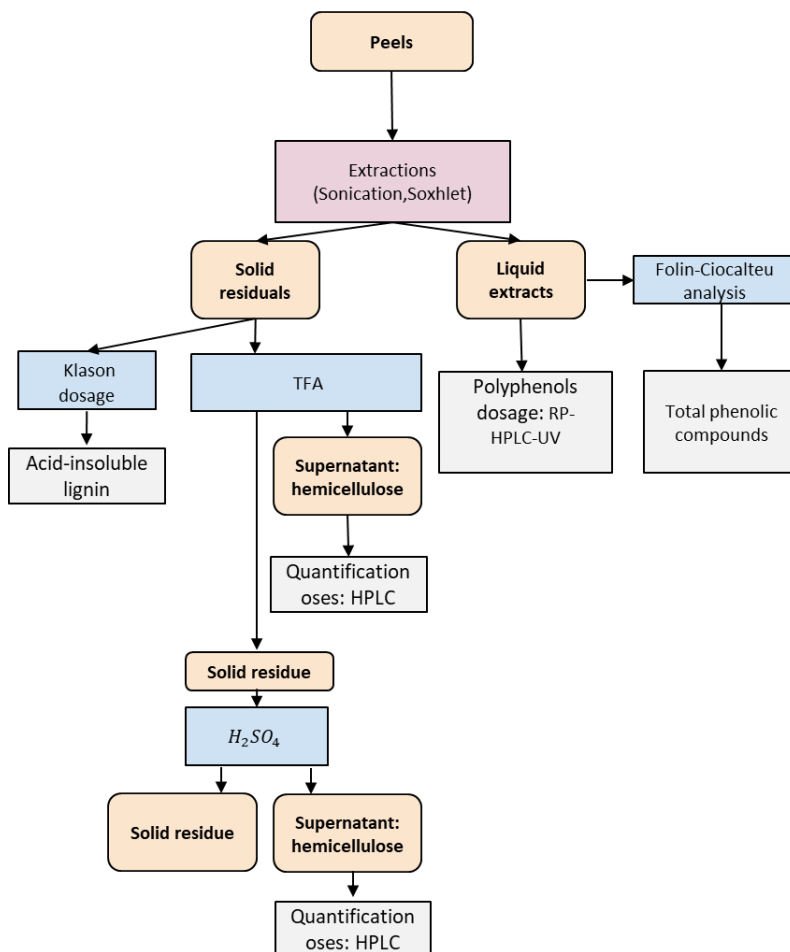


Figure VI.15: Biochemical analysis work flow

VI.3.2.3. Soxhlet Extraction procedures

The dried potato peel mass was extracted with a Soxhlet using a solution ethanol (96 °)/H₂O (2:1 v/v) for at least 7 h to allow extractions of pigments. Then, Soxhlet extraction with ethanol (96 °) for at least 6 h was carried out to extract lipids. Subsequently, Soxhlet extraction with deionized water was run for at least 9 h which allowed extraction of the water-soluble compounds such as sugars, pectin, proteins and tannins. Finally, the cartridge was immersed for 30 s in acetone before being placed in air-dryer at 50 °C for at least 6 days. The residue was weighted and designated as non-extractible content.

Chapter VI

VI.3.2.3.1. Ultrasound assisted maceration extraction method

The present protocol will be referred as sonication process in following sections. Thawed potato peels (50 g) were thoroughly mixed with a solution composed of ethanol and water (pH = 2 adjusted with HCl) (50:50 v/v). 5 g of dried potato peels were mixed with 200 mL of ethanol/water solution. The starting mixture was subjected to sonication (10.000 Hz) for 15 min in a water bath. Maximum temperature was 60 °C. Then sonicated preparation was placed contained in a closed Erlenmeyer and stirred for 2 h at 30 °C. Samples were then passed successively through a 250 µm sieve filter and a 20 µm cotton cellulose filter. The supernatant was collected in a flask. Oxygen was removed from the vial by nitrogen injection. The vial was then stored in a refrigerator at 4 °C. Two more extractions were performed starting from the previous extracted residue where 200 mL of solution ethanol: acidified water (50:50 v/v) was added. Samples were done in duplicates.

VI.3.2.3.2. Quantification of Cellulose & Hemicellulose

Quantification of cellulose and hemicellulose fractions was assessed with successive hydrolysis with trifluoroacetic acid (TFA) and sulfuric acid (H₂SO₄) degrading the hemicelluloses and celluloses, respectively. The protocol is shown in Figure VI.16.

TFA hydrolysis

First, 10 mg of biomass residue is mixed with 50 µL of fucose (2.5 g/L, standard solution) and 500 µL of TFA (2.5 M) and placed in oven at 110 °C for 2 h. After centrifugation, supernatant was water diluted with ratio 1:250 v/v and filtered with Anotop disc filters (aluminum oxide membrane, 45 µm) mounted on syringe in HPLC vials. Then samples were analyzed by high-performance anion-exchange chromatography (HPAEC) with a system consisting of a CarboPac PA-1 column (guard column 4x 50 mm and analytical column 4 x 250 mm) (Dionex) coupled to a pulsed amperometric detector (Dionex ED 40).

H₂SO₄ hydrolysis

Following TFA hydrolysis, the material was washed by centrifugation with water (3 mL), two times with ethanol and once with acetone (1.5 mL each time). Then they were freeze-dried. Then, 50 µL of fucose (2.5 g/L, standard solution) and 125 µL of 72 % H₂SO₄ was added and homogenized under magnetic stirring for 1 h under ambient conditions. Then, 1.5 mL of H₂O was added to the solution and placed for 2 h at 100 °C in oven. Finally, the supernatant was

Chapter VI

collected, water diluted with ratio 1:500 v/v and filtered with Anotop disc filters (aluminum oxide membrane, 45 μm) mounted on syringe in HPLC vials. Then samples were analyzed with HPAEC-PAD apparatus.

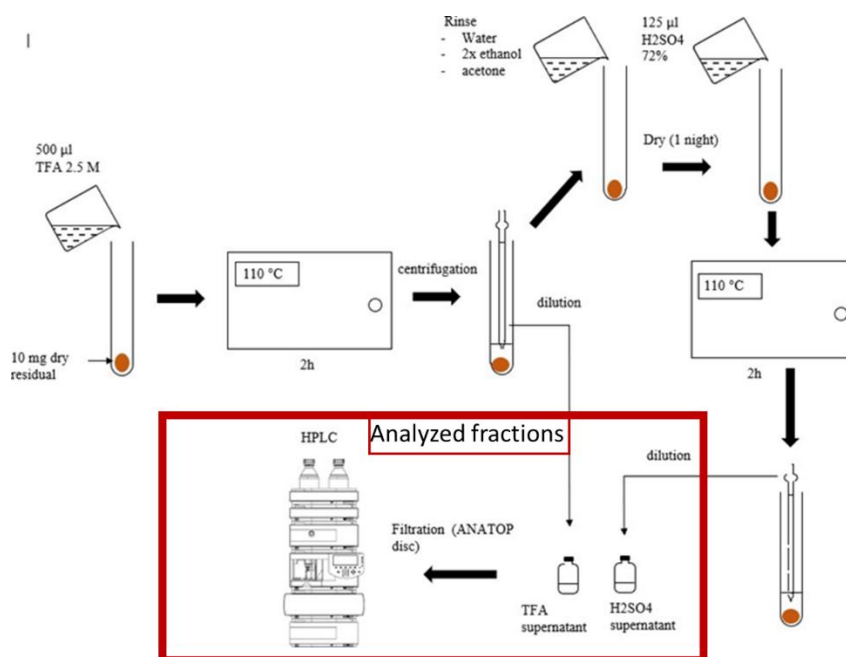


Figure VI.16: General diagram of the determination of cellulose/hemicelluloses content with successive hydrolysis using TFA and H₂SO₄ followed by HPLC analysis

VI.3.2.3.3.Lignin

The lignin content was measured by the Klason method, on the solid extraction residues. The Klason method is a gravimetric method of determination of lignin. It consists in hydrolyzing in acid medium (sulfuric acid solution) the constituents of the plant walls other than lignin and weighting the residue (Dence, 1992). First, 300 mg of residue were incubated in 72 % H₂SO₄ (3 mL) for 2 h under ambient conditions. Then residue was mixed with 5 % H₂SO₄ and placed in a sand bath for 3 h at 100 °C. The insoluble residue corresponds to the Klason lignin and is recovered by filtration (Whatman filter, glass fiber GF/A 47mm) and dried in an oven at 100 °C overnight. After being cooled in a desiccator, crucible was weighted. The Klason lignin was corrected by the ash content determined by incinerating the filter at 550 °C for 3 h.

Chapter VI

VI.3.2.4.Folin-Ciocalteu Assay

Total reducing compounds were assessed by Folin-Ciocalteu assay according to the protocol of (Caderby et al., 2013). After being subjected to sonication, 1 mL of sonicated residue and 5 mL of Folin-Ciocalteu reagent (diluted 10 times in ultrapure water) were thoroughly mixed in a vortex for 5 s. Four min later, 4 mL of 75 g/L Na₂CO₃ was added and subjected to vortex for 5 s. After being stored for 1 h in the dark under ambient conditions, the absorbance of the solution was read at 760 nm using a UV-vis spectrophotometer. The realization of a standard range using chlorogenic acid allows to calculate the concentration of phenolic compounds from 0 to 100 mg/L. The total phenolic content was expressed as chlorogenic acid equivalents.

VI.3.2.5.Reverse phase high performance liquid chromatography-UV detection (RP-HPLC-UV)

The phenolic compounds were quantified using a RP-HPLC-UV analysis. Compounds were separated by a C18 reversed phase silica gel column (50x 2 mmx 2.8 µm). Solvents for the mobile phase were acetonitrile acidified with formic acid at 0.1 % for the phase A and ultrapure water with formic acid at 0.1 % for the phase B. Ortho-coumaric acid was used as internal standard. Prior to assay, each sample was ultrafiltered on 0.45 µm cut-off filters. Injection flow rate was set to 0.5 mL/min. Elution conditions were as follows: from 0 to 25 minutes 1% A, 99% B; from 25 to 30 minutes 30% A 70% B.

VI.3.2.6. Fabrication of biodegradable items

VI.3.2.6.1.Thermoplastic films of potato peels/starch blends by casting

Starch/peel films were prepared through the casting technique using a film-forming solution at 5wt% dry content in water. Table VI.3 gives the individual formulations. The solution was heated for 30 min at 90 °C under magnetic stirring, subsequently mixed with an ultra-turrax for 45 s at 2000 rpm before glycerol was introduced at a concentration of 0.20 g/g dry content. Finally, the solution was poured in Teflon Petri dish and dried under vacuum at 40 °C.

Chapter VI

Table VI.3: Experimental design for preparation of potato peels:starch blends with glycerol

| Starch: Peels | Plasticizer | Volume H ₂ O (mL) | Starch weight (g) | Peels weight (g) |
|---------------|----------------|------------------------------|-------------------|------------------|
| 100 :0 | 0.6 g Glycerol | 57 | 3 | |
| 80 :20 | | | 2,4 | 0,6 |
| 70 :30 | | | 2,1 | 0,9 |
| 50 :50 | | | 1.5 | 1.5 |
| 30 :70 | | | 0,9 | 2.1 |
| 20 :80 | | | 0,6 | 2.4 |
| 0 :100 | | | | 3 |

VI.3.2.6.2.Films of potato peels by dissolution in formic acid

The following protocol was adapted to previous work done by (Giovanni Perotto et al., 2018). Powder of dried potato peels was mixed with a water solution of formic acid (2M). A solution of 20 mL/g of potato peels was prepared and placed in water-bath for 12 h at 40 °C under vigorous stirring. Finally, the solution was poured in Teflon Petri dish and let dry for 48-72 h under a fume hood and ambient conditions.

VI.3.2.6.3.Thermoplastic films of potato peels/starch blends by thermocompression

Potato peels, starch and glycerol with a content of 0.25 g/ g of dry starch were mixed. Weight ratio of starch: potato peels blend (dry content) was varied as follow: 29:71 w/w %, 44:54 w/w %, 50:50 w/w % and 66:33 w/w %. Formulations were processed by thermo-compression molding at 130 °C and up to 150 bar (thermocompression press model 15T, Scamex, France). They were heated pressed for 1 min and then compressed successively to 150 bar and 10 bar for 3 and 6 min, respectively. Aluminum foils of 3 mm were used to reach a thickness of 1 mm.

VI.4.Results and discussion

VI.4.1.Chemical composition of potato peels

Table VI.4 shows the chemical composition of potato peel mass with two different extraction methods. Both extraction methods gave approximatively the same amount of structural polysaccharides. Successive dissolution of hemicellulose and cellulose was done with the use

Chapter VI

of TFA and H₂SO₄. Hemicellulose was the major constituent of potato peels and accounted for about 18 % while cellulose represented about 10 %. As for lignin, upon both extraction methods gave the same result and represented 5 wt % of potato peel mass. Comparison with literature showed that, the lignin, hemicellulose and cellulose content correlate well with the data found from (Katariina et al., 2015). The major difference between both extraction techniques, i.e. sonication and soxhlet, was highlighted from the results of the extractible fractions which accounted for 33 and 55 wt %, respectively. In the present, starch content could not be determined. It can be estimated to be comprised between 10 and 20 % based on the material balance deficit (Table VI.4) and from literature (Borah, Das, & Badwaik, 2017; Camire et al., 1997; Liang & McDonald, 2014).

Table VI.4: Chemical composition of potato peel mass with different extraction methods

| Extraction method | Sonication (% d.m) | Soxhlet Ethanol: H₂O (% d.m) |
|--------------------------|---------------------------|--|
| Extractible | 33 | 55 |
| Lignin | 5.5±1 | 5±1 |
| Hemicellulose | H | 19.6 |
| Arabinose | 2.7 | 0.6 |
| Galactose | 2.4 | 2.2 |
| Glucose | 9.9 | 16.8 |
| Xylose | 1.1 | 0 |
| Cellulose | 12 | 7 |
| Starch | n.a | n.a |

n.a.: non analyzed

VI.4.2. Analysis of phenolic compounds in potato peels

After sonication, the extractible fraction was analyzed to explore composition of phenolic compounds in potato peels. The total phenolic compound within potato peels after ultrasound assisted extraction was assessed following Folin-Ciocalteu method and gave polyphenol content of 24.2± 0.7 mg of chlorogenic acid equivalent per grams of dried potato peels. In comparison phenolic compounds in sugar cane was calculated to be around 28-39 mg/g of dry matter (Caderby et al., 2013) or 33 mg/g in dry apple peels (Balasundram, Sundram, & Samman, 2006).

Chapter VI

The extractable fraction was further analyzed with RP-HPLC –UV and results are shown in Figure VI.17. Chlorogenic acid was present in its three isomeric forms, *i.e.* 3-O-caffeoylquinic acid (retention time $rt= 3.0$ min), 5-O-caffeoylquinic acid ($rt= 6.0$ min) and 4-O-caffeoylquinic acid ($rt= 5.6$ min). Moreover, caffeic acid ($rt= 4.7$ min) and ferulic acid ($rt= 8.1$ min) were present within potato peel fraction. Quantification results are gathered in Table VI.5. These phenolic compounds present high added-value compounds. Based on potato processor material flow with annual quantity of over 53,000 T, extraction and purification of these phenolic compounds could represent a great source of antioxidants molecule for various applications such as food or pharmaceutical to replace synthetic compounds (Jeddou et al., 2016; Rehman et al., 2004).

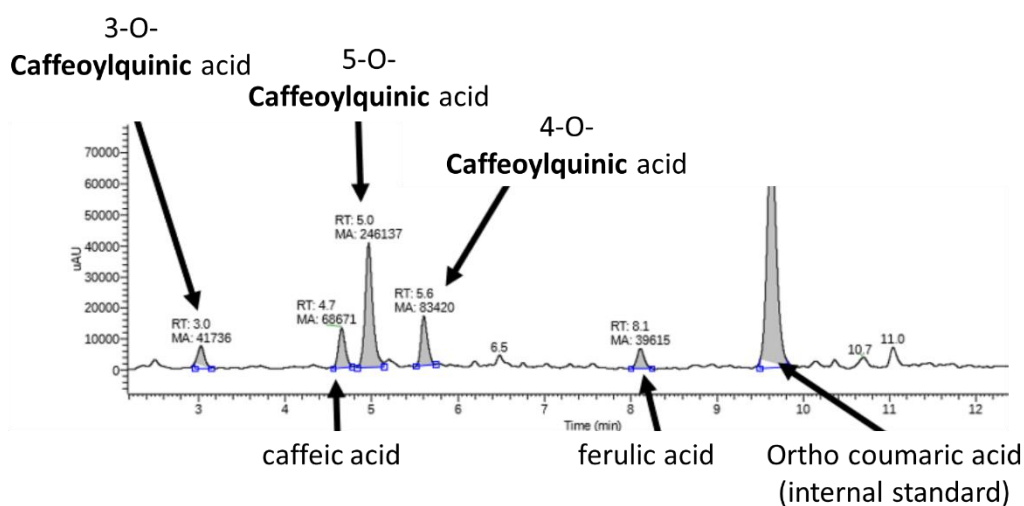


Figure VI.17: Chromatogram of the molecules determined by HPLC on extractible residue obtained ultrasound assisted extraction

Table VI.5: Extraction quantities of phenolic compounds after sonication extraction

| Phenolic compounds | Extracted mass (mg/g potato peels) |
|--------------------|------------------------------------|
| Chlorogenic acid | 0.695 ± 0.070 |
| Caffeic acid | 0.058 ± 0.004 |
| Ferulic acid | 0.028 |

The present study highlighted the effectiveness of sonication extraction method to isolate phenolic compounds present in potato peels. Following Folin-Ciocalteu method, yield of extraction went up to 25 mg/g of chlorogenic acid equivalent per grams of dried potato peels. Chlorogenic acid represents more than 88 wt % of phenolic compounds within potato peels

Chapter VI

while caffeic and ferulic acid are minor fractions. The potential valorization of by-products in high added-value molecule should be realized in a biorefinery approach as suggested in Figure VI.18 and described thereafter. In the proposed approach, three solvent streams will be required: water, ethanol and hydrochloric acid (water acidification). Minimization of their quantities will be required, therefore recycling loops must be considered with the objective of minimization of consumption while concentrating extracted molecules. Based on the results obtained previously, the ultra-sound assisted process was found to be a viable solution for separation of structural constituents and extractable fraction of potato peels. When considering three successive steps of sonication, it can be estimated that the third extraction will extract only very small fraction of molecules compared to the two previous ones. Therefore, solvent of the third extraction could be reinjected in the first one allowing concentration of molecules as well as reduction of solvent incomes. The recycling loop of water can also be considered a gradient of temperature will be generated along the process as follows: the cold water flow entering the plate heat exchanger exits at a hot temperature, so it can be used to heat the distillation column and finally reused for preparation of ethanol/water solution.

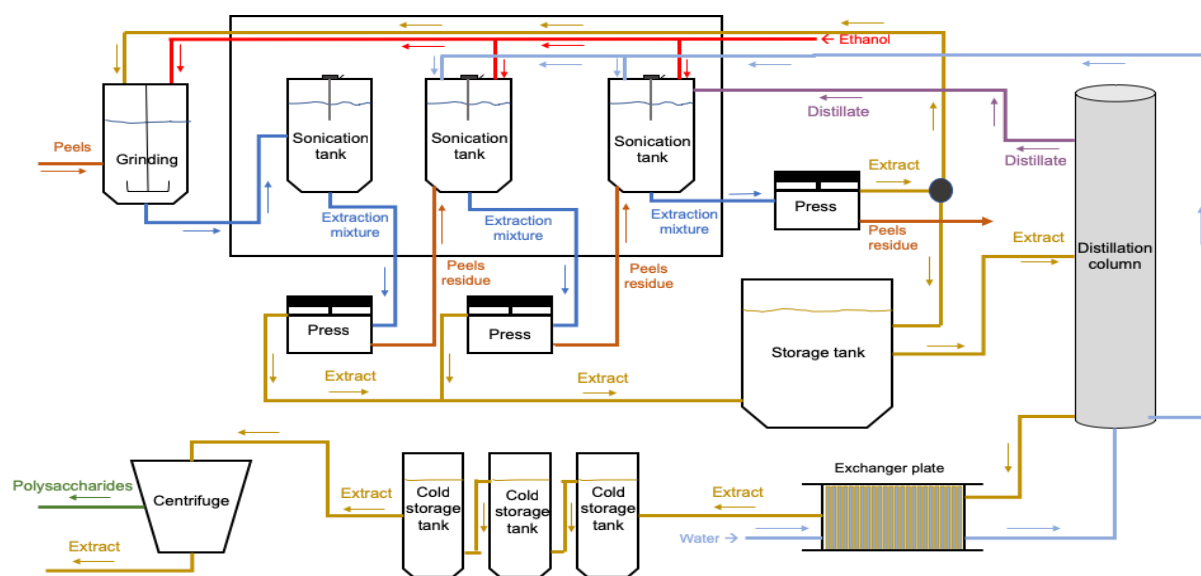
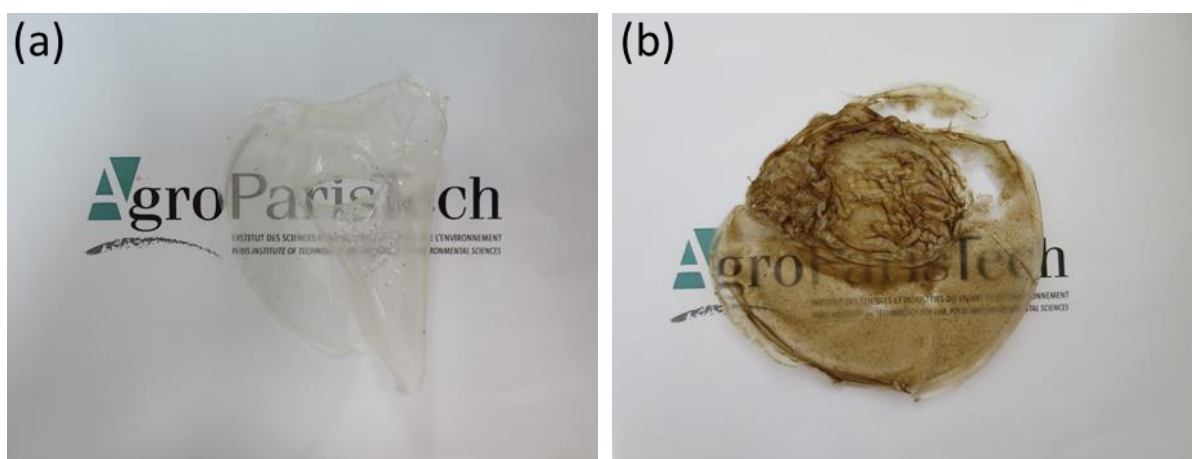


Figure VI.18: Schematic representation of a potential extraction and purification process of high value-added molecules implemented a biorefinery type approach.

VI.4.3. Thermoplastic starch/peel blends obtained by casting

Blends of starch and potato peels with fixed content of glycerol were obtained from solution-casting. Photographs in Figure VI.19(a-b) show that free standing films of potato by-products were obtained upon casting. All samples showed film forming ability. Differences in their visual aspects and mechanical resistance were probed by hand. Evaluation of their visual aspect showed that thermoplastic starch blank film was transparent (Figure VI.19(a)), while addition of potato peels within mixture resulted in brownish color. The brownish color reflected the typical color of potato peels caused by oxidation dehydrogenation of polyphenols (Busch, 1999). Moreover, the roughness of the film as probed by hand presented difference between both sides. The surface of the film in contact with Teflon was smooth while a granular aspect was observed at the other side. This effect was even more pronounced with increased peel content and could be attributed to presence of aggregates. The mechanical resistance as probed by hand showed that film of pure starch was stiff and brittle, which was attributed to strong retrogradation of starch (Van Soest & Knooren, 1997). On the contrary, addition of potato peels resulted in malleable materials but resistance to tearing was poor. Taking into account brittleness, texture and potential valorization of raw by-products, mixture comprising 20 wt% of starch and 80 wt % potato peels with addition of glycerol showed the best film forming ability. To further demonstrate the ability to make thermoplastic items with potato peels, solution casting was performed on larger scale using Teflon recipient as shown in Figure VI.19(f).



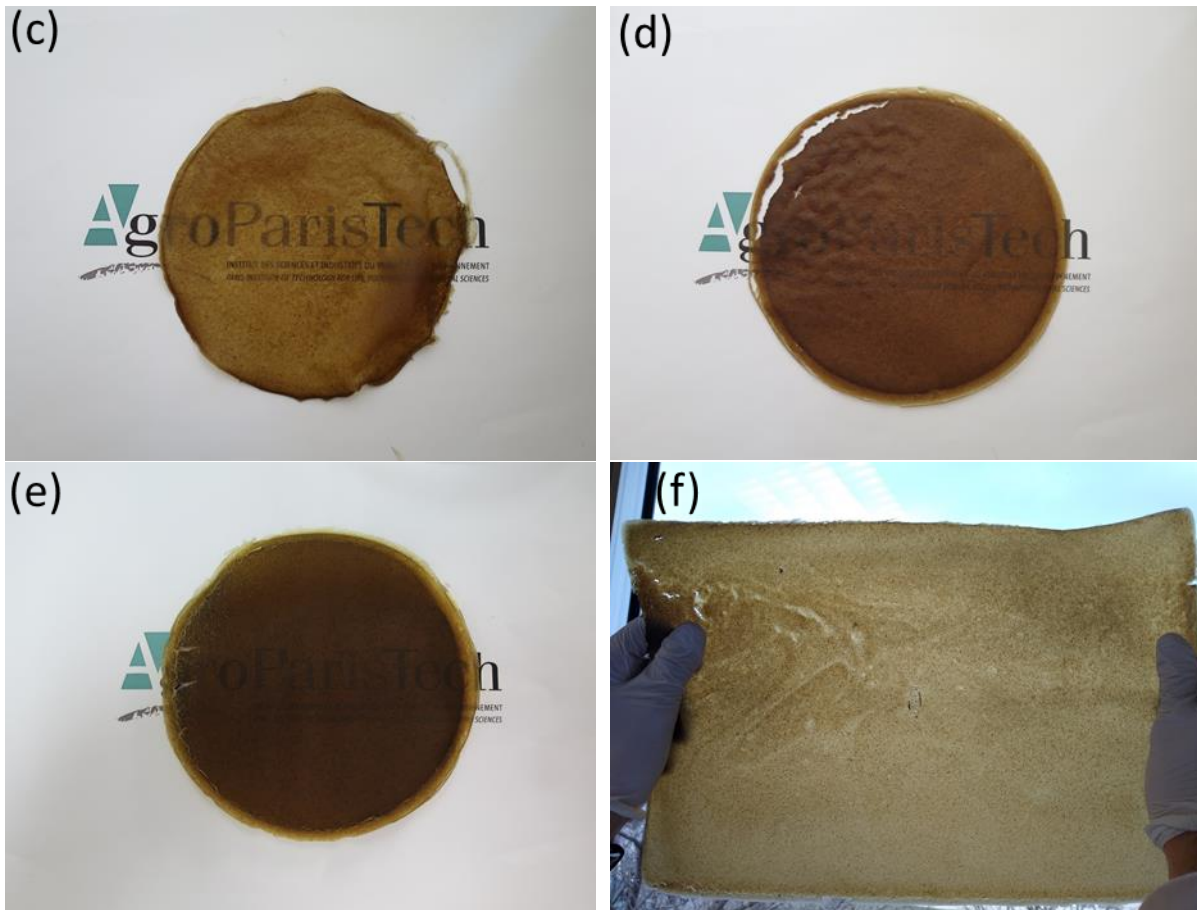


Figure VI.19: Appearance of starch: potato peels blend films with addition of glycerol with varying weight ratio a)100:0, b) 80:20, c) 50:50, d) 20:80, e) 0:100, f) 20:80 made from larger scale

VI.4.4. Films of potato peels by dissolution in formic acid

Films made only of potato peels were successfully achieved by the use of formic acid (no photography can be shown). Thanks to the higher volatility of formic acid compared to water, films could be obtained in less than 24 h. Obtained film showed very promising results by displaying, as probed by hand, malleable behavior and higher ductility when compared to plasticized potato peel film. As observed by (G. Perotto et al., 2020), carrot powder could be used to fabricate a bio-based film. Comparison between HCl and formic acid treatment gave rise to the formic acid treatment since resulting films had reduced degree of crystallinity and evidenced presence of pectin and aliphatic polyester from NMR. However, potato peels are not only composed of cellulose and pectins but also of starch. It has been shown than solution of formic acid/acid could reduce the gelatinization down to 56 °C in 40 % formic acid (Divers, Pillin, Feller, Levesque, & Grohens, 2004). Therefore, by properly controlling the temperature reaction, gelatinization of starch can be induced at low temperature. Investigations on the impact of RH on the mechanical properties should be considered.

VI.4.5. Potato peel films by thermo-compression

Thermo-compression molding was explored to obtain potato peels items based on the same scheme as BIOTREM (Wysocki, 2003). Compression forces and heat were imposed to induce gelatinization of starch, evaporation of water as well as compaction of the mixture to obtain a 1 mm thick material (Figure VI.21). In this way, varying weight ratio of starch: potato peels were investigated using an experimental design as shown in Figure VI.20. The amount of starch was incremented by 5 % between each sample (from left to right). Visual aspect visualization and mechanical resistance as probed by hand showed that low amount of thermoplastic starch (< 20 %) did not lead to film forming ability since obtained materials were friable. On the contrary, inclusion of large content of thermoplastic starch (>80 %) led to brittle material caused by retrogradation of starch. Balanced mechanical resistance were obtained with thermoplastic starch content of about 30 % and 70 %.

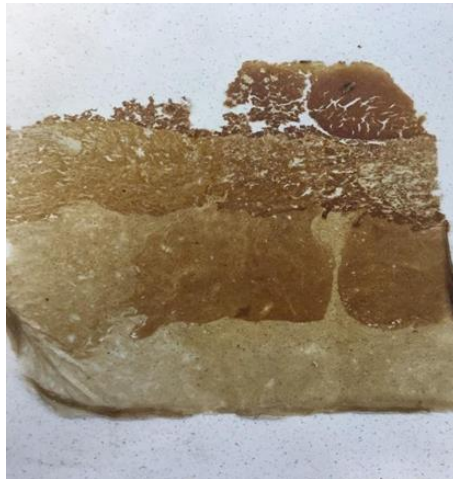


Figure VI.20: Experimental results after thermo-compression molding for varying weight ratio of starch: potato peels

To further explore the ability of turning potato peels materials in disposable products, 4 starch: potato peels ratios were selected: 29:71 w/w %, 44:54 w/w %, 50:50 w/w % and 66:33 w/w %.

Chapter VI

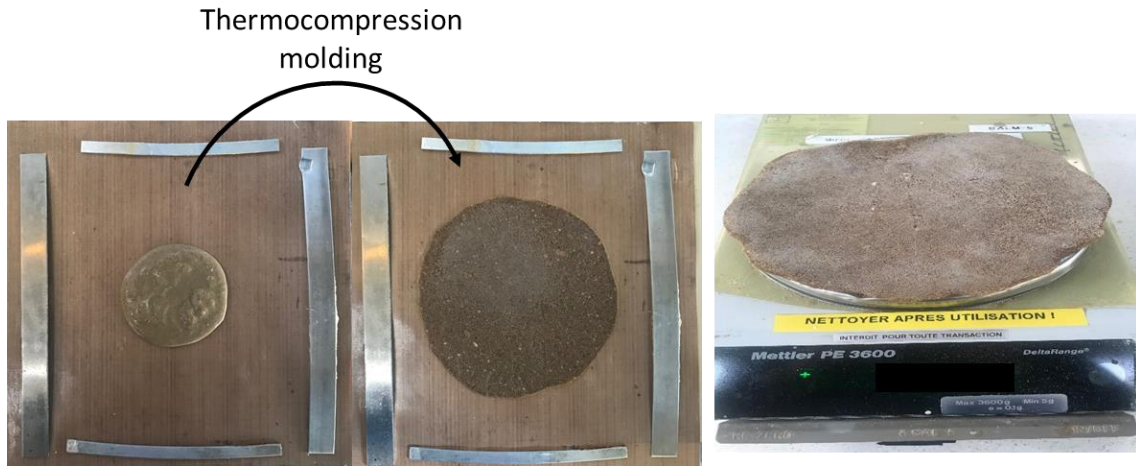


Figure VI.21: Successive steps for fabrication of starch: potato peels items from thermo-compression molding

Developed implementation process was effective to evaporate water content within the starch: potato peels mixture since a dried material was obtained as shown in Figure VI.21. Based on naked-eye evaluation, no significant differences between materials were observed as shown in Figure VI.22. However, the behavior of the obtained material deviated from solution casting where a more compact and rigid material was obtained whatever the starch content.

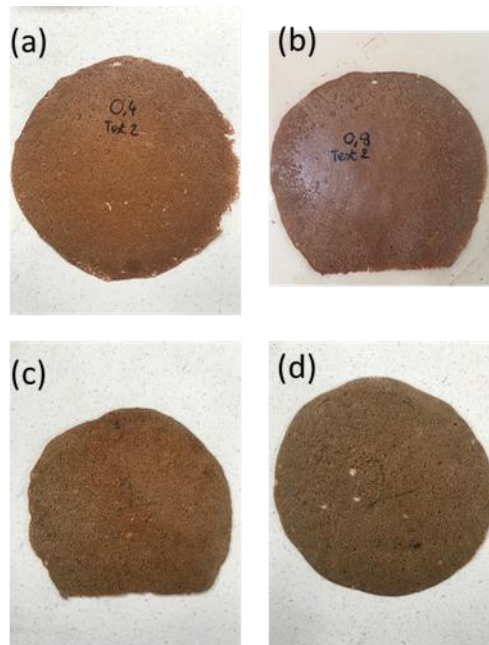


Figure VI.22: Visual aspects of thermo-compressed items of starch: potato peels upon varying weight ratio with a) 29:71 w/w %, b) 44:54 w/w %, c) 50:50 w/w % and d) 66:33 w/w %

VI.5. Conclusion

The generation of over 53.000 T of potato peel annually for a potato processor represents a waste costly to treat. However, it can be a source for extraction of phenolic compounds such as chlorogenic acid. Finally, both by-products potato starch and peels could be turned into bio-based and biodegradable items. First, potato peels-based material produced from a conventional solution casting method showed its film forming ability with malleable free-standing films. Towards another approach, more rigid materials were obtained from thermo-compression molding and could be addressed for production of items with very short service life. This study demonstrates various valorization ways for agri-food industries to be addressed for their by-products from negative or zero value to higher-value product.

Chapter VI

Conclusion and Perspectives

Bio-based and biodegradable packaging with food contact ability suitable for conditioning of frozen French fries were developed. The bio-based and biodegradable poly(3-hydroxybutyrate-co-3-hydroxyvalerate) (PHBV) was selected thanks to its ability to be produced from food by-products. The concept of short supply chain with valorization of by-products involved in a circular economy fits with Corporate Social Responsibility and sustainable development of the potato food processor. To explore the development of highly innovative bio-based and biodegradable packaging, a commercially available PHBV was used. PHBV has high stiffness and brittleness which makes it difficult to be used for flexible food packaging, lack of melt strength which hinders its processability and glass transition temperature (T_g) between 0 and 5 °C. This last property is important when considering applications in freezer conditions. The adopted strategy was melt blending with a highly ductile home compostable aliphatic polyester, poly(butylene succinate-co-adipate) (PBSA). The main findings are summarized as follows:

Investigation of melt blending of PHBV and PBSA with varying weight ratio showed immiscibility between both phases. A droplet-in-matrix morphology was obtained for PHBV or PBSA content of 70 % while a co-continuous blend morphology was observed in 50/50 PHBV/PBSA blend. The addition of PBSA in PHBV was efficient to soften PHBV-based films with decreased Young Modulus. The evolution of the mechanical properties was successfully modeled with the Equivalent Box Model (EBM) which accounts for immiscible polymer blends. Introduction of an adhesion parameter in the prediction of strength showed that a low interfacial adhesion factor needed to be assumed to describe the behavior of the blends at high PBSA content. As a result, blends showed brittle fracture even when PBSA was the main constituent. In the aim to maximize the PHBV content, the PHBV/PBSA ratio of 70/30 wt% was selected for the design of interfacial compatibility using reactive extrusion.

To improve interfacial compatibility *in-situ* reactive compatibilization was performed with the addition of dicumyl peroxide (DCP) as free radical initiator. Addition of DCP up to 0.2 phr led to the formation of long chain branched structure as evidenced from the gel content and rheological measurements with apparition of a frequency dependent behavior in low frequency range. Mechanical properties were positively impacted with maximum stress similar to PHBV blank resulting from improved interfacial adhesion. Best formulations, i.e. PHBV/PBSA 70/30 and PHBV/PBSA 70/30+0.1 and 0.2 phr DCP could be processed by film blowing extrusion. As a key result, we have been able to produce blown PHBV-based films with PHBV content as

Conclusion and Perspectives

high as 70 wt%. In-depth characterizations of obtained films were conducted with a special attention given to PHBV/PBSA 70/30+0.1phr DCP since it showed the best results. Packaging aging under freezer conditions and in contact with fatty food showed a decrease in elongation at break of about 20 % after 2 weeks and further a stabilization over time. However, introduction of DCP led to no improvement in ductility.

The inclusion use of Acetyl Tributyl Citrate (ATBC) as plasticizer was tested to further improve ductility and process-ability of PHBV/PBSA blends. DCP was replaced with Luperox® 101E, because of the requalification of DCP in a new hazard category having Reproductive toxicity 1B with interdicts its use in Food Contact Materials. Preliminary tests of PHBV/PBSA blends with 0.1 phr DCP showed that an optimal ATBC content was reached at 10 wt % with decreased T_m , T_c , and T_g , lower stiffness and increased elongation at break. Low miscibility between PHBV and ATBC above 5 wt % ATBC was evidenced by Fox law while PBSA/ATBC showed good miscibility in the investigated range 5-20 wt %. Based on the previous study, plasticized and unplasticized blends with 0.1 or 0.2 phr LUPEROX® and fixed content of ATBC, i.e. 10 wt %, was performed at lab scale. The optimal performances were reached with an organic peroxide content of 0.2 phr while addition of ATBC did not impart cross-linking and showed higher tensile strength and elongation at break when compared to plasticized blends with DCP. These improvements were attributed to enhanced interfacial adhesion between PHBV and PBSA. Finally, semi-pilot scale film blowing extrusion was performed. PHBV/PBSA/ATBC 63/27/10+ 0.2phr LUPEROX® showed remarkable good processability. Synergic effects resulting from combination of Luperox® and ATBC allowed production of PHBV-based film with improved toughness, higher elongation at break and featuring flexibility even at -20 °C. This result opens up the ability to process PHBV-based film with a PHBV content up to 63 wt % for large scale production scale and to be addressed for flexible film packaging of frozen food intended to come in contact with fatty food. The food contact compliance testing according to EU 10/2011 is in progress and results will be obtained just after submission of the manuscript. Food Contact Migration is assessed by means of overall migration tests. Two simulants were selected: water/ethanol 50/50 (v/v) and alternative fatty food simulants iso-octane. Overall migration is performed by total immersion for 10 days at 40 °C.

Despite the very promising result, the developed formulation still shows some drawbacks regarding their ductility. Several strategies for improving the overall mechanical properties of PHBV may be put in perspectives:

Conclusion and Perspectives

Increasing HV content in the copolymer PHBV

The commercially used PHBV contained only 3 mol% HV and displayed very brittle fracture. From literature, PHBV with higher HV content have been found to decrease T_m , T_g as well as the crystallinity degree resulting in more amorphous polymer. However, their crystallization rate may hinder their application since it was observed that crystallization rates decrease rapidly above 10 mol% HV (Yoshie, Saito, & Inoue, 2001). An extrusion campaign using PHBV 25 mol% HV was realized during the thesis. A micro-compounder equipped conical twin-screw was used. The obtained film after thermo-compression molding was very sticky despite the use of Teflon sheets and could be peeled off after aging of about 1 h. Therefore, addition of nucleated agent should be investigated. Although films of PHBV-25 mol% HV were obtained, the mechanical resistance as probed by hand, showed limited improvement. It can be estimated that, PHBV with 15-25mol% HV will still be difficult to comply with severe technical specifications. The developed strategy of blending, *in-situ* compatibilization and plasticization for improvement in rheological, thermal and mechanical properties may be applied while keeping its bio-based and biodegradable character. Moreover, inclusion of external plasticizer within PHBV-high HV content is expected to be improved since lower crystallinity degree will be obtained. However, main drawback to date for the use of such PHBV, is its very high cost which limits its potential use for food packaging.

Optimization of the blend structure – lamellar blends

Another strategy that could be adopted and that has already been demonstrated in literature results from structuration of blends. (Boufarguine et al., 2013) blended poly(lactic acid) (PLA) with PHBV in proportion of 90/10 wt% using a multilayer co-extrusion process. This process allows multiplication of the number of alternate layers of PLA and PHBV. As a result, authors observed an increase in ductility when compared to PLA blank and PLA/PHBV blends from 18 % (PLA blank) up to 52 % (129 theoretical layers).

Use of co-extrusion techniques – multilayer packaging

Finally another strategy that has been shown to be effective for food packaging is co-extrusion process of bi-layered films (Cunha et al., 2015; Teixeira et al., 2020). Designed film shows premature fracture when submitted to stretching and addition of second layer could play a role of sacrificial layer when submitted to large deformations. Selection of the second layer is important to keep its biodegradable character while behaving as ductile at low temperature, i.e. – 20 °C. In this way, co-extrusion film blowing with PBSA as external layer would be

Conclusion and Perspectives

interesting thanks to its low T_g , high elongation at break and commercially available with grade for film blowing.

Chapter VII

**Résumé du travail de thèse en
français**

VII.1.Introduction générale

Les emballages alimentaires jouent un rôle majeur dans la production, la distribution et la consommation des aliments. Les enjeux environnementaux requièrent la conception d'emballages raisonnés permettant de maintenir leurs fonctions principales tout en diminuant leur impact environnemental (Marsh & Bugusu, 2007). De nos jours, les polyoléfines, incluant le polyéthylène (PE) et le polypropylène, sont les polymères les plus couramment utilisés et permettent de répondre au cahier des charges d'un emballage alimentaire grâce à leurs excellentes propriétés thermomécaniques, leur très bonne capacité de mise en œuvre et un coût de production faible. Le polyéthylène basse densité (PEBD) peut notamment être adressé pour les emballages d'aliments surgelés. En effet, le PEBD a une faible température de transition vitreuse (- 100 °C) permettant d'être ductile à -20 °C, une structure branchée compatible avec la technique d'extrusion soufflage de film et apte au contact alimentaire. Cependant, sa persistance dans l'environnement et son difficile recyclage pour le contact alimentaire impacte négativement son empreinte environnementale. Le développement de nouveaux matériaux biosourcés et biodégradables se positionne ainsi comme une stratégie pertinente pour répondre à ces enjeux.

D'un autre côté, les industries agro-alimentaires (IAA) sont quant à elles utilisatrices de ces emballages thermoplastiques. Ces matériaux, qui sont pour la majorité non-biodégradables sont destinés à des applications de courte durée de vie et pose donc un enjeu environnemental majeur. En effet, leur persistance dans l'environnement couplé à la faible durée de vie du couple aliment/emballage encourage les industries agro-alimentaires à trouver de nouvelles stratégies vis-à-vis de leurs matériaux d'emballage. Or, les IAA génèrent une grande quantité de co-produits organiques tout au long des opérations unitaires de la production des aliments. Ce constat s'applique notamment aux industries de la transformation de la pomme de terre, en générant de grandes quantités d'amidon mais également de pelures. L'une des stratégies pouvant être employée pour la valorisation de ces co-produits est la transformation de ces co-produits en tant que matière première pour la production des éléments d'un emballage. Cette démarche s'inscrit dans un nouveau paradigme d'économie circulaire pour la production d'un emballage biodégradable à partir des co-produits industriels.

VII.2. Positionnement de la thèse

Le projet de thèse se positionne dans un contexte industriel qui cherche à concevoir un emballage flexible bio-sourcé et biodégradable pour l'emballage alimentaire de produits surgelés dans une démarche de circuit court. Ce positionnement se base sur la valorisation des co-produits d'une industrie agro-alimentaire en utilisant du poly(3-hydroxybutyrate-co-3-hydroxyvalérate) (PHBV). En effet, ce polymère est à la fois bio-sourcé mais également biodégradable. De plus, celui-ci peut être produit à partir de co-produits permettant ainsi de répondre à la démarche de valorisation des co-produits. Dans cette démarche d'économie circulaire, la Figure VII.1 illustre ce concept avec la production simultanée de l'aliment, mais également des composants de l'emballage en réemployant les flux de matière et d'énergie générés lors des différentes opérations unitaires. Le PHBV qui est issu de la famille des polyhydroxyalcanoates à courtes chaînes est un polymère apte au contact alimentaire et commercialement disponible (Anjum et al., 2016). Cependant, le PHBV est un polymère fragile et rigide et sa mise en œuvre par extrusion-soufflage de gaine est négativement impactée à cause de sa faible viscosité au fondu (Cunha et al., 2015; Teixeira et al., 2020). Malgré la possibilité de moduler la teneur en hydroxyvalérate (HV) et en prenant en compte le cahier des charges requis pour être utilisé en tant qu'emballage flexible d'aliments surgelés, les opportunités données par le PHBV seul sont limitées (Anjum et al., 2016; Corre et al., 2012; Lemechko et al., 2019).

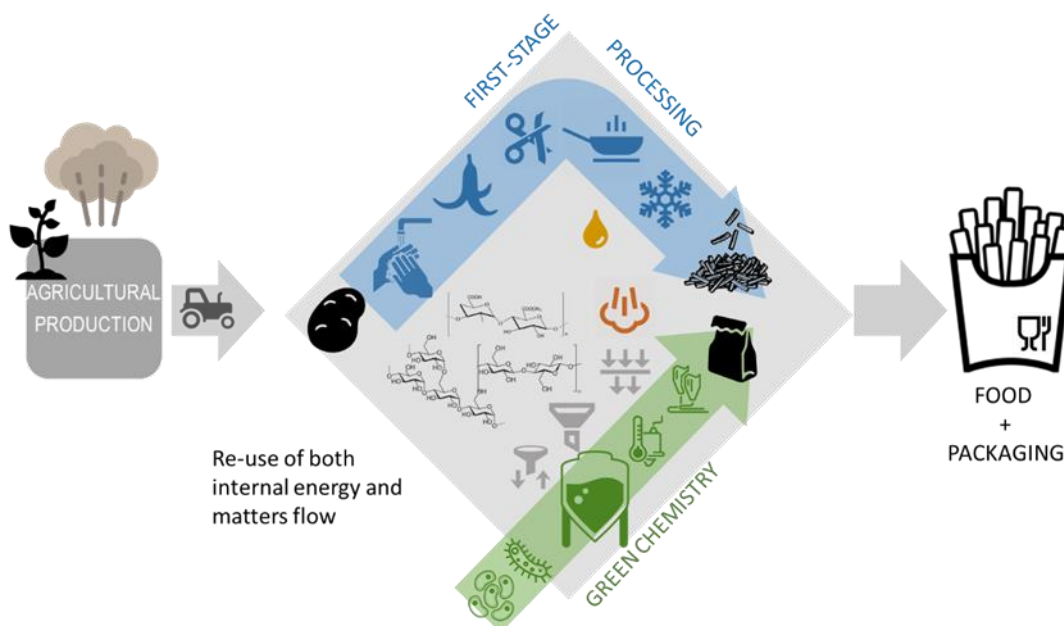


Figure VII.1: Principe de co-production de l'aliment et des composants de l'emballage

VII.3.Objectifs et approche

L'objectif général des travaux est la **conception d'un emballage flexible bio-sourcé et biodégradable apte au contact alimentaire pour les aliments surgelés et pré-frits**. Au-delà des conditions de stockage des aliments qui impacteront très fortement l'emballage et son contenu, la conception de l'emballage doit également prendre en compte les conditions de mise en œuvre. En effet, les emballages flexibles sont le plus souvent obtenus par extrusion soufflage de gaine. Ainsi, le matériau utilisé pour l'emballage doit répondre à un cahier des charges strict sur une grande plage de température tel qu'illustré dans la Figure VII.2. Cette technique de mise en œuvre requiert à la fois de l'élasticité au fondu, mais également de la viscosité extensionnelle.

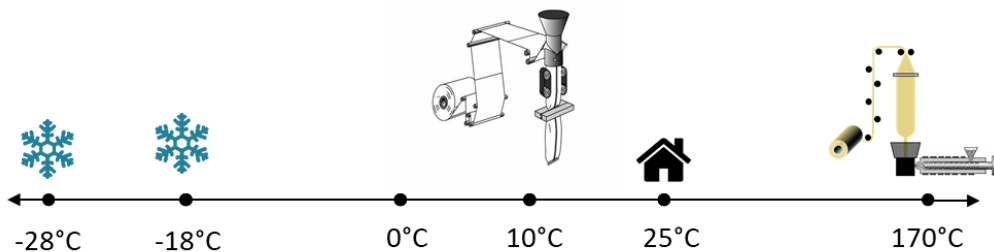


Figure VII.2: illustration des différentes températures auxquelles sera soumis l'emballage de sa mise en œuvre par extrusion soufflage de gaine à son application finale pour l'emballage des aliments surgelés

Afin de répondre à l'objectif général de la présente thèse et en considérant les propriétés thermomécaniques insuffisantes du PHBV, la stratégie adoptée est le mélange de polymères afin d'avoir un contrebalancement des propriétés thermo-mécaniques en mélangeant un polymère fragile et rigide avec un polymère ductile. Le polyester aliphatique poly(butylène succinate-co-adipate) (PBSA) a ainsi été sélectionné en se basant sur son caractère biodégradable et sa température de transition vitreuse située à $-45\text{ }^{\circ}\text{C}$. Par ailleurs, la revue littéraire détaillée dans le Chapter I permet de mettre en évidence que les polymères sont le plus souvent immiscibles et requiert une compatibilisation *ex-situ* ou *in-situ* afin d'améliorer l'adhésion interfaciale entre les deux phases de polymères. Dans le cadre de ces travaux, la compatibilisation *in-situ* en utilisant un initiateur de radicaux libres. De plus, une étude de la plastification de la phase amorphe a également été réalisée.

Les objectifs spécifiques sont les suivants :

- *Modification de la phase cristalline du PHBV*
 - Ajout d'un second polymère
- *Modification de la compatibilité interfaciale*

Chapter VII

- Addition d'un initiateur de radicaux libres
- *Modification de la phase amorphe*
 - Addition d'un plastifiant

Afin de répondre aux objectifs, la démarche adoptée est une méthode en cascade. La première étude porte sur le mélange du PHBV et du PBSA à l'état fondu en utilisant un mélangeur interne suivi par l'évaluation des propriétés morphologiques, rhéologiques et thermo-mécaniques. Cette étude a été poursuivie par la compatibilisation *in-situ* par extrusion réactive avec l'utilisation d'un initiateur de radicaux libres. Cette étude a été menée premièrement avec un mélangeur interne puis sur un module d'extrusion gonflage à l'échelle laboratoire permettant ainsi de valider la faisabilité de la formulation. Enfin, la meilleure formulation a été modifiée par l'ajout d'un plastifiant en utilisant le mélangeur interne avant d'être mise en forme à l'échelle pilote. En effet, cette dernière étude portant sur la formulation de PHBV s'est concentrée sur sa capacité à être gonflé afin d'analyser par la suite les interactions entre l'aliment et l'emballage en conditions de surgélation. Enfin la dernière étude de cette thèse s'est portée sur le développement de nouveaux matériaux à partir des co-produits d'une industrie agro-alimentaire. Cette étude s'est basée sur l'utilisation d'amidon et de pelures en proposant des méthodes de conception simple à l'échelle laboratoire.

VII.4.Principaux résultats

VII.4.1.Caractérisation d'un nouveau mélange de polymères biosourcés et biodégradables : Application aux mélanges poly(3-hydroxybutyrate-co-3-hydroxyvalérate) / poly(butylène-co-succinate-co-adipate)

La première étude s'est portée sur le mélange binaire du PHBV et du PBSA. Les différents mélanges ont été préparés par mélangeur interne à l'état fondu avant d'être mis en forme par thermocompression. Le PHBV et le PBSA sont des polymères immiscibles. L'évolution de la viscosité complexe en fonction de la fréquence, comme illustrée en Figure VII.3, permet de mettre en évidence le comportement Newtonien du PHBV tandis que le PBSA montre une dépendance de la viscosité en fonction de la fréquence. Les différents mélanges de PHBV/PBSA montrent quant à eux, que l'augmentation de la phase de PBSA dans la phase de PHBV conduit à une augmentation de la viscosité complexe et tend à se comporter comme le PBSA pur.

Chapter VII

Par ailleurs, en s'appuyant sur l'évolution de la viscosité complexe en fonction de la fréquence, le calcul du ratio des viscosités, défini comme étant $\lambda = \eta_{dispersed}/\eta_{continuous}$, permet de prédire la morphologie résultante dans la borne de fréquence définie entre 30 et 100 Hz. Ainsi, les ratios de viscosité η_{PBSA}/η_{PHBV} (PBSA comme phase dispersée) et η_{PHBV}/η_{PBSA} (PHBV comme phase dispersée) ont été évaluées à 3.6-2.8 and 0.2-0.1, respectivement. La valeur haute λ prédit ainsi que le PBSA sera présent sous forme de larges gouttelettes dans la phase continue de PHBV tandis que la faible valeur de λ prédit une dispersion de petits nodules de PHBV dans la phase continue de PBSA.

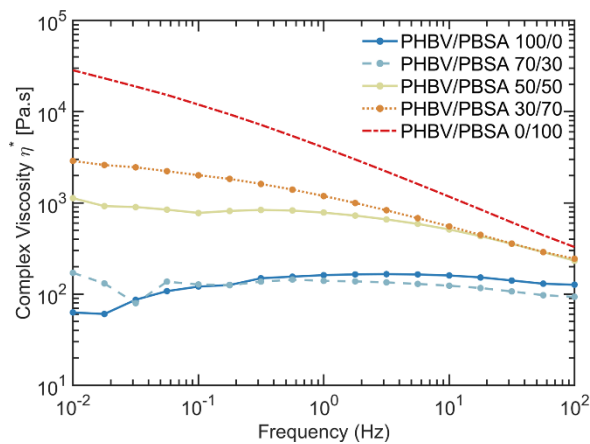


Figure VII.3: Evolution de la viscosité complexe du PHBV, PBSA et des mélanges PHBV/PBSA à 185 °C après mélangeur interne. Les données ont été enregistrées en débutant des hautes fréquences.

Les morphologies développées corréleront avec la prédiction issue du ratio des viscosités et sont typiques des polymères immiscibles avec une séparation de phase entre le PHBV et le PBSA tel qu'illustrées dans la Figure VII.4(a-e). En effet, lorsque le PHBV est en phase majoritaire, les nodules de PBSA sont dispersés dans la phase continue de PHBV. Lorsque les deux polymères sont en proportions équivalents, une morphologie de type co-continue est observée tandis que l'augmentation de la proportion en PBSA conduit à une inversion de phase où le PHBV se trouve sous forme de nodules dispersés dans la phase continue de PBSA.

Chapter VII

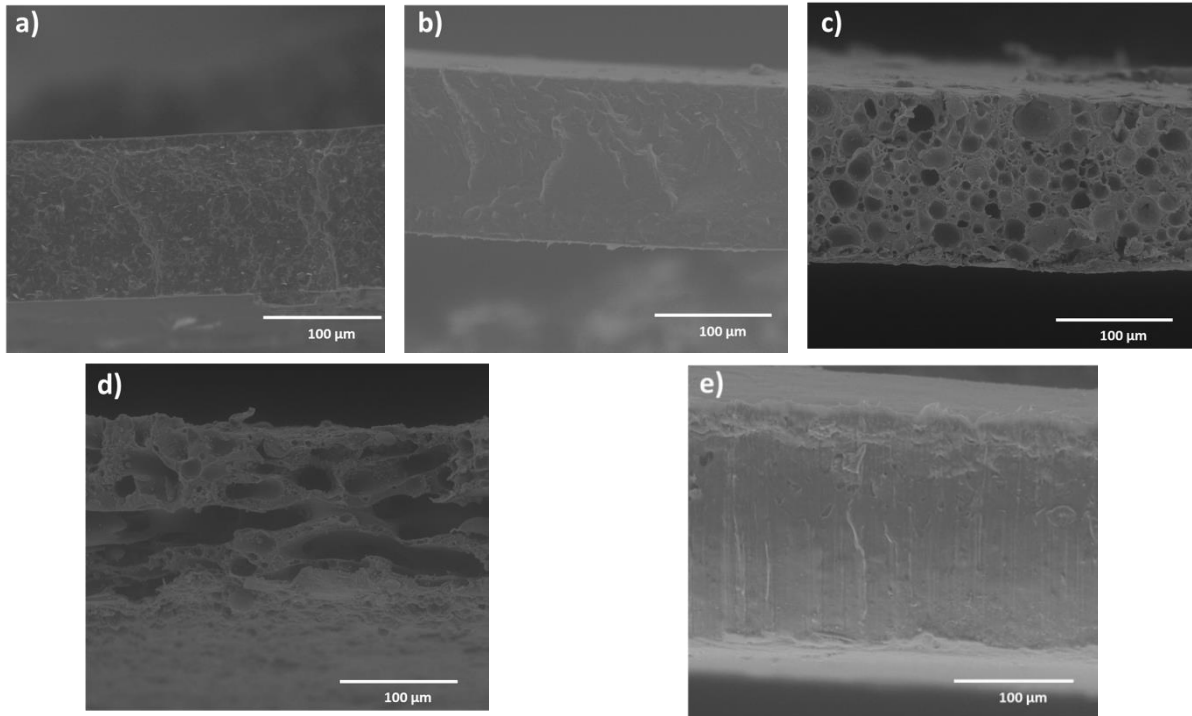


Figure VII.4: Images MEB des échantillons cryo-fracturés de PHBV, PBSA et mélanges PHBV/PBSA avec: (a) PHBV, (b) PBSA, (c) 70/30, (d) 50/50 et (e) 30/70

Les propriétés mécaniques ont été évaluées par tests de traction et les résultats sont récapitulés dans le Table VII.1. L'évolution du module élastique en fonction de la teneur en PBSA montre une diminution de la rigidité avec l'inclusion d'un polymère ductile. Cependant, l'augmentation de l'élongation à la rupture reste très minime avec une valeur de 3,1 % avec 70 % de PBSA . Cette faible amélioration de l'élongation à la rupture a pu notamment être expliquée par une faible adhésion interfaciale entre le PHBV et le PBSA tel qu'introduit par le « Equivalent Box Model » (EBM) selon Eq. VII.1 (Kolařík, 1996) :

$$S_b = S_1 v_{1p} + S_2 v_{2p} + A S_2 v_s, \quad \text{Eq. VII.1}$$

Où $S_1 > S_2$ et S_1, S_2 sont les valeurs de contraintes de la phase 1 et 2, respectivement. Tandis que A peut-être identifié comme un niveau d'adhésion interfaciale.

Table VII.1: Détermination des propriétés mécaniques des mélanges PHBV/PBSA par tests de traction

| Sample | Young modulus* (MPa) | Stress at yield (MPa) | Elongation at break (%) |
|--------|----------------------|-----------------------|-------------------------|
| 100/0 | 3485±63 | 22±2 | 0.98±0.1 |
| 70/30 | 2227±108 | 19±2.5 | 1.48±0.4 |
| 50/50 | 1360±125 | 12±1.9 | 1.48±0.2 |
| 30/70 | 833±147 | 12±1.6 | 3.1±0.8 |
| 0/100 | 332±8 | 15±1.4 | 134.8±48 |

*experiments carried out without extensometer

Chapter VII

La Figure VII.5 montre ainsi qu'un faible niveau d'adhésion interfaciale entre le PHBV et le PBSA peut être assumé pour un taux d'inclusion de PBSA supérieur à 50 %. En effet, au-delà de cette valeur seuil, il en résulte une forte diminution du niveau d'adhésion interfaciale.

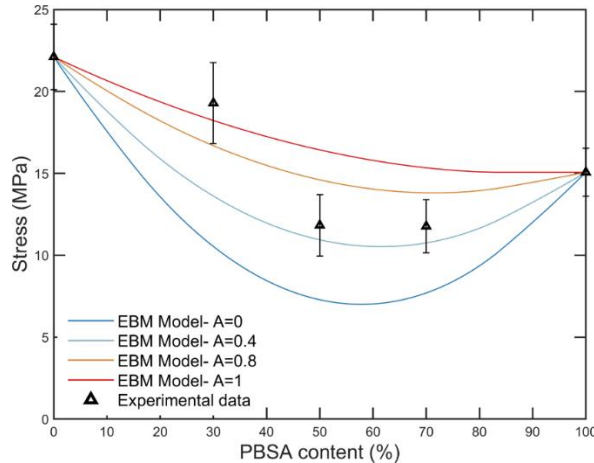


Figure VII.5: Évolution de la contrainte de traction des mélanges PHBV/PBSA avec représentation du modèle EBM avec différents niveaux d'adhésion interfaciale (A) entre le PHBV et le PBSA

D'après les résultats obtenus, l'inclusion de PBSA dans la matrice de PHBV conduit à une diminution de la rigidité ainsi qu'un changement dans le comportement rhéologique au fondu. Cependant, l'amélioration de l'élongation à la rupture reste limitée et corrèle avec une faible adhésion interfaciale entre le PHBV et le PBSA et nécessitant une compatibilisation entre les deux polymères.

VII.4.2. Compatibilisation *in situ* de mélanges binaires de poly(3-hydroxybutyrate-co-3-hydroxyvalérate) / poly(butylène-co-succinate-co-adipate) en utilisant un initiateur de radicaux libres

La compatibilisation interfaciale entre le PHBV et le PBSA s'est faite par extrusion réactive en introduisant un initiateur de radicaux libres, le peroxyde de dicumyle, dans le mélange PHBV/PBSA 70/30. La première partie de cette étude s'est portée sur la compatibilisation entre le PHBV et le PBSA en utilisant un mélangeur interne. La Figure VII.6(a) montre l'évolution de la viscosité complexe en fonction de la fréquence pour différentes teneurs en peroxyde de dicumyle et montre ainsi que la viscosité complexe du mélange PHBV/PBSA+ 0.02 phr DCP est identique au mélange non compatibilisé. Cependant, l'augmentation de la proportion en peroxyde conduit à une augmentation de deux ordres de grandeurs de la viscosité complexe. De

Chapter VII

plus, pour une teneur supérieure à 0.1 phr DCP, les mélanges montrent une viscosité complexe dépendante de la fréquence avec une augmentation de celle-ci aux basses fréquences. Ce comportement est typique des polymères avec une structure ramifiée (Eslami & Kamal, 2013a; Tian et al., 2006). De plus, l'évolution de la teneur en gel en fonction de la teneur en DCP, Figure VII.6(b), qui est sensible à la réticulation entre le PHBV et le PBSA avec PHBV-g-PBSA, confirme la réaction entre le PHBV et le PBSA tel qu'introduit par (Ma et al. 2012). En effet, l'inclusion de DCP dans le mélange PHBV/PBSA conduit à une forte augmentation de la teneur en gel jusqu'à 36 %. Le mécanisme de réaction conduit à la génération de radicaux libres sur les chaînes macromoléculaires de PHBV et de PBSA et par recombinaison conduit à la réticulation.

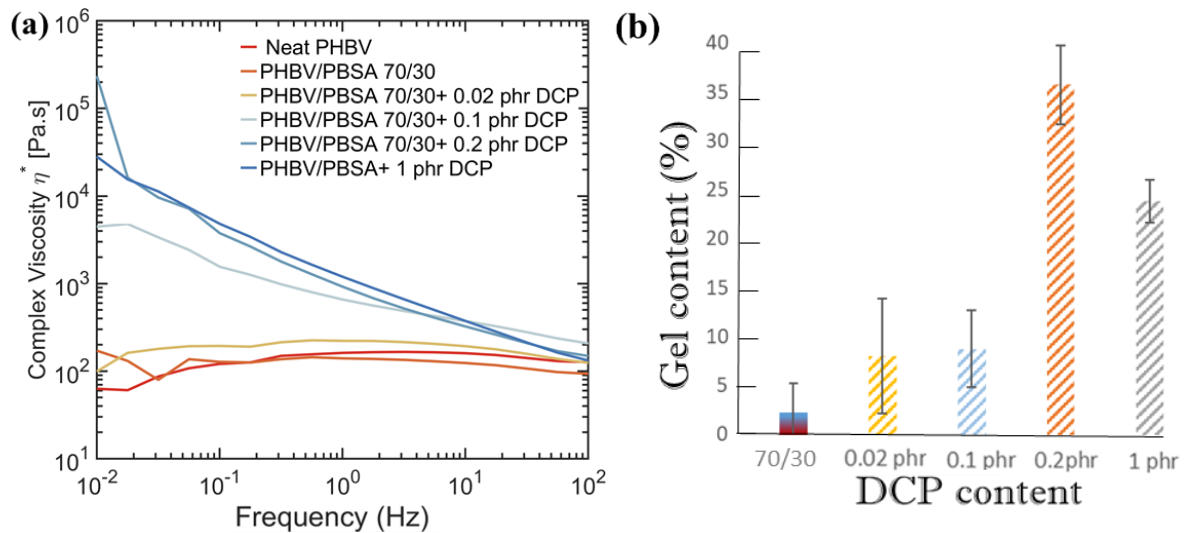


Figure VII.6: Evolution de la viscosité complexe en fonction de la fréquence des mélanges PHBV/PBSA avec différentes teneurs en peroxyde de dicumyle à 185 °C et (b) teneur en gel en fonction de la teneur en peroxyde de dicumyle

L'introduction d'un initiateur de radicaux libres a positivement impacté la mise en œuvre par extrusion soufflage de gaine le mélange à base de PHBV comme illustré en Figure VII.7(a). En effet, l'introduction de PBSA dans la matrice de PHBV permet de gonfler la bulle tandis que l'introduction du peroxyde de dicumyle permet d'apporter de la stabilité à la bulle. Cependant, il est à noter qu'une teneur trop importante de DCP conduit à la présence d'agrégats qui sont considérés comme des points de gels dû à une réticulation trop importante entre le PHBV et le PBSA. Ces derniers empêchant alors de gonfler la bulle à cause de la présence de points de fragilité.

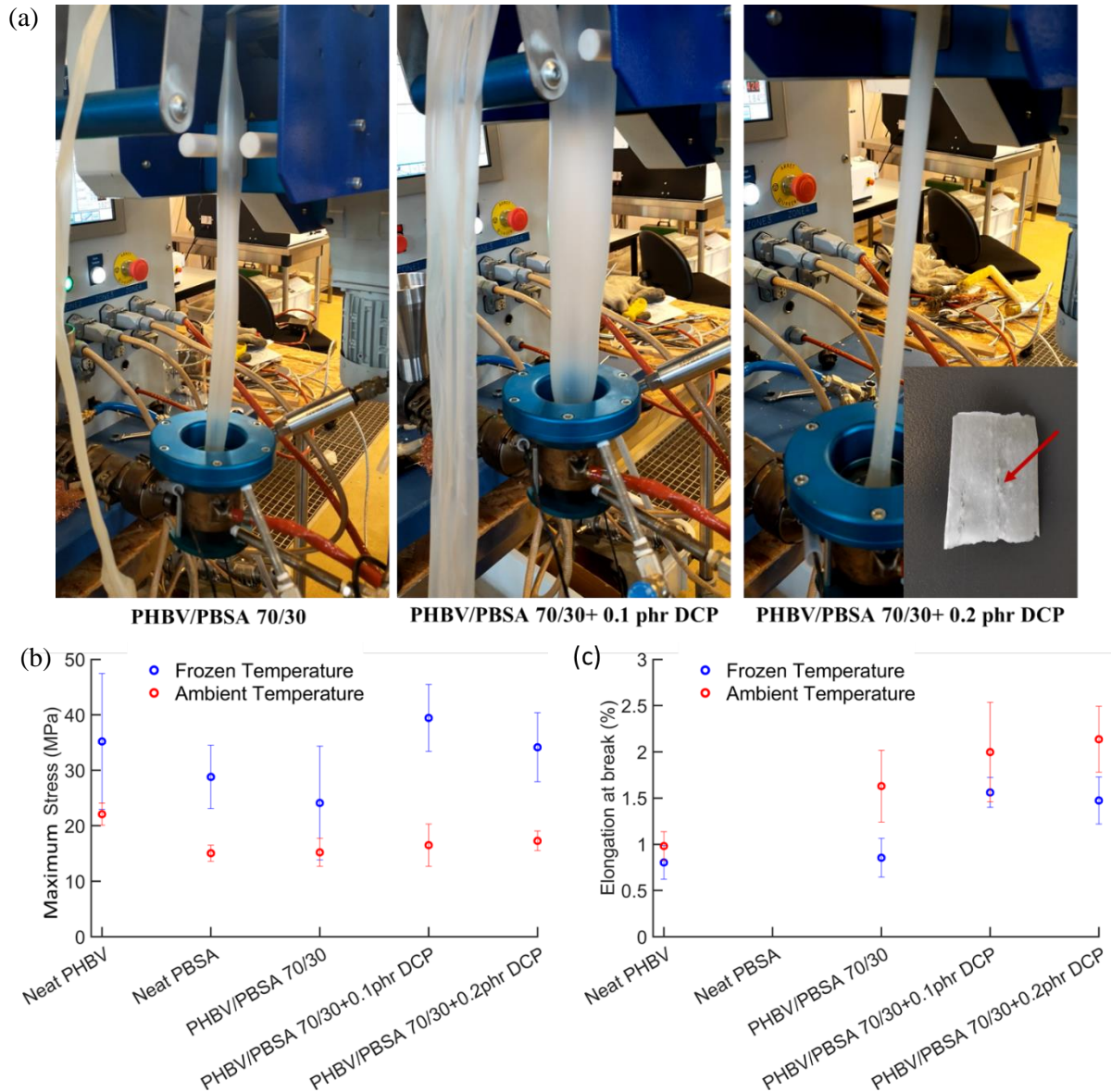


Figure VII.7: (a) Extrusion soufflage de gain du PHBV/PBSA avec addition de peroxyde de dicumyle après extrusion réactive, évolution de (a) la contrainte maximale et (b) de l'élongation à la rupture des mélanges de PHBV/PBSA en fonction de la teneur en DCP

Les propriétés mécaniques ont ensuite été évaluées par tests de traction dans des conditions ambiantes, mais également dans des conditions de surgélation ($-20\text{ }^{\circ}\text{C}$). L'évolution de la contrainte maximale et de l'élongation à la rupture sont illustrée Figure VII.7(b) et Figure VII.7(c), respectivement. Les résultats montrent que l'introduction du DCP (0.1 phr) induit une augmentation de la contrainte maximale avec une valeur de contrainte à $-20\text{ }^{\circ}\text{C}$ supérieure au mélange non compatibilisé et comparable à celle du PHBV. Cette contrainte supérieure a alors été interprété comme une amélioration de la compatibilité interfaciale entre le PHBV et le PBSA. Cependant, une amélioration minimale de l'élongation à la rupture du mélange est obtenue avec une valeur de 2 % à 0.1 phr DCP. Une tendance comparable de l'évolution de l'élongation à la rupture est observée sur une grande plage de température entre $-20\text{ }^{\circ}\text{C}$ et $20\text{ }^{\circ}\text{C}$.

Chapter VII

Cette étude montre ainsi que l'introduction d'un initiateur de radicaux libres impacte positivement la capacité de mise en œuvre du PHBV par extrusion soufflage et démontrant ainsi sa viabilité pour être transformé par une technique de mise en œuvre conventionnelle pour l'emballage flexible. Par ailleurs, les propriétés mécaniques montrent que l'élongation à la rupture entre $-20\text{ }^{\circ}\text{C}$ et $20\text{ }^{\circ}\text{C}$ sont comparables. Cependant, l'introduction du DCP ne conduit pas une amélioration significative de la ductilité du mélange. Les meilleurs résultats ont ainsi été obtenus pour une teneur en DCP de 0.1 phr. La modification de la phase amorphe du mélange a alors été étudiée par l'addition d'un agent plastifiant.

VII.4.3.Improvement of the thermo-mechanical properties of PHBV-based blend through plasticization using Acetyl Tributyl Citrate

La modification de la phase amorphe du mélange PHBV/PBSA+ 0.1 phr DCP a été étudiée par l'ajout de l'acétylcitrate de tributyle (ATBC) en tant qu'agent plastifiant. Les propriétés mécaniques sont détaillées dans le Chapter V: et montrent que l'inclusion d'ATBC conduit à une forte diminution de la rigidité du mélange jusqu'à atteindre une valeur-limite située aux alentours de 500 MPa pour une teneur en ATBC de 10 %. Ce seuil est également observé pour l'élongation à la rupture avec une valeur maximale atteinte à 2.9 % avec 10 % d'ATBC. Cette amélioration minime a ainsi été corrélée à une miscibilité partielle entre l'ATBC et le PHBV. La prédiction de la température de transition vitreuse en fonction de la teneur en ATBC a été estimée à partir de l'équation empirique de Fox tel que :

$$\frac{1}{T_{g,i}} = \frac{w_{1,i}}{T_{g1,i}} + \frac{1-w_{1,i}}{T_{g2}}, \quad \text{Eq. VII.2}$$

Où $T_{g1,i}$ est la température de transition vitreuse du PHBV ou du PBSA phase, T_{g2} est la température de transition vitreuse de l'ATBC, tandis que $w_{1,i}$ est la fraction massique de $i = \text{PHBV, PBSA}$

La Figure VII.8(a) montre qu'il y a une stabilisation de la température de transition de PHBV au-delà d'une teneur en ATBC de 5 % et dévie de l'équation de Fox. A l'opposé, les résultats expérimentaux illustrés à la Figure VII.8(b), montre que les résultats expérimentaux pour la phase de PBSA corrèle avec la prédiction de l'équation de Fox. Ce résultat permettant d'interpréter qu'il y a une bonne miscibilité entre l'ATBC et la phase de PBSA. Par conséquence, malgré l'ajout d'un agent plastifiant dans la phase amorphe, les propriétés mécaniques résultantes seront assujétis au comportement de la phase PHBV. Ainsi, la formulation comprenant 10 % d'ATBC montre les meilleurs résultats.

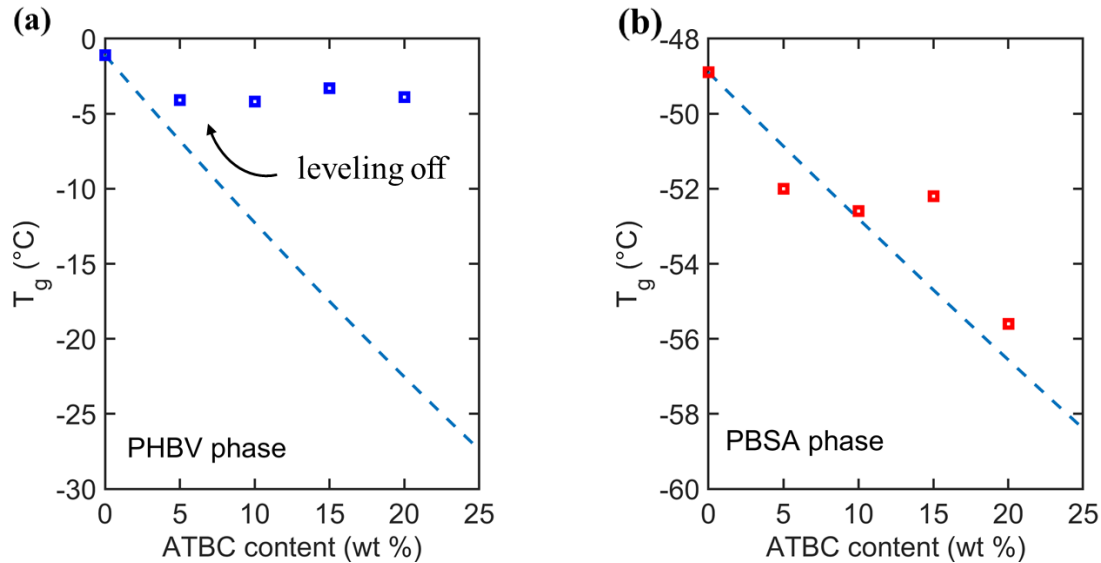


Figure VII.8: Température de transition vitreuse des phases de (a) PHBV et (b) PBSA en fonction de la teneur en ATBC. Les résultats expérimentaux sont représentés sous forme de symbole tandis que l'équation de Fox est représentée en pointillée

VII.4.4. Conception d'un emballage flexible à base de poly(3-hydroxybutyrate-co-3-hydroxyvalérate)-pour l'emballage de produits surgelés

Au cours des travaux, un changement de la réglementation vis-à-vis de la classification du peroxyde de dicumyle a conduit à substituer ce dernier par un peroxyde organique équivalent. Ainsi, le DCP a été remplacé par le Luperox® 101 et l'étude portant sur la formulation du PHBV et du PBSA en présence du Luperox® et de l'ATBC et mis en œuvre par mélangeur interne est décrite en détail dans le Chapter V, Part I.

La capacité de changer d'échelle de production d'un emballage flexible est dépendante de sa capacité à être mise en œuvre par la technique d'extrusion soufflage de gaine. La validation de cette montée en échelle a ainsi été réalisée à l'échelle semi-pilote et le film obtenu lors de la mise en œuvre est présenté dans la Figure VII.9. La formulation mise en œuvre montre une très bonne stabilité de la bulle et démontre ainsi sa viabilité à mettre produit à l'échelle semi-pilote par une technique d'extrusion soufflage.



Figure VII.9: Extrusion-soufflage de gaine de la formulation plastifiée PHBV/PBSA/ATBC 63/27/10+ 0.2 phr Luperox® avec un Blow Up Ratio de 3.8, la taille de la bulle est d'environ 180 cm

Les propriétés rhéologiques, thermiques et mécaniques de la formulation PHBV/PBSA/ATBC 63/27/10+ 0.2 phr Luperox® sont regroupés dans le Table VII.2. Les résultats montrent une anisotropie dans la direction transversale et longitudinale. Par ailleurs, les propriétés mécaniques ont été évaluées à température ambiante ainsi qu'à température de surgélation ($-20\text{ }^{\circ}\text{C}$). La diminution de la température induit une augmentation du module élastique ainsi que de la contrainte maximale cependant, l'élongation à la rupture montre des valeurs similaires sur la grande plage de température (ca. $\Delta T \cong 40\text{ }^{\circ}\text{C}$). En conclusion, le mélange PHBV/PBSA/ATBC/Luperox apparaît comme un candidat potentiel pour être utilisé en tant qu'emballage flexible pour les aliments surgelés.

Chapter VII

Table VII.2: Tableau synoptique des propriétés de la formulation PHBV/PBSA/ATBC 63/27/10+ 0.2 phr Luperox® obtenu par extrusion gonflage

| Methods | | Units | Values | |
|------------------------------|----------|-------------------|-------------|---------------|
| General properties | | | | |
| η_0 | / | Pa.s | 16,800 | |
| MFI (190°C; 2,16kg) | ISO 1133 | g/10 min | 15.5± 0.3 | |
| Thermal properties | | | PHBV | PBSA |
| T_g | / | °C | -3.9± 0.3 | -53.2± 0.3 |
| T_m | / | °C | 162± 1 | 77± 1 |
| T_c | / | °C | 111± 1 | 55± 1 |
| Mechanical properties | | | 23°C | -20 °C |
| Maximum stress | MD | Mpa | 14±2 | 37±3 |
| | TD | | 11±2 | 29±3 |
| Elongation at break | MD | ISO 527-2 | 4.2±0.5 | 4.8±0.5 |
| | TD | | % | 2.5±0.7 |
| Elastic Modulus | MD | Mpa | 1115±94 | 1774±354 |
| | TD | | 1064±94 | 1731±412 |
| Charpy Impact test (Notched) | ISO 179 | kJ/m ² | 7.7± 0.5 | |

VII.5.Principales conclusions

La recherche d'une solution alternative au polyéthylène basse densité pour être adressé à l'emballage flexible d'aliments surgelés doit répondre à un cahier des charges spécifiques comprenant la mise en œuvre par extrusion soufflage et l'obtention d'un emballage flexible. Dans cette perspective, le polymère biosourcé et biodégradable poly(3-hydroxybutyrate-co-3-hydroxyvalerate) (PHBV) apparaît comme un candidat potentiel. Cependant, sa rigidité et sa fragilité ainsi que sa faible viscosité au fondu requiert une formulation raisonnée. Dans ce cadre, la stratégie adoptée dans le cadre de ces travaux de recherche s'est appuyée sur le mélange binaire entre le PHBV et le PBSA. Découlant d'une méthodologie en cascade (tests de formulation à petite échelle, sélection des meilleurs candidats pour tests et construction de prototypes à l'échelle semi-pilote) ont abouti à une formulation basée sur le mélange entre le PHBV et le PBSA ainsi que l'introduction d'un agent plastifiant et d'un initiateur de radicaux.

Chapter VII

Les expériences finales ont ainsi montré que le mélange à base de PHBV était apte à être mis en forme par extrusion soufflage de gaine, mais peut potentiellement être adressé pour des conditions de surgélations avec des valeurs d'élongation à la rupture identique entre -20 °C et 20 °C .

References

- ADEME, T. M., FRD, CVG. (2015). *Panorama des coproduits et résidus biomasse à usage des filières chimie et matériaux biosourcés en France*. Retrieved from
- Aiken, W., Alfrey, T., Janssen, A., & Mark, H. (1947). CREEP BEHAVIOR OF PLASTICIZED VINYLITE VYNW. *Journal of Polymer Science*, 2(2), 178-198. doi:10.1002/pol.1947.120020206
- Anjum, A., Zuber, M., Zia, K. M., Noreen, A., Anjum, M. N., & Tabasum, S. (2016). Microbial production of polyhydroxyalkanoates (PHAs) and its copolymers: a review of recent advancements. *International journal of biological macromolecules*, 89, 161–174.
- Avérous, L. (2004). Biodegradable Multiphase Systems Based on Plasticized Starch: A Review. *Journal of Macromolecular Science, Part C*, 44(3), 231-274. doi:10.1081/MC-200029326
- Averous, L., & Boquillon, N. (2004). Biocomposites based on plasticized starch: thermal and mechanical behaviours. *Carbohydrate Polymers*, 56(2), 111-122. doi:<https://doi.org/10.1016/j.carbpol.2003.11.015>
- Avrami, M. (1939). Kinetics of Phase Change. I General Theory. *The Journal of Chemical Physics*, 7(12), 1103-1112. doi:10.1063/1.1750380
- Avrami, M. (1940). Kinetics of Phase Change. II Transformation-Time Relations for Random Distribution of Nuclei. *The Journal of Chemical Physics*, 8(2), 212-224. doi:10.1063/1.1750631
- Avrami, M. (1941). Granulation, Phase Change, and Microstructure Kinetics of Phase Change. III. *The Journal of Chemical Physics*, 9(2), 177-184. doi:10.1063/1.1750872
- Balasundram, N., Sundram, K., & Samman, S. (2006). Phenolic compounds in plants and agri-industrial by-products: Antioxidant activity, occurrence, and potential uses. *Food Chemistry*, 99(1), 191-203. doi:<https://doi.org/10.1016/j.foodchem.2005.07.042>
- Baptist, J. N., Ziegler, John B. (1965). United States Patent No.
- Barham, P. J., & Keller, A. (1986). THE RELATIONSHIP BETWEEN MICROSTRUCTURE AND MODE OF FRACTURE IN POLYHYDROXYBUTYRATE. *Journal of Polymer Science Part B-Polymer Physics*, 24(1), 69-77. doi:10.1002/polb.1986.180240108
- Bayer, I. S., Guzman-Puyol, S., Heredia-Guerrero, J. A., Ceseracciu, L., Pignatelli, F., Ruffilli, R., . . . Athanassiou, A. (2014). Direct Transformation of Edible Vegetable Waste into Bioplastics. *Macromolecules*, 47(15), 5135-5143. doi:10.1021/ma5008557
- BIOTREM. (2016). Retrieved from <https://biotrem.pl/en/>
- Bittmann, B., Bouza, R., Barral, L., Castro-Lopez, M., & Dopico-Garcia, S. (2015). Morphology and thermal behavior of poly (3-hydroxybutyrate-co-3-hydroxyvalerate)/poly(butylene adipate-co-terephthalate)/clay nanocomposites. *Polymer Composites*, 36(11), 2051-2058. doi:10.1002/pc.23115
- Borah, P. P., Das, P., & Badwaik, L. S. (2017). Ultrasound treated potato peel and sweet lime pomace based biopolymer film development. *Ultrasonics Sonochemistry*, 36, 11-19. doi:10.1016/j.ultsonch.2016.11.010
- Boufarguine, M., Guinault, A., Miquelard-Garnier, G., & Sollogoub, C. (2013). PLA/PHBV Films with Improved Mechanical and Gas Barrier Properties. *Macromolecular Materials and Engineering*, 298(10), 1065-1073. doi:10.1002/mame.201200285
- Brunel, D. G., Pachekoski, W. M., Dalmolin, C., & Agnelli, J. A. M. (2014). Natural additives for poly (hydroxybutyrate - CO - hydroxyvalerate) - PHBV: effect on mechanical properties and biodegradation. *Materials Research*, 17, 1145-1156.

- Bul on, A., Colonna, P., Planchot, V., & Ball, S. (1998). Starch granules: structure and biosynthesis. *International journal of biological macromolecules*, 23(2), 85-112. doi:[https://doi.org/10.1016/S0141-8130\(98\)00040-3](https://doi.org/10.1016/S0141-8130(98)00040-3)
- Busch, J. M. (1999). Enzymic browning in potatoes: A simple assay for a polyphenol oxidase catalysed reaction. *Biochemical Education*, 27(3), 171-173. doi:[https://doi.org/10.1016/S0307-4412\(99\)00033-3](https://doi.org/10.1016/S0307-4412(99)00033-3)
- Buzarovska, A., & Grozdanov, A. (2009). Crystallization kinetics of poly(hydroxybutyrate-co-hydroxyvalerate) and poly(dicyclohexylitaconate) PHBV/PDCHI blends: thermal properties and hydrolytic degradation. *Journal of Materials Science*, 44(7), 1844-1850. doi:10.1007/s10853-008-3236-3
- Caderby, E., Baumberger, S., Hoareau, W., Fargues, C., Decloux, M., & Maillard, M.-N. (2013). Sugar Cane Stillage: A Potential Source of Natural Antioxidants. *Journal of Agricultural and Food Chemistry*, 61(47), 11494-11501. doi:10.1021/jf4039474
- Cai, L., Qi, Z., Xu, J., Guo, B., & Huang, Z. (2019). Study on the Photodegradation Stability of Poly(butylene Succinate-co-butylene Adipate)/TiO₂ Nanocomposites. *Journal of Chemistry*, 2019, 5036019. doi:10.1155/2019/5036019
- Camire, M. E., Violette, D., Dougherty, M. P., & McLaughlin, M. A. (1997). Potato Peel Dietary Fiber Composition: Effects of Peeling and Extrusion Cooking Processes. *Journal of Agricultural and Food Chemistry*, 45(4), 1404-1408. doi:10.1021/jf9604293
- Chakar, F. S., & Ragauskas, A. J. (2004). Review of current and future softwood kraft lignin process chemistry. *Industrial Crops and Products*, 20(2), 131-141. doi:<https://doi.org/10.1016/j.indcrop.2004.04.016>
- Charlon, S., Follain, N., Dargent, E., Soulestin, J., Sclavons, M., & Marais, S. (2016). Poly[(butylene succinate)-co-(butylene adipate)]-Montmorillonite Nanocomposites Prepared by Water-Assisted Extrusion: Role of the Dispersion Level and of the Structure-Microstructure on the Enhanced Barrier Properties. *The Journal of Physical Chemistry C*, 120(24), 13234-13248. doi:10.1021/acs.jpcc.6b00339
- Chen, D., Lawton, D., Thompson, M. R., & Liu, Q. (2012). Biocomposites reinforced with cellulose nanocrystals derived from potato peel waste. *Carbohydrate Polymers*, 90(1), 709-716. doi:10.1016/j.carbpol.2012.06.002
- Chikh, A., Benhamida, A., Kaci, M., Pillin, I., & Bruzaud, S. (2016). Synergistic effect of compatibilizer and sepiolite on the morphology of poly(3-hydroxybutyrate-co-3-hydroxyvalerate)/poly(butylene succinate) blends. *Polymer Testing*, 53, 19-28. doi:10.1016/j.polymertesting.2016.05.008
- Choi, J. S., & Park, W. H. (2004). Effect of biodegradable plasticizers on thermal and mechanical properties of poly(3-hydroxybutyrate). *Polymer Testing*, 23(4), 455-460. doi:10.1016/j.polymertesting.2003.09.005
- CITEO. (2019). Le recyclage des films en plastique m nagers progresse. Retrieved from <https://www.citeo.com/le-mag/435/>
- Clark, F. W. (1941). *Chem. Ind.* 225-230, 60, .
- Colby, R. H. (1989). Breakdown of time-temperature superposition in miscible polymer blends. *Polymer*, 30(7), 1275-1278. doi:[https://doi.org/10.1016/0032-3861\(89\)90048-7](https://doi.org/10.1016/0032-3861(89)90048-7)
- Comission, E. (2021). A European Green Deal. Retrieved from https://ec.europa.eu/info/strategy/priorities-2019-2024/european-green-deal_en
- Corre, Y.-M., Bruzaud, S., Audic, J.-L., & Grohens, Y. (2012). Morphology and functional properties of commercial polyhydroxyalkanoates: A comprehensive and comparative study. *Polymer Testing*, 31(2), 226-235. doi:<http://dx.doi.org/10.1016/j.polymertesting.2011.11.002>
- Correa, M. C. S., Branciforti, M. C., Pollet, E., Agnelli, J. A. M., Nascente, P. A. P., & Averous, L. (2012). Elaboration and Characterization of Nano-Biocomposites Based on

- Plasticized Poly(Hydroxybutyrate-Co-Hydroxyvalerate) with Organo-Modified Montmorillonite. *Journal of Polymers and the Environment*, 20(2), 283-290. doi:10.1007/s10924-011-0379-0
- Costa, S. S., Miranda, A. L., De Morais, M. G., Costa, J. A. V., & Druzian, J. I. (2019). Microalgae as source of polyhydroxyalkanoates (PHAs) — A review. *International journal of biological macromolecules*, 131, 536-547. doi:10.1016/j.ijbiomac.2019.03.099
- Cunha, M., Fernandes, B., Covas, J. A., Vicente, A. A., & Hilliou, L. (2015). Film blowing of PHBV blends and PHBV-based multilayers for the production of biodegradable packages. *Journal of Applied Polymer Science*, 133(2). doi:10.1002/app.42165
- Cunha, M., Fernandes, B., Covas, J. A., Vicente, A. A., & Hilliou, L. (2016). Film blowing of PHBV blends and PHBV-based multilayers for the production of biodegradable packages. *Journal of Applied Polymer Science*, 133(2), n/a-n/a. doi:10.1002/app.42165
- D'Haene, P., Remsen, E. E., & Asrar, J. (1999). Preparation and Characterization of a Branched Bacterial Polyester. *Macromolecules*, 32(16), 5229-5235. doi:10.1021/ma981911k
- De Gennes, P.-G. (1976). On a relation between percolation theory and the elasticity of gels. *Journal de Physique Lettres*, 37(1), 1-2. doi:10.1051/jphyslet:019760037010100
- de Koning, G. J. M., & Lemstra, P. J. (1993). Crystallization phenomena in bacterial poly[(R)-3-hydroxybutyrate]: 2. Embrittlement and rejuvenation. *Polymer*, 34(19), 4089-4094. doi:[https://doi.org/10.1016/0032-3861\(93\)90671-V](https://doi.org/10.1016/0032-3861(93)90671-V)
- Debuissy, T., Pollet, E., & Avérous, L. (2017). Synthesis and characterization of biobased poly(butylene succinate-ran-butylene adipate). Analysis of the composition-dependent physicochemical properties. *European Polymer Journal*, 87, 84-98. doi:<https://doi.org/10.1016/j.eurpolymj.2016.12.012>
- Delamare, L., & Vergnes, B. (1996). Computation of the morphological changes of a polymer blend along a twin-screw extruder. *Polymer Engineering & Science*, 36(12), 1685-1693. doi:<https://doi.org/10.1002/pen.10565>
- Dence, C. W. (1992). The Determination of Lignin. In S. Y. Lin & C. W. Dence (Eds.), *Methods in Lignin Chemistry* (pp. 33-61). Berlin, Heidelberg: Springer Berlin Heidelberg.
- Deroine, M., Cesar, G., Le Duigou, A., Davies, P., & Bruzard, S. (2015). Natural Degradation and Biodegradation of Poly(3-Hydroxybutyrate-co-3-Hydroxyvalerate) in Liquid and Solid Marine Environments. *Journal of Polymers and the Environment*, 23(4), 493-505. doi:10.1007/s10924-015-0736-5
- Deroiné, M., Le Duigou, A., Corre, Y.-M., Le Gac, P.-Y., Davies, P., César, G., & Bruzard, S. (2014). Accelerated ageing and lifetime prediction of poly(3-hydroxybutyrate-co-3-hydroxyvalerate) in distilled water. *Polymer Testing*, 39, 70-78. doi:<https://doi.org/10.1016/j.polymertesting.2014.07.018>
- Dharmalingam, S., Hayes, D. G., Wadsworth, L. C., Dunlap, R. N., DeBruyn, J. M., Lee, J., & Wszelaki, A. L. (2015). Soil Degradation of Polylactic Acid/Polyhydroxyalkanoate-Based Nonwoven Mulches. *Journal of Polymers and the Environment*, 23(3), 302-315. doi:10.1007/s10924-015-0716-9
- Divers, T., Pillin, I., Feller, J.-F., Levesque, G., & Grohens, Y. (2004). Starch Modification, Destructuration and Hydrolysis during O-Formylation. *Starch - Stärke*, 56(9), 389-398. doi:<https://doi.org/10.1002/star.200300270>
- Dong, W., Ma, P., Wang, S., Chen, M., Cai, X., & Zhang, Y. (2013). Effect of partial crosslinking on morphology and properties of the poly(β -hydroxybutyrate)/poly(D,L-lactic acid) blends. *Polymer Degradation and Stability*, 98(9), 1549-1555. doi:<https://doi.org/10.1016/j.polymdegradstab.2013.06.033>
- Dufresne, A., Dupeyre, D., & Vignon, M. R. (2000). Cellulose microfibrils from potato tuber cells: Processing and characterization of starch-cellulose microfibril composites.

- Journal of Applied Polymer Science*, 76(14), 2080-2092. doi:[https://doi.org/10.1002/\(SICI\)1097-4628\(20000628\)76:14<2080::AID-APP12>3.0.CO;2-U](https://doi.org/10.1002/(SICI)1097-4628(20000628)76:14<2080::AID-APP12>3.0.CO;2-U)
- Dufresne, A., & Vignon, M. R. (1998). Improvement of Starch Film Performances Using Cellulose Microfibrils. *Macromolecules*, 31(8), 2693-2696. doi:10.1021/ma971532b
- Eichhorn, S. J., Dufresne, A., Aranguren, M., Marcovich, N. E., Capadona, J. R., Rowan, S. J., . . . Peijs, T. (2010). Review: current international research into cellulose nanofibres and nanocomposites. *Journal of Materials Science*, 45(1), 1-33. doi:10.1007/s10853-009-3874-0
- El-Hadi, A., Schnabel, R., Straube, E., Müller, G., & Henning, S. (2002). Correlation between degree of crystallinity, morphology, glass temperature, mechanical properties and biodegradation of poly (3-hydroxyalkanoate) PHAs and their blends. *Polymer Testing*, 21(6), 665-674. doi:[https://doi.org/10.1016/S0142-9418\(01\)00142-8](https://doi.org/10.1016/S0142-9418(01)00142-8)
- Elain, A., Le Grand, A., Corre, Y.-M., Le Fellic, M., Hachet, N., Le Tilly, V., . . . Bruzaud, S. (2016). Valorisation of local agro-industrial processing waters as growth media for polyhydroxyalkanoates (PHA) production. *Industrial Crops and Products*, 80, 1-5. doi:10.1016/j.indcrop.2015.10.052
- Elkahoui, S., Bartley, G. E., Yokoyama, W. H., & Friedman, M. (2018). Dietary Supplementation of Potato Peel Powders Prepared from Conventional and Organic Russet and Non-organic Gold and Red Potatoes Reduces Weight Gain in Mice on a High-Fat Diet. *J Agric Food Chem*, 66(24), 6064-6072. doi:10.1021/acs.jafc.8b01987
- Eric, G. (2010). Soufflage de gaine. *Techniques de l'ingénieur Plasturgie : fabrications de corps creux, de films et de fils, base documentaire : TIB149DUO*(ref. article : am3702).
- Eslami, H., & Kamal, M. R. (2013a). Effect of a chain extender on the rheological and mechanical properties of biodegradable poly(lactic acid)/poly[(butylene succinate)-co-adipate] blends. *Journal of Applied Polymer Science*, 129(5), 2418-2428. doi:10.1002/app.38449
- Eslami, H., & Kamal, M. R. (2013b). Elongational rheology of biodegradable poly(lactic acid)/poly[(butylene succinate)-co-adipate] binary blends and poly(lactic acid)/poly[(butylene succinate)-co-adipate]/clay ternary nanocomposites. *Journal of Applied Polymer Science*, 127(3), 2290-2306. doi:10.1002/app.37928
- FAO. (2019). Food and Agriculture Organization of the United Nations. (2019). FAOSTAT statistical database.
- Fei, B., Chen, C., Chen, S., Peng, S., Zhuang, Y., An, Y., & Dong, L. (2004). Crosslinking of poly[(3-hydroxybutyrate)-co-(3-hydroxyvalerate)] using dicumyl peroxide as initiator. *Polymer International*, 53(7), 937-943. doi:10.1002/pi.1477
- Fukui, T., & Doi, Y. (1998). Efficient production of polyhydroxyalkanoates from plant oils by *Alcaligenes eutrophus* and its recombinant strain. *Applied Microbiology and Biotechnology*, 49(3), 333-336. doi:10.1007/s002530051178
- Gérard, T. (2013). *Elaboration and characterization of multiphasic polylactide (PLA) and polyhydroxyalkanoates (PHA) multiphasic blends*. Ecole Nationale Supérieure des Mines de Paris, Retrieved from <https://pastel.archives-ouvertes.fr/pastel-00874861>
- Gerard, T., & Budtova, T. (2012). Morphology and molten-state rheology of polylactide and polyhydroxyalkanoate blends. *European Polymer Journal*, 48(6), 1110-1117. doi:<https://doi.org/10.1016/j.eurpolymj.2012.03.015>
- Gerard, T., Budtova, T., Podshivalov, A., & Bronnikov, S. (2014). Polylactide/poly(hydroxybutyrate-co-hydroxyvalerate) blends: Morphology and mechanical properties. *Express Polymer Letters*, 8(8), 609-617. doi:10.3144/expresspolymlett.2014.64

- Gierer, J. (1980). Chemical aspects of kraft pulping. *Wood Science and Technology*, 14(4), 241-266. doi:10.1007/BF00383453
- Grace†, H. P. (1982). DISPERSION PHENOMENA IN HIGH VISCOSITY IMMISCIBLE FLUID SYSTEMS AND APPLICATION OF STATIC MIXERS AS DISPERSION DEVICES IN SUCH SYSTEMS. *Chemical Engineering Communications*, 14(3-6), 225-277. doi:10.1080/00986448208911047
- Grassie, N., Murray, E. J., & Holmes, P. A. (1984a). The thermal degradation of poly(-(d)-β-hydroxybutyric acid): Part 1—Identification and quantitative analysis of products. *Polymer Degradation and Stability*, 6(1), 47-61. doi:[https://doi.org/10.1016/0141-3910\(84\)90016-8](https://doi.org/10.1016/0141-3910(84)90016-8)
- Grassie, N., Murray, E. J., & Holmes, P. A. (1984b). The thermal degradation of poly(-(d)-β-hydroxybutyric acid): Part 2—Changes in molecular weight. *Polymer Degradation and Stability*, 6(2), 95-103. doi:[https://doi.org/10.1016/0141-3910\(84\)90075-2](https://doi.org/10.1016/0141-3910(84)90075-2)
- Grassie, N., Murray, E. J., & Holmes, P. A. (1984c). The thermal degradation of poly(-(d)-β-hydroxybutyric acid): Part 3—The reaction mechanism. *Polymer Degradation and Stability*, 6(3), 127-134. doi:[https://doi.org/10.1016/0141-3910\(84\)90032-6](https://doi.org/10.1016/0141-3910(84)90032-6)
- He, Y., Hu, Z. W., Ren, M. D., Ding, C. K., Chen, P., Gu, Q., & Wu, Q. (2014). Evaluation of PHBHHx and PHBV/PLA fibers used as medical sutures. *Journal of Materials Science-Materials in Medicine*, 25(2), 561-571. doi:10.1007/s10856-013-5073-4
- Hoffman, J. D., & Weeks, J. J. (1962). MELTING PROCESS AND EQUILIBRIUM MELTING TEMPERATURE OF POLYCHLOROTRIFLUOROETHYLENE. *Journal of Research of the National Bureau of Standards Section a-Physics and Chemistry*, 66(JAN-F), 13-+. doi:10.6028/jres.066A.003
- Hoover, R. (2001). Composition, molecular structure, and physicochemical properties of tuber and root starches: a review. *Carbohydrate Polymers*, 45(3), 253-267. doi:[https://doi.org/10.1016/S0144-8617\(00\)00260-5](https://doi.org/10.1016/S0144-8617(00)00260-5)
- Houwink, R. (1974). *Conference: Proc. XI Int. Cong. Pure Appl. Chem*, 575-583.
- Immirzi, B., Malinconico, M., Orsello, G., Portofino, S., & Volpe, M. G. (1999). Blends of biodegradable polyesters by reactive blending: preparation, characterisation and properties. *Journal of Materials Science*, 34(7), 1625-1639. doi:10.1023/A:1004584802030
- INSEE. (14/01/2020). Population par sexe et groupe d'âges, Données annuelles 2020. Retrieved from <https://www.insee.fr/fr/statistiques/2381474>
- Jandas, P. J., Mohanty, S., & Nayak, S. K. (2013). Sustainability, Compostability, and Specific Microbial Activity on Agricultural Mulch Films Prepared from Poly(lactic acid). *Industrial & Engineering Chemistry Research*, 52(50), 17714-17724. doi:10.1021/ie4023429
- Jeddou, K. B., Chaari, F., Maktouf, S., Nouri-Ellouz, O., Helbert, C. B., & Ghorbel, R. E. (2016). Structural, functional, and antioxidant properties of water-soluble polysaccharides from potatoes peels. *Food Chem*, 205, 97-105. doi:10.1016/j.foodchem.2016.02.108
- Jeziorny, A. (1978). Parameters characterizing the kinetics of the non-isothermal crystallization of poly(ethylene terephthalate) determined by d.s.c. *Polymer*, 19(10), 1142-1144. doi:[https://doi.org/10.1016/0032-3861\(78\)90060-5](https://doi.org/10.1016/0032-3861(78)90060-5)
- Kang, H. J., & Min, S. C. (2010). Potato peel-based biopolymer film development using high-pressure homogenization, irradiation, and ultrasound. *LWT - Food Science and Technology*, 43(6), 903-909. doi:10.1016/j.lwt.2010.01.025
- Karamfilova, E., & Sacher, M. (2016). *Food Contact Materials - Regulation (EC) 1935/2004 - European Implementation Assessment, Report. PE 581.411*. Retrieved from Brussels, Belgique:

- Katariina, R., Jenni, R., Jari, V., Ulla, H., Panu, L., Kaisu, H., & Raija, L. (2015). Potato peeling costreams as raw materials for biopolymer film preparation. *Journal of Applied Polymer Science*, *133*(5). doi:10.1002/app.42862
- Kennouche, S., Le Moigne, N., Kaci, M., Quantin, J.-C., Caro-Bretelle, A.-S., Delaite, C., & Lopez-Cuesta, J.-M. (2016). Morphological characterization and thermal properties of compatibilized poly(3-hydroxybutyrate-co-3-hydroxyvalerate) (PHBV)/poly(butylene succinate) (PBS)/halloysite ternary nanocomposites. *European Polymer Journal*, *75*, 142-162. doi:10.1016/j.eurpolymj.2015.12.009
- Kim, D. J., Kim, W. S., Lee, D. H., Min, K. E., Park, L. S., Kang, I. K., . . . Seo, K. H. (2001). Modification of poly(butylene succinate) with peroxide: Crosslinking, physical and thermal properties, and biodegradation. *Journal of Applied Polymer Science*, *81*(5), 1115-1124. doi:<https://doi.org/10.1002/app.1534>
- Kim, H.-S., Kim, H.-J., Lee, J.-W., & Choi, I.-G. (2006). Biodegradability of bio-flour filled biodegradable poly(butylene succinate) bio-composites in natural and compost soil. *Polymer Degradation and Stability*, *91*(5), 1117-1127. doi:<https://doi.org/10.1016/j.polymdegradstab.2005.07.002>
- Kirkpatrick, A. (1940). Some Relations Between Molecular Structure and Plasticizing Effect. *Journal of Applied Physics*, *11*(4), 255-261. doi:10.1063/1.1712768
- Knuthsen, P., Jensen, U., Schmidt, B., & Larsen, I. K. (2009). Glycoalkaloids in potatoes: Content of glycoalkaloids in potatoes for consumption. *Journal of Food Composition and Analysis*, *22*(6), 577-581. doi:<https://doi.org/10.1016/j.jfca.2008.10.003>
- Kolahchi, A. R., & Kontopoulou, M. (2015). Chain extended poly(3-hydroxybutyrate) with improved rheological properties and thermal stability, through reactive modification in the melt state. *Polymer Degradation and Stability*, *121*, 222-229. doi:<https://doi.org/10.1016/j.polymdegradstab.2015.09.008>
- Kolarik, J. (1996). Simultaneous prediction of the modulus and yield strength of binary polymer blends. *Polymer Engineering and Science*, *36*(20), 2518-2524. doi:10.1002/pen.10650
- Kolařík, J. (1996). Evaluation of the extent of interfacial debonding in polymer blends. *Polymer*, *37*(6), 887-891. doi:[https://doi.org/10.1016/0032-3861\(96\)87270-3](https://doi.org/10.1016/0032-3861(96)87270-3)
- Koning, C., Van Duin, M., Pagnouille, C., & Jerome, R. (1998). Strategies for compatibilization of polymer blends. *Progress in Polymer Science*, *23*(4), 707-757. doi:[https://doi.org/10.1016/S0079-6700\(97\)00054-3](https://doi.org/10.1016/S0079-6700(97)00054-3)
- Kumar, P., Ray, S., & Kalia, V. C. (2016). Production of co-polymers of polyhydroxyalkanoates by regulating the hydrolysis of biowastes. *Bioresour Technol*, *200*, 413-419. doi:10.1016/j.biortech.2015.10.045
- Laffargue, J. P. R. (2003). *Etude et modélisation des instabilités du procédé de soufflage de gaine*. Available from <http://www.theses.fr/2003ENMP1156>
- Lai, L. S., & Kokini, J. L. (1991). Physicochemical changes and rheological properties of starch during extrusion. (A review). *Biotechnology Progress*, *7*(3), 251-266. doi:10.1021/bp00009a009
- Landreau, E. (2008). *Matériaux issus de ressources renouvelables. Mélanges amidon plastifié/PA11 compatibles*. Retrieved from <http://www.theses.fr/2008REIMS005/document> Available from <http://www.theses.fr/2008REIMS005>
- Lascano, D., Quiles-Carrillo, L., Balart, R., Boronat, T., & Montanes, N. (2019). Toughened Poly (Lactic Acid)PLA Formulations by Binary Blends with Poly(Butylene Succinate-co-Adipate)PBSA and Their Shape Memory Behaviour. *Materials*, *12*(4), 14. doi:10.3390/ma12040622

- Laurichesse, S., & Avérous, L. (2014). Chemical modification of lignins: Towards biobased polymers. *Progress in Polymer Science*, 39(7), 1266-1290. doi:<https://doi.org/10.1016/j.progpolymsci.2013.11.004>
- Laycock, B., Halley, P., Pratt, S., Werker, A., & Lant, P. (2014). The chemomechanical properties of microbial polyhydroxyalkanoates. *Progress in Polymer Science*, 39(2), 397-442. doi:<http://dx.doi.org/10.1016/j.progpolymsci.2013.06.008>
- Le Delliou, B., Vitrac, O., & Domenek, S. (2020). Bringing New Function to Packaging Materials by Agricultural By-Products. In P. A. Chong, D. J. Newman, & D. A. Steinmacher (Eds.), *Agricultural, Forestry and Bioindustry Biotechnology and Biodiscovery* (pp. 227-257). Cham: Springer International Publishing.
- Lemechko, P., Le Fellic, M., & Bruzard, S. (2019). Production of poly(3-hydroxybutyrate-co-3-hydroxyvalerate) using agro-industrial effluents with tunable proportion of 3-hydroxyvalerate monomer units. *International journal of biological macromolecules*, 128, 429-434. doi:<https://doi.org/10.1016/j.ijbiomac.2019.01.170>
- Leong, Y. K., Show, P. L., Lan, J. C. W., Loh, H. S., Lam, H. L., & Ling, T. C. (2017). Economic and environmental analysis of PHAs production process. *Clean Technologies and Environmental Policy*, 19(7), 1941-1953. doi:10.1007/s10098-017-1377-2
- Li, G., Qi, R., Lu, J., Hu, X., Luo, Y., & Jiang, P. (2013). Rheological properties and foam preparation of biodegradable poly(butylene succinate). *Journal of Applied Polymer Science*, 127(5), 3586-3594. doi:<https://doi.org/10.1002/app.37744>
- Li, H., Lu, X., Yang, H., & Hu, J. (2015). Non-isothermal crystallization of P(3HB-co-4HB)/PLA blends. *Journal of Thermal Analysis and Calorimetry*, 122(2), 817-829. doi:10.1007/s10973-015-4824-5
- Liang, S., & McDonald, A. G. (2014). Chemical and Thermal Characterization of Potato Peel Waste and Its Fermentation Residue as Potential Resources for Biofuel and Bioproducts Production. *Journal of Agricultural and Food Chemistry*, 62(33), 8421-8429. doi:10.1021/jf5019406
- Liu, Q.-S., Zhu, M.-F., Wu, W.-H., & Qin, Z.-Y. (2009). Reducing the formation of six-membered ring ester during thermal degradation of biodegradable PHBV to enhance its thermal stability. *Polymer Degradation and Stability*, 94(1), 18-24. doi:<https://doi.org/10.1016/j.polyimdegradstab.2008.10.016>
- Liu, T., Mo, Z., Wang, S., & Zhang, H. (1997). Nonisothermal melt and cold crystallization kinetics of poly(aryl ether ether ketone ketone). *Polymer Engineering & Science*, 37(3), 568-575. doi:<https://doi.org/10.1002/pen.11700>
- Lopez-Manchado, M. A., Valentini, L., Biagiotti, J., & Kenny, J. M. (2005). Thermal and mechanical properties of single-walled carbon nano tubes-polypropylene composites prepared by melt processing. *Carbon*, 43(7), 1499-1505. doi:10.1016/j.carbon.2005.01.031
- Lourdin, D., Bizot, H., & Colonna, P. (1997). "Antiplasticization" in starch-glycerol films? *Journal of Applied Polymer Science*, 63(8), 1047-1053. doi:10.1002/(sici)1097-4628(19970222)63:8<1047::aid-app11>3.0.co;2-3
- Lu, X., & Weiss, R. A. (1992). Relationship between the glass transition temperature and the interaction parameter of miscible binary polymer blends. *Macromolecules*, 25(12), 3242-3246. doi:10.1021/ma00038a033
- Lyngaae-Jorgensen, J., Kuta, A., Sondergaard, K., & Poulsen, K. V. (1993). Structure and properties of polymer blends with dual phase continuity. *Polym. Networks Blends*, 3, 1-13.
- Ma, P., Cai, X., Zhang, Y., Wang, S., Dong, W., Chen, M., & Lemstra, P. J. (2014). In-situ compatibilization of poly(lactic acid) and poly(butylene adipate-co-terephthalate)

- blends by using dicumyl peroxide as a free-radical initiator. *Polymer Degradation and Stability*, 102, 145-151. doi:<https://doi.org/10.1016/j.polyimdegradstab.2014.01.025>
- Ma, P., Hristova-Bogaerds, D. G., Lemstra, P. J., Zhang, Y., & Wang, S. (2012). Toughening of PHBV/PBS and PHB/PBS Blends via In situ Compatibilization Using Dicumyl Peroxide as a Free-Radical Grafting Initiator. *Macromolecular Materials and Engineering*, 297(5), 402-410. doi:W
- Ma, P. M., Hristova-Bogaerds, D. G., Lemstra, P. J., Zhang, Y., & Wang, S. F. (2012). Toughening of PHBV/PBS and PHB/PBS Blends via In situ Compatibilization Using Dicumyl Peroxide as a Free-Radical Grafting Initiator. *Macromolecular Materials and Engineering*, 297(5), 402-410. doi:10.1002/mame.201100224
- Machaon : l'usine de recyclage de demain. Retrieved from <https://www.entreprendre.fr/machaon-usine/>
- Macosko, C. W., Guégan, P., Khandpur, A. K., Nakayama, A., Marechal, P., & Inoue, T. (1996). Compatibilizers for Melt Blending: Premade Block Copolymers. *Macromolecules*, 29(17), 5590-5598. doi:10.1021/ma9602482
- Marcilla, A., & Beltrán, M. (2012). 5 - MECHANISMS OF PLASTICIZERS ACTION. In G. Wypych (Ed.), *Handbook of Plasticizers (Second Edition)* (pp. 119-133). Boston: William Andrew Publishing.
- Marsh, K., & Bugusu, B. (2007). Food Packaging—Roles, Materials, and Environmental Issues. *Journal of Food Science*, 72(3), R39-R55. doi:<https://doi.org/10.1111/j.1750-3841.2007.00301.x>
- Martelli, S. M., Sabirova, J., Fakhoury, F. M., Dyzma, A., de Meyer, B., & Soetaert, W. (2012). Obtention and characterization of poly(3-hydroxybutyric acid-co-hydroxyvaleric acid)/mcl-PHA based blends. *Lwt-Food Science and Technology*, 47(2), 386-392. doi:10.1016/j.lwt.2012.01.036
- Martino, L., Berthet, M.-A., Angellier-Coussy, H., & Gontard, N. (2015). Understanding external plasticization of melt extruded PHBV–wheat straw fibers biodegradable composites for food packaging. *Journal of Applied Polymer Science*, 132(10). doi:10.1002/app.41611
- Mayer, F. (1998). Potato pulp: properties, physical modification and applications. *Polymer Degradation and Stability*, 59(1), 231-235. doi:[https://doi.org/10.1016/S0141-3910\(97\)00187-0](https://doi.org/10.1016/S0141-3910(97)00187-0)
- Mirzadeh, A., Ghasemi, H., Mahrous, F., & Kamal, M. R. (2015). Reactive extrusion effects on rheological and mechanical properties of poly(lactic acid)/poly (butylene succinate)-co-adipate /epoxy chain extender blends and clay nanocomposites. *Journal of Applied Polymer Science*, 132(48), 11. doi:10.1002/app.42664
- Modi, S., Koelling, K., & Vodovotz, Y. (2013). Assessing the mechanical, phase inversion, and rheological properties of poly- (R)-3-hydroxybutyrate-co-(R)-3-hydroxyvalerate (PHBV) blended with poly-(L-lactic acid) (PLA). *European Polymer Journal*, 49(11), 3681-3690. doi:10.1016/j.eurpolymj.2013.07.036
- Muthuraj, R., Misra, M., & Mohanty, A. K. (2018). Biodegradable compatibilized polymer blends for packaging applications: A literature review. *Journal of Applied Polymer Science*, 135(24), 45726. doi:10.1002/app.45726
- Ncobela, C. N., Kanengoni, A. T., Hlatini, V. A., Thomas, R. S., & Chimonyo, M. (2017). A review of the utility of potato by-products as a feed resource for smallholder pig production. *Animal Feed Science and Technology*, 227, 107-117. doi:<https://doi.org/10.1016/j.anifeedsci.2017.02.008>
- Nechporchuk, O., Belgacem, M. N., & Bras, J. (2016). Production of cellulose nanofibrils: A review of recent advances. *Industrial Crops and Products*, 93, 2-25. doi:10.1016/j.indcrop.2016.02.016

- Niranjana Prabhu, T., & Prashantha, K. (2018). A review on present status and future challenges of starch based polymer films and their composites in food packaging applications. *Polymer Composites*, 39(7), 2499-2522. doi:10.1002/pc.24236
- Nofar, M., Tabatabaei, A., Sojoudiasli, H., Park, C. B., Carreau, P. J., Heuzey, M. C., & Kamal, M. R. (2017). Mechanical and bead foaming behavior of PLA-PBAT and PLA-PBSA blends with different morphologies. *European Polymer Journal*, 90, 231-244. doi:<https://doi.org/10.1016/j.eurpolymj.2017.03.031>
- Ojijo, V., & Ray, S. S. (2015). Super toughened biodegradable polylactide blends with non-linear copolymer interfacial architecture obtained via facile in-situ reactive compatibilization. *Polymer*, 80, 1-17. doi:<https://doi.org/10.1016/j.polymer.2015.10.038>
- Ojijo, V., Sinha Ray, S., & Sadiku, R. (2012). Role of Specific Interfacial Area in Controlling Properties of Immiscible Blends of Biodegradable Polylactide and Poly[(butylene succinate)-co-adipate]. *ACS Applied Materials & Interfaces*, 4(12), 6690-6701. doi:10.1021/am301842e
- Ojijo, V., Sinha Ray, S., & Sadiku, R. (2013). Toughening of Biodegradable Polylactide/Poly(butylene succinate-co-adipate) Blends via in Situ Reactive Compatibilization. *ACS Applied Materials & Interfaces*, 5(10), 4266-4276. doi:10.1021/am400482f
- Olaizola, M. (2003). Commercial development of microalgal biotechnology: from the test tube to the marketplace. *Biomolecular Engineering*, 20(4), 459-466. doi:[https://doi.org/10.1016/S1389-0344\(03\)00076-5](https://doi.org/10.1016/S1389-0344(03)00076-5)
- Ozawa, T. (1971). Kinetics of non-isothermal crystallization. *Polymer*, 12(3), 150-158. doi:[https://doi.org/10.1016/0032-3861\(71\)90041-3](https://doi.org/10.1016/0032-3861(71)90041-3)
- Padermshoke, A., Katsumoto, Y., Sato, H., Ekgasit, S., Noda, I., & Ozaki, Y. (2004). Surface melting and crystallization behavior of polyhydroxyalkanoates studied by attenuated total reflection infrared spectroscopy. *Polymer*, 45(19), 6547-6554. doi:<https://doi.org/10.1016/j.polymer.2004.07.051>
- Pakalapati, H., Chang, C.-K., Show, P. L., Arumugasamy, S. K., & Lan, J. C.-W. (2018). Development of polyhydroxyalkanoates production from waste feedstocks and applications. *Journal of Bioscience and Bioengineering*, 126(3), 282-292. doi:10.1016/j.jbiosc.2018.03.016
- Peelman, N., Ragaert, P., De Meulenaer, B., Adons, D., Peeters, R., Cardon, L., . . . Devlieghere, F. (2013). Application of bioplastics for food packaging. *Trends in Food Science & Technology*, 32(2), 128-141. doi:10.1016/j.tifs.2013.06.003
- Perotto, G., Ceseracciu, L., Simonutti, R., Paul, U. C., Guzman-Puyol, S., Tran, T.-N., . . . Athanassiou, A. (2018). Bioplastics from vegetable waste via an eco-friendly water-based process. *Green Chemistry*, 20(4), 894-902. doi:10.1039/C7GC03368K
- Perotto, G., Simonutti, R., Ceseracciu, L., Mauri, M., Besghini, D., & Athanassiou, A. (2020). Water-induced plasticization in vegetable-based bioplastic films: A structural and thermo-mechanical study. *Polymer*, 200, 9. doi:10.1016/j.polymer.2020.122598
- Phua, Y. J., Pegoretti, A., Araujo, T. M., & Ishak, Z. A. M. (2015). Mechanical and thermal properties of poly(butylene succinate)/poly(3-hydroxybutyrate-co-3-hydroxyvalerate) biodegradable blends. *Journal of Applied Polymer Science*, 132(47). doi:10.1002/app.42815
- Pietrosanto, A., Scarfato, P., Di Maio, L., Nobile, M. R., & Incarnato, L. (2020). Evaluation of the Suitability of Poly(Lactide)/Poly(Butylene-Adipate-co-Terephthalate) Blown Films for Chilled and Frozen Food Packaging Applications. *Polymers*, 12(4). doi:10.3390/polym12040804

- Platzer, N. (1982). The technology of plasticizers, J. Kern Sears and Joseph R. Darby, SPE Monograph Series, Wiley, New York, 1982, 1166 pp. Price: \$130.00. *Journal of Polymer Science: Polymer Letters Edition*, 20(8), 459-459. doi:10.1002/pol.1982.130200810
- Posada, J. A., Naranjo, J. M., Lopez, J. A., Higuera, J. C., & Cardona, C. A. (2011). Design and analysis of poly-3-hydroxybutyrate production processes from crude glycerol. *Process Biochemistry*, 46(1), 310-317. doi:10.1016/j.procbio.2010.09.003
- Pouteau, C., Dole, P., Cathala, B., Averous, L., & Boquillon, N. (2003). Antioxidant properties of lignin in polypropylene. *Polymer Degradation and Stability*, 81(1), 9-18. doi:[https://doi.org/10.1016/S0141-3910\(03\)00057-0](https://doi.org/10.1016/S0141-3910(03)00057-0)
- Puente, J. A. S., Esposito, A., Chivrac, F., & Dargent, E. (2013). Effects of Size and Specific Surface Area of Boron Nitride Particles on the Crystallization of Bacterial Poly(3-hydroxybutyrate-co-3-hydroxyvalerate). *Macromolecular Symposia*, 328(1), 8-19. doi:10.1002/masy.201350601
- Rahimi, A., & Garcia, J. M. (2017). Chemical recycling of waste plastics for new materials production. *Nature Reviews Chemistry*, 1(6), 11. doi:10.1038/s41570-017-0046
- Ralet, M.-C., Buffetto, F., Capron, I., & Guillon, F. (2016). Chapter 2 - Cell Wall Polysaccharides of Potato. In J. Singh & L. Kaur (Eds.), *Advances in Potato Chemistry and Technology (Second Edition)* (pp. 33-56). San Diego: Academic Press.
- Rehman, Z.-u., Habib, F., & Shah, W. H. (2004). Utilization of potato peels extract as a natural antioxidant in soy bean oil. *Food Chemistry*, 85(2), 215-220. doi:<https://doi.org/10.1016/j.foodchem.2003.06.015>
- Ren, M., Song, J., Song, C., Zhang, H., Sun, X., Chen, Q., . . . Mo, Z. (2005). Crystallization kinetics and morphology of poly(butylene succinate-co-adipate). *Journal of Polymer Science Part B: Polymer Physics*, 43(22), 3231-3241. doi:10.1002/polb.20539
- Ridley, B. L., O'Neill, M. A., & Mohnen, D. (2001). Pectins: structure, biosynthesis, and oligogalacturonide-related signaling. *Phytochemistry*, 57(6), 929-967. doi:[https://doi.org/10.1016/S0031-9422\(01\)00113-3](https://doi.org/10.1016/S0031-9422(01)00113-3)
- Robeson, L. M. (2007). *Polymer Blends: A Comprehensive Review* (HANSER Ed.).
- Rodriguez-Gonzalez, F. J., Ramsay, B. A., & Favis, B. D. (2004). Rheological and thermal properties of thermoplastic starch with high glycerol content. *Carbohydrate Polymers*, 58(2), 139-147. doi:<https://doi.org/10.1016/j.carbpol.2004.06.002>
- Roland, C. M., & Ngai, K. L. (1991). Dynamical heterogeneity in a miscible polymer blend. *Macromolecules*, 24(9), 2261-2265. doi:10.1021/ma00009a021
- Ruellan, A., Ducruet, V., & Domenek, S. (2015). CHAPTER 5 Plasticization of Poly(lactide). In *Poly(lactic acid) Science and Technology: Processing, Properties, Additives and Applications* (pp. 124-170): The Royal Society of Chemistry.
- Ruellan, A., Ducruet, V., Gratia, A., Saelices Jimenez, L., Guinault, A., Sollogoub, C., . . . Domenek, S. (2016). Palm oil deodorizer distillate as toughening agent in polylactide packaging films. *Polymer International*, 65(6), 683-690. doi:10.1002/pi.5114
- Ruellan, A., Guinault, A., Sollogoub, C., Ducruet, V., & Domenek, S. (2015). Solubility Factors as Screening Tools of Biodegradable Toughening Agents of Polylactide. *Journal of Applied Polymer Science, Special Issue: Manufacturing of Advanced Biodegradable Polymeric Components*(in print). doi:DOI: 10.1002/APP.42476
- Salomez, M., George, M., Fabre, P., Touchaleaume, F., Cesar, G., Lajarrige, A., & Gastaldi, E. (2019). A comparative study of degradation mechanisms of PHBV and PBSA under laboratory-scale composting conditions. *Polymer Degradation and Stability*, 167, 102-113. doi:<https://doi.org/10.1016/j.polymdegradstab.2019.06.025>
- Sampaio, S. L., Petropoulos, S. A., Alexopoulos, A., Heleno, S. A., Santos-Buelga, C., Barros, L., & Ferreira, I. C. F. R. (2020). Potato peels as sources of functional compounds for

- the food industry: A review. *Trends in Food Science & Technology*, 103, 118-129. doi:<https://doi.org/10.1016/j.tifs.2020.07.015>
- Sánchez Maldonado, A. F., Mudge, E., Gänzle, M. G., & Schieber, A. (2014). Extraction and fractionation of phenolic acids and glycoalkaloids from potato peels using acidified water/ethanol-based solvents. *Food Research International*, 65, 27-34. doi:<https://doi.org/10.1016/j.foodres.2014.06.018>
- Scheller, H. V., & Ulvskov, P. (2010). Hemicelluloses. *Annual Review of Plant Biology*, 61(1), 263-289. doi:10.1146/annurev-arplant-042809-112315
- Schieber, A., & Saldaña, M. D. (2009). *Potato peels: A source of nutritionally and pharmacologically interesting compounds - A review*.
- Sehaqui, H., Liu, A., Zhou, Q., & Berglund, L. A. (2010). Fast preparation procedure for large, flat cellulose and cellulose/inorganic nanopaper structures. *Biomacromolecules*, 11(9), 2195-2198. doi:10.1021/bm100490s
- Serrano, D. P., Aguado, J., & Escola, J. M. (2012). Developing Advanced Catalysts for the Conversion of Polyolefinic Waste Plastics into Fuels and Chemicals. *ACS Catalysis*, 2(9), 1924-1941. doi:10.1021/cs3003403
- Shabna, A., Saranya, V., Malathi, J., Shenbagarathai, R., & Madhavan, H. N. (2014). Indigenously produced polyhydroxyalkanoate based co-polymer as cellular supportive biomaterial. *Journal of Biomedical Materials Research Part A*, 102(10), 3470-3476. doi:10.1002/jbm.a.35029
- Shah, J., Jan, M. R., Mabood, F., & Jabeen, F. (2010). Catalytic pyrolysis of LDPE leads to valuable resource recovery and reduction of waste problems. *Energy Conversion and Management*, 51(12), 2791-2801. doi:<https://doi.org/10.1016/j.enconman.2010.06.016>
- Sheldon, R. A. (2014). Green and sustainable manufacture of chemicals from biomass: state of the art. *Green Chemistry*, 16(3), 950-963. doi:10.1039/c3gc41935e
- Song, H., & Lee, S. Y. (2006). Production of succinic acid by bacterial fermentation. *Enzyme and Microbial Technology*, 39(3), 352-361. doi:<https://doi.org/10.1016/j.enzmictec.2005.11.043>
- Sun, R., Lawther, J. M., & Banks, W. B. (1997). A tentative chemical structure of wheat straw lignin. *Industrial Crops and Products*, 6(1), 1-8. doi:[https://doi.org/10.1016/S0926-6690\(96\)00170-7](https://doi.org/10.1016/S0926-6690(96)00170-7)
- Sun, S., Liu, P., Ji, N., Hou, H., & Dong, H. (2017). Effects of low polyhydroxyalkanoate content on the properties of films based on modified starch acquired by extrusion blowing. *Food Hydrocolloids*, 72, 81-89. doi:10.1016/j.foodhyd.2017.05.030
- Szuman, K., Krucinska, I., Bogun, M., & Draczynski, Z. (2016). PLA/PHA-BIODEGRADABLE BLENDS FOR PNEUMOTHERMIC FABRICATION OF NONWOVENS. *Autex Research Journal*, 16(3), 119-127. doi:10.1515/aut-2015-0047
- Taniguchi, I., Kagotani, K., & Kimura, Y. (2003). Microbial production of poly(hydroxyalkanoate)s from waste edible oils. *Green Chemistry*, 5(5), 545-548. doi:10.1039/B304800B
- Taylor, G. I. (1932). The viscosity of a fluid containing small drops of another fluid. *Proceedings of the Royal Society of London. Series A, Containing Papers of a Mathematical and Physical Character*, 138(834), 41-48. doi:10.1098/rspa.1932.0169
- Taylor, G. I. (1934). The formation of emulsions in definable fields of flow. *Proceedings of the Royal Society of London. Series A, Containing Papers of a Mathematical and Physical Character*, 146(858), 501-523. doi:10.1098/rspa.1934.0169
- Teixeira, P. F., Covas, J. A., Suarez, M. J., Angulo, I., & Hilliou, L. (2020). Film Blowing of PHB-Based Systems for Home Compostable Food Packaging. *International Polymer Processing*, 35(5), 440-447. doi:10.1515/ipp-2020-350506

- Tian, J., Yu, W., & Zhou, C. (2006). The preparation and rheology characterization of long chain branching polypropylene. *Polymer*, 47(23), 7962-7969. doi:<https://doi.org/10.1016/j.polymer.2006.09.042>
- Tri, P. N., Domenek, S., Guinault, A., & Sollogoub, C. (2013). Crystallization behavior of poly(lactide)/poly(-hydroxybutyrate)/talc composites. *Journal of Applied Polymer Science*, 129(6), 3355-3365. doi:10.1002/app.39056
- Tserki, V., Matzinos, P., Pavlidou, E., Vachliotis, D., & Panayiotou, C. (2006). Biodegradable aliphatic polyesters. Part I. Properties and biodegradation of poly(butylene succinate-co-butylene adipate). *Polymer Degradation and Stability*, 91(2), 367-376. doi:<https://doi.org/10.1016/j.polymdegradstab.2005.04.035>
- Utracki, L. A. (1991). ON THE VISCOSITY-CONCENTRATION DEPENDENCE OF IMMISCIBLE POLYMER BLENDS. *Journal of Rheology*, 35(8), 1615-1637. doi:10.1122/1.550248
- Utracki, L. A. (2002). Compatibilization of Polymer Blends. *The Canadian Journal of Chemical Engineering*, 80(6), 1008-1016. doi:10.1002/cjce.5450800601
- Vaccaro, E., DiBenedetto, A. T., & Huang, S. J. (1997). Yield strength of low-density polyethylene-polypropylene blends. *Journal of Applied Polymer Science*, 63(3), 275-281. doi:[https://doi.org/10.1002/\(SICI\)1097-4628\(19970118\)63:3<275::AID-APP1>3.0.CO;2-K](https://doi.org/10.1002/(SICI)1097-4628(19970118)63:3<275::AID-APP1>3.0.CO;2-K)
- Van Soest, J. J. G., & Knooren, N. (1997). Influence of glycerol and water content on the structure and properties of extruded starch plastic sheets during aging. *Journal of Applied Polymer Science*, 64(7), 1411-1422. doi:[https://doi.org/10.1002/\(SICI\)1097-4628\(19970516\)64:7<1411::AID-APP21>3.0.CO;2-Y](https://doi.org/10.1002/(SICI)1097-4628(19970516)64:7<1411::AID-APP21>3.0.CO;2-Y)
- Vardon, D. R., Franden, M. A., Johnson, C. W., Karp, E. M., Guarnieri, M. T., Linger, J. G., . . . Beckham, G. T. (2015). Adipic acid production from lignin. *Energy & Environmental Science*, 8(2), 617-628. doi:10.1039/c4ee03230f
- Vergheese, K., Lewis, H., Lockrey, S., & Williams, H. (2015). Packaging's Role in Minimizing Food Loss and Waste Across the Supply Chain. *Packaging Technology and Science*, 28(7), 603-620. doi:10.1002/pts.2127
- Verlinden, R. A. J., Hill, D. J., Kenward, M. A., Williams, C. D., Piotrowska-Seget, Z., & Radecka, I. K. (2011). Production of polyhydroxyalkanoates from waste frying oil by *Cupriavidus necator*. *Amb Express*, 1, 8. doi:10.1186/2191-0855-1-11
- Vieira, M. G. A., da Silva, M. A., dos Santos, L. O., & Beppu, M. M. (2011). Natural-based plasticizers and biopolymer films: A review. *European Polymer Journal*, 47(3), 254-263. doi:<https://doi.org/10.1016/j.eurpolymj.2010.12.011>
- Voragen, A. G. J., Coenen, G.-J., Verhoef, R. P., & Schols, H. A. (2009). Pectin, a versatile polysaccharide present in plant cell walls. *Structural Chemistry*, 20(2), 263. doi:10.1007/s11224-009-9442-z
- Waigh, T. A., Gidley, M. J., Komanshek, B. U., & Donald, A. M. (2000). The phase transformations in starch during gelatinisation: a liquid crystalline approach. *Carbohydrate Research*, 328(2), 165-176. doi:[https://doi.org/10.1016/S0008-6215\(00\)00098-7](https://doi.org/10.1016/S0008-6215(00)00098-7)
- Wallen, L. L., & Rohwedder, W. K. (1974). Poly-.beta.-hydroxyalkanoate from activated sludge. *Environmental Science & Technology*, 8(6), 576-579. doi:10.1021/es60091a007
- Wan, C. Y., Heeley, E. L., Zhou, Y. T., Wang, S. F., Cafolla, C. T., Crabb, E. M., & Hughes, D. J. (2018). Stress-oscillation behaviour of semi-crystalline polymers: the case of poly(butylene succinate). *Soft Matter*, 14(45), 9175-9184. doi:10.1039/c8sm01889h
- Wan, T., Zhang, J., Liao, S., & Du, T. (2015). An investigation of stress oscillation in poly(butylene succinate-co-cyclohexanedimethylene succinate). *Polymer Engineering & Science*, 55(4), 966-974. doi:<https://doi.org/10.1002/pen.23966>

- Wang, X., Chen, Z., Chen, X., Pan, J., & Xu, K. (2010). Miscibility, crystallization kinetics, and mechanical properties of poly(3-hydroxybutyrate-co-3-hydroxyvalerate)(PHBV)/poly(3-hydroxybutyrate-co-4-hydroxybutyrate)(P3/4HB) blends. *Journal of Applied Polymer Science*, *117*(2), 838-848. doi:<https://doi.org/10.1002/app.31215>
- Weinmann, S., & Bonten, C. (2019). Thermal and rheological properties of modified polyhydroxybutyrate (PHB). *Polymer Engineering & Science*, *59*(5), 1057-1064. doi:10.1002/pen.25075
- Wu, F., Misra, M., & Mohanty, A. K. (2019). Super Toughened Poly(lactic acid)-Based Ternary Blends via Enhancing Interfacial Compatibility. *ACS Omega*, *4*(1), 1955-1968. doi:10.1021/acsomega.8b02587
- Wysocki, J. (2003). Material for making biodegradable mouldings from bran and method thereof. In: Google Patents.
- Xu, J., & Guo, B.-H. (2010). Poly(butylene succinate) and its copolymers: Research, development and industrialization. *Biotechnology Journal*, *5*(11), 1149-1163. doi:10.1002/biot.201000136
- Yim, H., Haselbeck, R., Niu, W., Pujol-Baxley, C., Burgard, A., Boldt, J., . . . Van Dien, S. (2011). Metabolic engineering of *Escherichia coli* for direct production of 1,4-butanediol. *Nature Chemical Biology*, *7*(7), 445-452. doi:10.1038/nchembio.580
- Yoshie, N., Saito, M., & Inoue, Y. (2001). Structural Transition of Lamella Crystals in a Isomorphous Copolymer, Poly(3-hydroxybutyrate-co-3-hydroxyvalerate). *Macromolecules*, *34*(26), 8953-8960. doi:10.1021/ma0113071
- Zembouai, I., Bruzaud, S., Kaci, M., Benhamida, A., Corre, Y. M., Grohens, Y., . . . Lopez-Cuesta, J. M. (2014). Poly(3-Hydroxybutyrate-co-3-Hydroxyvalerate)/Polylactide Blends: Thermal Stability, Flammability and Thermo-Mechanical Behavior. *Journal of Polymers and the Environment*, *22*(1), 131-139. doi:10.1007/s10924-013-0626-7
- Zembouai, I., Kaci, M., Bruzaud, S., Benhamida, A., Corre, Y.-M., & Grohens, Y. (2013). A study of morphological, thermal, rheological and barrier properties of Poly(3-hydroxybutyrate-Co-3-Hydroxyvalerate)/polylactide blends prepared by melt mixing. *Polymer Testing*, *32*(5), 842-851. doi:10.1016/j.polymertesting.2013.04.004
- Zhang, B., Sun, B., Bian, X., Li, G., & Chen, X. (2017). High Melt Strength and High Toughness PLLA/PBS Blends by Copolymerization and in Situ Reactive Compatibilization. *Industrial & Engineering Chemistry Research*, *56*(1), 52-62. doi:10.1021/acs.iecr.6b03151
- Zhang, K., Misra, M., & Mohanty, A. K. (2014). Toughened Sustainable Green Composites from Poly(3-hydroxybutyrate-co-3-hydroxyvalerate) Based Ternary Blends and Miscanthus Biofiber. *ACS Sustainable Chemistry & Engineering*, *2*(10), 2345-2354. doi:10.1021/sc500353v
- Zhang, K., Mohanty, A. K., & Misra, M. (2012). Fully Biodegradable and Biorenewable Ternary Blends from Polylactide, Poly(3-hydroxybutyrate-co-hydroxyvalerate) and Poly(butylene succinate) with Balanced Properties. *ACS Applied Materials & Interfaces*, *4*(6), 3091-3101. doi:10.1021/am3004522
- Zhang, M., & Thomas, N. L. (2011). Blending polylactic acid with polyhydroxybutyrate: The effect on thermal, mechanical, and biodegradation properties. *Advances in Polymer Technology*, *30*(2), 67-79. doi:10.1002/adv.20235
- Zhang, X. M., Elkoun, S., Ajji, A., & Huneault, M. A. (2004). Oriented structure and anisotropy properties of polymer blown films: HDPE, LLDPE and LDPE. *Polymer*, *45*(1), 217-229. doi:<https://doi.org/10.1016/j.polymer.2003.10.057>

- Zhu, Y., Nguyen, P.-M., & Vitrac, O. (2019). Risk assessment of migration from packaging materials into food. In G. Robertson (Ed.), *Elsevier Food Science Reference Module* (pp. 64). Amsterdam, NL: Elsevier.
- Zytner, P., Wu, F., Misra, M., & Mohanty, A. K. (2020). Toughening of Biodegradable Poly(3-hydroxybutyrate-co-3-hydroxyvalerate)/Poly(ϵ -caprolactone) Blends by In Situ Reactive Compatibilization. *ACS Omega*, 5(25), 14900-14910. doi:10.1021/acsomega.9b04379

Titre : Conception de films de poly(3-hydroxybutyrate-co-3-hydroxyvalérate) pour l'emballage alimentaire flexible en contact avec des aliments gras et dans des conditions de surgélation

Mots clés : Polymères biosourcés, polymères biodégradables, PHBV, valorisation co-produits, emballage alimentaire

Résumé : L'objectif principal de cette thèse est de concevoir un matériau d'emballage biosourcé et biodégradable adapté au conditionnement de frites surgelées en utilisant les sous-produits de leur fabrication. Deux stratégies ont été étudiées. La première stratégie consistait à fabriquer des mélanges de polymères à base de poly(3-hydroxybutyrate-co-3-hydroxyvalérate) (PHBV), qui peuvent être obtenus par fermentation de sous-produits. Les mélanges PHBV-poly(butylènesuccinate-co-adipate) (PBSA) ont été conçus dans le but d'améliorer sa mise en oeuvre ainsi que d'augmenter la ductilité du PHBV. Les deux polymères étant immiscibles, la compatibilité interfaciale devait être optimisée. La compatibilisation réactive à l'aide de peroxyde de dicumyle (DCP) a été couronnée de succès et a permis la fabrication de films PHBV/PBSA par extrusion-soufflage à l'échelle du laboratoire. L'effet du DCP sur les propriétés morphologiques, thermiques, mécaniques et rhéologiques a été

évalué dans le but d'optimiser la composition du mélange à l'échelle laboratoire. Pour améliorer les propriétés mécaniques des films, le plastifiant acétyl tri-butyl citrate (ATBC) a été utilisé. L'amélioration de la résistance à la fusion et de la viscosité élongationnelle des mélanges optimisés a permis de réaliser une campagne d'extrusion gonflage réussie à l'échelle pilote en utilisant l'ATBC et un peroxyde organique alternatif LUPEROX® 101, les deux molécules étant admises pour les matériaux en contact avec les aliments. La deuxième stratégie était l'utilisation directe de déchets d'amidon et de pelures de pommes de terre. Pour cela, la caractérisation biochimique des pelures de pomme de terre a été réalisée, et le potentiel d'extraction de molécules à haute valeur ajoutée a été évalué. La possibilité de produire des pelures de pomme de terre et des matériaux à base d'amidon adaptés à la fabrication d'articles à très courte durée de vie a été étudiée.

Title : Design of poly(3-hydroxybutyrate-co-3-hydroxyvalerate)-based films for flexible food packaging in contact with fatty food and under frozen conditions

Keywords : Bio-based polymers, biodegradable polymers, PHBV, valorization of by-products, food packaging

Abstract : The main objective of the present thesis is to design a bio-based and biodegradable packaging material suitable for frozen French fries using the by-products of their fabrication. Two strategies were investigated. The first strategy was the fabrication of polymer blends based on poly(3-hydroxybutyrate-co-3-hydroxyvalerate) (PHBV), which could be obtained by fermentation of by-products. PHBV-poly(butylene succinate-co-adipate) (PBSA) blends were designed with the aim to increase the processability and ductility of PHBV. Both polymers are immiscible, therefore the interfacial compatibility needed to be optimized. Reactive compatibilization using dicumyle peroxide (DCP) was successful and allowed the fabrication of PHBV/PBSA films by film blowing extrusion at the laboratory scale. The effect of DCP on morphological, thermal, mechanical and rheological properties was

Evaluated in the aim to optimize the composition at laboratory scale. To improve the mechanical properties of the films, the plasticizer acetyl tributyl citrate (ATBC) was used. The improved melt strength and extensional viscosity of the optimized blends allowed to perform a successful film blowing scale-up experiment to the small pilot scale using ATBC and an alternative organic peroxide LUPEROX® 101, both molecules being admitted for food contact materials. The second strategy was the direct use of waste starch and potato peels. For that, the biochemical characterization of potato peels was carried out, and the potential of extraction of high added value molecules from potato peels was assessed. The possibility to produce potato peels and starch-based materials suitable for the fabrication of items with very short service life was investigated.